Identification of anti-resorptive and anti-cancer activities of epigenetic inhibitors

Na Wu

Brasenose College

Nuffield Department of Orthopaedics, Rheumatology and

Musculoskeletal Sciences

University of Oxford

Thesis submitted for the degree of Doctor of Philosophy

Trinity 2017

Identification of anti-resorptive and anti-cancer activities of epigenetic inhibitors

Na Wu

Brasenose college

Abstract

Multiple myeloma is a plasma cell malignancy and develops in the bone marrow. The myeloma bone disease is present in the majority of the myeloma patients and is characterised by the excessive numbers and increased resorptive functions of osteoclasts. In order to identify novel targets controlling both osteoclastogenesis and myeloma cell growth, a library of epigenetic compounds was screened in an osteoclast differentiation assay and myeloma cell viability assay. Some compound classes, such as BET bromodomain inhibitors and HDAC inhibitors, showed inhibitory effects on both osteoclast differentiation and myeloma cell proliferation, suggesting that chromatin modifying reagents are possible therapeutic targets in multiple myeloma treatment. To rapidly screen for anti-osteoclast effects, an osteoclast RANKL gene card was successfully developed and applied to selected inhibitors in osteoclast assays. Moreover, the transcriptomic analysis was used to investigate the underlying mechanisms of selected epigenetic compounds in myeloma cells, and we found that cell cycle related pathways have been regulated by several inhibitors. Furthermore, an antibody panel for CyTOF (Mass cytometry) has been developed to characterise the bone marrow microenvironment of myeloma patients, and the CyTOF experiments demonstrated that GSK-J4 and rocilinostat activate the apoptosis marker caspase3 only in myeloma cells without affecting other cell populations. GSK-J4, an inhibitor for KDM5 and KDM6, was shown to upregulate the metallothioneins and induce the ATF4-mediated stress response in myeloma cells, whereas the KDM5B inhibitors causes cell cycle arrest rather than apoptosis.

Acknowledgements

I would like to thank Professor Udo Oppermann, Dr James Dunford and Dr Anthony Tumber for their support, encourage and guidance through my entire D.Phil project. I am grateful to present and former members of the Oppermann group who have helped me with the work of this thesis, including but not limited to Dr Manman Guo, Dr Edward Hookway, Dr Clarence Yapp and Dr Laurynas Pliuskys.

I would like to thank the following people for their friendship in the Botnar Research Centre, including Dr Kelly Rooke, Dr Anneke Kramm, Mr Yanda Xin, Mr Henry Lee and Mr Chao Jiang. Special thanks to Miss Ying-chun Chen for her consistent support and our precious friendship.

Finally, I would like to thank my husband Dr Zhiqiao Wang for his support, accompany and love in these years. I would also like to thank my parents Mr Wenyong Wu, Mrs Baolan Zhang and my parents-in-law Mr Jun Wang and Mrs Jihong Chu for their constant love, mental and financial support for my D.Phil study.

Associated Publications

Tumber, A., A. Nuzzi, E. S. Hookway, S. B. Hatch, S. Velupillai, C. Johansson, A. Kawamura, P. Savitsky, C. Yapp, A. Szykowska, **N. Wu**, C. Bountra, C. Strain-Damerell, N. A. Burgess-Brown, G. F. Ruda, O. Fedorov, S. Munro, K. S. England, R. P. Nowak, C. J. Schofield, N. B. La Thangue, C. Pawlyn, F. Davies, G. Morgan, N. Athanasou, S. Müller, U. Oppermann, and P. E. Brennan. 2017. "Potent and Selective KDM5 Inhibitor Stops Cellular Demethylation of H3K4me3 at Transcription Start Sites and Proliferation of MM1S Myeloma Cells." Cell Chem Biol 24 (3):371-380. doi: 10.1016/j.chembiol.2017.02.006.

Johansson, C., S. Velupillai, A. Tumber, A. Szykowska, E. S. Hookway, R. P. Nowak, C. Strain-Damerell, C. Gileadi, M. Philpott, N. Burgess-Brown, **N. Wu**, J. Kopec, A. Nuzzi, H. Steuber, U. Egner, V. Badock, S. Munro, N. B. LaThangue, S. Westaway, J. Brown, N. Athanasou, R. Prinjha, P. E. Brennan, and U. Oppermann. 2016. "Structural analysis of human KDM5B guides histone demethylase inhibitor development." Nat Chem Biol 12 (7):539-45. doi: 10.1038/nchembio.2087.

Table of Contents

Figure list

Figure 8.7 GSK-467 and KDM5-70C did not induce apoptosis in MM1S myeloma cells

Table list

Abbreviations

AAR: amino acid response
ACTB: actin beta
ASCT: autologous stem cell transplant
ASNS: asparagine synthetase
ASS1: arginosuccinate synthetase 1
ATF4: activating transcription factor 4
B2M: beta-2-microglobulin
BCR: B-cell receptor
BCL-2: B-cell lymphoma 2
BCMA: B-cell maturation antigen
BET: Bromo- and Extra-Terminal domain
BM: bone marrow
BMSCs: bone marrow stromal cells
BMP: bone morphogenetic protein
BMU: basic multicellular unit
BRD: bromodomain
CAR: chimeric antigen receptor
CDK: cyclin-dependent kinases
CDKN2A: cyclin-dependent kinase Inhibitor 2A
ChIPseq: chromatin immunoprecipitation sequencing
CKIs: cyclin-dependent kinase inhibitors
CR: complete response
CRD: chromodomain
CyTOF: cytometry by time of flight
DC-STAMP: dendritic cell-specific transmembrane protein
DDIT3: DNA damage inducible transcript 3
DNMT: DNA methyltransferase
EC_{50}: half maximal effective concentration
FACS: fluorescence-activated cell sorting
FAD: flavin adenine dinucleotide

FDA: Federal Drug Administration

GCN2: general control non-depressible 2

H3K4: methylation of histone 3 lysine 4

HAT: histone acetyltransferase

HDAC: histone deacetylases

HMT: histone methyltransferase

IGF-1: insulin growth factor 1

IL-6: interleukin 6

IL-7: interleukin 7

IL-12: interleukin 12

IL-15: interleukin 15

INHBE: inhibin beta E subunit

JAK: Janus kinase

JmjC: Jumonji C

JNK: c-Jun N-terminal kinase

KDM: histone lysine demethylase

KMT: histone lysine methyltransferases

LEF1: lymphoid enhancer factor 1

LSD1: Lysine specific demethylase 1A

M-CSF: macrophage colony-stimulating factor

MBD: myeloid bone disease

MGUS: monoclonal gammopathy of undetermined significance

MIP-1α: macrophage inflammatory protein 1α

MiRNA: microRNA

MM: multiple myeloma

MMP: matrix metalloproteases

mRNA: messenger RNA

MT: metallothionein

MTF1: metal regulatory transcription factor 1

NAC: N-acetyl-cysteine

ncRNAs: non-coding RNAs

NF-kB: nuclear factor kappa B

NFATc1: nuclear factor of activated T-cells 1

NGS: Next Generation Sequencing

NK cells: natural killer cells

OB: osteoblast

OC: osteoclast

OPG: osteoprotegerin

PADI4: peptidyl arginine deiminase, type IV

PARP: poly ADP ribose polymerase

PBMCs: peripheral blood mononuclear cells

PCL: plasma cell leukaemia

PDGFR: platelet-derived growth factor receptor

PI: propidium iodide

PRMT: protein arginine methyltransferases

PSAT1: phosphoserine aminotransferase 1

PTMs: post-translational modifications

RANK: receptor activator of nuclear factor kappa B

RANKL: receptor activator of nuclear factor kappa B ligand

Rb: retinoblastoma

RISC: RNA-induced silencing complex

RNAseq: RNA sequencing

SAHA: suberoylanilide hydroxamic acid

SD: standard deviation

SDF-1: stromal cell-derived factor 1

SLAMF7: signalling lymphocyte activation molecule F7

SPADE: spanning-tree progression analysis of density-normalized events

STAT3: signal transducer and activator of transcription

TCF: T-cell factor

TGF-β: transforming growth factor-β

TI-2: T-cell-independent type 2

TNF-α: tumour necrosis factor-α

TRAF6: tumour necrosis factor receptor-associated factor

TRAP: Tartrate-resistant acid phosphatase

VCAM-1: vascular cell adhesion molecule-1

VEGF: vascular endothelial growth factor

VGPR: very good partial remission

Chapter 1 Introduction

1.1 Multiple myeloma

1.1.1 Development of Multiple myeloma

Multiple myeloma (MM) is a haematological malignancy which results from the clonal expansion of malignant plasma cells, leading to plasma cells producing aberrant antibodies (Eslick and Talaulikar 2013, Kumar et al. 2017). MM accounts for approximately 10% of all hematologic cancers and the median age of patients at the time of diagnosis is 65 years (Rajkumar and Kyle 2005, Kyle and Rajkumar 2004). With the advancement of more effective therapeutic agents and improvements in supportive treatment, the median survival of MM has been increased from 3 years to > 6 years in the past two decades (Röllig, Knop, and Bornhäuser 2015).

The development of multiple myeloma includes the initial malignant transformation of plasma cells and the progression from asymptomatic stages of the disease including monoclonal gammopathy of undetermined significance (MGUS) and smouldering myeloma. As stated in **Table 1.1**, the clinical diagnostic criteria for MGUS, smouldering myeloma and myeloma are the level of M protein, plasma cell percentage in bone marrow and the related organ or tissue damages which include hypercalcaemia, renal failure, anaemia, and bone lesions (referred to as CRAB features). Over 95% of the plasma cells in multiple myeloma patients are malignant cells, defined as abnormal antigen expression profile comparing with plasma cells in healthy donors (Ribourtout and Zandecki 2015).

Table 1.1 Diagnostic criteria for multiple myeloma, smouldering myeloma and MGUS

Disease	MGUS	Smouldering Myeloma	Multiple Myeloma
	Asymptomatic		Symtomatic
Monoclonal protein (M protein)	Serum M protein<30g/L	Serum M protein (IgG or IgA) ≥30 g/L or urinary M protein ≥500 mg per 24h	M protein in serum or urine
Bone marrow plasma cells	<10%	10–60%	≥10%
Related organ or tissue impairment	No related organ or tissue impairment	No related organ or tissue impairment. Absence of myeloma defining events* or amyloidosis	Biopsy-proven bony or extramedullary plasmacytoma and any one or more of the myeloma defining events*

*Myeloma defining events:
• Evidence of end organ damage that can be attributed to the underlying plasma cell proliferative disorder, specifically:
• Hypercalcaemia: serum calcium >0·25 mmol/L (>1 mg/dL) higher than the upper limit of normal or >2·75 mmol/L (>11 mg/dL)
• Renal insufficiency: creatinine clearance <40 mL per min† or serum creatinine >177 µmol/L (>2 mg/dL)
• Anaemia: haemoglobin value of >20 g/L below the lower limit of normal, or a haemoglobin value <100 g/L
• Bone lesions: one or more osteolytic lesions on skeletal radiography, CT, or PET-CT‡
• Any one or more of the following biomarkers of malignancy:
• Clonal bone marrow plasma cell percentage* ≥60%
• Involved:uninvolved serum free light chain ratio§ ≥100
• >1 focal lesions on MRI studies

This table is produced according to the diagnostic criteria for multiple myeloma made by International Myeloma Working Group (Rajkumar et al. 2014).

There are several other related plasma cell disorders which may progress to multiple myeloma eventually. For example, solitary plasmacytoma (SP) is characterised by biopsy-proven solitary lesions of bone or soft tissue with clonal plasma cells. Based on the presence or absence of the clonal plasma cells in bone marrow, SP can be subtyped into solitary plasmacytoma without bone marrow plasma cells and solitary plasmacytoma with low marrow involvement (Rajkumar et al. 2014).

Plasma cell leukaemia (PCL) is a rare and aggressive form of plasma malignancy characterised by circulating neoplastic plasma cells. PCL may present *de novo*

(primary PCL) or occurs in patients with relapsed/refractory multiple myeloma (secondary PCL). The diagnosis criteria of PLC is over 20% and 2×10^9/L of plasma cells in the peripheral blood (Fernández de Larrea et al. 2013). Both forms of PCL are severe and life-threatening diseases.

The tumorigenesis of plasma cells happens in the germinal centre and often during the mutation-prone events of immunoglobulin class switching and somatic hypermutations (Seifert, Scholtysik, and Kuppers 2013). Serial transplantation models and clonogenic in-vitro assays indicate that a putative multiple myeloma stem cell is part of the subset of $CD38^-CD19^+CD27^+$ B cell precursors, which do not express the classic multiple myeloma markers CD38 or CD138 (Matsui et al. 2008). The initial mutations may serve as a starting point for further myeloma oncogenesis. After that, the original clone develops into a malignant plasma cell, which happens in bone marrow (Morgan, Walker, and Davies 2012). The malignant progressions of plasma cells include activation of MYC, FGFR3, KRAS and NRAS, and NF-κB pathways (Keats et al. 2007, Bergsagel and Kuehl 2005, Annunziata et al. 2007).

MM is a heterogeneous disease, with its wide ranges of aggressive progressions and inevitable therapeutic resistance, both caused by different genetic mutations and individually evolving clones due to various malignant cellular malfunctions (Kuehl and Bergsagel 2012). Some myeloma patients may live a decade or more after the initial diagnosis while others suffer from rapid and aggressive relapse of the disease and die within 24 months. In spite of the recent advances in the development of more effective therapeutic strategies and improvements in supportive care, MM still is an incurable disease, which is characterised by rapid recurrence and broad treatment refractoriness in its late stages (Mateos et al. 2013, Smith and Yong 2013).

1.1.2 Local bone marrow microenvironment supports myeloma maintenance and progression

The generation and development of B cells occurs in both the bone marrow and the peripheral lymphoid tissue, such as the spleen, through several stages and checkpoints. In the bone marrow, B-cell generation occurs via pro-B cell, pre-B-cell and immature-B-cell stages. The first key checkpoint in the process of B-cell generation is the expression of a functional B-cell receptor (BCR) by immature B cells. Cells which successfully pass this checkpoint will exit the bone marrow and differentiate into naïve and then follicular and marginal-zone B cells in the spleen (Cambier et al. 2007).

As shown in **Figure 1.1**, the plasma cells can be generated from follicular B cells, marginal zone B cells, activated germinal-centre B cells or memory B cells. Marginal-zone B cells can recognise T-cell-independent type 2 (TI-2) antigens, and the immunisation with TI-2 antigen allows marginal-zone B cells to move out of the marginal zone and differentiate into plasma cells (Lopes-Carvalho and Kearney 2004). When follicular B cells encounter T-cell-dependent antigens, they can either undergo plasmacytic differentiation or establish a germinal centre (McHeyzer-Williams, Driver, and McHeyzer-Williams 2001). In the germinal centres, antigen-induced T cell-dependent B cell activation occurs, which then results in the development of either memory B cells or plasma cells (Liu and Arpin 1997).

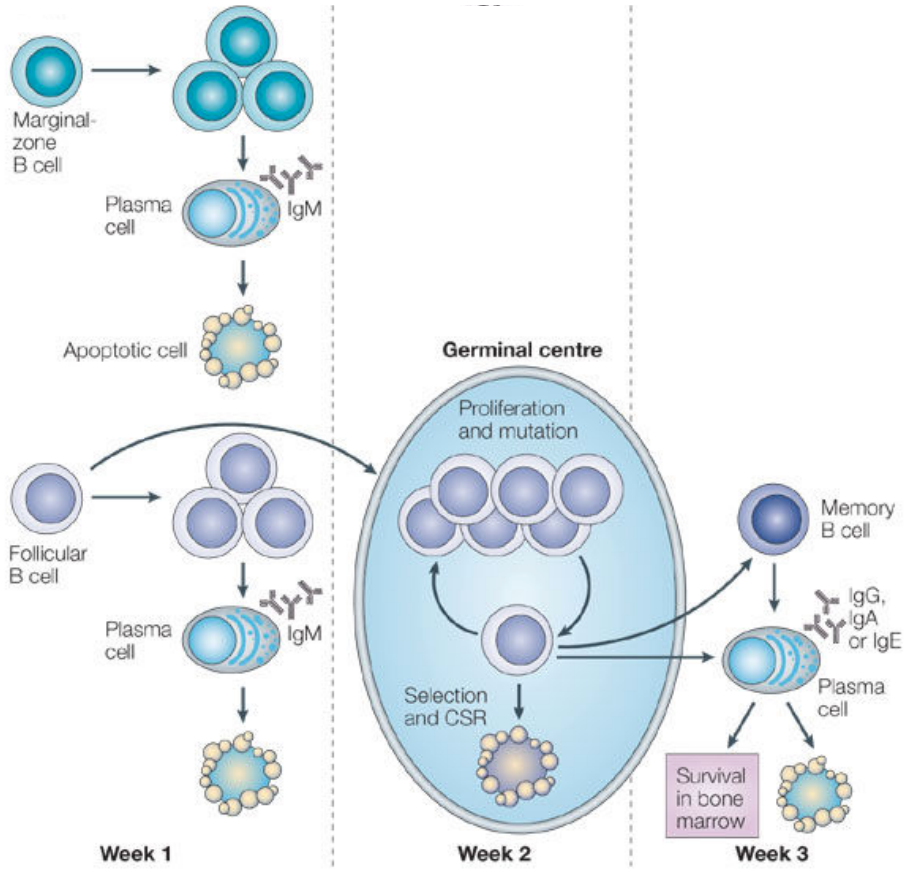

Figure 1.1 Development of plasma cells

The plasma cells can be generated from follicular B cells, marginal zone B cells, activated germinal-centre B cells or memory B cells. This figure is from the original artwork from (Shapiro-Shelef and Calame 2005), reprinted with permission.

Most of the extrafollicular plasma cells are short-lived. However, the post-germinal-centre plasma cells will exit from the germinal centre and home to the bone marrow niches and become long-lived (Warde 2010, Rizzi et al. 2010). In the premalignant or early stage of MM, myeloma/plasma cells live in specialised niches of the bone marrow (BM) (Radbruch et al. 2006, Manz et al. 1998). Analyses of serum immunoglobulin titers against viral antigens or vaccines in rituximab-treated patients, whose B cells were eliminated, indicated that $CD20^-$ long-lived plasma cells could

persist for years and some of the long-lived plasma cells in the BM are replaced by newly generated plasma cells during acute immune responses (Hoyer et al. 2004). When MM progresses, and cells accumulate more mutations, malignant plasma cells can also survive outside the supporting niche of the BM (Varettoni et al. 2010).

The local bone marrow microenvironment plays a supportive role in the development and maintenance of multiple myeloma (Kawano et al. 2017). The BM microenvironment is a cellular compartment, including hematopoietic cells, bone marrow stromal cells, immune cells, adipocytes, osteoblasts and osteoclasts. In local BM microenvironment, the myeloma cells are involved in the cytokine-mediated cross talk which includes a variety of cells and characterises the BM microenvironment (Kumar et al. 2017). The continuous and complex interactions between these cells lead to the conditions that favour myeloma survival and progression(Nair et al. 2011, Kawano et al. 2017). The cytokines and soluble factors generated by the resident cells in this BM microenvironment also stimulate tumour proliferation and downregulate apoptotic pathways. These cytokines and soluble factors include insulin growth factor 1 (IGF-1), interleukin 6 (IL-6), interleukin 12 (IL-12), Interleukin 15 (IL-15), Wnt3A, platelet-derived growth factor receptor (PDGFR), vascular endothelial growth factor (VEGF), tumour necrosis factor-α (TNF-α), and numerous others (Lawasut et al. 2013, Bianchi and Munshi 2015, Bergsagel and Kuehl 2005). For example, IL-6, which is mainly produced by BM stromal cells and macrophages, is essential for the survival and propagation of both normal and malignant plasma cells and induces the production of the survival signals for myeloma to ensure their proliferation and increase their drug resistance (Xu et al. 1998, Chauhan et al. 1995). Myeloma cell lines have been found to have increased expression of the IL-6 receptor, and inhibition of IL-6 slows down myeloma cell

proliferation (Nilsson, Jernberg, and Pettersson 1990). Plasma cell adhesion to bone marrow stroma promotes stromal IL-6 secretion, resulting in a self-augmenting feedback loop and tumour growth (Uchiyama et al. 1993). IL-6 has also been reported to be a promoter of plasma cell survival and inhibitor of plasma cell apoptosis through various pathways such as upregulation of Bcl-xL and Mcl-1 (Puthier et al. 1999).

Moreover, the guidance of plasma cells to their residential niches is a result of changing the responsiveness to tissue-specific chemokines. For example, downregulation of germinal centre-related chemokine receptors, such as CXCR5, as well as upregulation of CXCR4, causes plasma cell homing to their niches with high expression of the CXCR4 ligand CXCL12, which is produced by the resident cells in the BM microenvironment, for instance, stromal cells (Wehrli et al. 2001, Tokoyoda et al. 2004).

CD28 is usually expressed on T cells, providing costimulatory signals essential for T cell survival and activation. Studies showed that plasma cells also express CD28, and that CD28 signalling supports myeloma cell survival thus helping them to escape from apoptosis (Nair et al. 2011). Mice deficient for CD28 have been used to investigate the function of CD28 in plasma cells (Good-Jacobson et al. 2012), and the interactions between CD28 and its ligands (B7.1, and B7.2) negatively regulate the antibody secretion of plasma cells (Njau et al. 2012).

Taken together, the BM microenvironment cannot be neglected in the study of multiple myeloma progression and suppression. The bone marrow microenvironment with the continuous interactions of these cytokines and soluble factors affects the balance of pro-apoptotic and anti-apoptotic mechanisms within the malignant plasma

cells and promotes tumour growth. At the same time, these cytokines and soluble factors and its receptor systems and signalling pathways are potential therapeutic targets for myeloma treatment.

1.2 Osteoclasts and myeloma induced bone disease

1.2.1 Bone remodelling

Bone provides a highly vascular environment rich in nutrients, growth factors, and cellular niches that both attract, maintain and promote the survival and growth of tumours, such as multiple myeloma. Bone remodelling is a dynamic and continuous process which involves the resorption of bone by osteoclasts and the synthesis of new bone by osteoblasts (**Figure 1.2**). The bone remodelling cycle lasts about 200 days in normal bone and takes place on the surface of trabeculae (Eriksen 1986). Osteoclasts (OCs) are large multinucleated cells which are derived from monocyte/macrophage precursors. The key cytokines involved in survival, activation and differentiation of osteoclasts are macrophage colony-stimulating factor (M-CSF) and receptor activator of nuclear factor kappa B (NF-kB) ligand (RANKL)(Zhao et al. 2007). Osteoblasts (OBs) are the bone forming cells which are differentiated from mesenchymal stem cells (MSCs). In general, OBs produce collagen and mineralise the collagen matrix to form the rigid structure of bone. When osteoblasts are incorporated into the bone matrix, they become osteocytes. Osteoblast differentiation is regulated among others by Vitamin D3, TGF-β, bone morphogenetic protein (BMP) and Wnt/β-Catenin signalling pathways (Crockett et al. 2011).

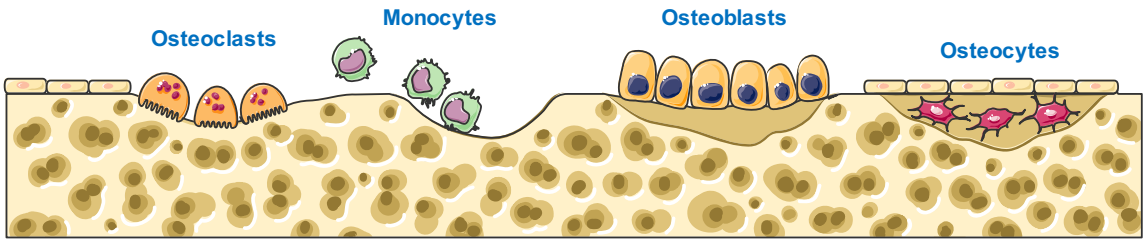

Figure 1.2 Bone remodelling cycle

The bone remodelling cycle involves the resorption of bone by osteoclasts and the synthesis of new bone by osteoblasts. Monocytes are precursors for osteoclasts. Osteocytes can generate signals that control the bone remodelling procedure.

Osteoclastic resorption initiates the bone remodelling process by the formation of a resorption lacuna, the depth of which varies from 60μm in young individuals to 40μm in older individuals. The median duration of the resorption process is 30-40 days and the process of bone formation, which follows the resorption, is over 150 days (Eriksen, Melsen, and Mosekilde 1984, Eriksen et al. 1984). The result of the remodelling process in normal bone is complete refilling of the resorption lacuna with new bone, which is secured by the tight coupling of bone resorption and bone formation. However, in disease states like MBD and osteoporosis, the main problem is that the excessive number of osteoclasts and reduced activity of osteoblasts lead to insufficient refilling of the resorption lacuna, which results in a net loss of bone (Eriksen et al. 1990).

1.2.2 Osteoclast differentiation process

Osteoclasts are formed by the fusion of mononuclear osteoclast precursors which are differentiated from hematopoietic cells in the BM. As mentioned above, the main function of osteoclasts is to resorb bone, which starts from attached to the bone surface and forming a sealing zone with the ruffled border membrane on it. The ruffled border membrane of osteoclasts is similar to endosomal/lysosomal membrane (Stenbeck 2002). After that, osteoclasts secrete proteolytic enzymes to degrade the bone matrix. The degraded bone material is then removed and released to the extracellular environment by transcytosis (Salo et al. 1997). The enzymes involved in this process include cathepsin K, and matrix metalloproteases (MMP) and TRAP (Väänänen et al. 2000, Hayman 2008). It was found previously that the activation of osteoclastogenesis requires M-CSF, Vitamin D3 and bone derived stromal cells (Fujikawa et al. 1996, Yasuda et al. 1998), but does not require the involvement of bone (Fuller et al. 2010).

The first group of genes involved in the osteoclast precursor cell generation and osteoclast differentiation includes M-CSF (Lagasse and Weissman 1997), Csf1r/c-Fms (encoding M-CSF receptor) (Dai et al. 2002) and the transcription factor PU.1 (McKercher et al. 1996). A deficiency of these genes results in the lack of both osteoclasts and macrophages. M-CSF supports the survival and activates the proliferation of osteoclast precursor cells asbesides upregulating RANK expression (Arai and Yamamura 1990, Ross and Teitelbaum 2005). The myeloid lineage master transcription factor PU.1 binds to the promoter region of Csf1r and upregulates transcription (Zhang et al. 1994). The importance of this factor in osteoclast biology is evidenced by depletion of PU.1 in mice resulting in an osteopetrotic phenotype

(Tondravi et al. 1997). The transcription factor MITF (microphthalmia-associated transcription factor) is activated by M-CSF signalling (Weilbaecher et al. 2001) and binds to the Bcl-2 promoter in the osteoclast lineage (McGill et al. 2002). Animals, either with a mutation at the MITF locus or deficient in Bcl-2, display an osteopetrotic phenotype (Hodgkinson et al. 1993, McGill et al. 2002).

The second group of genes involved in osteoclastogenesis consists of NF-κB (Franzoso et al. 1997, Iotsova et al. 1997), RANKL (Kong et al. 1999), RANK (Dougall et al. 1999, Li et al. 2000), NFATc1 (Asagiri et al. 2005), c-Fos (Johnson, Spiegelman, and Papaioannou 1992, Wang et al. 1992), TRAF6 (Lomaga et al. 1999, Kobayashi et al. 2003) and Fc receptor common γ subunit (FcRγ)/DNAX-activated protein 12 (DAP12) (Koga et al. 2004, Mócsai et al. 2004), as shown in **Figure 1.3**. The deletion of these genes results in reduced numbers of multinucleated osteoclasts despite a normal or increased number of osteoclast precursors.

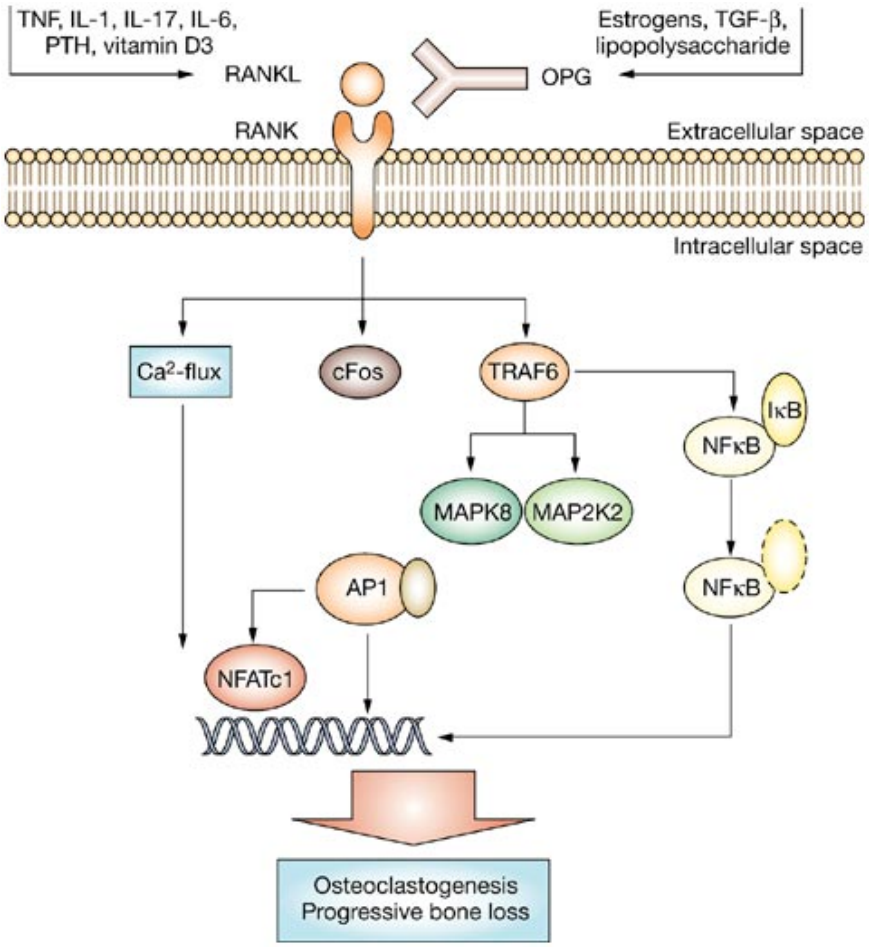

Figure 1.3 RANK-RANKL signalling pathway in osteoclast

When RANKL binds to RANK, RANK can trigger the signalling pathway inside the cell membrane, which leads to osteoclastogenesis and bone resorption. This figure is from the artwork from (Drees et al. 2007), reprinted with permission.

NFκB is a transcription factor which consists of different subunits, such as p50/105, p52/p100, p65/RelA, RelB and c-Rel. It regulates numerous genes which play important roles in many cellular activities including the immune response (Hayden and Ghosh 2004). Osteoclast formation requires the involvement of subunits p50 and p52 (Franzoso et al. 1997, Xing et al. 2002). Moreover, receptor activator of NFκB ligand (RANKL) of the RANKL-RANK pathway was identified as an essential ligand during osteoclastogenesis (Lacey et al. 1998, Yasuda et al. 1998). RANKL,

also known as TNFSF11, is a TNF superfamily cytokine mainly expressed by BMSCs and osteoblasts. The RANK receptor is a member of the TNF receptor superfamily and is expressed in osteoclast progenitors. The binding of RANKL to RANK receptor activates tumour necrosis factor receptor-associated factor 6 (TRAF6), which is a mediator of RANK and binds to three different sites on the RANK receptor (Gohda et al. 2005). Major signalling pathways have been identified downstream of TRAF6, including NFκB, nuclear factor of activated T-cells 1 (NFATc1), c-Jun N-terminal kinase (JNK) (Ikeda et al. 2004), and calcium/calcineurin (Hwang and Putney 2011).

Although initially identified in T cells, NFATc1 is a transcription factor which is induced by NF-κB in osteoclast progenitors (Takayanagi et al. 2002, Ishida et al. 2002). NFATc1 interacts with AP-1 and induces the expression of many genes involved in cell fusion, such as ATP6V0D2 (Kim et al. 2008), dendritic cell-specific transmembrane protein (DC-STAMP) (Yagi et al. 2005) and Gab2 (Wada et al. 2005). However, the deletion of these genes in mice leads to a less severe osteopetrosis phenotype.

The third group of genes, which is involved in the resorptive activities of osteoclasts, includes c-Src (Soriano et al. 1991), LTBP3 (Dabovic et al. 2005), ClC-7 (CLCN7) (Kornak et al. 2001), ATP6V0A3 (known as Atp6i or TCIRG1) (Li et al. 1999) and CTSK (cathepsin K) (Saftig et al. 1998, Li et al. 2006). The depletion of these genes in mice leads to osteoclasts with no or little resorptive function.

1.2.3 MM-induced bone disease

Myeloma bone disease (MBD) is present in 70%-80% of MM patients and can severely affect the quality of life and survival rate of patients (Panaroni, Yee, and Raje 2017). Therefore, it is necessary and beneficial to understand the pathology of bone disease in MM. The underlying cause of MBD is the bone remodelling imbalance which includes an excessive level of activated osteoclasts (OCs) and insufficient osteoblastic activity (Terpos et al. 2014). Without suitable treatment, patients with MBD are expected to experience more than two skeletal-related events per year, which include pathologic fractures, vertebral body compression fractures, hypercalcemia, pain and need for radiation or surgery (Vallet and Raje 2011). Therefore, patients suffering from MBD will probably require either anabolic or (more often) anti-osteoclastic treatment (Vallet and Raje 2011).

The interaction between myeloma cells and bone marrow stromal cells (BMSCs) is through vascular cell adhesion molecule-1 (VCAM-1), which binds to $\alpha 4\beta 1$ integrin on myeloma cells and results in generation and activation of osteoclasts (Hameed et al. 2014). The cytokines, which promote osteoclastogenesis and increase resorptive ability, are produced either by myeloma cells or by BMSCs which are activated by myeloma cells (Papamerkouriou et al. 2015). Over-expression of osteoclastogenesis-related genes provide evidence for the involvement of osteoclasts and MM cells, leading to drug resistance of MM cells (Moreaux et al. 2011). In addition to these factors, myeloma cells also mediate the RANKL-osteoprotegerin (OPG) system which is essential for maintaining balanced bone remodelling (Silbermann and Roodman 2013).

1.2.4 Interactions between tumour cells and osteoclasts

Osteolytic destructions in MM patients are caused by increased osteoclast numbers and activities, which can be mediated by various factors and signalling pathways. These include soluble and membrane-bound proteins (RANKL, M-CSF) as well as other cytokines and chemokines, integrins and matrix proteases. These factors can promote tumour growth through direct action on myeloma cells and by increasing angiogenesis. All of these molecules are either secreted by myeloma cells themselves or induced in the local bone marrow microenvironment by the presence of myeloma cells (Kovacic, Croucher, and McDonald 2014, Silbermann and Roodman 2013)

IL-7 is involved in MBD with increased levels detected in bone marrow plasma cells of myeloma patients (Giuliani, Mangoni, and Rizzoli 2009). The expression of IL-7 by myeloma cells may activate osteoclast differentiation by stimulation of RANKL production by T cells. Receptors for IL-7 are found on bone marrow stromal cells (BMSCs), and coculture of osteoblast precursors with myeloma cells showed less osteoblast formation, while inhibition of IL-7 can improve osteoblast generation as well as the bone formation (Giuliani, Mangoni, and Rizzoli 2009, Giuliani and Rizzoli 2007). Taken together, IL-7 expression by myeloma is related to increased osteoclast differentiation and reduced osteoblastic activity.

IL-8, which is a pro-inflammatory chemokine, induces the expression of RANKL and activates osteoclast differentiation directly by binding to receptor CXCR1 on osteoclast precursors (Aggarwal, Ghobrial, and Roodman 2006). BMSCs from patients with myeloma produce elevated levels of IL-8, which takes part in NF-κB-mediated resistance of myeloma cells to the proteasome inhibitor bortezomib

(Markovina et al. 2010). Therefore, IL-8 production in myeloma favours tumour growth as well as the bone destruction caused by MBD.

Stromal cell-derived factor 1 (SDF-1) is secreted by various cell types in the bone environment, favours homing and migration of myeloma cells. Also, SDF-1 induces osteoclastogenesis through binding to its receptor, CXCR4, which is expressed by human monocytes (Wright et al. 2005). Myeloma cells produce SDF-1, and increased levels of serum SDF-1 leads to osteolytic bone lesions (Zannettino et al. 2005, Aggarwal, Ghobrial, and Roodman 2006, Ooi and Dunstan 2009). Moreover, *in vitro* studies showed that recombinant human SDF-1 promotes the resorptive activity of osteoclasts while inhibition of CXCR4 mitigated the increased resorptive activities induced by myeloma cell conditioned medium and the disruption of the CXCL12/CXCR4 axis reduces osteolysis in a murine model of myeloma-associated bone loss (Zannettino et al. 2005, Diamond et al. 2009).

Macrophage inflammatory protein 1α (MIP-1α), which is a chemokine produced by myeloma cells, promotes osteoclastogenesis via binding to CCR1 and CCR5 receptors on osteoclast precursors (Terpos et al. 2017, Vallet and Anderson 2011). However, the activation of CCR5 by recombinant MIP-1α was not able to activate osteoclastogenesis in RANK-deficient mice, indicating its effect in myeloma needs the presence of RANK signalling (Terpos et al. 2017).

Taken together, a complex network of interactions exists between myeloma cells and cells of the local BM environment. These interactions between myeloma cells and the bone microenvironment provide support and encouragement for myeloma cell proliferation and migration. Most importantly, myeloma cells directly break the balance of bone remodelling which results in the development of osteolytic bone

lesions by direct activation of osteoclastogenesis. These myeloma cell-induced modifications are further enhanced indirectly via bone marrow residing cells. Because of the complex nature of myeloma cells and the interactions with other cells, further study is needed to improve the efficacy of myeloma and MBD treatment.

1.3 Treatment of multiple myeloma

In the past decades, traditional treatments used for multiple myeloma were combinations of alkylating agents and glucocorticoids (Bergsagel et al. 1967). Currently, the treatment strategies for myeloma patients is decided mainly based on the suitability for an Autologous Stem Cell Transplant (ASCT), a treatment which provides an increase in median overall survival by about 12 months (Attal et al. 1996, Mateos et al. 2015, Moreau and Attal 2014). Fitness for ASCT is normally determined by the presence of other medical morbidities and the age of the patient, which means patients over 70 years old are typically not suggested to receive ASCT. Corticosteroids including dexamethasone and prednisolone have been used for many years as a treatment for myeloma as well as other haematological malignancies. Although corticosteroids can induce apoptosis in myeloma cells, they have a number of side-effects including increased risk of infections and osteoporosis (Buchman 2001). The use of lower doses of dexamethasone in combination with lenalidomide provides a higher survival rate than high-dose dexamethasone and lenalidomide (Rajkumar et al. 2010). More myeloma drugs, including immunomodulatory drugs, proteasome inhibitors, monoclonal antibodies, epigenetic inhibitors and CAR T-cell therapies, are now part of the standard therapy or under investigation in clinical trials (Palumbo and Anderson 2011).

1.3.1 Proteasome inhibitors

The proteasome is a multi-subunit enzyme complex which can selectively and efficiently degrade damaged or unneeded protein by proteolysis with the collaboration of ubiquitin. It plays an essential role in the control of many cellular activities including cell-cycle progression and apoptosis and therefore becomes a therapeutic target for myeloma and mantle cell lymphoma (Kubiczkova et al. 2014, Manasanch et al. 2014). Proteasome inhibition encourages the accumulation of misfolded and ubiquitin marked intracellular proteins and reduces the degradation of pro-apoptotic factors (Siegel et al. 2012).

Bortezomib is a potent inhibitor of the 26S proteasome and the forerunner of its drug class. The effectiveness of bortezomib in myeloma cells is not only due to the high efficiency of inducing apoptosis (Lu, Punj, and Chaudhary 2008) but also by sensitising cells to other chemotherapeutic agents (Nikrad et al. 2005). Moreover, bortezomib stabilises IκB, a regulatory subunit of NF-κB and results in reduced expression of anti-apoptotic proteins such as B-cell lymphoma 2 (BCL-2), the proliferative cyclin D and adhesion molecules such as VCAM-1 (Hideshima et al. 2002, Li et al. 2008). Bortezomib also induces the unfolded protein response in MM (Obeng et al. 2006). In 2003, bortezomib was first approved by the Federal Drug Administration (FDA) for multiple myeloma, and since then became a first-line treatment in combination with a range of drugs such as dexamethasone and lenalidomide (Painuly and Kumar 2013). Apart from bortezomib, some next-generation proteasome inhibitors are currently available as well. For example, carfilzomib, which binds to the 20S proteasome, can reduce its chymotrypsin-like activity and increase the accumulation of pro-apoptotic polyubiquitinated proteins.

These functions of carfilzomib lead to inhibition of tumorigenesis, cell cycle arrest and programmed cell death (Stewart et al. 2015, Hideshima et al. 2002).

1.3.2 Immunomodulatory drugs

There are a number of immunomodulatory drugs, such as thalidomide, lenalidomide and pomalidomide, currently available for multiple myeloma treatment. The initial clinical trials about thalidomide showed that the known anti-angiogenic action of this compound has anti-tumour activity in refractory myeloma (Singhal et al. 1999). Lenalidomide is a more potent molecular analogue of thalidomide and inhibits myeloma cell angiogenesis and induces myeloma cell apoptosis (Syed 2017). Besides, recent study suggests that lenalidomide also enhances immune checkpoint blockade-induced immune response (Görgün et al. 2015). Pomalidomide has effects on myeloma cells as well as their local bone marrow microenvironment and inhibits both intracellular and extracellular myeloma growth promoters (Subramaniam et al. 2014). Moreover, pomalidomide downregulates proinflammatory cytokines, enhances the cytotoxicity of natural killer cells and constraining regulatory T cells, therefore weakening immune tolerance of myeloma cells. Also, by downregulating of the transcription factor PU.1, pomalidomide reduces bone resorption in myeloma patients (Touzeau and Moreau 2016). In 2013, FDA approved the use of pamalidomide as a single drug or in combination with dexamethasone in relapsed/refractory MM patients (Naymagon and Abdul-Hay 2016).

1.3.3 Monoclonal antibodies

Monoclonal antibodies, including elotuzumab, daratumumab and several others, constitutes a novel drug class for multiple myeloma. Elotuzumab is an immunostimulatory monoclonal antibody targeting signalling lymphocyte activation molecule F7 (SLAMF7, also known as CS1), which is found consistently expressed in myeloma cells and rarely expressed in other tissues including hematopoietic elements (Liu, Szmania, and van Rhee 2014). Elotuzumab directly increases the cytotoxicity of natural killer cells against myeloma cells via CS1 ligation (Collins, Bakan, et al. 2013). Moreover, the use of elotuzumab in combination with lenalidomide and low-dose dexamethasone shows anti-tumour efficacy in MM patients with relapse or therapy resistance (Mateos et al. 2016).

Daratumumab is a human IgG1k monoclonal antibody against CD38, which is a regulator of cell adhesion and highly expressed on normal and malignant plasma cells. As a regulator of intracellular calcium signalling, CD38 is also associated with the signalling pathways which regulate cell cycle progress and apoptosis of myeloma cells. Moreover, CD38 can interact with several immune cells, including B cells, T cells, and NK cells, and therefore impacts the immune tolerance of malignant plasma cells. Binding of daratumumab to CD38 is thought to mediate phagocytosis of MM cells by macrophages (Overdijk et al. 2015, Khagi and Mark 2014). Importantly, daratumumab showed efficacy in patients with relapsed myeloma as single therapeutic agent (Lokhorst et al. 2015). Similarly, isatuximab (also known as SAR650984) is a monoclonal antibody against CD38 and can directly induce apoptosis in myeloma cells (Jiang et al. 2016).

Nowadays, there are more emerging monoclonal antibody based therapies available for multiple myeloma. For example, GSK2857916 is a novel anti–B-cell maturation antigen (BCMA) antibody-drug conjugate. It can induce cell cycle arrest and apoptosis in myeloma cells in the presence of BMSCs. This effect can be further enhanced in combination with lenalidomide (Tai et al. 2014).

1.3.4 Epigenetic inhibitors

Epigenetic inhibitors are a class of novel therapeutic agents for multiple myeloma. The first-generation HDAC inhibitor vorinostat (SAHA) has demonstrated efficacy in combination with lenalidomide and dexamethasone from relapsed/refractory myeloma patients (Siegel et al. 2014). Panobinostat, which targets class I, II and IV of HDACs, has demonstrated effectiveness in clinical trials in myeloma patients who have already been treated with a proteasome inhibitor (Ibragimova et al. 2013). FDA approved the use of panobinostat in the treatment for myeloma patients in 2015. Rocilinostat (also known as ACY-1215) is a novel HDAC6-specific inhibitor. Rocilinostat in combination with carfilzomib showed synergistic toxicity to bortezomib-resistant myeloma cells. Moreover, inhibition of HDAC6 by rocilinostat disrupts the formation and function of the aggresome where misfolded and ubiquitinated proteins are accumulated (Mishima et al. 2015). The combination of rocilinostat and bortezomib reduces myeloma cell growth in a murine model of myeloma (Santo et al. 2012).

1.3.5 CAR T-cell therapies

The chimeric antigen receptor (CAR) T-cell therapies have brought the drug development for hematologic malignancies into a new era. CAR T-cell therapy is a customised treatment consisting of the collection of a patient's own T cells and transferring genetically reprogrammed T cells back to the patient. The genetic modifications of T cells will guide the T cells to the specific targets (tumour cells) and destroy them. This novel therapeutic strategy has demonstrated dramatic effectiveness in B cell acute lymphoblastic leukaemia (Davila et al. 2014, Lee et al. 2015). BCMA targeted CAR T-cell therapy is currently undergoing phase I clinical trial in patients with relapsed/refractory myeloma. The initial results show that 80% of patients reach the criteria of a complete response (CR) or very good partial remission (VGPR) (Fan et al. 2017). There are several other CAR T-cell therapies under investigation as well, such as CD138 targeted CAR T-cell therapy, or kappa light chain targeted CAR T-cell therapy (D'Agostino, Boccadoro, and Smith 2017).

1.4 Epigenetics

Although having the same DNA sequence, an individual eukaryotic organism contains many different cell types with distinct transcriptional profiles. Transcriptomic analysis reveals that only a small proportion of the genome is actively transcribed in any period (Djebali et al. 2012). Thus, there is a mechanism tightly controlling the gene expression both in a cell-type specific and a temporal manner.

The field of "epigenetics" comprises the study of heritable phenotypic alterations in gene expression without changes in the underlying DNA sequence. Epigenetics has been widely accepted to play a major role in embryogenesis, cancer development

and other complex processes which are associated with regulating the level of gene expression and controlling the phenotype of the cell (Egger et al. 2004).

Cellular differentiation is an example of epigenetic changes. During human embryogenesis, the undifferentiated totipotent zygote gives rise to distinct cell populations in the blastocyst of the trophoblast, the pluripotent cells of the trophoblast and the inner cell mass(Wu, Yamauchi, and Izpisua Belmonte 2016). As embryogenesis progresses, the cells become highly differentiated and are unable to differentiate into other cell types. Multipotent stem cells, such as the mesenchymal stem cells, can differentiate into a limited number of related cell types whereas terminally differentiated cells, such as plasma cells, have lost the ability to change into other cell types under normal physiological conditions (Wu, Yamauchi, and Izpisua Belmonte 2016). However, in rare cases, cells undergo the process of transdifferentiation, in which cells re-differentiate into other cell types without an intermediate pluripotent state (Kokabu, Lowery, and Jimi 2016). Therefore, to achieve the cellular differentiation from the original zygote to multipotent stem cells or terminally differentiated cells, epigenetic mechanisms define and make a specific and restricted gene-expression programme for each cell type. The genes required for later development in multipotent stem cells are repressed short-timely, while in terminally differentiated cells, the epigenetic silencing is often long-term (Reik 2007).

1.4.1 Molecular mechanism of epigenetic regulations

An epigenetic modification is a stable and heritable change which does not associate with underlying DNA sequence consisting of the four nitrogen-containing bases

(adenine (A), thymine (T), guanine (G) and cytosine (C)) attached to a deoxyribose-phosphate backbone (Kanwal, Gupta, and Gupta 2015). Therefore, most mechanisms of epigenetic modification are relying on the structure of DNA and the composition of chromatin. Double-stranded DNA interacts with proteins within the cell nucleus to form chromatin, which is a more structured and condensed molecule which allows DNA to be packaged into the nucleus of micrometre range. A nucleosome is the smallest unit of chromatin. The nucleosome consists of a histone octamer, containing two copies of each of histone subunits H2A, H2B, H3 and H4, and 146 base pairs of DNA wrapped around the histone octamer(Travers and Muskhelishvili 2015, Waldmann and Schneider 2013).

The results of epigenetic modifications are chromatin remodelling, gene expression changes and cellular phenotype alterations. In general, there are three different types of events that are found to initiate and maintain epigenetic modifications, including DNA methylation, RNA-associated silencing and histone modification (Egger et al. 2004). Covalent modifications of histones and DNA methylation are potential molecular carriers of epigenetic inheritance to facilitate correct storage, organisation and interpretation of genetic information (Bernstein, Meissner, and Lander 2007).

1.4.1.1 Histone modifications

Post-translational modifications (PTMs) of histone proteins is one of the most critical mechanisms of epigenetic regulation (Patel et al. 2012). Common PTMs include acetylation of lysine residues, phosphorylation of serine, threonine and tyrosine

residues, and methylation of lysine and arginine residues. Other less common PTMs include for example sumoylation and ubiquitylation of lysine residues (Khoury, Baliban, and Floudas 2011). The majority of these mechanisms are found in the flexible N- and C-terminal ‘tail’ domains, which protrude from the nucleosome and do not have a defined secondary structure. The functional impacts of PTMs on gene expression and transcription include acting directly on the physical properties of individual nucleosomes and the recruitment of specialised “reader” domains to recognize the specific modifications (Bannister and Kouzarides 2011). Based on these functions, the protein families which mediate epigenetic modifications can be divided into three different categories: “writers”, such as histone methyltransferases (HMTs), histone acetyltransferases (HATs), protein arginine methyltransferases (PRMTs); “erasers”, such as histone deacetylases (HDACs), histone lysine demethylases (KDMs); and “reader” proteins, such as proteins containing bromodomains (BRDs), chromodomains (CRDs) and Tudor domains (Falkenberg and Johnstone 2014).

1.4.1.1.1 Bromodomains

Bromodomains (BRDs) containing proteins are “reader” enzymes which read epigenetic marks by recognising and binding to acetyl-lysine on histones. The BET proteins (bromo- and extra-terminal domain), including BRD2, BRD3 and BRD4, manage the assembly of histone acetylation-dependent chromatin complexes (Gallenkamp et al. 2014). The BRDs usually work with other protein-interaction modules to increase the targeting specificity (Muller, Filippakopoulos, and Knapp 2011). Moreover, the BET proteins also play an important role in cell cycle control

since the overexpression of BRD4 can cause cell cycle arrest in the G1-S phases (Maruyama et al. 2002, Dey et al. 2000) while the genetic knockdown of BRD4 in cultured human cells significantly reduces cell growth (Wu et al. 2006). BRD4 contains two bromodomains and binds extensively to the enhancer and super-enhancer regions of DNA, which causes the upregulation of some oncogenic genes. For example, inhibition of BRD4 from binding to acetylated residues reduced the expression of MYC, which contributes to the genesis of many human cancers (Grayson et al. 2014). Therefore, the inhibition of bromodomain containing proteins provides possibilities in the development of novel drugs for cancers.

1.4.1.1.2 Histone deacetylation

Histone deacetylases (HDACs) are “eraser” enzymes which remove acetyl groups from a ε-N-acetyl lysine on histones and restore the positive charge on the side-chain. There are 18 enzymes identified belonging to this group. Based on sequence homology, these enzymes are subdivided into four major classes including class I (HDAC 1-3 and HDAC 8) and class II (HDAC 4-7 and HDAC 9-10), class III (Sirtuin 1-7) and class IV (HDAC11) (Hull, Montgomery, and Leyva 2016). Studies show that HDAC expression is often aberrantly regulated in a number of malignancies (West and Johnstone 2014). Moreover, HDACs can not only interact with oncogenes, such as BCL6, but also reverse some of the aberrant gene repression profiles, thereby leading to cell growth arrest and apoptosis in malignant cells (Bereshchenko, Gu, and Dalla-Favera 2002, Federico and Bagella 2011).

1.4.1.1.3 Histone methylation

Histone methylation refers to transfer of methyl groups to the ε-amino moiety of the lysine side-chain or to nitrogen atoms on arginine side-chains, found on histone tails. Different from acetylation, methylation does not change the overall charge state of the histone protein. Lysine residues may be mono-, di-, or tri- methylated, while arginine residues may be mono- or di-methylated, and the latter being symmetrically or asymmetrically methylated. Numerous research projects have been conducted to study the functions of lysine methylation of histones, which then reveals that methylation of histone 3 lysine 4 (H3K4, abbreviations in the following are in an according manner), H3K36, H3K79 is often associated with activation of transcription whereas methylation of H3K9, H3K27 is associated with repression of transcription (Barski et al. 2007). Moreover, cytogenetic studies and Next Generation Sequencing (NGS) of various cancer genomes suggest that recurrent translocation and/or coding mutations occur to many histone lysine methyltransferases (KMTs), such as EZH2 and MLL family members (Dawson and Kouzarides 2012).

Both under and over-expression of different histone lysine demethylases (KDMs) are associated with a cancer phenotype (Johansson et al. 2014). Lysine specific demethylase 1A (also known as LSD1, KDM1A) and its paralogue LSD2 belong to a class of demethylases which act via an amine oxidation reaction with flavin adenine dinucleotide (FAD) as a cofactor (Shi et al. 2004, Fang et al. 2010). The second and significantly larger class of lysine demethylases of the Jumonji C (JmjC)-domain-containing family was identified through sequence comparisons and subsequent biochemical studies (Clissold and Ponting 2001, Tsukada et al. 2006). To date, recurrent coding mutations have been found in KDM5A (JARID1A), KDM5C

(JARID1C) and KDM6A (UTX) (van Haaften et al. 2009, Dalgliesh et al. 2010, de Rooij et al. 2013). Inhibitors targeting these two families are at various stages of drug development, and the preclinical data has shown the therapeutic potential of compounds that inhibit LSD1 in acute myeloid leukaemia (Barretina et al. 2012, Schenk et al. 2012).

1.4.1.2 DNA methylation

The addition of a methyl group to the cytosine residues at carbon atom 5 is the dominant form of modification to DNA. DNA methylation is the basis for various epigenetic phenomena, such as imprinting or X chromosome inactivation. The most well-studied DNA methylation event in cancer development is the methylation changes at cytosines in the sequence CpG. The cytosine nucleotide in CpG sites is followed by a guanine nucleotide in the sequence of bases along its 5' → 3' direction (Sharma, Kelly, and Jones 2010). CpG islands are present in about 70% of all mammalian promoters whereas the methylation level of CpG islands tends to be higher during tumourigenesis. Hypermethylation of CpG sites affects the expression of both protein coding genes and some noncoding RNAs, resulting in malignant transformation (Jones 1986). In almost all species where DNA methylation is present, gene body methylation is also present in highly transcribed genes, and it has been suggested that this may inhibit anti-sense transcription or RNA splicing (Aran et al. 2011). The enzymes responsible for transferring the methyl group to DNA are DNA methyltransferases (DNMTs). There are three catalytically active members of the DNMT family: DNMT1, DNMT3A and DNMT3B. The *de novo* DNA methyltransferases, including DNMT3A and DNMT3B, show specificity for both

unmethylated and hemimethylated DNA and act independently of replication. The "maintenance" DNA methyltransferase, DNMT1, shows a preference for hemimethylated DNA and acts during DNA replication (Subramaniam et al. 2014).

1.4.1.3 Non-coding RNAs

A further mechanism of epigenetic regulation is through the expression of non-coding RNAs (ncRNAs), which can be categorised into small (< 200 nucleotides) and large ncRNAs (> 200 nucleotides). Non-coding RNAs are transcribed from the genome and often undergo post-transcriptional processing, including polyadenylation or splicing, but do not lead to a protein product being formed. These ncRNAs are increasingly accepted to be essential for normal development and possibly diseases such as cancer (Dawson and Kouzarides 2012). Long ncRNAs are usually transcribed from gene loci which are overlapping and interspersed among coding genes. Although long ncRNAs were believed to be transcriptional ‘noise’, it has been suggested that many long ncRNAs, which are expressed in tightly regulated temporal and regional patterns, may have important biological functions (Bracken and Helin 2009).

A microRNA (miRNA) is a small ncRNA (19-24 nucleotides) responsible for post-transcriptional gene silencing. The genes regulated by miRNAs are involved in diverse cellular functions including cell growth, haematopoiesis and apoptosis (Rana 2007). The RNA-induced silencing complex (RISC) containing miRNA provides possibilities for gene editing in both biological research and gene therapy development. Apart from miRNA, there are some other types of small ncRNAs,

including small interfering RNAs (siRNA) and Piwi-interacting RNAs (piRNAs). With complementary nucleotide sequences, siRNA can silence the expression of the specific gene by degrading its related mRNA (Agrawal et al. 2003). piRNA is involved in RNA silencing by the interaction with Piwi proteins and formation of a RISC. The Piwi subfamily proteins found in rat, mouse, and zebrafish are Riwi, Miwi (Miwi, Miwi2, Mili), and Ziwi (Ziwi, Zili), respectively (Choudhuri 2010).

1.4.2 Epigenetics in multiple myeloma and MBD

As a result of DNA changes, protein expression and/or function are altered, which contributes to the malignant transformation of cells. The classic cancer hallmarks include self-sufficiency for growth signals, insensitivity to anti-growth signals, evasion of growth suppression, escape from cell death, replicative immortality, sustained angiogenesis and metastasis (Hanahan and Weinberg 2011). Moreover, dysregulated expression or modification of a normal protein without alterations in DNA sequence can underlie the development and maintenance of cancer. Epigenetic changes, such as aberrant DNA and histone methylation, have been found to contribute to the pathogenesis of MM (Sharma et al. 2010, Dimopoulos, Gimsing, and Grønbæk 2013). These mechanisms provide novel approaches for rescuing cells from the malignant state by targeting the underlying epigenetic modifications which are involved in cancer development instead of only depending on traditional cytotoxic chemotherapies (Azad et al. 2013).

1.4.2.1 Cell cycle control in MM - Cyclin/CDK/Rb pathway

The cell cycle is a process in which a cell duplicates its DNA and divides into two daughter cells with equal cellular components. The cell cycle process consists of G1 phase, S phase, G2 phase and M phase. G1 phase is responsible for checking whether the cell should enter S phase to continue cell division or enter G0 phase for arrest/apoptosis. All the chromosomes are duplicated in S phase, and rapid protein synthesis and cell growth occur in G2 to prepare for the following M phase where the chromosome starts to separate. After M phase, the cell undergoes cytokinesis which divides the cell into two daughter cells with same cellular components. For normal cellular growth, it is essential to tightly control the cell cycle, and accordingly disrupting the cell cycle regulation may induce malignant transformation(Williams and Stoeber 2012, Medema and Macůrek 2012). CDK4 and CDK6 (cyclin-dependent kinases 4 and 6) are induced in the G1 phase and form complexes with Cyclin D molecules, which leads to phosphorylation and suppression of the Rb (retinoblastoma) protein. This event will then activate the CDK2/Cycline A/E complex and members of the E2F transcription factor family, causing the cell cycle to progress from G1 to S phase. Cyclin-dependent kinase inhibitors (CKIs) are negative mediators for this process and include members of the INK4 family which inhibit CDK4/6 and members of the Cip/Kip family which controls CDK2 (Deshpande, Sicinski, and Hinds 2005, Chohan et al. 2015).

In myeloma, overexpression of Cyclin D happens in most cases, which contributes to the development of the disease at an early stage (Bergsagel and Kuehl 2003). Moreover, several studies have pointed out the issue of downregulation of CKIs by hypermethylation in promoter regions in MM (Dimopoulos, Gimsing, and Grønbæk

2014, Chim, Kwong, and Liang 2008). Although inactivating mutations or deletions of cyclin-dependent kinase Inhibitor 2A (CDKN2A) are not common in MM, hypermethylation of CDKN2A and cell cycle inhibitor p15 and p16 occurs in about 40% of patient samples with newly diagnosed MM and are associated with the poor prognosis in MM patients (Ng et al. 1997, Mateos et al. 2002, Krämer et al. 2002). However, the reported methylation frequency varies, possibly explained by different methodologies used in the studies (Dimopoulos, Gimsing, and Grønbæk 2014). Similarly, hypermethylation of CDKN2B promoter varies from 10%-80% in the MM patient samples examined (Dimopoulos, Gimsing, and Grønbæk 2014, Wei et al. 2016, Krämer et al. 2002).

1.4.2.2 The WNT/β-Catenin pathway

Wnt signalling is responsible for many cellular functions, including hematopoiesis and tissue homeostasis and the regulation of bone remodelling (Niehrs 2012). The promoters of several tumour suppressor genes have been found hypermethylated in MGUS or MM patients. These genes include SFRP1, SFRP4 and SFRP5, which are inhibitors of the Wnt pathway (Dimopoulos, Gimsing, and Grønbæk 2014). Induction of the Wnt signalling pathway leads to intranuclear accumulation of β-catenin, which then binds to lymphoid enhancer factor 1/T-cell factor (LEF1/TCF) and forms a transcription factor complex. β-catenin/LEF1/ transforming growth factor (TGF) induces the expression of several target genes, which are known to be upregulated in MM, such as STAT3, CCDN1 (coding for cyclin D1) and MYC (Klaus and Birchmeier 2008, Sekiguchi et al. 2014, Szabo et al. 2016).

1.4.2.3 IL-6 and JAK/STAT signalling

Apart from the role in osteoclastogenesis which has been mentioned above, the upregulated secretion of IL-6 by BMSCs followed by activation of the IL-6 receptor and Janus kinase/signal transducer and activator of transcription 3 (JAK/STAT3) pathway, is pivotal for the anti-apoptotic features of myeloma cells (Gadó et al. 2000, Rosean et al. 2014, Noll et al. 2014). The promoter hypermethylation of tumour suppressor genes involved in inhibition of the JAK/STAT pathway, including SOCS1, SOCS3 and SHP1, have variable reported frequencies in MGUS/MM patients (Dimopoulos, Gimsing, and Grønbæk 2014, Galm et al. 2003). Moreover, the upregulation of the miRNA-17-92 cluster that directly targets SOCS1 and SOCS3 is another mechanism of increased JAK/STAT signalling in MM (Pichiorri et al. 2008, Collins, McCoy, et al. 2013).

1.5 AIMS of the thesis

Since epigenetic regulation of gene expression is highly dynamic and reversible, it is becoming increasingly evident that a number of epigenetic proteins are involved in the development of various human diseases, therefore supporting the hypothesis that the modulations of epigenetic signalling can lead to novel therapeutic targets. Based on that, in this thesis, I aim to first identify novel epigenetic inhibitors targeting both MM cell proliferation and OC differentiation. Secondly, I will define an OC RANKL genecard for different stages of OC development and use it to reveal the functions of the compounds in osteoclastogenesis. At last, with the application of

novel techniques, such as NGS and CyTOF (Cytometry by Time of Flight), I will investigate the underlying mechanisms of some compounds in myeloma cells.

Chapter 2 Materials and Methods

2.1 Cell culture for myeloma cell lines

Four human myeloma cells (JIM3, MM1S, KMS11 and U266) were obtained from Professor Gareth Morgan, Institute of Cancer Research, London. Another human myeloma cell line (JJN3) and one mouse myeloma cell line (5TGM1) were obtained from Dr Claire Edwards, NDORMS, University of Oxford.

JJN3 cells were cultured in 50% Dulbecco's Modified Eagle Medium (DMEM) (Sigma) with 50% Iscove's Modified Dulbecco's Medium (IMDM) (Sigma) (supplemented with 10% (v/v) Fetal Calf Serum (FCS) (Invitrogen) and 2mM/L glutamine (Sigma)) at 37°C, 5% CO_2. All other myeloma cell lines, KMS11, MM1S, U266, JIM3 and 5TGM1 were cultured in RPMI (Sigma) (supplemented with 10% (v/v) FCS (Invitrogen) and 2mM/L glutamine (Sigma)) at 37°C, 5% CO_2.

2.2 Mycoplasma test

Mycoplasma test was performed twice a year to ensure that the cell culture was mycoplasma-free. 1ml media from growing cultures was taken and spun down at 280 x g for 5 min to sediment the cells. 500μl supernatant was taken and transferred to a fresh tube and spun down at 14000 rpm, followed by removal of supernatant. 50μl 1xTE buffer (10 mM Tris-HCl, 1 mM disodium EDTA, pH 8.0) was added to the pellet (normally invisible) and the mix was heated to denature DNA at 95°C for 3 min. Afterwards, PCR (40 cycles) was performed using the primers below which have an

annealing temperature of 60°C and extension temperature of 72°C. PCR products were analysed on 1% agarose gel with appropriate negative and positive controls. A band visualized at about 450bp indicates the presence of mycoplasma infection. The infected cells were discarded immediately.

Forward primer: 5'GTGGGGAGCAAAYAGGATTAGA3' (Y means an equal mix of C and T)

Reverse primer: 5'GGCATGATGATTTGACGTCRT3'

2.3 Cell viability assay in Myeloma cells

JJN3 cells were cultured in 50% DMEM with 50% IMDM (supplemented with 10% (v/v) FCS and 2mM glutamine) and all other myeloma cells were cultured in RPMI (supplemented with 10% (v/v) FCS and 2mM glutamine) at 37°C, 5% CO_2. The cells were treated with compounds and incubated for 72 hours or 7 days. The viability of the cells was measured using PrestoBlue® Assay (Thermo Fisher Scientific) according to the manufacturer's instructions. Plates were read on a FLUOstar Optima (BMG Labtech) and values were normalized to vehicle control.

2.4 RNA extraction

0.5 to 1 million cells were harvested in 350μl Trizol (Thermo Fisher Scientific) and mixed with an equal volume of 100% ethanol. Total RNA was extracted with Direct-zol™ RNA MiniPrep Kit (Zymo Research). RNA was eluted with 30μl nuclease-free water and stored at -80°C until needed.

2.5 cDNA synthesis

RNA samples were quantified using a Nanodrop 1000 spectrophotometer (Thermo Scientific) according to the manufacturer's instructions. The purity of RNA was assessed by measurement of the absorbance ratio at 260:280nm and 260:230nm. A ratio above 1.8 was considered acceptable. 1-2μg of RNA was converted to cDNA by using High Capacity cDNA Reverse Transcription Kits (Applied Biosystems) according to the manufacturer's instructions. The final product was stored at -20°C until needed.

2.6 Quantitative PCR

Real time PCR reaction was performed on the ViiA 7 RTPCR cycler (Thermo Fisher Scientific) using Fast SYBR Green Master Mix (Applied Biosystems), 200nM of primers and 20ng of cDNA in a final volume of 10μl. Differences in expression were calculated using the relative quantification method ($\Delta\Delta C_T$). The programme is described in the tables below.

Table 2.1 Programme of quantitative PCR

	Hold Stage	PCR Stage		Melt Curve Stage		
		Cycles: 40		Continuous		
	Step 1	Step 1	Step 2	Step 1	Step 2	Step 3 (Dissociation)
Temp	95°C	95°C	60°C	95°C	60°C	95°C
Time	20s	1s	20s	15s	1m	15s

2.7 Osteoclast differentiation assay

2.7.1 Assay optimisation

To study osteoclast formation, monocytes were isolated from blood donations of healthy individuals obtained from the National Health Service (NHS). Briefly, peripheral blood mononuclear cells (PBMCs) were separated by centrifugation on a gradient of Ficoll (Histopaque, Sigma). Then three different monocyte isolation methods were compared in their ability to support osteoclast formation: isolation based on magnetic separation with CD14+ beads (CD14 Isolation Kit by Miltenyi Biotec) (Helfrich and Ralston 2012), gradient separation with Percoll (Martinez 2012) and adhesion of monocytes from PBMC fraction (Knowles and Athanasou 2009). After isolation, monocytes were resuspended in αMEM (Sigma) (supplemented with 10% (v/v) FCS (Invitrogen), 2mM glutamine (Sigma) and 100U/ml Penicillin/Streptomycin (Thermo Fisher Scientific)) and plated at a density of 7.8 $x10^4$, 1.6 $x10^5$ and 2.3 $x10^5$ cells per cm^2 in 96 well-plates. Cells were then treated with Macrophage Colony-Stimulating Factor (M-CSF) (25ng/ml, Peprotech).

2.7.2 Osteoclast differentiation

On day 2 of the culture, cells appeared as macrophages. At this point, various inhibitor compounds were added. 6 hours after start of compound treatment, Receptor Activator of Nuclear Factor Kappa-B Ligand (RANKL) (50ng/ml, Peprotech) was added to initialise osteoclast differentiation. After 5-7 days, cells appeared as macrophages and cells then started to enlarge and fuse into multinuclear cells. On day 21, multinuclear cells were obtained representing osteoclasts.

2.7.3 Fixation and Tartrate-Resistant Acid Phosphatase (TRAP) staining

From Day 14 to Day 21, osteoclast formation was examined by light microscopy (Zeiss AxioObserver); by phase contrast or bright field. On Day 21, cells were fixed with 4% paraformaldehyde and stained with 0.6g/L fast violent B (Sigma) and 0.3g/L Napthol AS-Bi phosphate (Sigma) dissolved in sodium acetate buffer (pH 5.0) containing 0.1mM sodium tartrate. The stained cells were examined by light microscopy (Nikon Eclipse TE300). Multinuclear cells, which contain more than 2 nuclei, and larger than 50 μm in diameter, were counted in TRAP staining as osteoclasts.

2.7.4 Bone resorption assay

Dentine slices (OsteoSite Dentine Discs, Immunodiagnostic systems Ltd, Boldon, UK), which were about 5mm in diameter and 0.3 mm in thickness, were plated in the bottom of the wells before plating monocytes. The monocytes were cultured as described in **Section 2.7.2**. On day 21, dentine slices were retrieved and cleaned. The dentine slices were then scanned by confocal microscopy (Zeiss LSM710) with the help of Dr Clarence Yapp in our research group.

2.8 Next generation sequencing (NGS)

Total RNA, extracted by Direct-zol™ RNA MiniPrep Kit (Zymo Research), was used to perform mRNA isolation, fragmentation and priming. RNA was quantified using a Nanodrop 1000 spectrophotometer, and RNA quality assessed using a Tape Station (Agilent) giving a RIN number (where an index >9 indicates high quality RNA). Poly-adenylated RNA was enriched from the extracted total RNA using the NEBNext

Poly(A) mRNA magnetic isolation module (New England Biolabs) according to manufacturer's instruction. The Poly-A selected RNA was used to prepare the library for sequencing using NEBNext Ultra Directional RNA Library Prep Kit for Illumina (New England Biolabs). The pooled library was quantified by both TapeStation (Agilent) and Kapa Library Quantification Kit (Kapa) according to the manufacturer's instructions. The library was diluted to 4nM and mixed with an equal volume of 0.2M NaOH. After 5 min incubation at room temperature, the same volume of 200mM Tris-HCl (PH=8) was added to the library. Finally, the library was diluted by HT1 (Illumina) to 1.8pM and loaded onto the Nextseq 500 sequencing platform (Illumina). 75bp paired-end reads or 42 bp single reads were obtained.

Data were processed by Dr Reshma Nibhani in the research group. Sequence reads were aligned using Hisat2 to a human reference genome (Hg38). FeatureCounts program was then applied to counts mapped reads for genomic feature (coding exon). Differential expression analysis of count data (quantification and statistical inference of systematic changes between conditions) was performed with DESeq2 (false discovery rate(FDR) = 0.01 was used for the analysis). After that, differentially expressed genes were extracted based on the threshold of p value = 0.05 and $\log_2$ fold change = 1.5. The pathway analysis was performed by using Metacore or Reactome database.

2.9 Cell cycle analysis by flow cytometry

MM1S cells were plated at 200,000/well in 6-well plates. After incubation for 4 hours, cells were treated with compounds or DMSO as solvent vehicle. After 7 days of culture, the samples were fixed by cold 70% ethanol overnight and then

resuspended in PBS containing 0.1% Nonidet P40 (SIGMA), 0.1% sodium citrate (SIGMA), 25μg/ml propidium iodide (PI) (Abcam) and 12.5μg/ml RNase (Thermofisher Scientific) for 30 minutes. The samples were analysed by LSRFortessa flow cytometer (BD Biosciences). Data was analysed through Cytobank by gating on the intensity of PI.

2.10 Apoptosis analysis by flow cytometry

MM1S cells were plated at 200,000/well in a 6-well plate. After incubation for 4 hours, cells were treated with compounds or DMSO as solvent vehicle. After 7 days of culture, the samples were stained by Annexin V Apoptosis Detection Kit APC (Abcam). Then samples were analysed by LSRFortessa flow cytometer (BD Biosciences). Apoptosis was assessed by detecting phosphatidylserine by FITC-conjugated Annexin V. Data was analysed through Cytobank by gating on the intensity of Annexin V and PI.

2.11 Myeloma patient sample preparation

Myeloma patient bone marrow samples were obtained through the Oxford Biobank from Dr Karthik Ramasamy, Churchill Hospital (Oxford, UK) (Ethics code: 09/H0606/5+5). Bone marrow samples were mixed with an equal volume of PBS, layered on 15ml of HISTOPAQUE(Sigma) and spun down with 500g for 20 min without brake. Afterwards, the middle layer of the mononuclear cells was aspirated and washed with PBS (Sigma) twice. Cells were counted and resuspended in storage buffer which contained 90% (v/v) FCS and 10% (v/v) DMSO. Cells were split into aliquots of 10-20 million cells each in cryovials and were stored at -80°C.

The patient sample information is listed in Appendices Table 4.

2.12 Mass cytometry (CyTOF)

2.12.1 Sample preparation

Cells were cultured in Bone Marrow Max medium (Sigma) in Nunc™ Non-treated Flasks (Thermo Fisher Scientific), which prevents cell adhesion, at a cell density of 1 million cells per ml at 37°C, 5% CO_2. To determine live cells after culturing for 48 hours, cells were stained with intercalator-103Rh (1:1000) at room temperature for 20 min (MaxPar).

2.12.2 Surface marker staining

After a wash step with Staining Buffer (MaxPar), cells were resuspended in 50μl Cell Buffer (MaxPar) with 5ul TruStain FcX (Biolegend) and incubated at room temperature for 10 min. After blocking, 50μl antibody mix was added and incubated for 30 min at 4°C.

2.12.3 Intracellular marker staining

After incubation, cells were washed twice with staining buffer (MaxPar) and fixed by adding 1ml of 1X Fix I Buffer (MaxPar) and incubated at room temperature for 15 min. Then cells were washed by Perm Buffer (MaxPar) and resuspended in 50μl Perm Buffer. 50μl antibody mix was added to cell suspension and incubated for 30 min at 4degree C. After incubation, cells were washed twice with staining buffer and stained with intercalator-Ir (1:1000) (MaxPar) for overnight at 4°C.

2.12.4 CyTOF sample preparation

Cells were washed by staining buffer (MaxPar) twice and water (MaxPar) twice. Then cells were analysed using the CyTOF Helios platform (Fluidigm). CyTOF data was analysed in CytoBank using spanning-tree progression analysis of density-normalized events (SPADE analysis) and viSNE analysis to identify populations in multidimensional flow cytometry data files.

Detailed antibody list is shown in Appendices Table 3.

2.13 Determination of inhibitor EC_{50}

Cells were plated and cultured at the same condition as detailed in the viability assay chapter. Compounds were diluted to 10 concentrations ranging from 50μM to 97nM (1:2 dilution series). The cells were treated with compounds and incubated for 72 hours or 7 days. The viability of the cells was measured using PrestoBlue® Assay (Thermo Fisher Scientific) according to the manufacturer's instructions. Plates were read on a FLUOstar Optima (BMG Labtech) and values were normalized to blank and vehicle control. The viability curve was plotted using GraphPad Prism and was plotted by Log (Concentration) vs viability. EC_{50} values were calculated by fitting the curve to the following equation using Prism: $y = \frac{top-bottom}{1+10^{(logIC50*hill\ slope)}}$.

2.14 Cysteine depletion experiment

JJN3 cells were resuspended in normal DMEM medium or Cysteine/Methionine deficient DMEM medium (Thermo Fisher Scientific) (supplemented with 10% FCS

(Invitrogen) and 2mM glutamine (Sigma)) at a density of 500,000 cells/ml and plated in 24-well plates. Methionine (Sigma), Cysteine (Sigma), N-acetyl-cysteine (Sigma) and Cystine (Sigma) were added to pre-treat the cells for 1 hour. Then DMSO (0.1%) or GSK-J4 (5μM) were added and cells were incubated for 6 hours. Cells were then harvested in 350μl Trizol (Thermo Fisher Scientific).

Chapter 3 Screening of epigenetic compounds

3.1 Introduction

Multiple myeloma (MM) is a malignancy of plasma cells and is the second most common hematologic cancer (Kyle and Rajkumar 2004). Myeloma bone disease, which is caused by the uncoupling of bone resorption from bone production is present in most of MM patients and seriously affects the quality of life and survival rate of MM patients (Rajkumar 2016, Hameed et al. 2014). Excessive numbers and increased resorptive functions of osteoclasts not only lead to severe bone destruction in bone cancer such as multiple myeloma, but also stimulate tumour growth. Based on the interactions between osteoclasts and myeloma or other bone tumour cells, inhibition of osteoclast differentiation and myeloma cell growth at the same time might be beneficial for control of tumour growth and related bone disease.

The epigenetic regulation of DNA-templated processes has been demonstrated to be involved in the genesis of cancer (Dawson and Kouzarides 2012). To identify novel targets that control osteoclast differentiation and myeloma cell proliferation, a focused library consisting of >70 novel epigenetic small molecule inhibitors (**Table 3.1**) was screened in this study. This library was compiled based on literature data and furthermore in collaboration with the Structural Genomics Consortium (SGC). Some of the compounds have proven *in vivo* activities, such as SAHA (Olsen et al. 2007), but many of the compounds have not yet been used in *in vivo* studies.

Table 3.1 Epigenetic compounds used in this study

Class	Target	Compound	Assay Conc.(μM)
Bromodomain	BAZ2A/B	BAZ-ICR	1
Bromodomain	BRD9&7	LP99	10
Bromodomain	BRPF	NI57	1
Bromodomain	BRPF	PFI-4	1
Bromodomain	BRPF	OF-1	0.5
Bromodomain	SMARCA2/4, PB1(5)	PFI-3	1
Bromodomain	BRD4	(+)-JQ1	0.1
Bromodomain	inactive form of JQ1 (+), ctrl cpd	(-)-JQ1	0.1
Bromodomain	BRD4	PFI-1 (BET)	5
Bromodomain	CBP, BRD4	CBP/BRD4 (0383)	5
Bromodomain	SMARCA, PB1	SMARCA	2.5
Bromodomain	BRD4	I-BET	1
Bromodomain	BAZ2B/A	GSK2801	1
Bromodomain	pan-Bromodomain	Bromosporin	1
Bromodomain	CREBBP, EP300	I-CBP112	1
Bromodomain	BET, BD2	RVX-208	5
Bromodomain	CREBBP, EP300	SGC-CBP30	1
HDAC/Bromo	Dual specific inhibitor BET/HDAC	DUAL946	1
HDAC	Class 1,2,3, (8)	CI-994	1
HDAC	Class 1	CXD101	1
HDAC	pan-HDAC	Valproic acid	1000
HDAC	ortho-amino anilides- Class 2	Entinostat (MS-275)	0.1
HDAC	hydroxamic acids-Class 1&2	Trichostatin A	0.1
HDAC	hydroxamic acids-Class 1&2	SAHA	0.5
HDAC	hydroxamic acids-Class 1&2	Belinostat	1
HDAC	SIRT1 activator	SRT1720	1
HDAC	SIRT1	EX 527	1
HDAC	HDAC 3	RGFP 966	1
HDAC	HDAC 6	Tubastatin A HCl	10
HDAC	HDAC 8	PCI-34051	5
HDAC	HDAC 6	Rocilinostat	1
DNMT	DNMT1/3	5-Aza-deoxy-cytidine	5
DNMT	DNMT1/3	5-Azacitidine (AZA)	10
Class	**Target**	**Compound**	**Assay Conc.(μM)**

Halofuginol		MAZ1805	1
Halofuginone		MAZ1392	1
HAT	CBP/ P300	C646	1
Histone demethylase	pan- JmjC	JIB-04	0.05
Histone demethylase	Pan-JmjC	Methylstat	0.5
Histone demethylase	H3K27/H3K4	KDOBA67	10
Histone demethylase	JMJD2E	ML324	5
Histone demethylase	LSD1	Tranylcypromine	20
Histone demethylase	H3K27	GSK-J4	10
Histone demethylase	Inactive form of GSK-J4	GSK-J5	10
Histone demethylase	pan-2-OG	IOX1 (5COOH-8HQ)	40
Histone demethylase	LSD1	GSK-LSD1	5
Histone demethylase	JARID1B	KDOAM-25	25
Histone demethylase	JARID1B	GSK467	25
Prolyl-Hydroxylases	PHD2 (EGLN1)	IOX2	10
Kinase inhibitor	ATP competitive-PIM	K00135	1
Kinase inhibitor	ATP mimetic - Haspin	HASPIN	1
Methyl Lysine Binder	L3MBTL3	UNC1215	5
Methyl Lysine Binder	WRD5	IOCR-9429	1
Protein Arginine Deiminase	PADI4	GSK484	1
PARP	PARP1	Rucaparib	10
PARP	PARP1	Olaparib	1
Histone methyltransferase	DOT1L	SGC0946	7.5
Histone methyltransferase	SETD7	(R)-PFI-2	2
Histone methyltransferase	G9a/GLP	UNC0642	1
Histone methyltransferase	G9a	UNC0638	1
Histone methyltransferase	SUV39H1	Chaetocin	0.01
Histone methyltransferase	G9a/GLP	A-366	2
Histone methyltransferase	EZH2	GSK343	3
Histone methyltransferase	EZH1/2	UNC1999	1
Histone methyltransferase	EZH1/2	CPI.360	0.1
Class	**Target**	**Compound**	**Assay Conc.(μM)**

Histone methyltransferase	EZH1/2	CPI.413	0.1
Histone methyltransferase	SMYD2	LLY507	1
Histone methyltransferase	SUV420H1/H2	A196	25
Histone methyltransferase	SMYD2	BAY598	25
Arginine methyltransferase	PRMT3	SGC707	1
Arginine methyltransferase	PRMT5	J556-42R	10
Arginine methyltransferase	PRMT5	J556-63R	10
Arginine methyltransferase	PRMT5	J556-70P	10
Arginine methyltransferase	PRMT5	J556-143	1

3.2 Epigenetic compound screening in osteoclast differentiation assay

3.2.1 Assay optimization

Initially, three methods for monocyte isolation were tested, including CD14 magnetic bead selection, Percoll gradient and Peripheral blood mononuclear cell (PBMC) adhesion. Cells were cultured in the presence of M-CSF and RANKL for 21 Days for osteoclast differentiation, as described in **Section 2.7**. Based on this comparison of osteoclast formation (**Figure 3.1**), the use of CD14+ magnetic beads selection was identified as the optimal method for osteoclast assay screens. Another parameter tested was cell density, and it emerged that a density window exists for optimal osteoclast formation. The optimal density was 1.6 $x10^5$ to 2.3 $x10^5$ cells per cm^2

(**Figure 3.1**); this is equivalent to plating 5x10^4 to 7.5 x10^4 cells/well in a 96 well plate (this format was used for TRAP staining) and 5x10^5 cells per well in a 24 well plate (used for RNA isolation).

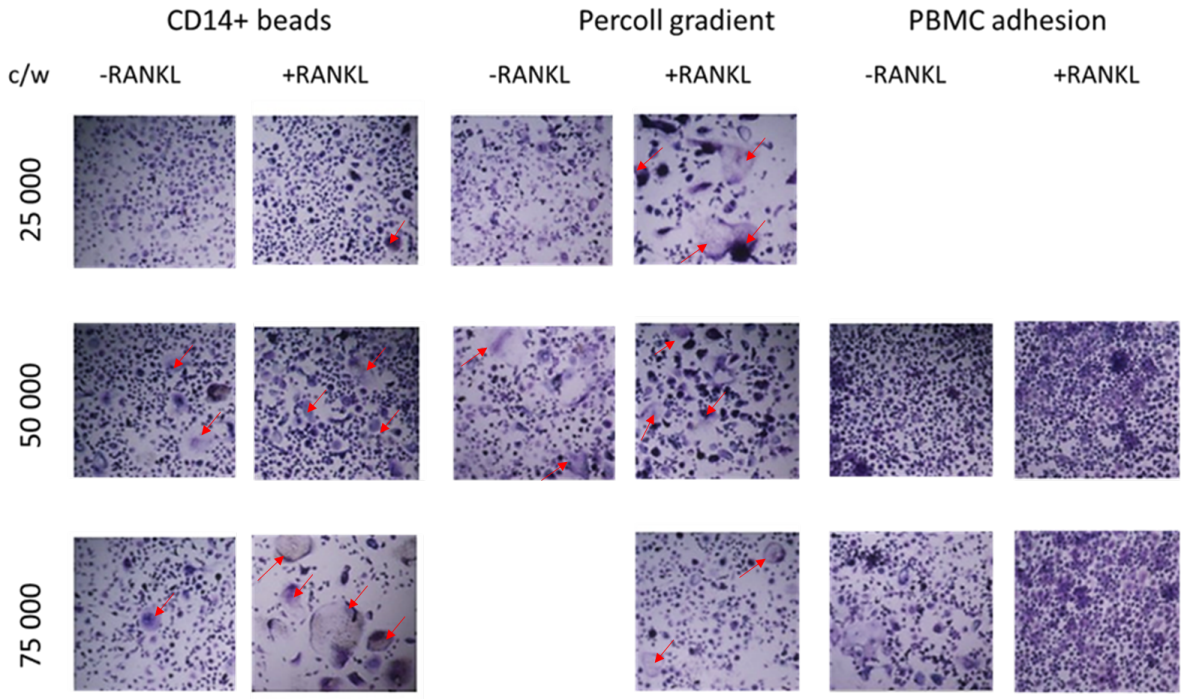

Figure 3.1 Tartrate-resistant acid phosphatase (TRAP) staining results of different PBMCs isolation methods and different cell densities

For both CD14+ beads and Percoll gradient methods, RANKL treated samples of different cell densities generated many osteoclasts. There were still some osteoclasts spontaneously generated in non-RANKL treated samples, however, the difference between positive control and negative control is obvious. In PBMC adhesion methods, there were no osteoclasts generated and there was contamination by lymphocytes. Red arrows refer to osteoclasts and c/w refers to number of cells per well in 96 well plates.

3.2.2 Identification of epigenetic inhibitors of osteoclast differentiation

An experiment was first conducted to adjust the concentration of each compound, since at some of the initial concentrations the compounds were too toxic for the cells, which was determined by significantly reduced osteoclast precursor number observed under bright-field microscopy. Once the appropriate concentration had been determined, experiments to identify epigenetic inhibitors with anti-resorptive activities were undertaken. 65 small molecule inhibitors were tested in an osteoclast differentiation assay and the experiments were successfully repeated up to 9 times using different donors. The number of osteoclasts in different conditions was counted based on the Tartrate-resistant acid phosphatase (TRAP) staining and divided by osteoclast number counted in the positive control sample, which contains only vehicle control DMSO. The results are summarised in **Figure 3.2** below. Several compound-treated conditions showed more than 70% reduction in osteoclast numbers compared to control. Particularly, some compound classes showed a strong inhibitory ability of osteoclast differentiation including bromodomain inhibitors (such as (+)-JQ1, I-BET, PFI-1 and bromosporine), histone deacetylase inhibitors (such as SAHA), or histone demethylase inhibitors (such as GSK-J4).

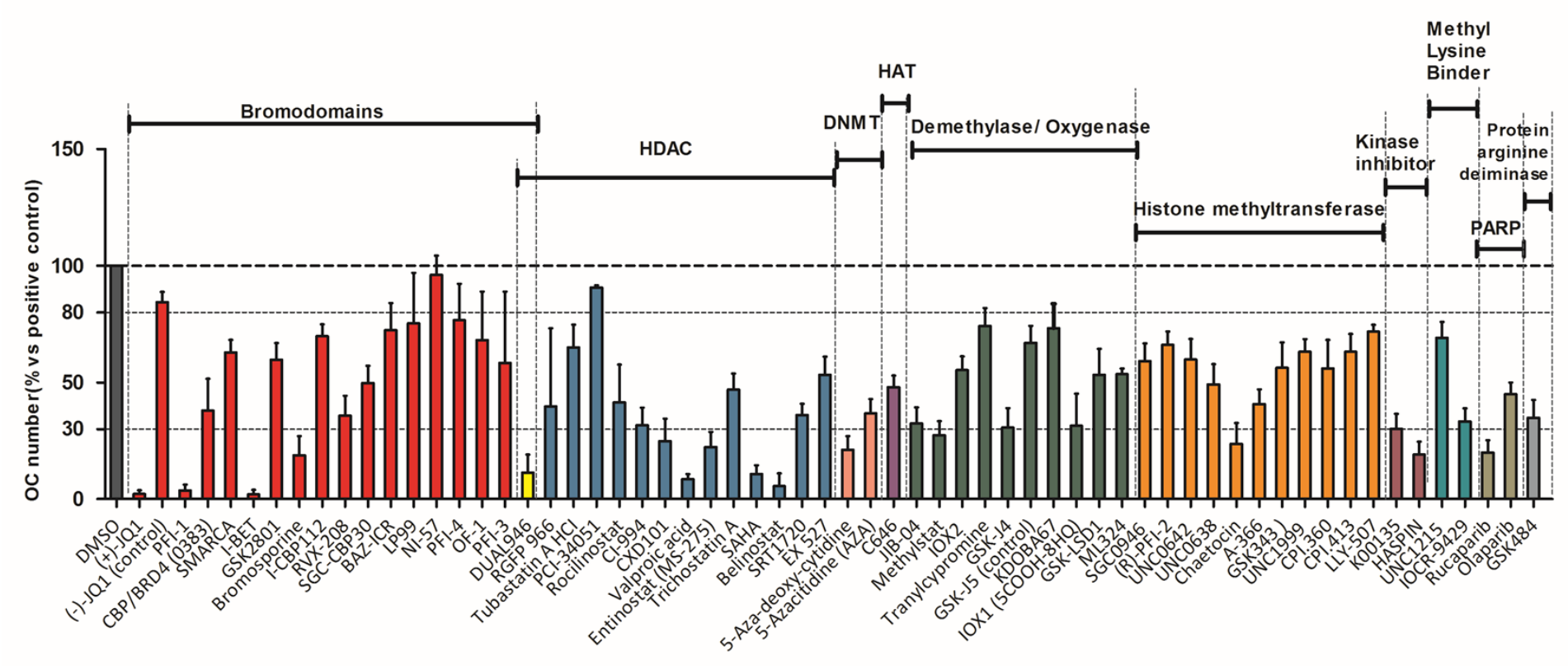

Figure 3.2 Osteoclast numbers in different compound treatment vs positive control

Several inhibitors showed >80% inhibitory ability for osteoclast differentiation, such as (+)-JQ1, PFI-1, I-BET, SAHA. Positive control refers to osteoclast treated with M-CSF, RANKL and 0.1% DMSO. Data plotted represent the mean plus SD of 3 to 9 biological replicates.

3.2.3 Selected inhibitors for osteoclast differentiation

Based on the TRAP staining results of the osteoclast differentiation assay, a dentine resorption assay was conducted for selected compounds to confirm their anti-resorptive abilities. **Figure 3.3** shows the comparison of TRAP staining and dentine resorption results of negative and positive controls. The appearance of multinucleated cells in positive control (M-CSF+RANKL) correlates with the resorption pits on the surface of the dentine slice as determined by the scanning of dentine slices.

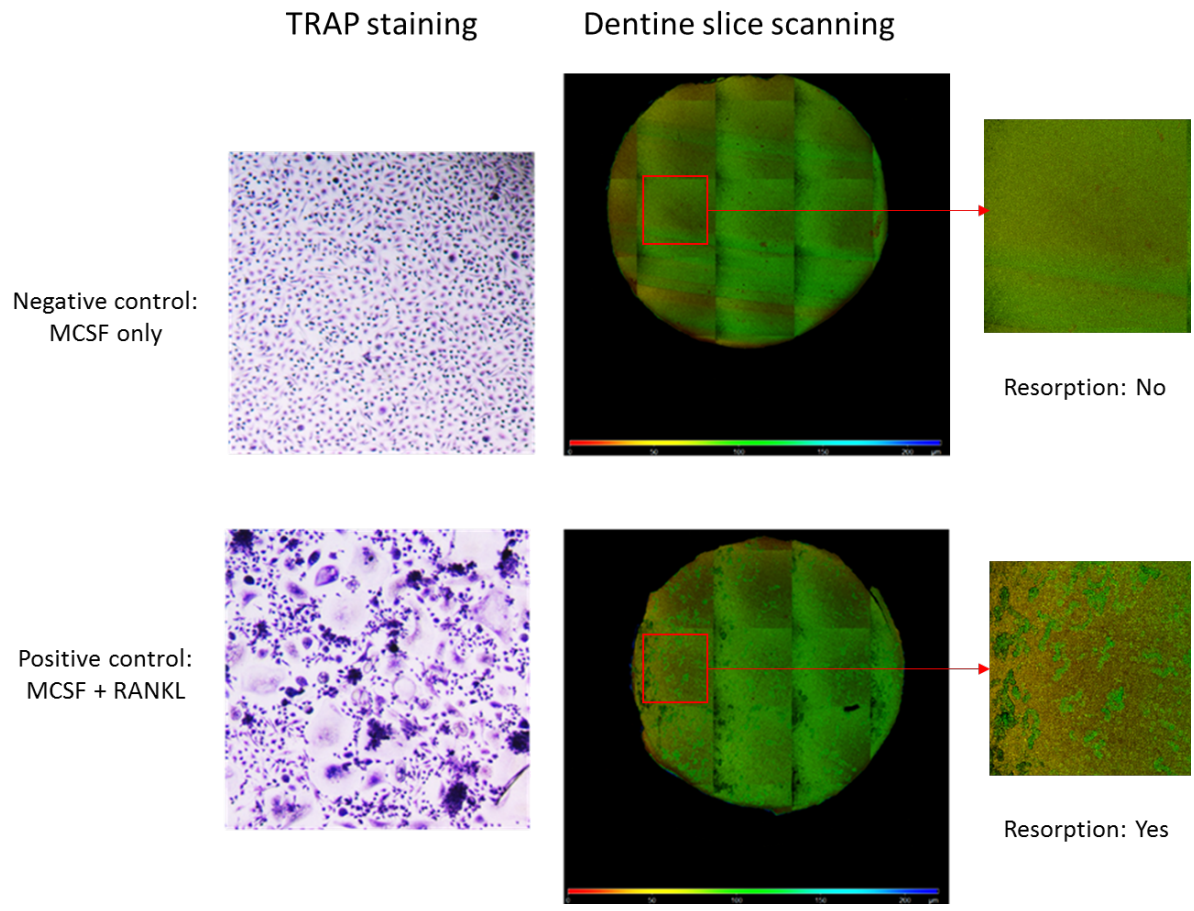

Figure 3.3 Trap staining and dentine resorption results of negative and positive control

Negative control refers to the sample with only M-CSF treatment and have no resorption pits on the dentine slides surface. Positive control refers to the sample with M-CSF and RANKL

treatment and have resorption pits on the dentine slides surface. The methods of TRAP staining and dentine slice scanning were described in ***Section 2.7.***

3.2.3.1 Bromodomain Inhibitors

Figure 3.4 shows the chemical structures for (+)-JQ1, bromosporine, I-BET, PFI-1, which were selected as representatives for BET bromodomain inhibitors. From the TRAP staining results in **Figure 3.5 and 3.6,** it is concluded that (+)-JQ1, I-BET and PFI-1, which are all BET inhibitors, have a strong inhibitory ability of osteoclast generation. In the (+)-JQ1 treated sample, only a few osteoclasts were generated and the cell morphology showed elongated macrophages, suggesting that BET bromodomains are essential for monocyte to osteoclast differentiation. A similar situation was also found in I-BET and PFI-1 treated samples. This indicates that the osteoclast differentiation process has been inhibited by (+)-JQ1, I-BET and PFI-1 at a very early stage. It has been recently reported that (+)-JQ1, as a BET bromodomain inhibitor, can inhibit osteoclast differentiation by interfering with BRD4-dependent RANKL activation of NFATc1 transcription (Lamoureux et al. 2014). As a control for off-target effects, stereoisomers (such as (-)-JQ1, which is an inactive form of (+)-JQ1) were employed whenever possible, resulting in indistinguishable osteoclast numbers compared to control (RANKL, no inhibitor) treatments, indeed indicating a specific on-target effect of BET inhibition.

Intriguingly, **Figure 3.6** shows that even though there were some fused cells in 0.5μM PFI-1 treated samples, the dentine resorption assay did not give any evidence of actual resorption, indicating that the fused cells in 0.5μM PFI-1 treated samples were not activated osteoclasts. With higher concentrations (5μM), PFI-1 can prevent

the cells from fusing, while with lower concentrations it inhibits the resorptive activities.

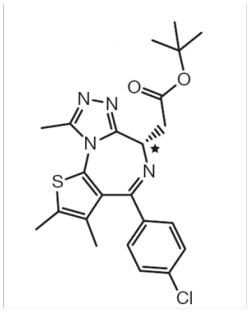

(+)-JQ1

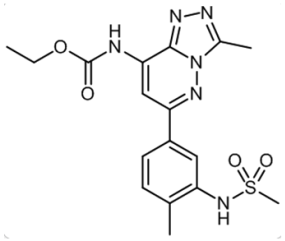

Bromosporine

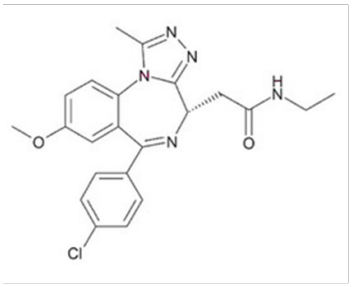

I-BET

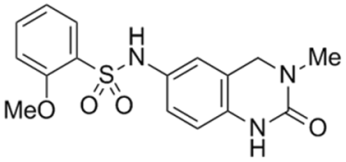

PFI-1

Figure 3.4 The chemical structures of (+)-JQ-1, Bromosporine, I-BET and PFI-1

The chemical structures were obtained from Structural Genomics Consortium (http://www.thesgc.org/chemical-probes).

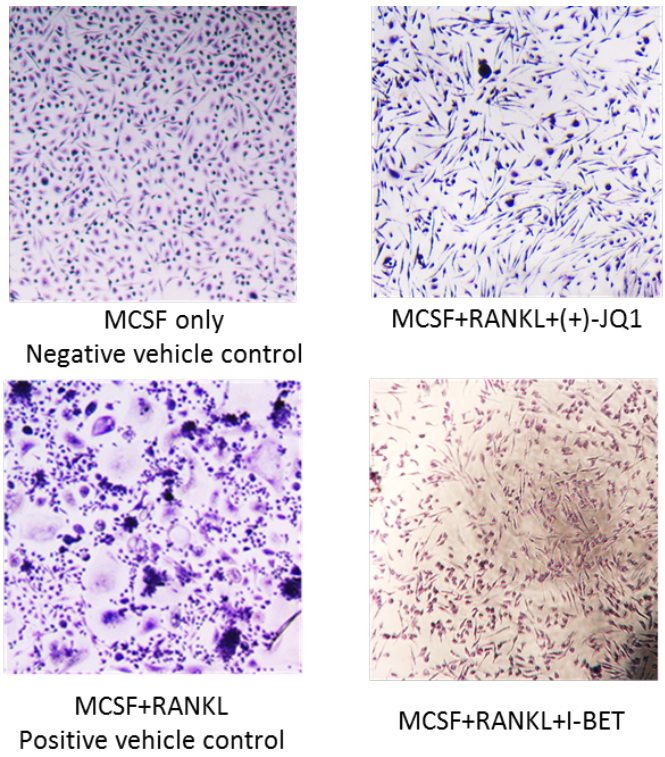

Figure 3.5 TRAP staining results for (+)-JQ1 and I-BET treated macrophages comparing with control samples

The cells treated with (+)-JQ1 and I-BET are still elongated macrophage-like cells and the cell densities remain acceptable. The concentration of (+)-JQ1 and I-BET used in this assay was 0.1μM and 1μM. Cells are elongated macrophages in (+)-JQ1 and I-BET treated samples.

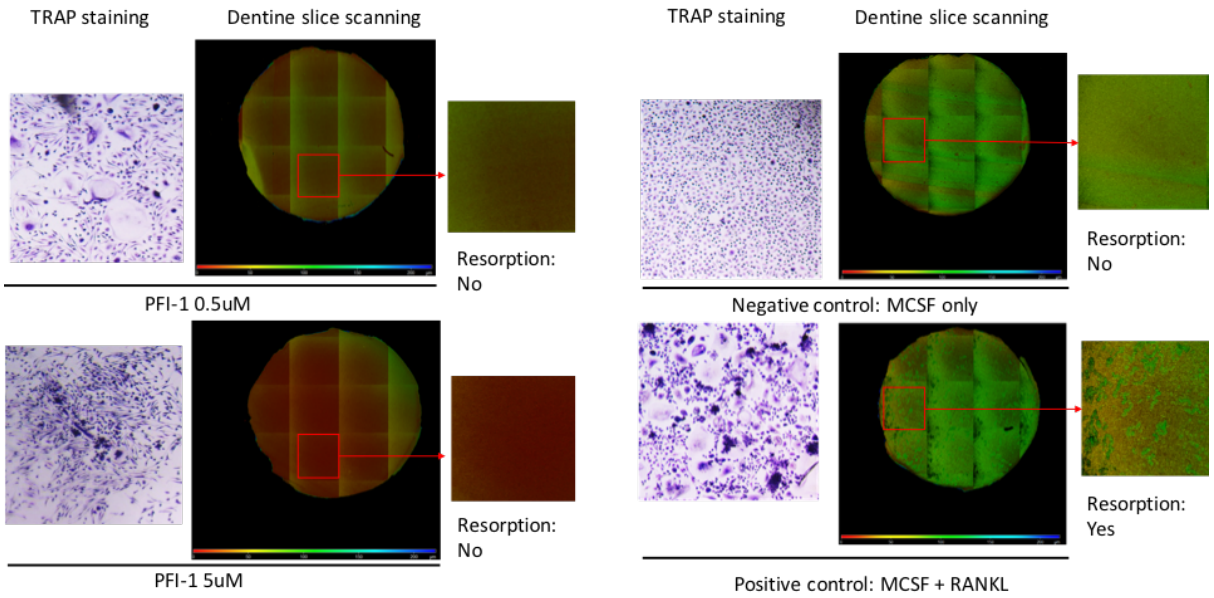

Figure 3.6 TRAP staining and dentine resorption results of PFI-1 treated samples

Compared with negative and positive controls, both concentrations of PFI-1 can inhibit the bone resorption. However, the TRAP staining shows some of 0.5 μM PFI-1 treated cells are multinucleated cells.

Bromosporine (**Figure 3.4**) is a broad-spectrum inhibitor for bromodomains, which showed efficacy in inhibition of osteoclast formation (over 80% inhibition of OC numbers vs control at 1μM). The dentine resorption assay corroborates that bromosporine is an inhibitor for osteoclast function (**Figure 3.7**). Under the treatment of 1uM bromosporine, most of the cells appeared as elongated macrophages. Some of the cells were fused but the dentine resorption assay showed them as resorption-inactive. Therefore, bromosporine reduces the fusion of osteoclast precursors and results (when fused) in mostly inactive osteoclasts.

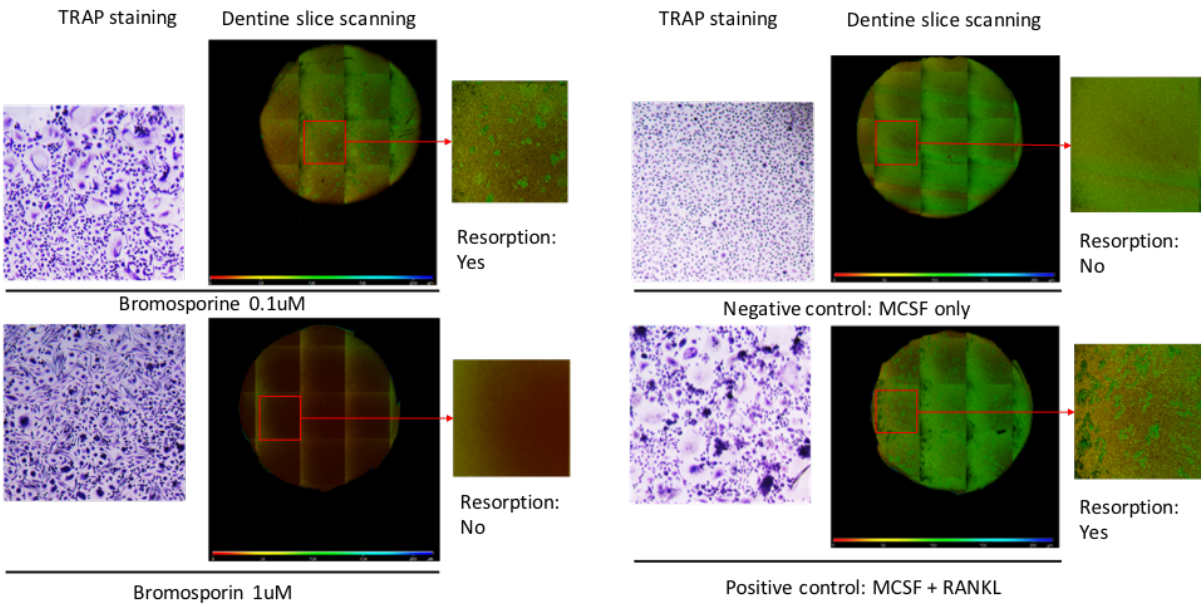

Figure 3.7 TRAP staining and dentine resorption result of bromosporine treated samples

Compared with negative and positive controls, 1μM of bromosporine can inhibit osteoclastogenesis and bone resorption.

3.2.3.2 Demethylase inhibitors

Another target class that emerged from the screen comprised histone demethylases. For example, GSK-J4 (**Figure 3.8**), which is a selective inhibitor for H3K27 and H3K4 demethylases, showed potent inhibition of osteoclast differentiation (**Figure 3.9**). However, KDOBA67, an analogue of GSK-J4, did not show the similar inhibition in the osteoclast assay (**Figure 3.9**).

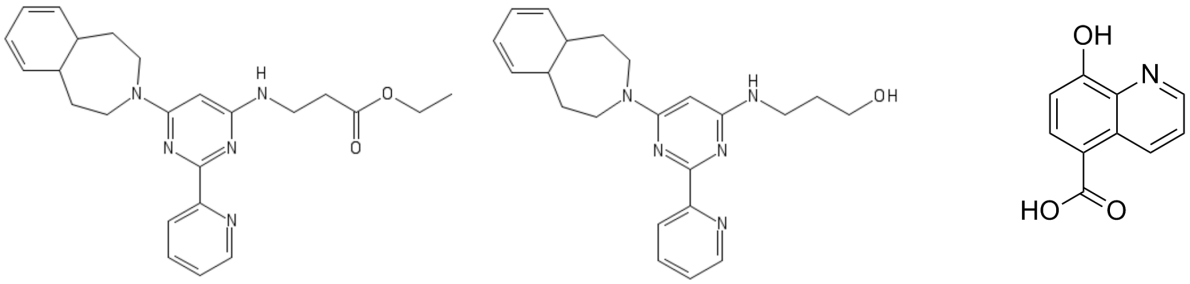

Figure 3.8 The chemical structures of GSK-J4, KDOBA67 and IOX1

The chemical structures were obtained from Structural Genomics Consortium (http://www.thesgc.org/chemical-probes). KDOBA67 is a cell-permeable derivative for GSK-J4 without intracellular esterase activation

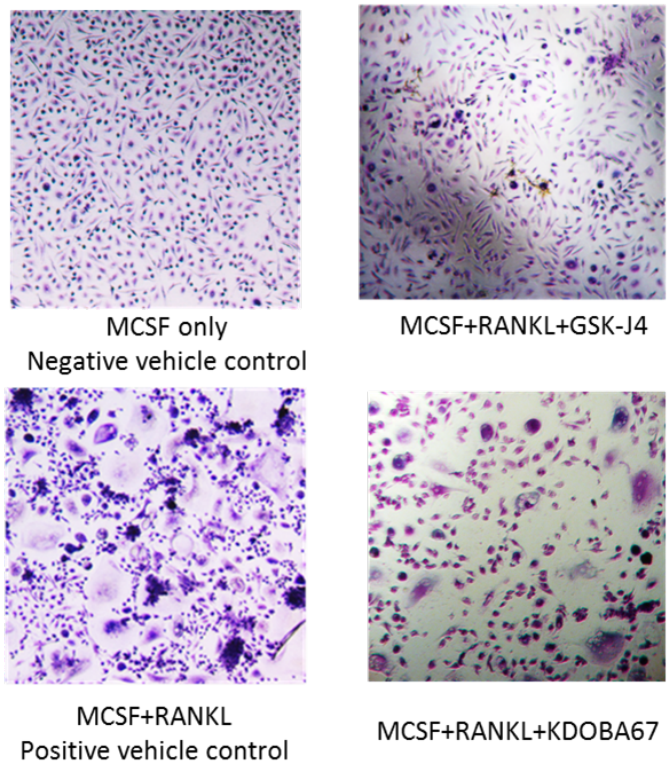

Figure 3.9 TRAP staining results for GSK-J4 and KDOBA67 treated samples compared to control samples

The concentration of GSK-J4 and KDOBA67 used in this assay was 10μM. Cells are elongated macrophages in GSK-J4 treated sample while there are a few osteoclasts generated in KDOBA67 treated sample.

Moreover, IOX1 (**Figure 3.8**), which is a cell-penetrating and active pan-histone demethylase inhibitor, showed good inhibitory ability in osteoclast differentiation, both in the TRAP staining result and the dentine resorption analysis (**Figure 3.10**). However, from the TRAP staining of a 40μM IOX1 treated sample, the cell density was much lower than the control samples. Therefore, treatment with a high concentration of IOX1 has reduced the number of monocytic osteoclast precursors, which might be one reason for lower osteoclastogenesis. In the 4μM IOX1 treated sample, both the osteoclast number and dentine resorption has been decreased slightly, which confirmed the anti-resorptive ability of IOX1.

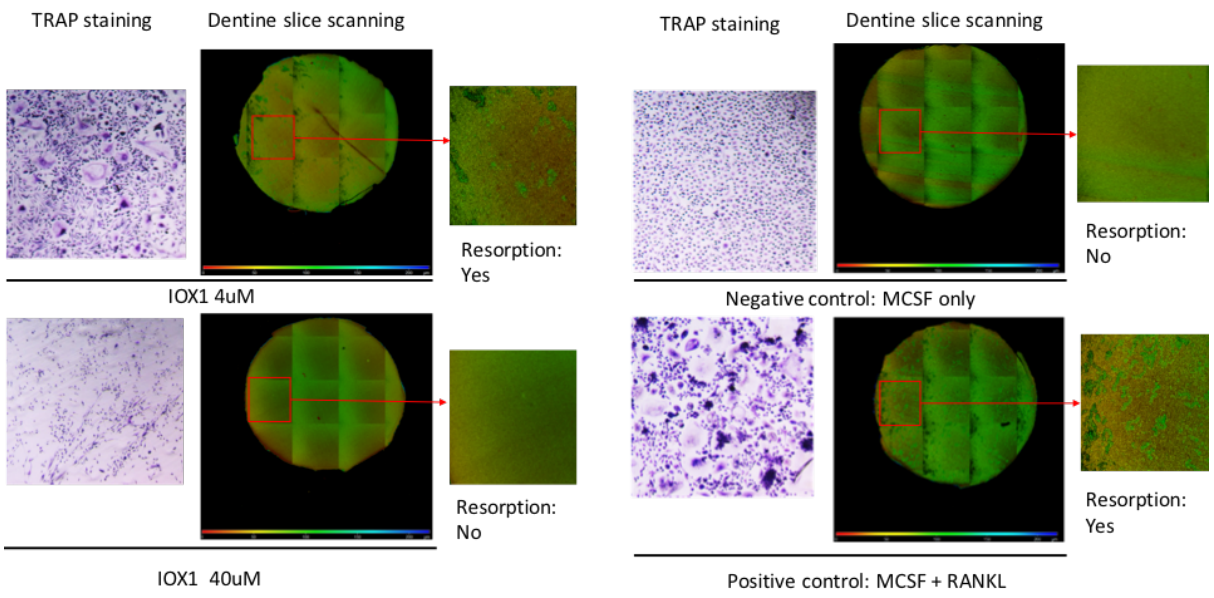

Figure 3.10 TRAP staining and dentine resorption results of IOX1 treated samples

Compared with negative and positive controls, 40μM of IOX1 can inhibit osteoclastogenesis and bone resorption.

3.2.3.3 HDAC inhibitors

It has been reported that HDAC inhibitors targeting both Class I and II HDACs are effective at inhibiting osteoclast development, e.g. previously SAHA (Class I and II) has shown good inhibitory ability (IC_{50} =12 nM) (Cantley et al. 2011). In this work, SAHA and CXD101 (**Figure 3.11**), which target Class I HDACs, showed good inhibitory ability against osteoclast differentiation at a very early stage (**Figure 3.12**). Moreover, rocilinostat (**Figure 3.11**), which targets HDAC6, has shown inhibition of osteoclastogenesis from the TRAP staining results (**Figure 3.12**), however, the high SD in **Figure 3.2** indicates a possible donor dependency of the observed effect. Since both bromodomain and HDAC inhibitors have been shown to inhibit osteoclastogenesis, DUAL946 (**Figure 3.11**), which simultaneously targets both epigenetic classes, was included in the screening. Although DUAL946 did show some inhibitory ability in our osteoclastogenesis assay (**Figure 3.12**), its potency was lower than its parent compounds, which are SAHA and I-BET.

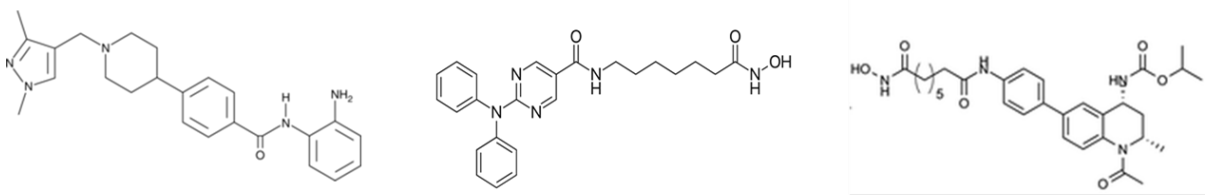

CXD101 Rocilinostat DUAL946

Figure 3.11 The chemical structures of CXD101, Rocilinostat and DUAL946.

The chemical structures were obtained from Structural Genomics Consortium (http://www.thesgc.org/chemical-probes).

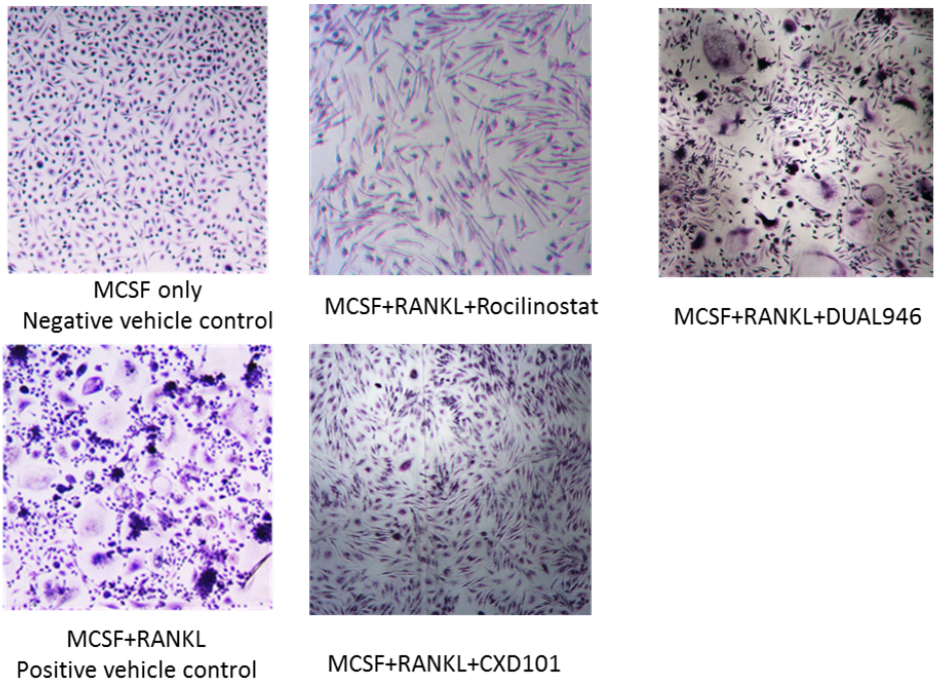

Figure 3.12 TRAP staining results for rocilinostat, CXD101 and DUAL946 treated samples comparing with control samples

The concentration of rocilinostat, CXD101 and DUAL946 used in this assay was 1μM. Cells are elongated macrophages in rocilinostat and CXD101 treated samples while there are a few osteoclasts generated in DUAL946 treated sample.

3.3 Epigenetic compound screening in Multiple Myeloma

To identify anti-proliferative epigenetic inhibitors for multiple myeloma, the compound library (**Table 3.1**) was tested on several myeloma cell lines using a cell viability assay as the primary readout.

3.3.1 Prestoblue® cell viability assay (3-day time course)

The library of small molecule inhibitors was screened against six myeloma cell lines which included 5 human myeloma cell lines and 1 mouse myeloma cell line. Using

the readout from the Prestoblue® assay as proxy for proliferation after 3-days of treatment, several hits emerged as active against all the six multiple myeloma cell lines used, such as (+)-JQ1 and I-BET from the bromodomain inhibitors, rocilinostat and CXD101 from the HDAC class, besides GSK-J4 and KDOBA67 from the demethylase class **(Figure 3.13)**.

Figure 3.13 (below) Small molecule screening in myeloma cell lines (3-day treatment)

*The concentration of each compound is shown in **Table 3.1** (compound list). The results represent the viability as a percentage of the vehicle treated control, which is 0.1% DMSO treated sample. Data presents the mean of 4 biological replicates. The full list of SD for each plot is shown in Appendices Table 5*

.

Class	Compound	JJN3	JIM3	KMS11	5TGM1	U266	MM1S
Bromodomain	BAZ-ICR						
Bromodomain	LP99						
Bromodomain	NI57						
Bromodomain	PFI-4						
Bromodomain	OF-1						
Bromodomain	PFI-3						
Bromodomains	(+)-JQ1						
Bromodomains	(-)-JQ1						
Bromodomains	PFI-1 (BET)						
Bromodomains	CBP/BRD4 (0383)						
Bromodomains	SMARCA						
Bromodomains	I-BET						
Bromodomains	GSK2801						
Bromodomains	Bromosporin						
Bromodomains	I-CBP112						
Bromodomains	RVX-208						
Bromodomains	SGC-CBP30						
HDAC/Bromo	DUAL946						
HDAC	CI-994						
HDAC	CXD101						
HDAC	Valproic acid						
HDAC	Entinostat (MS-275)						
HDAC	Trichostatin A						
HDAC	SAHA						
HDAC	Belinostat						
HDAC	SRT1720						
HDAC	EX 527						
HDAC	RGFP 966						
HDAC	Tubastatin A HCl						
HDAC	PCI-34051						
HDAC	Rocilinostat						
DNMT	5-Aza-deoxy-cytidine						
DNMT	5-Azacitidine (AZA)						
Halofuginol	MAZ1805						
Halofuginone	MAZ1392						
HAT	C646						
Histone demethylase	JIB-04						
Histone demethylase	Methylstat						
Histone demethylase	KDOBA67						
Histone demethylase	ML324						
Histone demethylase	Tranylcypromine						
Histone demethylase	GSK-J4						
Histone demethylase	GSK-J5						
Histone demethylase	IOX1 (5COOH-8HQ)						
Histone demethylase	GSK-LSD1						
Prolyl-Hydroxylases	IOX2						
Kinase inhibitor	K00135						
Kinase inhibitor	HASPIN						
Methyl Lysine Binder	UNC1215						
Methyl Lysine Binder	IOCR-9429						
Protein Arginine Deiminase	GSK484						
PARP	Rucaparib						
PARP	Olaparib						

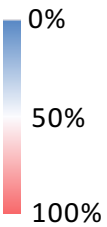

3.3.2 Prestoblue® assay (10-day time course)

Previously, several of these molecules (e.g. for the methyltransferase and some of demethylase inhibitor classes) have shown a long onset of effect (i.e. > 3 days). Based on this knowledge, an extended treatment length was used to assess the effect of selected compounds, accordingly a longer time course was identified and 7 to 10 days of inhibition was determined as suitable treatment length for the methyltransferase and some demethylase inhibitors.

The inhibitors were screened in all six myeloma cell lines after a 10-day treatment, and results are shown in **Figure 3.14**. Histone methyltransferase inhibitors, chaetocin and A196, and most of the arginine methyltransferase inhibitors, indeed show a significant inhibition of viability (>50%) in all six myeloma cell lines.

Class	Compound	JJN3	JIM3	KMS11	5TGM1	U266	MM1S
Histone methyltransferase	SGC0946						
Histone methyltransferase	(R)-PFI-2						
Histone methyltransferase	UNC0642						
Histone methyltransferase	UNC0638						
Histone methyltransferase	Chaetocin						
Histone methyltransferase	A-366						
Histone methyltransferase	GSK343						
Histone methyltransferase	UNC1999						
Histone methyltransferase	CPI.360						
Histone methyltransferase	CPI.413						
Histone methyltransferase	LLY507						
Histone methyltransferase	A196						
Histone methyltransferase	BAY598						
Arginine methyltransferase	SGC707						
Arginine methyltransferase	J556-42R						
Arginine methyltransferase	J556-63R						
Arginine methyltransferase	J556-70P						
Arginine methyltransferase	J556143						
Histone demethylase	KDOAM-25						
Histone demethylase	GSK467						

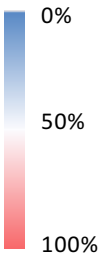

Figure 3.14 Small molecule screening in myeloma cell lines (10-day treatment)

*The concentration of each compound can be found in **Table 3.1** (compound list). The results represent the viability as a percentage of the vehicle treated control, which is 0.1% DMSO treated. Data plotted represents the mean of 4 biological replicates. The full list of SD for each plot is shown in Appendices Table 5.*

3.4 Selected epigenetic compounds have both anti-resorptive and anti-proliferative activity

3.4.1 Comparison of screening in osteoclast differentiation assay and myeloma viability assay (JJN3 cell line)

To identify anti-resorptive and anti-proliferative epigenetic inhibitors, the screening results of both the osteoclast differentiation assay and the myeloma viability assay were compared, which is shown in **Figure 3.15**. The JJN3 cell line was selected as a representative cell line based on the high similarity of screening results between JJN3 cells and the other cell lines. Several compounds from the bromodomain group of compounds, such as (+)-JQ1 and PFI-1, and several compounds from the HDAC group of compounds, such as CXD101 and rocilinosat, showed strong inhibition for both osteoclast differentiation and myeloma cell proliferation. Moreover, GSK-J4, which is a histone demethylase inhibitor, showed strong inhibition in both the osteoclast assay and the myeloma viability assay, whereas GSK-J5, the inactive control of GSK-J4, did not show any inhibition in both assays. These compounds were then investigated further to identify their molecular inhibitory mechanisms.

Figure 3.15 (below) Comparison of compound screening in osteoclast differentiation assay (top) and myeloma cell viability assay (bottom).

Data of screening in myeloma cell represents the screening results of JJN3 cell line. Each plot represents the mean plus SD of 3 to 9 biological replicates for osteoclast results and 4 biological replicates for myeloma results.

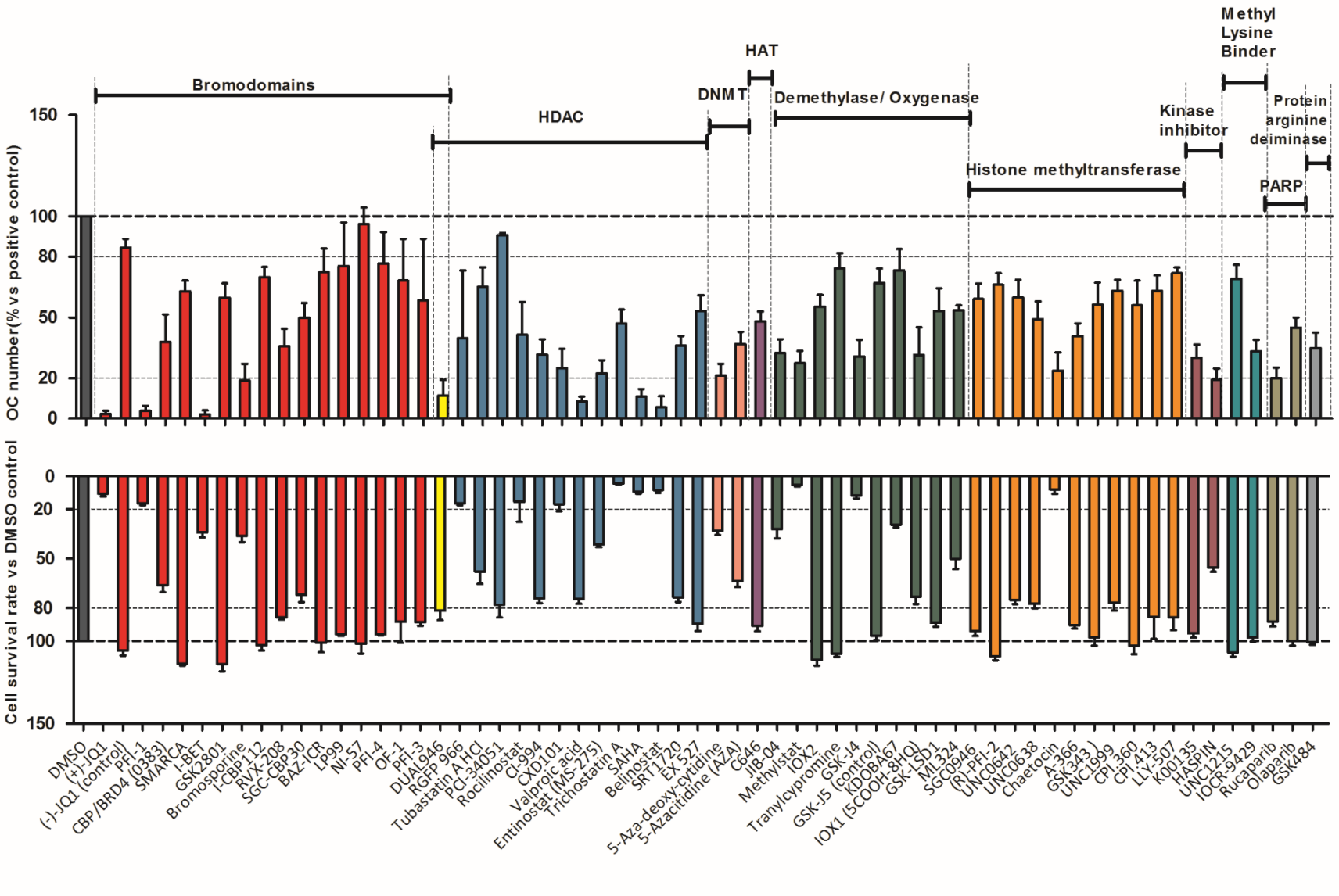
Bromodomains
HDAC
DNMT
HAT
Demethylase/ Oxygenase
Histone methyltransferase
Kinase inhibitor
Methyl Lysine Binder
Protein arginine deiminase
PARP
OC number(% vs positive control)
Cell survival rate vs DMSO control
150
100
80
50
20
0
0
20
50
80
100
150
DMSO
(+)-JQ1
(-)-JQ1 (control)
CBP/BRD4 (0383)
PFI-1
SMARCA
I-BET
GSK2801
Bromosporine
I-CBP112
RVX-208
SGC-CBP30
BAZ-ICR
LP99
NI-57
PFI-4
OF-1
PFI-3
DUAL946
RGFP 966
Tubastatin A HCl
PCI-34051
Rocilinostat
CI-994
CXD101
Valproic acid
Entinostat (MS-275)
Trichostatin A
SAHA
Belinostat
SRT1720
EX 527
5-Aza-deoxy-cytidine
5-Azacitidine (AZA)
C646
JIB-04
Methylstat
IOX2
Tranylcypromine
GSK-I4
GSK-J5 (control)
KDOBA67
IOX1 (5COOH-8HQ)
GSK-LSD1
ML324
SGC0946
(R)-PFI-2
UNC0642
UNC0638
Chaetocin
A-366
GSK343)
UNC1999
CPI-360
CPI-413
LLY-507
K00135
HASPIN
UNC1215
IOCR-9429
Rucaparib
Olaparib
GSK484

3.4.2 Selected compounds have an EC_{50} in the nanomolar or low micromolar range in myeloma cell lines.

Based on the results described above, seven compounds against different targets were selected based on pronounced anti-proliferative ability of all six myeloma cell lines. These compounds have an EC_{50} in the nanomolar or low micromolar range in all six myeloma cell lines. Details of EC_{50} determinations of each compound are shown in **Table 3.2**.

Table 3.2 EC_{50} values (μM) for selected compounds in various myeloma cell lines

Target	Compound	Cell line					
		JJN3	5TGM1	JIM3	KMS11	MM1S	U266
Bromodomain	CBP/BRD4(0380)	7.6	7.5	3.3	9.4	3.6	7.8
Bromodomain	(+)-JQ1	0.1	0.1	0.2	0.1	0.0	0.1
Bromodomain/HDAC	DUAL946	2.3	4.4	17.2	5.0	1.0	4.5
DNMT	5-Aza-deoxy-cytidine	1.3	0.1	1.8	1.5	>50	3.6
HDAC	Rocillinostat	1.8	2.2	4.7	4.9	2.9	5.5
HDAC	CXD101	0.1	0.1	0.1	0.3	0.3	0.2
Histone demethylase	GSK-J4	1.5		1.0	2.3	1.9	1.6

Part of the EC_{50} of GSK-J4 was obtained from Dr Edward Hookway in our group. The EC_{50} of GSK-J4 in 5TGM1 cells was not tested. Data plotted represents the mean for three biological replicates. The full list of confidential intervals (95%) for each plot is shown in Appendices Table 4.

3.5 Discussion

In this chapter, a focused library of small molecules (73 molecules) against specific epigenetic targets was screened in osteoclast differentiation and myeloma cell viability (proliferation) assays. The Prestoblue® cell viability assay results of myeloma cells screened against the inhibitor library demonstrated that several compounds, such as (+)-JQ1, GSK-J4 and CXD101, showed growth inhibition across all six myeloma cell lines used. However, some compounds only showed inhibition for certain cell lines, such as methylstat which only inhibited JJN3 cells. It is apparent that several compounds, including bromodomain inhibitors such as (+)-JQ1, HDAC inhibitors such as rocilinostat and CXD101, as well as histone demethylase inhibitors like GSK-J4 or a set of PRMT5 inhibitors have an overlapping inhibitory effect on both osteoclast differentiation and myeloma cell proliferation.

The results clearly showed recurring patterns: for example, BET bromodomain inhibitors (JQ1, PFI-1, I-BET, bromosporine) show clear anti-proliferative and anti-resorptive effects. Since these compounds represent distinct chemical scaffolds, and negative control compounds such as (-)-JQ1 (or GSK-J5 for demethylases) were employed with no significant effects, the experiments provide strong evidence for specific on-target effects. Moreover, comparing with (+)-JQ1, the molecule CBP/BRD4(0383) is less potent in inhibiting both osteoclast differentiation and myeloma proliferation and since it has significant BRD4 activity, it is concluded that its observed effects are more likely related to BET inhibition than to CBP inhibition.

HDAC inhibitors have been reported to inhibit myeloma cell proliferation, for example, HDAC inhibitor panobinostat, which targets class I, II and IV of HDACs, has demonstrated its effectiveness in clinical trials for myeloma treatment (Laubach et al.

2015). The results presented here confirm and extend these earlier observations. However, less data on CXD101 and rocilinostat have been reported (compared to classical HDAC inhibitors such as SAHA or TSA) and these molecules were therefore selected for further studies to be conducted in this thesis.

There are several inhibitors from the demethylase class, which showed strong potency in both osteoclast assay and myeloma viability assay. Impressively, GSK-J4 showed the ability to inhibit both osteoclast differentiation and myeloma proliferation. KDOBA67, which is a derivative of GSK-J4, showed inhibitory ability in all six myeloma cell lines as well. Previously, GSK-J4 was shown to reduce the TNF-α production in human primary macrophages in an H3K27-dependent manner (Kruidenier et al. 2012).

More recently, several arginine methyltransferase (PRMT5) inhibitors became available, and therefore have not been applied to the osteoclast differentiation assay yet. However, the compound screening in myeloma proliferation assays have shown this group of compounds to be potent. However, the reason why these compounds had slower effects on the cells than compounds from other target classes was still unclear.

In summary, several epigenetic compound classes were identified or confirmed as potent anti-proliferative and anti-resorptive inhibitors, and prototypic molecules of these classes were now selected for further mode of action studies.

Chapter 4 Development of RANKL gene card to understand osteoclast biology

4.1 Introduction

Bone remodelling is a dynamic and continuous process which involves the resorption of bone by osteoclasts and the synthesis of new bone matrix by osteoblasts. Osteoclasts are large multinucleated cells which are derived from monocyte/macrophage precursors. It has been reported that an excessive number and resorptive function of osteoclasts is the main cause of bone destruction in many osteolytic diseases, such as post-menopausal osteoporosis, primary bone cancer, multiple myeloma or bone metastasis, thereby seriously affecting the quality of patients' lives. Moreover, the growth factors released by osteoclasts enhance the proliferation of tumour cells; accordingly control of osteoclast differentiation can inhibit both bone destruction and tumour growth.

The key cytokines involved in osteoclast differentiation and activation are macrophage colony-stimulating factor (M-CSF) and receptor activator of nuclear factor kappa B (NF-kB) ligand (RANKL). M-CSF plays an important role in maintaining the survival of mature osteoclasts and osteoclast precursors. Differently, the binding of RANKL to receptor activator of nuclear factor kappa B (RANK) activates the differentiation process. There are many genes involved in the osteoclast activation and differentiation process, which has been discussed in **Chapter 1**. Therefore, it is important to identify the genes which closely related with

the RANK signalling pathway and characterize how our epigenetic compounds can affect this process.

4.2 Development of a RANKL target gene card

The gene selection for the quantitative Real Time PCR (qPCR) study is based both on literature mining. RANKL is a well-studied cytokine and many publications address functional and gene expression patterns elicited by the cytokine in human macrophages and monocytes. We selected genes induced by RANKL for which functional evidence for their role in formation or function of osteoclasts had previously been reported. In addition, an RNAseq study of RANKL stimulated monocytes was used to select novel genes, which was done by our former group member Dr Laurynas Pliuskys.

In total, 34 genes related to osteoclast differentiation (full list in **Appendices Table 1**) were selected and validated by quantitative RealTime PCR, among them, 20 genes were selected for a RANKL gene card based on the clear gene expression difference between RANKL treated sample and non-RANKL treated sample (**Figure 4.1**). The PCR was done using ACTB (actin beta) and B2M (beta-2-microglobulin**)** as housekeeping genes for normalisation and the fold-change was calculated using 24 hours non-RANKL (vehicle control) treated sample as reference sample. Since the results of fold-changes were very similar between normalisations to ACTB or B2M, only the results normalised to ACTB are displayed in **Figure 4.1**. The genes that emerge as the best markers of RANKL activity are CA2, TCIRG1, MMP9, NFATC1, CTSK, CALCR, COL6A1, CDK7, CALM1, FBP1, FAM89A, IGFBP4, CDC42EP5, CKB, NEURL3, LIF, CSPG, MEGA6, PRPSAP1 and TMEM132A. The detailed

information of the genes and primers is displayed in **Table 4.1**. These primers were applied in compound screening studies to characterise the inhibitory mechanisms of compounds in osteoclast differentiation.

Specifically, **Figure 4.1** shows clear differences between RANKL treated samples and non-RANKL treated samples. Fold-change was calculated using non-RANKL treated sample of the same time point, with results displayed in **Table 4.2**. Most of the markers showed the largest difference between RANKL treated samples and non-RANKL treated samples after 14 days of treatment. Interestingly, after 7 days of treatment, the cells had not fused yet and the morphology of the cells showed no difference between RANKL treated and non-RANKL treated samples from observation under the microscope, but the expression level of some of the genes had already increased or decreased.

Accordingly, the primers can be classified as markers for early/intermediate/late and transient/stable differentiation events. Several genes emerged as stable markers for RANKL differentiation after 7 days and 14 days such as CKB, CDC42EP5, CSPG, TEME132A, NEURL3, COL6A1, MMP9 and CA2. These genes are known to be important in osteoclast biology, for example CA2 (Carbonic Anhydrase II) plays an important role in osteoclast differentiation by affecting steady-state intracellular pH and Ca^{2+} levels (Lehenkari et al. 1998). After 7 days of RANKL treatment, the expression level of CA2 gene was high compared with the MCSF only sample (2.88 fold), and this high level continues until the end of treatment (5.13 fold on Day 21). For MMP9 (matrix metallopeptidase 9), CKB (creatine kinase, brain), CDC42EP5 (CDC42 effector protein 5) and TMEM132A (transmembrane protein 132A), the gene expression was higher in RANKL treated samples compared with non-RANKL

treated samples from Day 7 until the end of culturing. However, CSPG (chondroitin sulfate proteoglycan), COL6A1 (collagen, type VI, alpha 1) and CALM1 (Calmodulin) only showed a high gene expression at Day 14 in RANKL treated sample.

Figure 4.1 (below) Real Time PCR of selective primers vs ACTB (actin beta)

*Figures **a** and **b** show 20 selected genes based on the clear gene expression difference between RANKL treated sample and non-RANKL treated sample and they were tested as osteoclast differentiation markers. Most of the markers showed the biggest differences between RANKL treated samples and non-RANKL treated samples at Day 14. Data plotted represents the mean plus/minus SD of three biological replicates.*

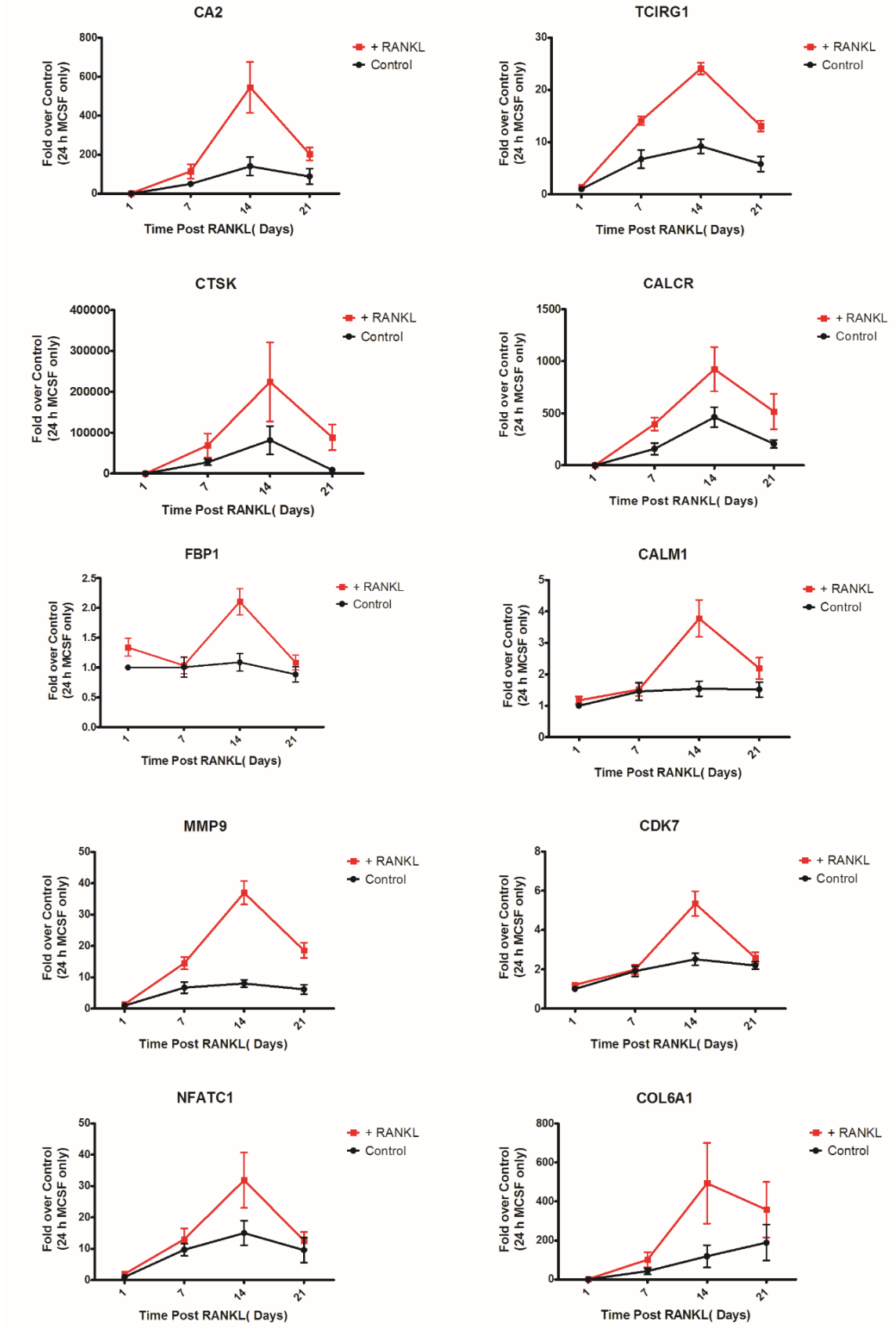
CA2
Fold over Control (24 h MCSF only)
800
600
400
200
0
+ RANKL
Control
1
7
14
21
Time Post RANKL(Days)
TCIRG1
Fold over Control (24 h MCSF only)
30
20
10
0
+ RANKL
Control
1
7
14
21
Time Post RANKL(Days)
CTSK
Fold over Control (24 h MCSF only)
400000
300000
200000
100000
0
+ RANKL
Control
1
7
14
21
Time Post RANKL(Days)
CALCR
Fold over Control (24 h MCSF only)
1500
1000
500
0
+ RANKL
Control
1
7
14
21
Time Post RANKL(Days)
FBP1
Fold over Control (24 h MCSF only)
2.5
2.0
1.5
1.0
0.5
0.0
+ RANKL
Control
1
7
14
21
Time Post RANKL(Days)
CALM1
Fold over Control (24 h MCSF only)
5
4
3
2
1
0
+ RANKL
Control
1
7
14
21
Time Post RANKL(Days)
MMP9
Fold over Control (24 h MCSF only)
50
40
30
20
10
0
+ RANKL
Control
1
7
14
21
Time Post RANKL(Days)
CDK7
Fold over Control (24 h MCSF only)
8
6
4
2
0
+ RANKL
Control
1
7
14
21
Time Post RANKL(Days)
NFATC1
Fold over Control (24 h MCSF only)
50
40
30
20
10
0
+ RANKL
Control
1
7
14
21
Time Post RANKL(Days)
COL6A1
Fold over Control (24 h MCSF only)
800
600
400
200
0
+ RANKL
Control
1
7
14
21
Time Post RANKL(Days)

a)

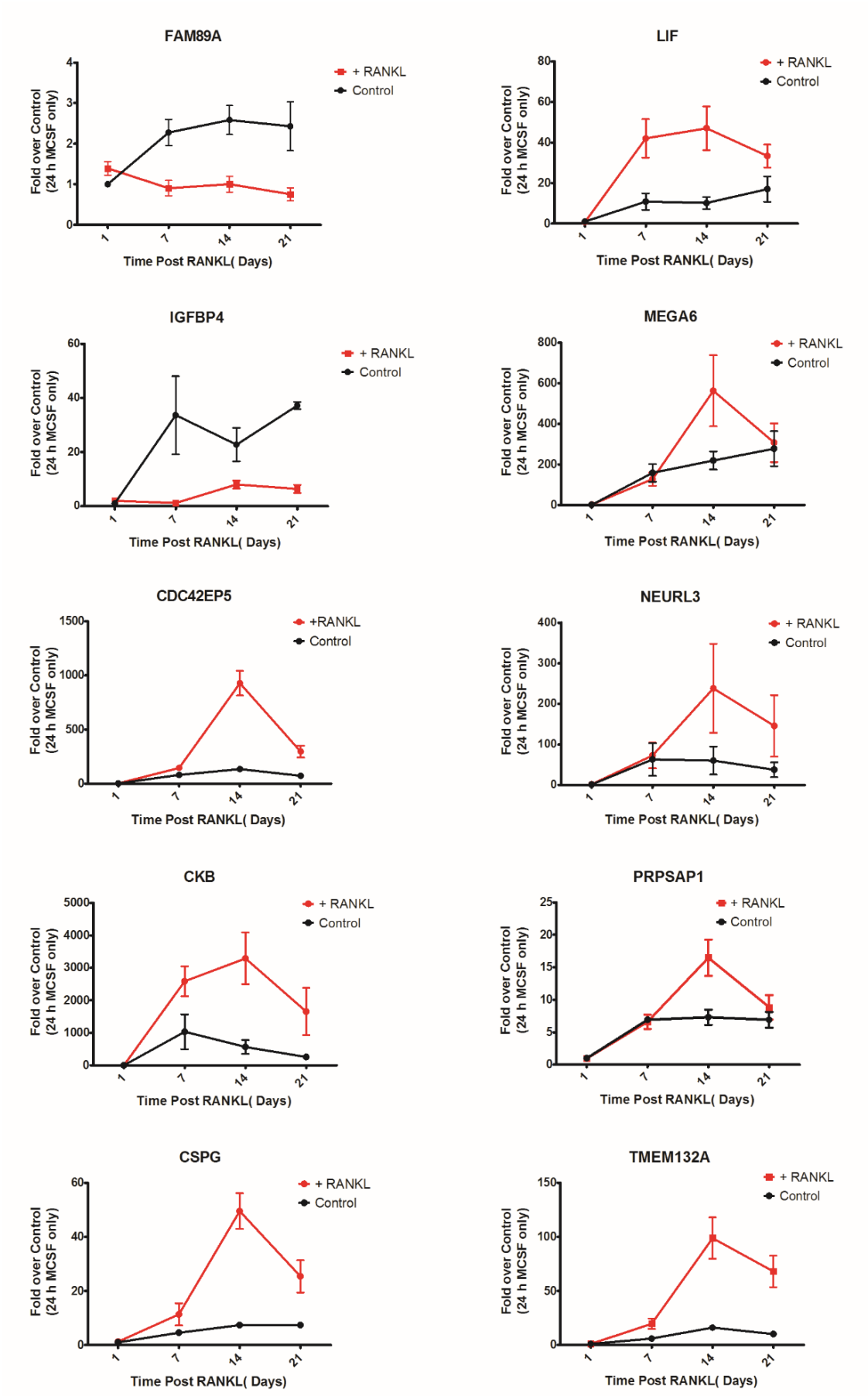
FAM89A
+ RANKL
Control
Fold over Control (24 h MCSF only)
Time Post RANKL(Days)
LIF
+ RANKL
Control
Fold over Control (24 h MCSF only)
Time Post RANKL(Days)
IGFBP4
+ RANKL
Control
Fold over Control (24 h MCSF only)
Time Post RANKL(Days)
MEGA6
+ RANKL
Control
Fold over Control (24 h MCSF only)
Time Post RANKL(Days)
CDC42EP5
+RANKL
Control
Fold over Control (24 h MCSF only)
Time Post RANKL(Days)
NEURL3
+ RANKL
Control
Fold over Control (24 h MCSF only)
Time Post RANKL(Days)
CKB
+ RANKL
Control
Fold over Control (24 h MCSF only)
Time Post RANKL(Days)
PRPSAP1
+ RANKL
Control
Fold over Control (24 h MCSF only)
Time Post RANKL(Days)
CSPG
+ RANKL
Control
Fold over Control (24 h MCSF only)
Time Post RANKL(Days)
TMEM132A
+ RANKL
Control
Fold over Control (24 h MCSF only)
Time Post RANKL(Days)

b)

Table 4.1 Selective primers used in the study

Gene	Gene description	Forward (5'-3')	Reverse (5'-3')	Efficiency (%)	Source
CALCR	Calcitonin receptor	TGGTGCCAACCACTATCCATGC	CACAAGTGCCGCCATGACAG	101.08	(Hattersley and Chambers 1989)
IGFBP4	Insulin-like growth factor binding protein 4	CCCACTCCCAAAGCTCAGACT	CCAAGCAGATGGTGCAACAA	116.33	(Fiorelli et al. 1996)
CA2	Carbonic anhydrase II	ACTGGGGTTCACTTGATGGA	CTGCACAGCTTTCCCAAAAT	102.56	(Lehenkari et al. 1998)
FBP1	Fructose-1,6-bisphosphatase 1	CATGGCGATGGACCGGGA	AGGTTTGTCAGCACCAGTGT	93.97	(Day et al. 2004)
CALM1	Calmodulin	GGCATTCCGAGTCTTTGACAA	CCGTCTCCATCAATATCTGCT	97.23	(Seales, Micoli, and McDonald 2006)
MMP9	Matrix metallopeptidase 9	CAGTCCACCCTTGTGCTCTT	CCAGAGATTTCGACTCTCCAC	106.33	(Sundaram et al. 2007)
CDK7	Cyclin-dependent kinase 7	ATGGCTCTGGACGTGAAGTC	CTTAATGGCGACAATTTGGTTG	100.15	(Rimondi et al. 2007)
NFATC1	Nuclear factor of activated T-cells, cytoplasmic, calcineurin-dependent 1	CGAGCCGTCATTGACTGTGC	GAGCGCTGGGAGCATTCGAT	99.63	(Takayanagi 2007)
CTSK	Cathepsin K	TGAGGCTTCTCTTGGTGTCCATAC	AAAGGGTGTCATTACTGCGGG	114.77	(Motyckova and Fisher 2002)
TCIBG1	T-cell, immune regulator 1, ATPase, H+ transporting, lysosomal V0 subunit A3	AGCTCGATGGAGGAGGGAGT	CAAACAGGAAGGGGAAGGTG	99.55	(Moscatelli et al. 2013)
FAM89A	Family with sequence similarity 89, member A	TGTCCTTGCTCTGCCAACTG	GCCGTTCTCCAGAGCGTAAG	106.87	RNAseq
COL6A1	Collagen, type VI, alpha 1	ACCTACACCGACTGCGCTAT	CGTCGGTCACCACAATCAGG	107.48	RNAseq
CDC42EP5	CDC42 effector protein (Rho GTPase binding) 5	GGCTAGAGCTGGAGTCGTGA	CGATCAGGCCGCTTCTTGG	117.11	RNAseq
CKB	Creatine kinase, brain	CACCATGCACCCCTGATGT	CTCTACCAAGGGTGACGGAAGT	108.87	RNAseq
CSPG	Chondroitin sulfate proteoglycan	CAGCTCTACTCTGGACGCCT	GATGGAGTCACTCAGCAGCG	95.95	RNAseq
LIF	Leukemia inhibitory factor	GTCTTGGCGGCAGTACACA	ACGACTATGCGGTACAGCTC	115.95	RNAseq

Gene	Gene description	Forward (5'-3')	Reverse (5'-3')	Efficiency (%)	Source
MEGA6	Multiple EGF-like-domains 6	CTGCCAGACAAGGTGCTCTT	GCCCAGTATCACAGGCTCTC	89.63	RNAseq
NEURL3	Neuralized E3 ubiquitin protein ligase 3	CCAAAGCCACACCAGGAGAG	CACTTGGCCGTATCGCTGAA	105.03	RNAseq
PRPSAP1	Phosphoribosyl pyrophosphate synthetase-associated protein 1	CCAGGGAAATGGAGGTATTG	AGAGGCCAACTGGATAGTAA	97.35	RNAseq
TMEM132A	Transmembrane protein 132A	TTCTGCTCCTACAGCCCTGG	GTAGGGCTCTGCTGGAGTCA	93.68	RNAseq

Table 4.2 Summary of RANKL responsive genes

Gene symbol	Gene description	Fold 1d RANKL/ 1d MCSF only	Fold 7d RANKL/ 7d MCSF only	Fold 14d RANKL/ 14d MCSF only	Fold 21d RANKL/ 21d MCSF only	Classification
CKB	Creatine kinase, brain	1.46	10.92	8.97	15.93	Intermediate Stable
CDC42EP5	CDC42 effector protein (Rho GTPase binding) 5	0.85	3.63	8.59	9.63	Intermediate Stable
CSPG	Chondroitin sulfate proteoglycan	1.14	4.23	8.12	4.28	Intermediate Transient
TMEM132A	Transmembrane protein 132A	0.96	7.73	7.62	9.58	Intermediate Stable
NEURL3	Neuralized E3 ubiquitin protein ligase 3	1.40	5.42	7.55	7.56	Intermediate Stable
COL6A1	Collagen, type VI, alpha 1	1.20	3.64	6.24	2.97	Intermediate Transient
MMP9	Matrix metallopeptidase 9	1.24	3.49	5.92	4.51	Intermediate Stable
CA2	Carbonic anhydrase II	2.58	2.88	5.43	5.13	Early Stable
LIF	Leukemia inhibitory factor	0.85	6.60	4.06	3.50	Early Transient
CTSK	Cathepsin K	3.95	3.38	3.69	8.37	Early Stable
TCIBG1	T-cell, immune regulator 1, ATPase, H+ transporting, lysosomal V0 subunit A3	1.28	3.51	3.49	3.73	Intermediate Stable
CALM1	Calmodulin	1.06	1.53	3.10	1.62	Intermediate Transient
PRPSAP1	Phosphoribosyl pyrophosphate synthetase-associated protein 1	0.85	1.27	3.09	1.53	Intermediate Transient
MEGA6	Multiple EGF-like-domains 6	1.45	1.11	2.81	1.28	Intermediate Transient
CDK7	Cyclin-dependent kinase 7	1.09	1.41	2.65	1.28	Intermediate Transient
NFATC1	Nuclear factor of activated T-cells, cytoplasmic, calcineurin-dependent 1	1.66	1.86	2.55	2.52	Intermediate Stable
CALCR	Calcitonin receptor	0.98	5.44	2.54	2.90	Early Transient
FBP1	Fructose-1,6-bisphosphatase 1	1.20	1.43	2.46	1.41	Intermediate Transient
IGFBP4	Insulin-like growth factor binding protein 4	1.71	0.19	1.81	0.19	Early Transient
FAM89A	Family with sequence similarity 89, member A	1.24	0.54	0.47	0.36	Early Transient

4.3 Application of RANKL gene card

After the RANKL gene card was established and validated, it was used to characterise the cellular mechanisms for selected compounds in the osteoclast differentiation assay (**Figure 4.2** and **Figure 4.3**). Eight compounds were selected based on previous results of the osteoclast assay. (+)-JQ1, I-BET and PFI-1 from the bromodomain family were selected based on their inhibition for osteoclast differentiation at a very early stage. (-)-JQ1 served as an inactive control for (+)-JQ1. For some genes, (+)-JQ1, I-BET and PFI-1 showed similar pattern of gene suppression (**Figure 4.2 and 4.3**). For example, the expression levels of CKB, CDC42EP5, CTSK were much lower in (+)-JQ1, I-BET and PFI-1 treated samples compared with the positive control. However, the level of expression was still higher than the expression levels in the negative control. Therefore, even though the morphology of the cells treated with bromodomain inhibitors looked very similar to the cells in the negative controls, the gene results showed that the expression levels of some genes related to the RANKL signalling pathway were changed. Since (+)-JQ1, I-BET and PFI-1 are all BET bromodomain inhibitors, it was expected that they would have similar molecular effects. However, for some genes, (+)-JQ1, I-BET and PFI-1 showed different results. For instance, I-BET and PFI-1 increased the expression of CALCR on both the Day 7 and Day 14, whereas (+)-JQ1 decreased the CALCR expression.

SAHA and Belinostat, which target HDACs, showed a stronger inhibition in the gene expression of the RANKL regulated genes than bromodomain inhibitors. In particular, CTSK as a key gene in osteoclastogenesis had lower expression levels in SAHA and

Belinostat treated samples than (+)-JQ1, I-BET and PFI-1 treated samples in both the Day 7 and Day 14 results.

However, DUAL946, which targets both bromodomain and HDAC, had less inhibition for the RANKL related genes. This correlated with the results of TRAP staining in Chapter 3 (**Figure 3.12**). Interestingly, methylstat, which showed good inhibitory ability in osteoclast differentiation from the results of TRAP staining, did not reduce expression level of many genes, such as CTSK, in this RANKL gene card in the Day 7 and Day 14 results. This may indicate that methylstat inhibits osteoclastogenesis at a later stage.

Figure 4.2 (below) Fold-change of gene expression in compound treated samples after 7 days of treatment

*Figure a and b showed the gene expression of compound treated samples over negative control of Day 7. M refers to negative control without RANKL treatment and MR refers to positive control with RANKL treatment. All compound treated samples were treated with RANKL as well. The concentrations of compounds used were same as the compound screening in Chapter 3 (**Table 3.1**). Data plotted represents the mean plus SD of three biological replicates.*

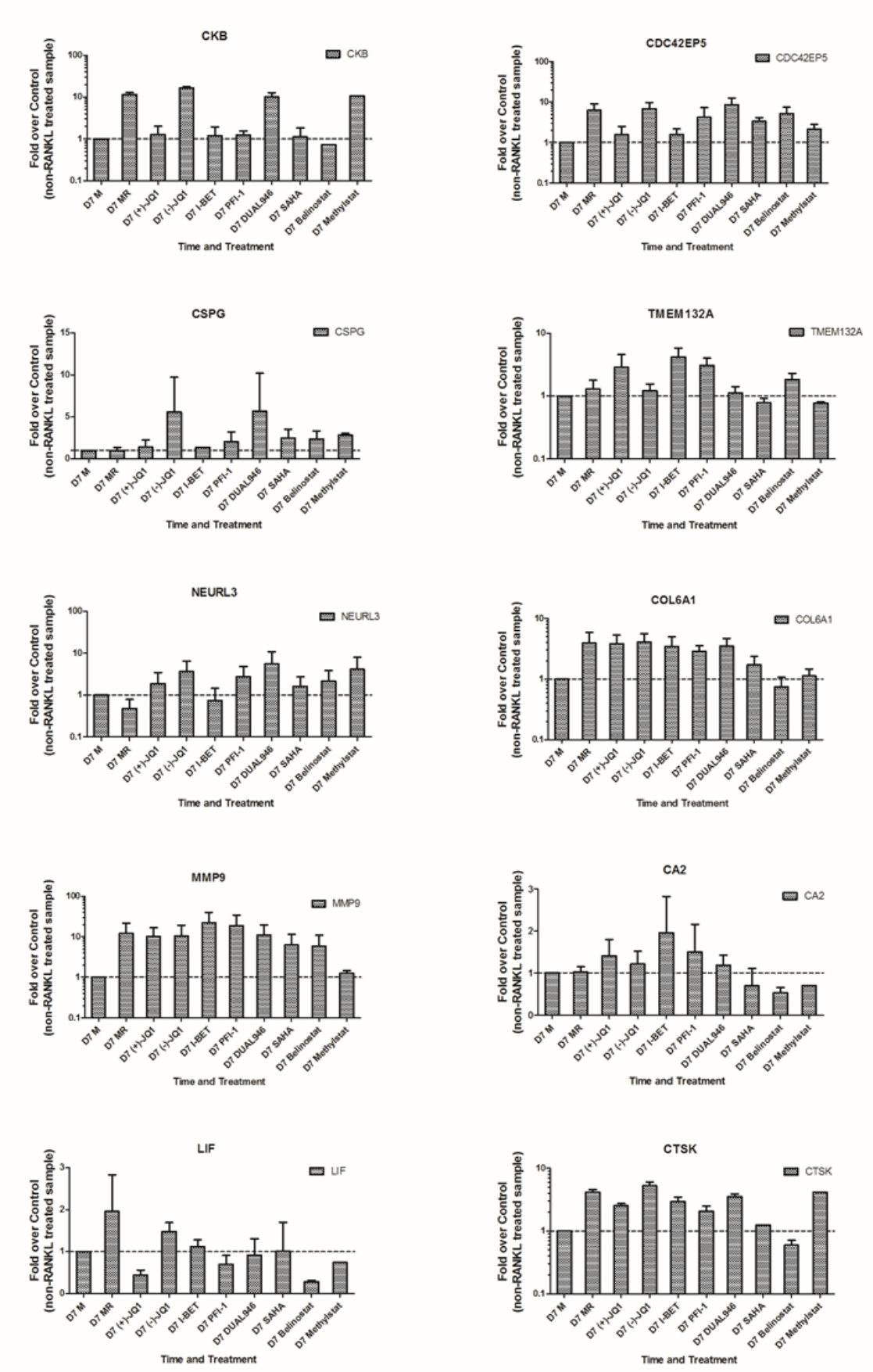
CKB
CDC42EP5
CSPG
TMEM132A
NEURL3
COL6A1
MMP9
CA2
LIF
CTSK
Fold over Control (non-RANKL treated sample)
Time and Treatment
D7 M
D7 MR
D7 (+)-JQ1
D7 (-)-JQ1
D7 I-BET
D7 PFI-1
D7 DUAL946
D7 SAHA
D7 Belinostat
D7 Methylstat

a)

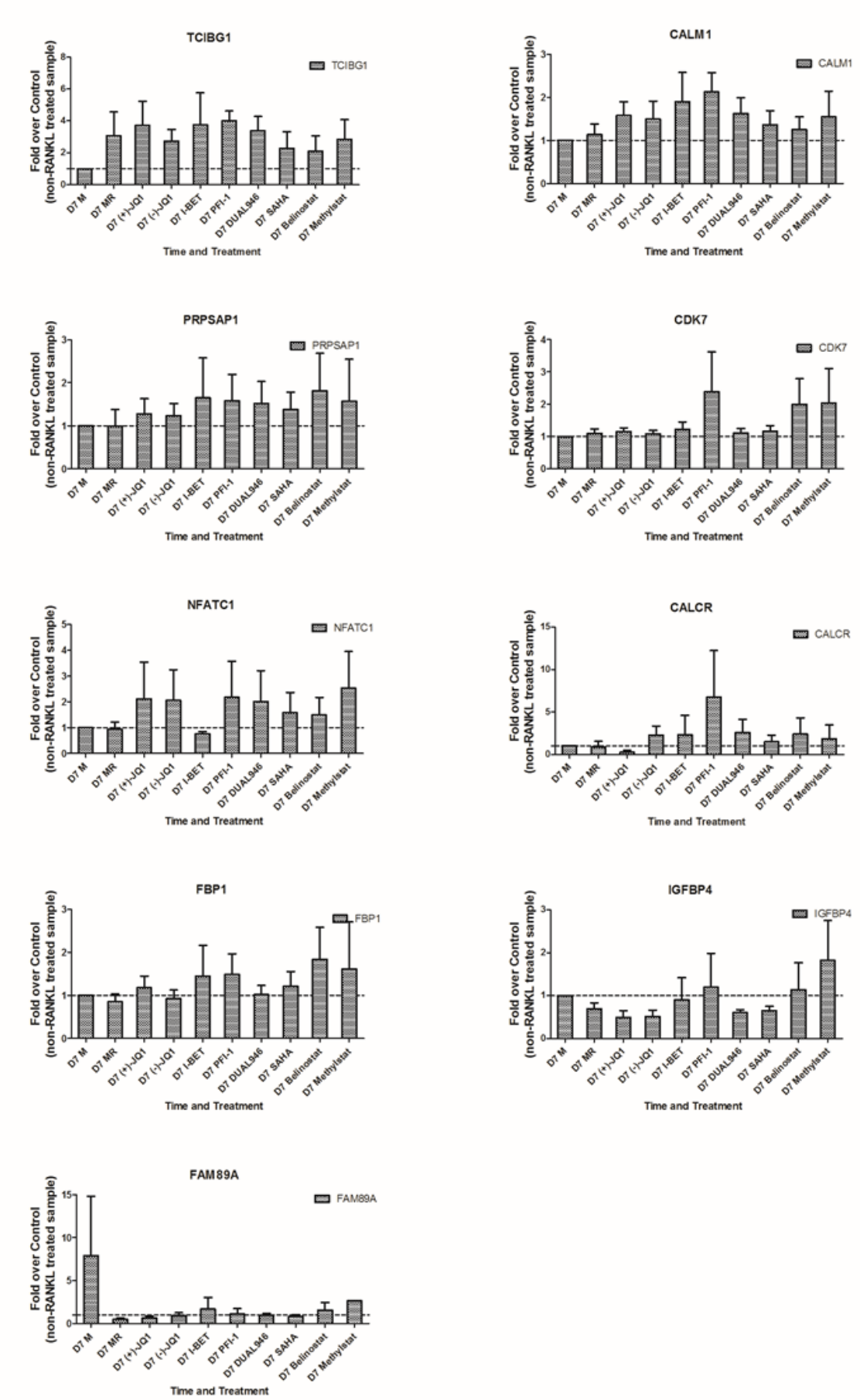
TCIBG1
TCIBG1
CALM1
CALM1
PRPSAP1
PRPSAP1
CDK7
CDK7
NFATC1
NFATC1
CALCR
CALCR
FBP1
FBP1
IGFBP4
IGFBP4
FAM89A
FAM89A
Fold over Control (non-RANKL treated sample)
Time and Treatment
D7 M
D7 MR
D7 (+)-JQ1
D7 (-)-JQ1
D7 I-BET
D7 PFI-1
D7 DUAL946
D7 SAHA
D7 Belinostat
D7 Methylstat

b)

Figure 4.3 (below) Fold change of gene expression in compound treated samples after 14 days of treatment

*Figure a and b showed the gene expression of compound treated samples over negative control of Day 14. M refers to negative control without RANKL treatment and MR refers to positive control with RANKL treatment. All compound treated samples were treated with RANKL as well. The concentrations of compounds used were same as the compound screening in Chapter 3 (**Table 3.1**). Data plotted represents the mean plus SD of three biological replicates.*

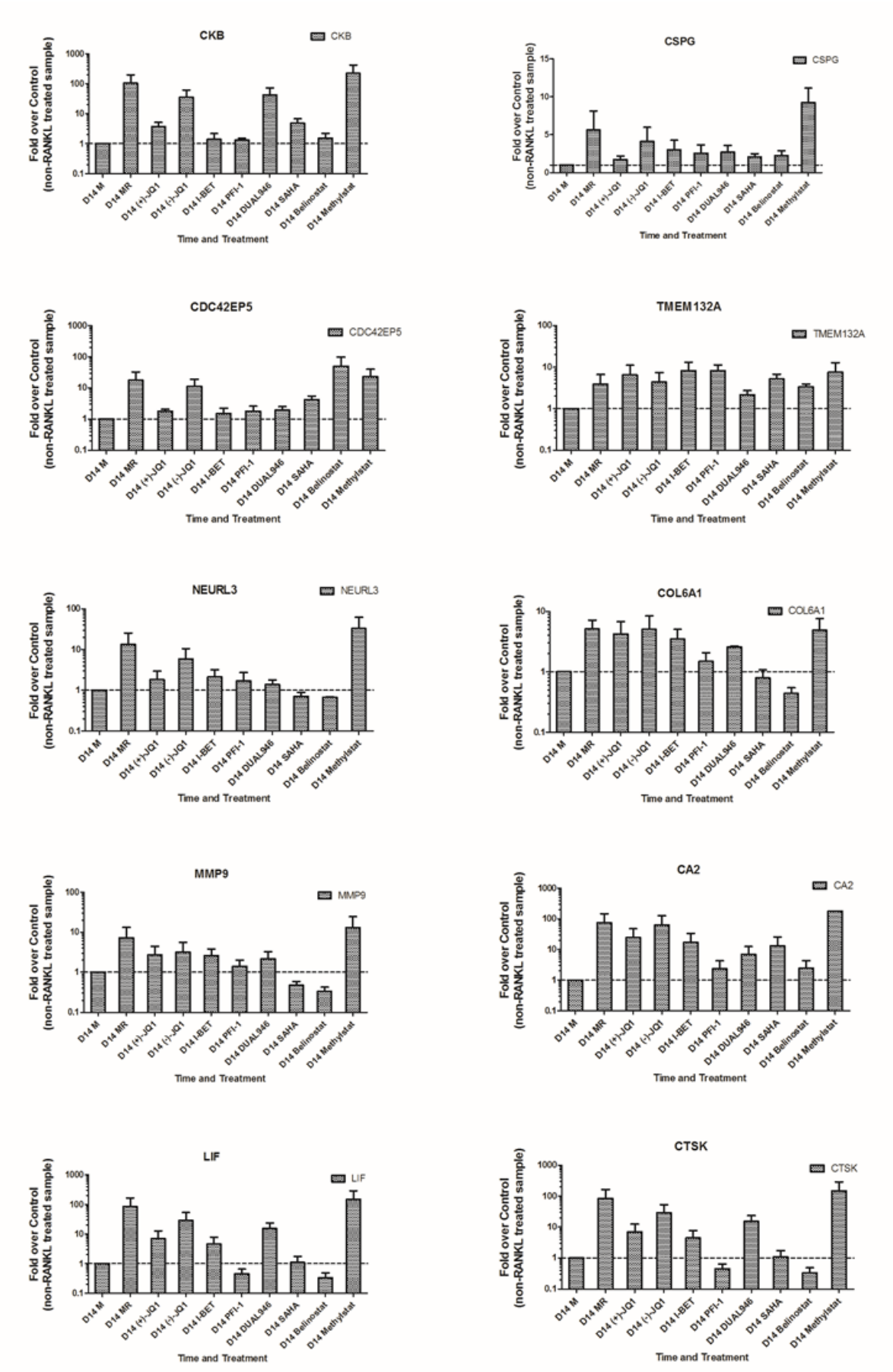
CKB
CKB
Fold over Control (non-RANKL treated sample)
1000
100
10
1
0.1
D14 M
D14 MR
D14 (+)-JQ1
D14 (-)-JQ1
D14 I-BET
D14 PFI-1
D14 DUAL946
D14 SAHA
D14 Belinostat
D14 Methylstat
Time and Treatment
CSPG
CSPG
Fold over Control (non-RANKL treated sample)
15
10
5
0
Time and Treatment
CDC42EP5
CDC42EP5
Fold over Control (non-RANKL treated sample)
Time and Treatment
TMEM132A
TMEM132A
Fold over Control (non-RANKL treated sample)
Time and Treatment
NEURL3
NEURL3
Fold over Control (non-RANKL treated sample)
Time and Treatment
COL6A1
COL6A1
Fold over Control (non-RANKL treated sample)
Time and Treatment
MMP9
MMP9
Fold over Control (non-RANKL treated sample)
Time and Treatment
CA2
CA2
Fold over Control (non-RANKL treated sample)
Time and Treatment
LIF
LIF
Fold over Control (non-RANKL treated sample)
Time and Treatment
CTSK
CTSK
Fold over Control (non-RANKL treated sample)
Time and Treatment

a)

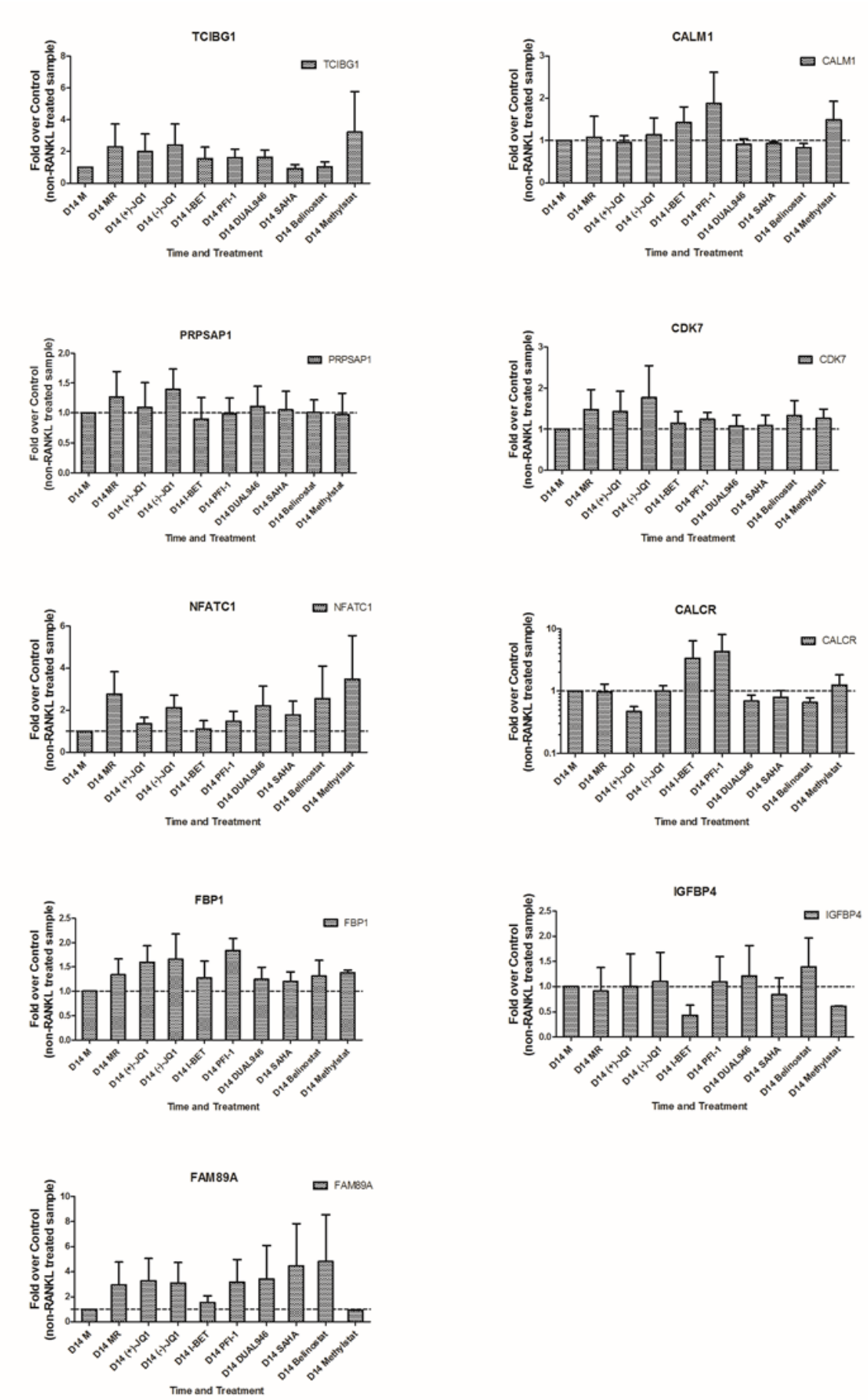
TCIBG1
TCIBG1
Fold over Control (non-RANKL treated sample)
Time and Treatment
CALM1
CALM1
PRPSAP1
PRPSAP1
CDK7
CDK7
NFATC1
NFATC1
CALCR
CALCR
FBP1
FBP1
IGFBP4
IGFBP4
FAM89A
FAM89A
D14 M
D14 MR
D14 (+)-JQ1
D14 (-)-JQ1
D14 I-BET
D14 PFI-1
D14 DUAL946
D14 SAHA
D14 Belinostat
D14 Methylstat

b)

4.4 Discussion

In this chapter, a RANKL gene card containing 20 genes has been established and validated. Some of these genes have clear validated roles in RANKL induced osteoclastogenesis, as reported previously in the literature (**Table 4.1**). These include for example CTSK and CA2, while the rest of these genes were novel targets, whose functions in osteoclastogenesis were still unclear, such as CKB and CSPG. These genes, based on their level and timing of expression, can be classified into early/intermediate markers. This RANKL gene card was useful for confirming the TRAP staining results of the osteoclast differentiation assay and for assessing the effect of the inhibitors in different stages of osteoclastogenesis. By comparing the three time points employed in analysis, which were Day 7, Day 14 and Day 21 after the monocytes were seeded, Day 14 was determined as the optimal time point to investigate the compound effects in osteoclast differentiation.

Based on the TRAP staining and dentine resorption results, eight compounds were selected from classes of bromodomain, HDAC and histone demethylase inhibitors. The elongated marcrophages-like cells showed that compounds such as (+)-JQ1 and I-BET (**Figure 3.5**) inhibited the osteoclastogenesis at an early stage. The reduction of gene expression of RANKL related genes in Day 7 qPCR results (**Figure 4.2**) confirms this conclusion. Moreover, almost all the Bromodomain and HDAC inhibitors, except DUAL946, suppress the gene expression on Day 7. By comparing the qPCR results, HDAC inhibitors, both SAHA and belinostat, normally showed stronger reduction in the gene expressions than Bromodomain inhibitors. Whereas HDAC inhibitors did not show inhibition for NFATc1, which is a transcription factor induced by NFκB in osteoclast precursors and regulates a number of genes

related to cell fusion (Takayanagi 2002, Ishida 2002 HC). Therefore, NFATc1 has been triggered by SAHA and belinostat while the TRAP staining results showed cell fusion has been inhibited in SAHA and belinostat treated samples (reduced over 90% osteoclast numbers, **Figure 3.2**).

However, the Day 7 and Day 14 qPCR results of RANKL gene card did not confirm the osteoclast inhibitory ability of methylstat, which is a histone demethylase inhibitor. In the TRAP staining assay in **Chapter 3**, methylstat treated samples showed a reduction of > 70% in osteoclast numbers compared to the positive controls (**Figure 3.2**). However, the expression level of resorption markers CTSK and TCIBG1 in methylstat treated sample was as high as the positive controls.

Although the qPCR analysis showed differences between the samples, all the BET bromodomain inhibitors ((+)-JQ1, I-BET and PFI-1) reduced the expression of common osteoclast differentiation markers, such as NFATc1 and CTSK, and some novel markers, such as CKB and CDC45EP5. Samples treated with (-)-JQ1, which is the inactive control analogue of (+)-JQ1, displayed a similar gene profile compared to the vehicle control (MR), which confirms that (+)-JQ1 has an on-target effect.

In particular, the mechanisms of the compound DUAL946, targeting both Bromodomain and HDAC genes, were not similar to either Bromodomain inhibitors or HDAC inhibitors. For example, DUAL946 treated samples show higher expression levels of CKB, which is a gene related with ATP synthesis within the cells, compared with samples treated with Bromodomain or HDAC inhibitors. Therefore, further studies need to be carried out to understand those differences in the mechanisms between compounds.

Taken together, the RANKL gene card has confirmed the inhibition in osteoclast differentiation of the compounds we selected except for methylstat. Importantly, the RANKL gene card analysis also indicates mechanistic differences for the mode of action of the compounds used. Although being a very useful rapid screening tool for analysis of osteoclastogenesis, with the limited number of genes that have been employed in the RANKL gene card, further studies need to be conducted to investigate the detailed functions of the selected compounds.

Chapter 5 Investigation of epigenetic inhibitors at transcriptomic level

5.1 Introduction

Some epigenetic inhibitors have shown their ability to reduce the cell viability of myeloma cells (**Figure 3.13** and **Figure 3.14**). However, the underlying mechanisms are still unclear. Several pathways of reduced cell viability have been studied in healthy and malignant cells, such as apoptosis, cell cycle arrest, senescence, autophagy and mitotic catastrophe (Okada and Mak 2004). For example, the tumour suppressor p53 is known as a key regulator of apoptosis. When the cells cannot repair DNA damage caused by genotoxic stress, the cells will undergo the process of apoptosis via the p53 pathway (Vogelstein, Lane, and Levine 2000).

The global analysis of mRNA expression used to be achieved by using the microarray which consists of thousands of DNA spots and measures the mRNA expression level by scanning the DNA spot hybridised with a cDNA sample. Compared with the microarray, RNA sequencing (RNAseq) is a relatively new and more efficient technology. RNA sequencing applies high-throughput next-generation technologies to sequence cDNA derived from extracted RNA and then to infer the gene expression level of mRNA. In this chapter, RNA sequencing was conducted in JJN3 myeloma cells to assess and understand the effects of selected compounds at transcriptomic level.

5.2 RNAseq reveals the gene expression regulated by selected epigenetic compounds

Six epigenetic compounds with different target enzymes were chosen based on the screening results in **Chapter 3** (**Figure 3.13** and **Figure 3.14**). JJN3 cells were selected as a representative myeloma cell line. Although the cell viability assay was done for a treatment length of 72 hours, we hypothesised the mRNA level changes occur in a much shorter period. Therefore, in this experiment, myeloma cells were treated with compounds for 24 hours. As stated in **Table 5.1**, the compound concentrations used in the treatment were around their IC_{80} value.

Table 5.1 Treatment information for compounds used in the experiment

Target	Target class	Compound name	Concentrations used in treatment	Treatment duration
Bromodomains	BET	(+)-JQ1	0.2uM	24hours
HDAC	Class 1	CXD101	0.2uM	24hours
HDAC/Bromo	BET/HDAC	DUAL946	10uM	24hours
HDAC	HDAC 8	Rocilinostat	3uM	24hours
DNMT	DNMT1/3	5-Aza-deoxy-cytidine	10uM	24hours
Histone demethylase	KDM6	GSK-J4	5uM	24hours

The bioinformatics analysis of the RNAseq data of these compound treated samples were conducted by group member Dr Reshma Nibhani (details of analysis in **Section 2.8**). **Figure 5.1** shows the number of upregulated and downregulated genes detected in each treatment, the analysis of which has the threshold of *p value* < 0.05 *and* $\log_2$ *fold change* > 1.5. After 24 hours treatment, GSK-J4, rocilinostat, CXD101 and DUAL946 induces upregulation or downregulation of over 500 genes in JJN3 myeloma cells, compared with cells treated with vehicle control DMSO.

However, most of the genes regulated by CXD101 and 5-Aza-deoxy-cytidine are upregulated, which may indicate a toxic effect of these compounds.

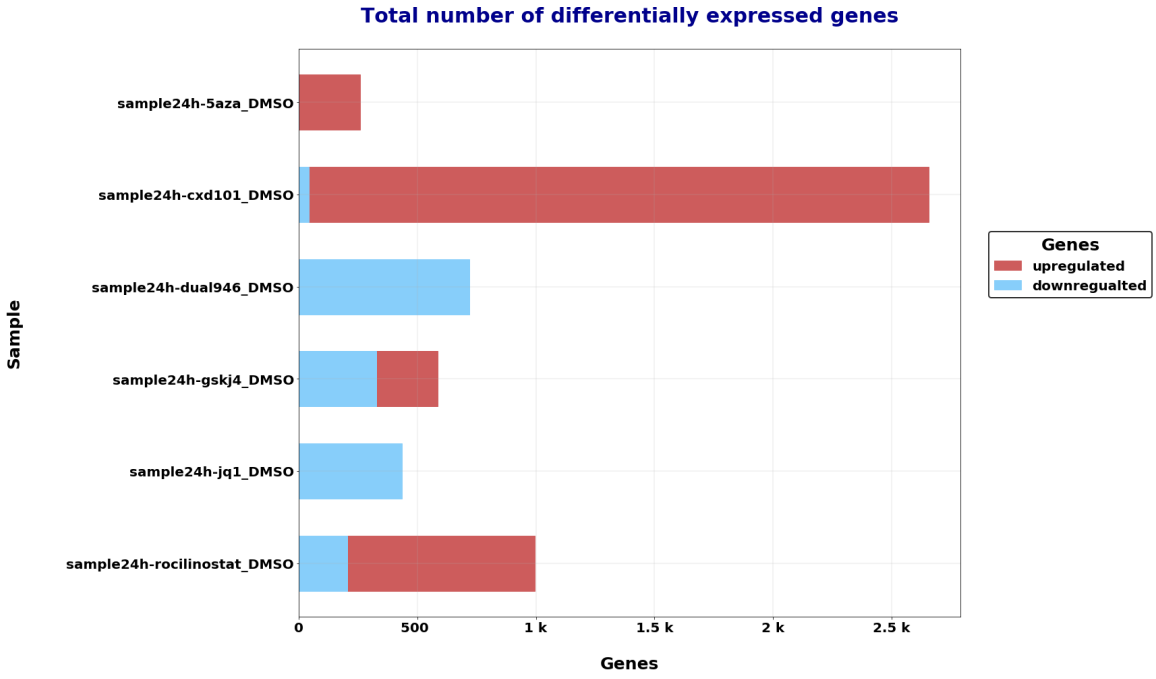

Figure 5.1 Summary of upregulated gene number and downregulated gene number for each treatment

The number of genes regulated by different compounds is ranging from hundreds to thousands. Most of the genes regulated by CXD101 and 5-Aza-deoxy-cytidine are upregulated. The threshold of the analysis is p value < 0.05 and log_2 fold change > 1.5.

5.2.1 Bromodomain inhibitors

(+)-JQ1 is a potent inhibitor mainly targeting BET family of bromodomain (including BRD2, BRD3 and BRD4), while DUAL946 can target both BET bromodomains and HDAC. Compared the regulated genes of samples treated by (+)-JQ1 and DUAL946

(**Figure 5.2**), there are over 600 genes significantly regulated by both (+)-JQ1 and DUAL946. By conducted pathway analysis using the Reactome pathway database, it has been found that most of the pathways highly regulated by (+)-JQ1 and DUAL946 are associated with cell cycle progression. This indicates that (+)-JQ1 and DUAL946 reduced the cell viability in myeloma cells by interrupted the cell cycle progress. The top ten upregulated and downregulated genes for both conditions are listed in **Table 5.4** and **Table 5.5**. However, the top regulated genes by these two compounds are not very similar. Moreover, the top regulated genes in the list are not closely related with the cell cycle progress as well. Therefore, the compounds induce cell cycle related pathways in a more general manner instead of highly inducing specific genes in the cell cycle related pathways.

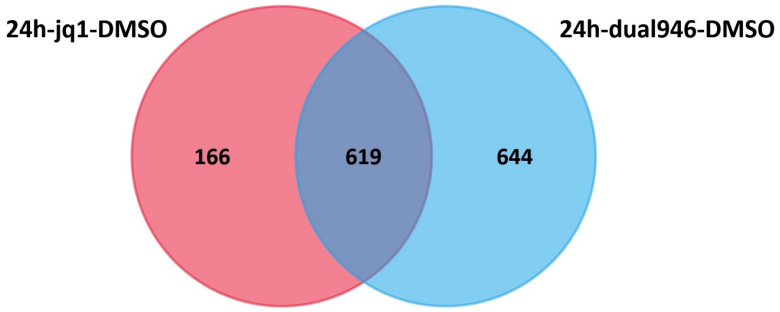

Figure 5.2 Overlapping of genes whose expression was regulated in (+)-JQ1 and DUAL946 treated samples

There are 619 genes are regulated by both (+)-JQ1 and DUAL946.

Table 5.2 Pathway analysis of regulated genes for (+)-JQ1 treated samples

Number	Pathway name	p value
1	Cell Cycle	1.37E-14
2	Cell Cycle, Mitotic	1.35E-13
3	Mitotic G1-G1/S phases	2.69E-11
4	Activation of E2F1 target genes at G1/S	5.69E-10
5	G1/S-Specific Transcription	5.69E-10
6	G1/S Transition	2.05E-08
7	DNA strand elongation	8.89E-08
8	Activation of ATR in response to replication stress	1.30E-07
9	Unwinding of DNA	4.91E-07
10	Activation of the pre-replicative complex	7.16E-07

There are several cell cycle related pathways regulated by (+)-JQ1. The pathway analysis was done using the Reactome pathway database

Table 5.3 Pathway analysis of regulated genes for DUAL946 treated samples

Number	Pathway name	p value
1	Mitotic G1-G1/S phases	1.46E-09
2	G1/S-Specific Transcription	9.15E-09
3	Activation of E2F1 target genes at G1/S	9.15E-09
4	G1/S Transition	9.91E-08
5	DNA strand elongation	1.10E-07
6	G0 and Early G1	1.71E-06
7	S Phase	2.29E-06
8	Unwinding of DNA	2.51E-06
9	DNA Replication	2.88E-06
10	Cell Cycle, Mitotic	4.38E-06

There are several cell cycle related pathways regulated by DUAL946. The pathway analysis was done using the Reactome pathway database

Table 5.4 Top ten upregulated and downregulated genes in (+)-JQ1 treated samples

Treatment	Gene	Description	log2_fold_change	p_value
(+)-JQ1	MFSD3	major facilitator superfamily domain containing 3 [Source:HGNC Symbol;Acc:HGNC:25157]	5.76	1.36E-08
	NBPF14	NBPF member 14 [Source:HGNC Symbol;Acc:HGNC:25232]	5.31	1.43E-03
	INTS4	integrator complex subunit 4 [Source:HGNC Symbol;Acc:HGNC:25048]	5.12	3.69E-03
	AL021997.3		4.98	4.79E-05
	AC005258.1		4.23	6.42E-03
	38596	septin 5 [Source:HGNC Symbol;Acc:HGNC:9164]	4.22	9.89E-95
	YPEL1	yippee like 1 [Source:HGNC Symbol;Acc:HGNC:12845]	4.03	9.21E-07
	C10orf142	chromosome 10 open reading frame 142 [Source:HGNC Symbol;Acc:HGNC:51236]	3.90	2.43E-41
	TBC1D3D	TBC1 domain family member 3D [Source:HGNC Symbol;Acc:HGNC:28944]	3.78	2.18E-06
	AL772284.2		3.68	3.21E-26
	HIRIP3	HIRA interacting protein 3 [Source:HGNC Symbol;Acc:HGNC:4917]	-8.06	2.01E-06
	PSMB7	proteasome subunit beta 7 [Source:HGNC Symbol;Acc:HGNC:9544]	-7.19	1.31E-03
	SPARCL1	SPARC like 1 [Source:HGNC Symbol;Acc:HGNC:11220]	-6.96	5.73E-03
	ALDH3B2	aldehyde dehydrogenase 3 family member B2 [Source:HGNC Symbol;Acc:HGNC:411]	-4.78	3.90E-03
	EID2	EP300 interacting inhibitor of differentiation 2 [Source:HGNC Symbol;Acc:HGNC:28292]	-4.56	2.38E-22
	DPT	dermatopontin [Source:HGNC Symbol;Acc:HGNC:3011]	-4.16	2.27E-04
	MATK	megakaryocyte-associated tyrosine kinase [Source:HGNC Symbol;Acc:HGNC:6906]	-4.10	8.34E-14
	CCDC127	coiled-coil domain containing 127 [Source:HGNC Symbol;Acc:HGNC:30520]	-3.82	3.88E-04
	CRH	corticotropin releasing hormone [Source:HGNC Symbol;Acc:HGNC:2355]	-3.71	8.73E-03
	ZHX1	zinc fingers and homeoboxes 1 [Source:HGNC Symbol;Acc:HGNC:12871]	-3.54	8.42E-05

The top genes regulated by (+)-JQ1 are not closely related with cell cycle progress.

Table 5.5 Top ten upregulated and downregulated genes in DUAL946 treated samples

Treatment	Gene	Description	log2_fold_change	p_value
DUAL946	PLA2G2C	phospholipase A2 group IIC [Source:HGNC Symbol;Acc:HGNC:9032]	6.45	8.73E-04
	SCN3B	sodium voltage-gated channel beta subunit 3 [Source:HGNC Symbol;Acc:HGNC:20665]	6.03	6.46E-03
	MFSD3	major facilitator superfamily domain containing 3 [Source:HGNC Symbol;Acc:HGNC:25157]	5.80	3.50E-10
	INTS4	integrator complex subunit 4 [Source:HGNC Symbol;Acc:HGNC:25048]	5.50	1.41E-04
	TMEM170A	transmembrane protein 170A [Source:HGNC Symbol;Acc:HGNC:29577]	5.17	9.63E-04
	NBPF14	NBPF member 14 [Source:HGNC Symbol;Acc:HGNC:25232]	5.11	1.86E-03
	LRRC29	leucine rich repeat containing 29 [Source:HGNC Symbol;Acc:HGNC:13605]	4.78	6.92E-03
	GAGE12E	G antigen 12E [Source:HGNC Symbol;Acc:HGNC:31905]	4.59	1.55E-04
	AC005258.1		4.42	7.20E-04
	AKAP3	A-kinase anchoring protein 3 [Source:HGNC Symbol;Acc:HGNC:373]	4.42	8.64E-04
	MCOLN2	mucolipin 2 [Source:HGNC Symbol;Acc:HGNC:13357]	-5.94	6.57E-21
	PSMB7	proteasome subunit beta 7 [Source:HGNC Symbol;Acc:HGNC:9544]	-5.48	9.02E-04
	EID2	EP300 interacting inhibitor of differentiation 2 [Source:HGNC Symbol;Acc:HGNC:28292]	-5.31	1.23E-28
	CCDC127	coiled-coil domain containing 127 [Source:HGNC Symbol;Acc:HGNC:30520]	-5.11	2.25E-05
	KISS1R	KISS1 receptor [Source:HGNC Symbol;Acc:HGNC:4510]	-4.81	1.55E-20
	DCAF4L1	DDB1 and CUL4 associated factor 4 like 1 [Source:HGNC Symbol;Acc:HGNC:27723]	-4.61	1.46E-20
	CYP26A1	cytochrome P450 family 26 subfamily A member 1 [Source:HGNC Symbol;Acc:HGNC:2603]	-4.45	2.47E-07
	HIRIP3	HIRA interacting protein 3 [Source:HGNC Symbol;Acc:HGNC:4917]	-4.33	2.50E-05
	MATK	megakaryocyte-associated tyrosine kinase [Source:HGNC Symbol;Acc:HGNC:6906]	-4.18	2.00E-17
	OR2T3	olfactory receptor family 2 subfamily T member 3 [Source:HGNC Symbol;Acc:HGNC:14727]	-4.12	2.28E-14

The top genes regulated by DUAL946 are not closely related with cell cycle progress.

5.2.2 HDAC inhibitors

There HDAC inhibitors CXD101, rocilinostat and DUAL946 were selected based on the screening results, and although the three compounds target different subclasses of HDAC, there were almost 900 genes showing overlapping changes in expression among the genes regulated by CXD101 and rocilinostat and about 200 genes overlapped among all three compounds (**Table 5.4**). The big difference between the number of overlapped genes may be caused by the multi-target effect of DUAL946. However, the pathway analysis for CXD101, rocilinostat and DUAL946 regulated genes are not very similar. The pathways mediated by CXD101 are more about immune responses, such as integrin and interleukin signalling, which may be caused by toxic effects or may be the actual effect of the compound. Rocilinostat and DUAL946 regulate more cell cycle related pathways (**Table 5.3, 5.4 and 5.5**). The top ten upregulated and downregulated genes for the three conditions are listed in **Table 5.5, Table 5.8** and **Table 5.9**. Interestingly, CD9 is the top one upregulated genes in the cells treated by CXD101 and rocilinostat. CD9 is a cell surface glycoprotein which complexes with integrins and other transmembrane 4 superfamily proteins. The interactions between CD9 and HDAC inhibitors CXD101 and rocilinostat is worthy to be investigated.

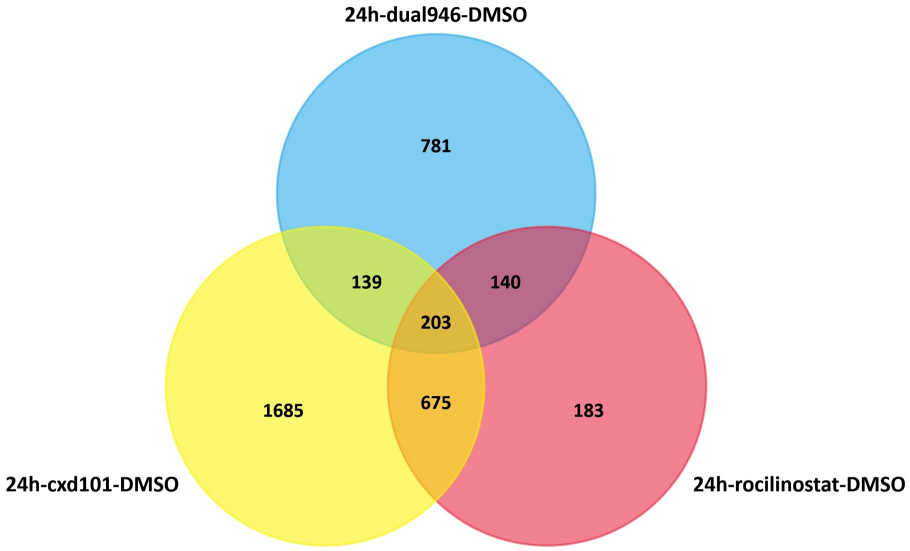

Figure 5.3 Overlapping of genes whose expression was regulated in CXD101, rocilinostat and DUAL946 treated samples

There are 203 genes regulated by CXD101, rocilinostat and DUAL946. There are 878 genes regulated by both CXD101 and rocilinostat.

Table 5.6 Pathway analysis of regulated genes for CXD101 treated samples

Number	Pathway name	p value
1	Interleukin-10 signaling	2.94E-05
2	Receptor-type tyrosine-protein phosphatases	9.04E-04
3	Integrin cell surface interactions	1.45E-03
4	ECM proteoglycans	1.59E-03
5	TP53 Regulates Transcription of Genes Involved in G1 Cell Cycle Arrest	3.20E-03
6	EPH-ephrin mediated repulsion of cells	3.21E-03
7	Syndecan interactions	4.32E-03
8	L1CAM interactions	6.11E-03
9	Interleukin-4 and 13 signaling	6.54E-03
10	MET activates PTK2 signaling	8.68E-03

There are immune response related pathways, such as IL-10, IL-4 and IL-13 pathways regulated by CXD101. The pathway analysis was done using the Reactome pathway database.

Table 5.7 Pathway analysis of regulated genes for rocilinostat treated samples

Number	Pathway name	p value
1	Activation of E2F1 target genes at G1/S	5.26E-06
2	G1/S-Specific Transcription	5.26E-06
3	Unwinding of DNA	7.00E-04
4	TP53 Regulates Transcription of Genes Involved in Cytochrome C Release	7.81E-04
5	G0 and Early G1	8.38E-04
6	TP53 Regulates Transcription of Cell Death Genes	2.99E-03
7	Mitotic G1-G1/S phases	3.10E-03
8	Intraflagellar transport	3.14E-03
9	Activation of the pre-replicative complex	3.83E-03
10	DNA strand elongation	6.91E-03

A few pathways regulated by rocilinostat are about cell cycle progress phases (such as G0, G1 and S phases). The pathway analysis was done using the Reactome pathway database.

Table 5.8 Top ten upregulated and downregulated genes in CXD101 treated samples

Treatment	Gene	Description	log2_fold_change	p_value
CXD101	CD9	CD9 molecule [Source:HGNC Symbol;Acc:HGNC:1709]	9.42	2.49E-18
	COG6	component of oligomeric golgi complex 6 [Source:HGNC Symbol;Acc:HGNC:18621]	9.37	3.61E-18
	BCAN	brevican [Source:HGNC Symbol;Acc:HGNC:23059]	9.17	1.17E-15
	ZNF385A	zinc finger protein 385A [Source:HGNC Symbol;Acc:HGNC:17521]	9.09	1.47E-15
	WFIKKN2	WAP, follistatin/kazal, immunoglobulin, kunitz and netrin domain containing 2 [Source:HGNC Symbol;Acc:HGNC:30916]	9.08	2.01E-30
	H1FX	H1 histone family member X [Source:HGNC Symbol;Acc:HGNC:4722]	9.07	1.08E-14
	BDH1	3-hydroxybutyrate dehydrogenase 1 [Source:HGNC Symbol;Acc:HGNC:1027]	8.96	1.25E-14
	GHR	growth hormone receptor [Source:HGNC Symbol;Acc:HGNC:4263]	8.82	1.62E-13
	RAB28	RAB28, member RAS oncogene family [Source:HGNC Symbol;Acc:HGNC:9768]	8.81	6.98E-13
	TNC	tenascin C [Source:HGNC Symbol;Acc:HGNC:5318]	8.70	8.02E-36
	CSF2RB	colony stimulating factor 2 receptor beta common subunit [Source:HGNC Symbol;Acc:HGNC:2436]	-3.55	2.13E-16
	IGLL1	immunoglobulin lambda like polypeptide 1 [Source:HGNC Symbol;Acc:HGNC:5870]	-3.46	3.22E-21
	F2RL3	F2R like thrombin/trypsin receptor 3 [Source:HGNC Symbol;Acc:HGNC:3540]	-2.38	5.06E-15
	PIP	prolactin induced protein [Source:HGNC Symbol;Acc:HGNC:8993]	-2.37	8.89E-21
	GPR68	G protein-coupled receptor 68 [Source:HGNC Symbol;Acc:HGNC:4519]	-2.19	2.12E-05
	FAS	Fas cell surface death receptor [Source:HGNC Symbol;Acc:HGNC:11920]	-2.13	9.37E-07
	OSTN	osteocrin [Source:HGNC Symbol;Acc:HGNC:29961]	-2.06	3.34E-14
	EN1	engrailed homeobox 1 [Source:HGNC Symbol;Acc:HGNC:3342]	-2.05	1.17E-13
	SYS1-DBNDD2	SYS1-DBNDD2 readthrough (NMD candidate) [Source:HGNC Symbol;Acc:HGNC:33535]	-2.03	2.89E-17
	PLCB3	phospholipase C beta 3 [Source:HGNC Symbol;Acc:HGNC:9056]	-2.02	3.00E-09

The top 10 upregulated genes have the expression change over 200 folds vs DMSO controls while the top 10 downregulated genes have the expression change only about 4-16 folds vs DMSO controls.

Table 5.9 Top ten upregulated and downregulated genes in rocilinostat treated samples

Treatment	Gene	Description	log2_fold_change	p_value
Rocilinostat	CD9	CD9 molecule [Source:HGNC Symbol;Acc:HGNC:1709]	9.01	2.71E-18
	CYP3A4	cytochrome P450 family 3 subfamily A member 4 [Source:HGNC	8.69	2.58E-15
	MYCN	MYCN proto-oncogene, bHLH transcription factor [Source:HGNC Symbol;Acc:HGNC:7559]	8.20	4.87E-11
	ZNF544	zinc finger protein 544 [Source:HGNC Symbol;Acc:HGNC:16759]	8.04	7.32E-10
	ZBTB41	zinc finger and BTB domain containing 41 [Source:HGNC Symbol;Acc:HGNC:24819]	7.97	2.53E-09
	COG6	component of oligomeric golgi complex 6 [Source:HGNC Symbol;Acc:HGNC:18621]	7.96	1.96E-09
	H1FX	H1 histone family member X [Source:HGNC Symbol;Acc:HGNC:4722]	7.94	2.77E-09
	BDH1	3-hydroxybutyrate dehydrogenase 1 [Source:HGNC Symbol;Acc:HGNC:1027]	7.88	6.85E-09
	TNC	tenascin C [Source:HGNC Symbol;Acc:HGNC:5318]	7.66	1.17E-31
	CHRD	chordin [Source:HGNC Symbol;Acc:HGNC:1949]	7.65	2.50E-07
	CSF2RB	colony stimulating factor 2 receptor beta common subunit [Source:HGNC Symbol;Acc:HGNC:2436]	-4.52	4.41E-34
	SAGE1	sarcoma antigen 1 [Source:HGNC Symbol;Acc:HGNC:30369]	-4.05	3.49E-04
	IGLL1	immunoglobulin lambda like polypeptide 1 [Source:HGNC Symbol;Acc:HGNC:5870]	-4.01	2.24E-39
	CCDC127	coiled-coil domain containing 127 [Source:HGNC Symbol;Acc:HGNC:30520]	-3.71	1.71E-03
	KCNE1B	potassium voltage-gated channel subfamily E regulatory subunit 1B [Source:HGNC Symbol;Acc:HGNC:52280]	-3.29	2.99E-55
	IL27RA	interleukin 27 receptor subunit alpha [Source:HGNC Symbol;Acc:HGNC:17290]	-3.27	3.83E-64
	MCOLN2	mucolipin 2 [Source:HGNC Symbol;Acc:HGNC:13357]	-3.25	2.69E-11
	GPR68	G protein-coupled receptor 68 [Source:HGNC Symbol;Acc:HGNC:4519]	-3.21	1.13E-13
	ZBTB43	zinc finger and BTB domain containing 43 [Source:HGNC Symbol;Acc:HGNC:17908]	-3.19	5.80E-35
	AC003002.4		-2.95	4.24E-10

The top 10 upregulated genes have larger expression differences than top 10 downregulated genes.

5.2.3 DNMT inhibitor

5-Aza-deoxy-cytidine, which targets both DNA methyltransferase (DNMT)1 and DNMT3, was selected from the compound screening as a representative compound for a DNMT inhibitor. After 24 hours treatment, there were only a few genes which had been highly upregulated and even fewer genes downregulated by 5-Aza-deoxy-cytidine (**Figure 5.1**). The pathway analysis showed most of the pathways regulated by the 5-Aza-deoxy-cytidine are about immune response and two pathways are related to the G1 phase of cell cycle (**Table 5.6**). The top ten upregulated and downregulated genes by 5-Aza-deoxy-cytidine are listed in **Table 5.11**.

Table 5.10 Pathway analysis of regulated genes for 5-Aza-deoxy-cytidine treated samples

Number	Pathway name	p value
1	Interleukin-4 and 13 signaling	4.76E-10
2	Cytokine Signaling in Immune system	4.06E-06
3	Interleukin-10 signaling	1.33E-05
4	Signaling by Interleukins	6.63E-05
5	Interferon alpha/beta signaling	5.99E-04
6	Immune System	7.95E-04
7	Interferon Signaling	8.54E-04
8	Interferon gamma signaling	9.05E-04
9	Cyclin D associated events in G1	2.90E-03
10	G1 Phase	2.90E-03

There are immune response and cell cycle related pathways regulated by 5-Aza-deoxy-cytidine. The pathway analysis was done using the Reactome pathway database.

Table 5.11 Top ten upregulated and downregulated genes in 5-Aza-deoxy-cytidine treated samples

Treatment	Gene	Description	log2_fold_change	p_value
5-Aza-deoxy-cytidine	THAP2	THAP domain containing 2 [Source:HGNC Symbol;Acc:HGNC:20854]	7.40	1.24E-04
	ZNF544	zinc finger protein 544 [Source:HGNC Symbol;Acc:HGNC:16759]	7.20	9.45E-04
	PGPEP1	pyroglutamyl-peptidase I [Source:HGNC Symbol;Acc:HGNC:13568]	7.15	1.62E-03
	WFIKKN2	WAP, follistatin/kazal, immunoglobulin, kunitz and netrin domain containing 2 [Source:HGNC Symbol;Acc:HGNC:30916]	6.35	4.07E-06
	FUT1	fucosyltransferase 1 (H blood group) [Source:HGNC Symbol;Acc:HGNC:4012]	5.87	8.64E-34
	LRRC37A3	leucine rich repeat containing 37 member A3 [Source:HGNC Symbol;Acc:HGNC:32427]	4.97	2.31E-04
	EPHB6	EPH receptor B6 [Source:HGNC Symbol;Acc:HGNC:3396]	4.97	5.94E-04
	AL021997.3		4.97	4.60E-04
	KCTD3	potassium channel tetramerization domain containing 3 [Source:HGNC Symbol;Acc:HGNC:21305]	4.77	6.64E-17
	TNC	tenascin C [Source:HGNC Symbol;Acc:HGNC:5318]	4.71	4.73E-03
	ZNF251	zinc finger protein 251 [Source:HGNC Symbol;Acc:HGNC:13045]	-1.89	5.49E-07
	ATXN7L1	ataxin 7 like 1 [Source:HGNC Symbol;Acc:HGNC:22210]	-1.74	2.74E-03
	E2F5	E2F transcription factor 5 [Source:HGNC Symbol;Acc:HGNC:3119]	-1.55	6.44E-03
	STEAP3	STEAP3 metalloreductase [Source:HGNC Symbol;Acc:HGNC:24592]	-1.33	3.47E-04
	FAM155B	family with sequence similarity 155 member B [Source:HGNC Symbol;Acc:HGNC:30701]	-1.30	6.34E-04
	SH3BGRL2	SH3 domain binding glutamate rich protein like 2 [Source:HGNC Symbol;Acc:HGNC:15567]	-1.28	6.17E-03
	POLR3G	RNA polymerase III subunit G [Source:HGNC Symbol;Acc:HGNC:30075]	-1.26	5.97E-03
	CENPC	centromere protein C [Source:HGNC Symbol;Acc:HGNC:1854]	-1.24	1.29E-05
	GABRG1	gamma-aminobutyric acid type A receptor gamma1 subunit [Source:HGNC Symbol;Acc:HGNC:4086]	-1.21	4.41E-03
	SOX2	SRY-box 2 [Source:HGNC Symbol;Acc:HGNC:11195]	-1.19	2.84E-07

The top 10 upregulated genes have much larger expression differences than top 10 downregulated genes.

5.2.4 Histone demethylase

GSK-J4 is a potent KDM6 and KDM5 inhibitor which showed inhibition in all six myeloma cell lines. The pathway analysis of genes regulated by GSK-J4 indicates the GSK-J4 induces stress response related apoptosis and cellular response to zinc ion (**Table 5.7**). Furthermore, **Table 5.13** shows that several genes of the metallothionein family have been highly activated by GSK-J4. Metallothioneins (MTs) are essential for maintaining the cellular metal ion (such as zinc ion) homeostasis (Davis and Cousins 2000). RNAseq and microarray analysis for GSK-J4 in myeloma cells has been conducted previously by our group member Dr Peter Cain and Dr Edward Hookway. This RNA sequencing result is consistent with the previous data, which further confirms that GSK-J4 reduces cell viability of myeloma cells by upregulating MTs and inducing the stress response and apoptosis.

Table 5.12 Pathway analysis of regulated genes for GSK-J4 treated samples

Number	Pathway name	p value
1	Cellular response to zinc ion	1.12E-12
2	Response to stress	4.22E-12
3	Intrinsic apoptotic signaling pathway in response to endoplasmic reticulum stress	4.28E-12
4	Single-organism metabolic process	1.47E-11
5	Organophosphate metabolic process	2.02E-11
6	Negative regulation of growth	3.42E-11
7	Single-organism cellular process	5.66E-11
8	Cellular response to metal ion	7.75E-11
9	Response to stimulus	9.75E-11
10	Granulocyte chemotaxis	2.15E-10

The stress response and cellular response to zinc ion turns out to be the top regulated pathways by GSK-J4. The pathway analysis was done using the Metacore

database in order to keep consistent with the RNAseq analysis from Dr Edward Hookway.

Table 5.13 Top ten upregulated and downregulated genes in GSK-J4 treated samples

Treatment	Gene	Description	log2_fold_change	p_value
GSK-J4	MT1H	metallothionein 1H [Source:HGNC Symbol;Acc:HGNC:7400]	11.19	6.65E-55
	MT1G	metallothionein 1G [Source:HGNC Symbol;Acc:HGNC:7399]	9.84	2.28E-57
	MT1M	metallothionein 1M [Source:HGNC Symbol;Acc:HGNC:14296]	9.76	1.54E-52
	MT1B	metallothionein 1B [Source:HGNC Symbol;Acc:HGNC:7394]	9.41	4.07E-20
	MT1E	metallothionein 1E [Source:HGNC Symbol;Acc:HGNC:7397]	8.10	4.96E-07
	GDF15	growth differentiation factor 15 [Source:HGNC Symbol;Acc:HGNC:30142]	7.58	6.43E-06
	TPSAB1	tryptase alpha/beta 1 [Source:HGNC Symbol;Acc:HGNC:12019]	7.57	6.48E-06
	INHBE	inhibin beta E subunit [Source:HGNC Symbol;Acc:HGNC:24029]	7.46	1.32E-100
	UNC5B	unc-5 netrin receptor B [Source:HGNC Symbol;Acc:HGNC:12568]	7.04	6.41E-11
	MT1HL1	metallothionein 1H like 1 [Source:HGNC Symbol;Acc:HGNC:31864]	6.97	2.10E-03
	MT-CO1	mitochondrially encoded cytochrome c oxidase I [Source:HGNC	-7.17	2.23E-76
	OCA2	OCA2 melanosomal transmembrane protein [Source:HGNC Symbol;Acc:HGNC:8101]	-6.87	2.14E-02
	MT-ND3	mitochondrially encoded NADH:ubiquinone oxidoreductase core subunit 3 [Source:HGNC Symbol;Acc:HGNC:7458]	-6.65	1.47E-76
	MT-CO2	mitochondrially encoded cytochrome c oxidase II [Source:HGNC	-6.63	2.01E-143
	MT-CO3	mitochondrially encoded cytochrome c oxidase III [Source:HGNC	-6.58	0.00E+00
	MT-ND4L	mitochondrially encoded NADH:ubiquinone oxidoreductase core subunit 4L [Source:HGNC Symbol;Acc:HGNC:7460]	-6.52	0.00E+00
	MT-CYB	mitochondrially encoded cytochrome b [Source:HGNC Symbol;Acc:HGNC:7427]	-6.45	2.92E-148
	MT-ND6	mitochondrially encoded NADH:ubiquinone oxidoreductase core subunit 6 [Source:HGNC Symbol;Acc:HGNC:7462]	-6.26	2.42E-149
	MT-ND4	mitochondrially encoded NADH:ubiquinone oxidoreductase core subunit 4 [Source:HGNC Symbol;Acc:HGNC:7459]	-6.25	7.51E-265
	MT-ATP6	mitochondrially encoded ATP synthase 6 [Source:HGNC Symbol;Acc:HGNC:7414]	-6.18	0.00E+00

Several members of metallothionein family are highly upregulated by the treatment of GSK-J4.

5.3 Discussion

In this chapter, RNAseq was conducted to investigate the underlying mechanisms of six epigenetic inhibitors which were selected based on the compound screening results in **Chapter 3**. It is not surprising that the analysis shows there are some overlapping genes between inhibitors targeting the same enzyme class (Bromodomains and HDACs). Moreover, the pathway analysis demonstrates that different compounds have distinct mechanisms to inhibit the myeloma cell growth. However, CXD101 and 5-Aza-deoxy-cytidine have been suggested to have a possible toxic effect on the myeloma cells rather than directly inhibit the cell growth while both compounds shows induction of immune response related pathways. The toxic effect might be caused by the high concentration or the biological mechanism of the compound, which needs further confirmation.

(+)-JQ1 is a very potent inhibitor in both myeloma viability assay and osteoclast differentiation assay. It has been reported to induce cell cycle arrest and cellular senescence in multiple myeloma (Delmore et al. 2011). The pathway analysis shows (+)-JQ1 affects cell cycle progression, which confirms the previous studies and increases the reliability of our RNAseq results. Moreover, DUAL946, which targets BET bromodomain as well, also showed effects on cell cycle progression. However, the top gene list of up- or down-regulated genes by the treatment of (+)-JQ1 and DUAL946 does not have many cell cycle progress associated genes. The impact of the bromodomain inhibitors on the cell cycle progress of myeloma cells may not be that significant. Therefore, the inhibition of BET bromodomain might induce cell cycle arrest in myeloma cells to some extent.

The RNAseq result of GSK-J4 is correspondence with the previous microarray and RANseq experiments which were done by our former group member Dr Edward Hookway. This further confirmed the reliability of the transcriptomic analysis in this chapter.

However, the transcriptomic analysis shown in this chapter is an experiment with some limitations. First of all, although many compounds showed inhibitory ability in both osteoclast differentiation assay and myeloma viability assay, only eight compounds were selected to be analysed in this chapter. Therefore, limited information of our compound library has been obtained. Secondly, the analysis in this chapter only includes the basic gene expression comparison and pathway analysis. The information of this RNAseq experiment could be explored further. Therefore, a few follow up works can be done in the future. For example, more compounds can be selected from the compound library. The overlapped genes regulated by the compounds (at least three to four) from the same target class can be investigated further. The pathway analysis based on the overlapped genes is worthy to do to reveal the function of the specific target enzymes. Furthermore, qPCR will be applied to validate the key genes involved in the important pathways, such as cell cycle related pathways. The qPCR will ensure the reliability of the transcriptomic analysis in this chapter.

Taken together, the RNAseq analysis indicates the possible underlying mechanisms of six selected epigenetic inhibitors. Some of the inhibitors, such as (+)-JQ1, has been well-studied in the past and our experiment confirms their results. Whereas some of the inhibitors, such as GSK-J4 and rocilinostat, which have not been deeply

investigated in myeloma cells, need us to further validate the mechanisms indicated by this RNAseq analysis.

Chapter 6 Effects of H3K27 demethylase inhibition in multiple myeloma cell lines

6.1 Introduction

Methylation of histone lysine residues plays an important role in the maintenance of both active and suppressed states of gene expression. Specifically, methylation of histone H3 at lysine residues -4, -36, and -79 (H3K4, H3K36, and H3K79) is involved in activation of transcription while methylation of histone H3 at lysine-9 and -27 (H3K9, H3K27) is associated with repression of transcription (Dawson and Kouzarides 2012, Barski et al. 2007). Methylated lysine residues of histone 3 lysine 27 (H3K27me) play essential roles in regulating gene expression by silencing through the polycomb-repressive complex (Bracken and Helin 2009).

By testing an inhibitor library against epigenetic targets in multiple myeloma cell lines (described in **Chapter 3)**, the demethylase inhibitors, especially the H3K27 demethylase inhibitor GSK-J4, showed strong inhibition in myeloma cells (see **Figure 3.13** and **Table 3.2**). In the screen, cell viability was not reduced by GSK-J5, an inactive form of GSK-J4, while another H3K27 demethylase inhibitor, KDOBA67, which is a derivative of GSK-J4, also showed inhibition of cell viability in all six myeloma cell lines. The combined results of GSK-J4, KDOBA67 and GSK-J5 in myeloma cell viability assays, therefore, suggests that reducing cell viability by GSK-J4 is caused by on-target effects rather than a generalised toxicity of the molecule.

The microarray and RNAseq, which was done by former group members Dr Peter Cain and Dr Edward Hookway, together with the RNAseq in **Chapter 6**, revealed GSK-J4 induced the expression of several members of the metallothionein (MT) family and activated ATF4-mediated stress response pathway in JJN3 myeloma cells. The genes, which are involved in the ATF4 stress response pathway and have identified by the microarray and RNAseq, include but are not limited to activating transcription factor 4 (ATF4), inhibin beta E subunit (INHBE), DNA damage inducible transcript 3 (DDIT3), asparagine synthetase (ASNS), arginosuccinate synthetase 1 (ASS1) and phosphoserine aminotransferase 1 (PSAT1).

The cellular stress response is a protective effect to a range of environmental and physiological stresses. ATF4 acts as a transcription factor to mediate the expression of genes involved in amino acid metabolism and resistance to oxidative stress (Harding et al. 2003). Moreover, ATF4 is able to activate the transcription of another transcription factor, CHOP, which is encoded by the gene DDIT3.

Cysteine is an important amino acid and is required for synthesis of proteins. It has been reported that the depletion of cysteine in HepG2/C3A human hepatocellular carcinoma cells activated the eIF2α kinase-mediated integrated stress response to inhibit global protein synthesis and increased expression of related genes, such as ATF4, INHBE and DDIT3 (Lee et al. 2008). Accordingly, the amino acid deprivation pathway, which is initiated by general control non-depressible 2 (GCN2) or eIF2 kinase 4, is mediated by a consequent increase in ATF4. It has been found that murine embryonic ATF4-/-fibroblasts required much higher amount of cysteine to defend against reduced glutathione depletion than wild-type cells (Harding et al.

2003), suggesting that ATF4-/-cells may be defective in import and/or metabolism of cysteine and be predisposed to oxidative stress.

In this chapter, GSK-J4 is studied in JJN3 myeloma cells for its cellular mechanisms following the results derived from cell viability assays and transcriptomic analyses.

6.2 GSK-J4 is a potent chemical probe for H3K27 demethylase

GSK-J1 is a potent and selective inhibitor for the H3K27 demethylases JMJD3 and UTX and is inactive against a panel of other demethylases of the jumonj (JMJ) family (Kruidenier et al. 2012). GSK-J4 is a pro-drug of GSK-J1 for cellular use (**Figure 6.1**) and is a cell permeable compound. GSK-J4 has been shown to reduce the viability of all six myeloma cell lines tested in this study (**Figure 3.13**). The EC_{50} of GSK-J4 in JJN3 myeloma cells is about 1.5uM as shown in **Figure 6.2** (details of assay in **Section 2.13**). The low EC_{50} of GSK-J4 indicates GSK-J4 can be used as a chemical probe to study the function of H3K27 demethylase in multiple myeloma. In this chapter, in order to investigate the effect of GSK-J4 in shorter time courses (6 hours to 24 hours), comparing with the 72 hours treatment used in the cell viability assay, the concentration of GSK-J4 used in JJN3 myeloma cells was 5μM, which is close to the EC_{80} value determined by the dose response experiment.

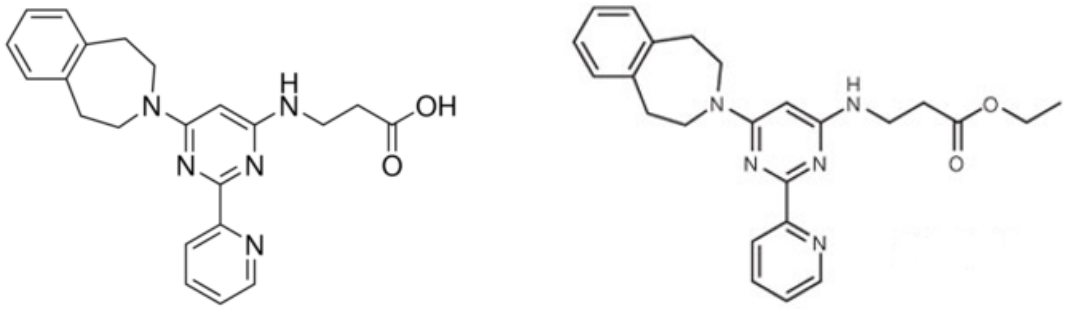

GSK-J1 GSK-J4

Figure 6.1 The chemical structures of GSK-J1 and GSK-J4

The chemical structures were obtained from Structural Genomics Consortium (http://www.thesgc.org/chemical-probes).

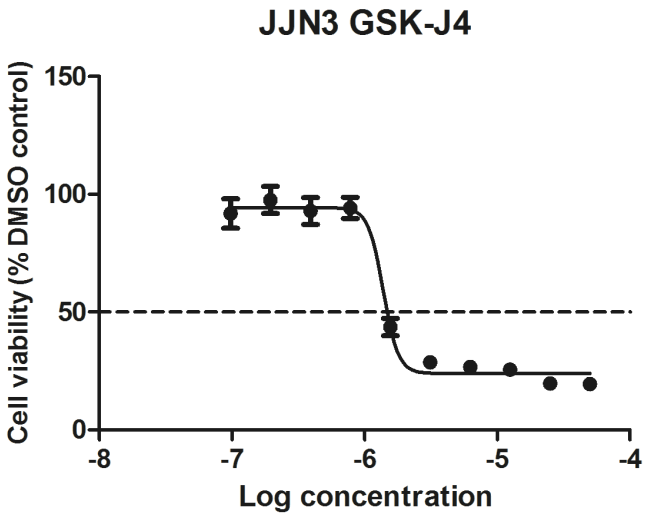

Figure 6.2 Dose response curve of GSK-J4 in JJN3 cells

The cells were treated with GSK-J4 or vehicle solvent (DMSO) for 72 hours and cell viability was measured by Prestoblue® assay. The EC_{50} value of GSK-J4 is about 5uM. Log concentration refers to mM concentration range. Data plotted represents three biological replicates plus/minus SD.

6.3 GSK-J4 induces metallothionein gene expression

The results of transcriptomic analysis for GSK-J4 treated JJN3 myeloma cells showed several members of the Metallothionein (MT) gene family to be induced. MTs constitute a family of cysteine-rich, low molecular weight proteins which are protective for the cells against metal toxicity and oxidative stress (Li, Chen, and Epstein 2004, Krizkova et al. 2012). Metallothionein 1X (MT1X) was chosen as a representative of the metallothionein family to validate this regulation in a time-course manner in JJN3 myeloma cells. As shown in **Figure 6.3**, GSK-J4 induced a large metallothionein response as measured by the expression of MT1X at 6h, by over 200 fold over the base line level. By 24 hours, the expression of MT1X had decreased from the high level observed at 6 hours in JJN3 cells.

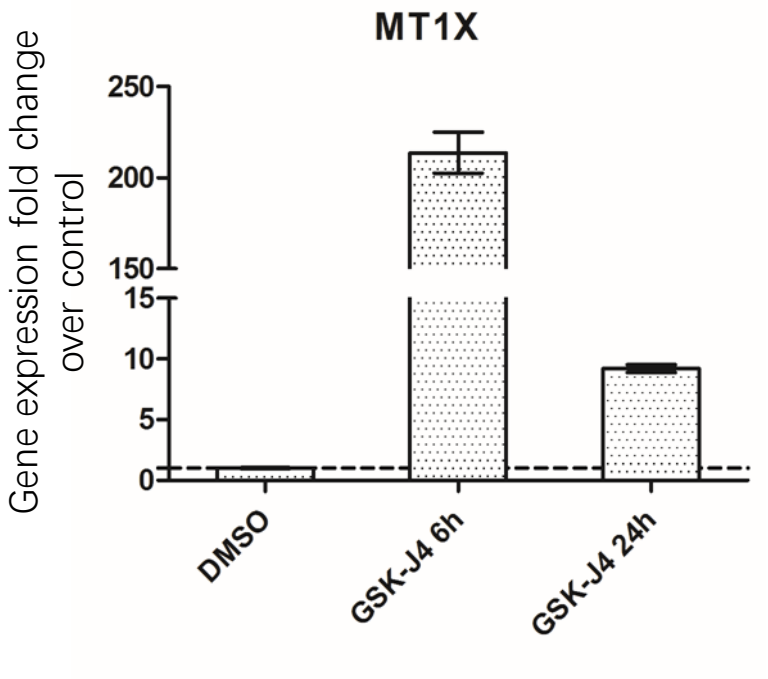

Figure 6.3 qPCR result of MT1X in JJN3 myeloma cells

JJN3 cells were treated with GSK-J4 (5μM) or DMSO (0.1%) for 6 or 24 hours. The expression level of MT1X was normalised to DMSO treated sample and ACTB served as a housekeeping gene. Under the treatment of GSK-J4, MT1X has the highest expression level at 6 hours post-treatment. Data plotted represents three biological replicates plus/minus SD.

6.4 GSK-J4 induces ATF4 stress response in myeloma cells

The ATF4-mediated stress response which might be induced by GSK-J4 was validated by qPCR. Based on the data from the microarray (which was done by Dr Peter Cain and Dr Edward Hookway) and the RNAseq in **Chapter 6**, genes were chosen to represent ATF4-mediated pathway include ATF4, INHBE, DDIT3, PSAT1, ASNS and ASS1. Two time points, 6 hours and 24 hours, were employed, and GSK-J4 is shown to induce the expression of ATF4 and its downstream targets, such as DDIT3, at 6 hours post-treatment with an increase up to 24 hours (**Figure 6.4**).

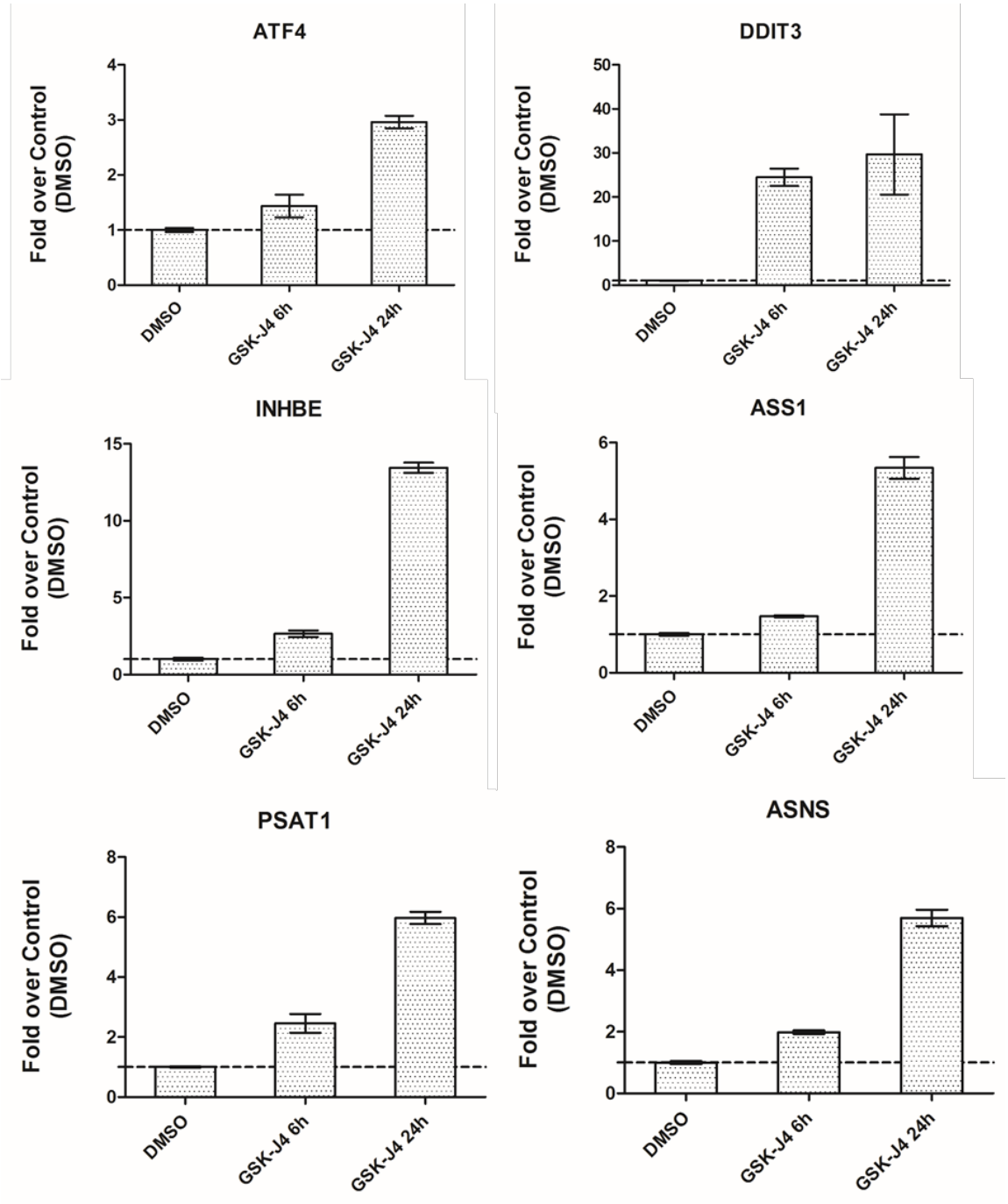

Figure 6.4 qPCR results of stress response related genes in JJN3 myeloma cells

JJN cells were treated with GSK-J4 (5μM) or DMSO (0.1%) for 6 or 24 hours. The expression level of each gene was normalised to DMSO treated sample and ACTB served as a housekeeping gene. The gene expression of all genes listed above have higher level at

24 hours post-treatment than 6 hours post-treatment. Data plotted represents three biological replicates plus/minus SD.

6.5 The overexpression of MT genes induces an ATF4 response

It was hypothesized that the observed expression of MT genes during GSK-J4 treatment may activate the ATF4 stress response, an observation which has not been reported yet in the literature. To validate this hypothesis, a construct coding for four metallothionein genes (MT1G, MT1H, MT1X and MT2A) genes separated by the self-cleaving porcine teschovirus-1 2A(p2A) peptide sequence (termed the “4xMT uebergene”) was generated by group member Dr Martin Philpott and transfected into a doxycycline-inducible flip-in HEK293 cell line (**Figure 6.5**) where stable lines were generated by Dr Federica Lari (Ludwig Institute, University of Oxford, UK). This was done after having first confirmed that GSK-J4 induces a metallothionein response and an ATF4-driven integrated stress response in HEK cells in a similar manner as in JJN3 myeloma cells.

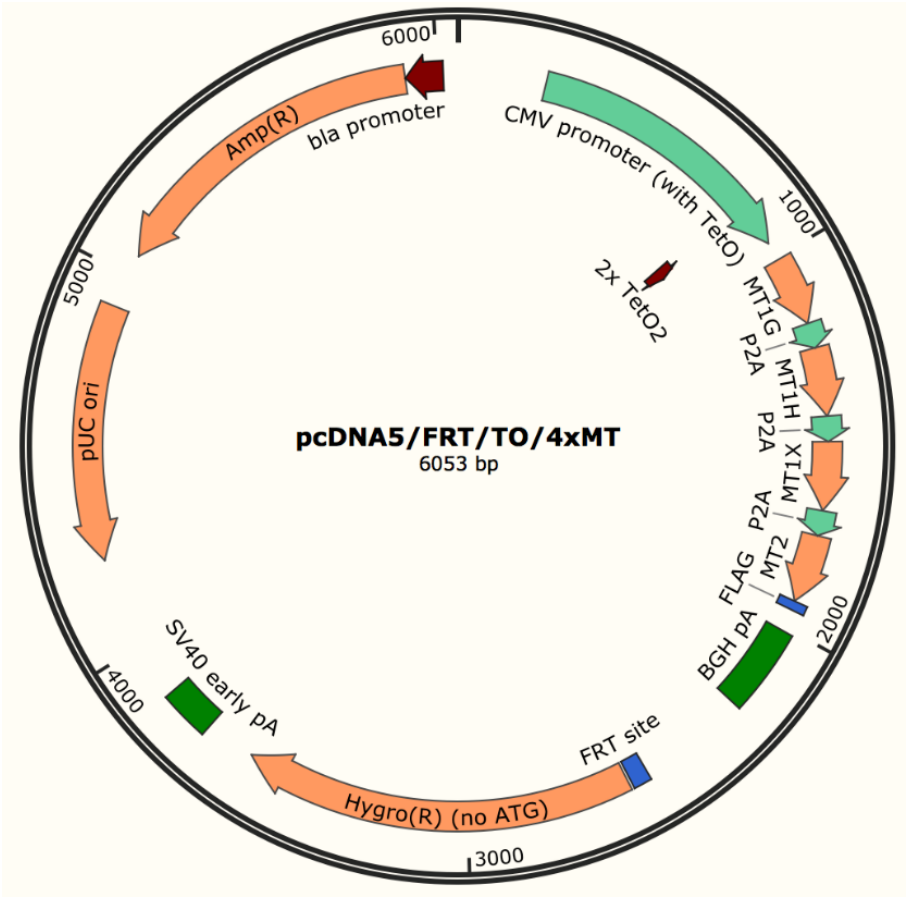

Figure 6.5 A plasmid map of "4xMT uebergene" (MT1G, MT1H, MT1X and MT2A), which was designed and generated by Dr Martin Philpott

A construct coding for four metallothionein genes (MT1G, MT1H, MT1X and MT2A) genes separated by the self-cleaving porcine teschovirus-1 2A(p2A) peptide sequence (termed the "4xMT uebergene") was generated by group member Dr Martin Philpott

The "4xMT uebergene" was induced by doxycycline and the expression level reached a peak after 24 hours doxycycline induction (**Figure 6.6)**. The expression of ATF4 was increased compared to untreated samples after 24 hours doxycycline induction, however, ATF4 was not activated at 6 hours and 12 hours post-treatment. The downstream targets of ATF4, such as DDIT3, INHBE and PSAT1, showed

increased expression level at 24 hours post-treatment as well. These results suggest that the overexpression of metallothionein genes may activate the ATF4 stress response. Compared with samples treated with GSK-J4, the activation of the ATF4 response was slower and weaker in samples with the expression of “4xMT uebergenes”.

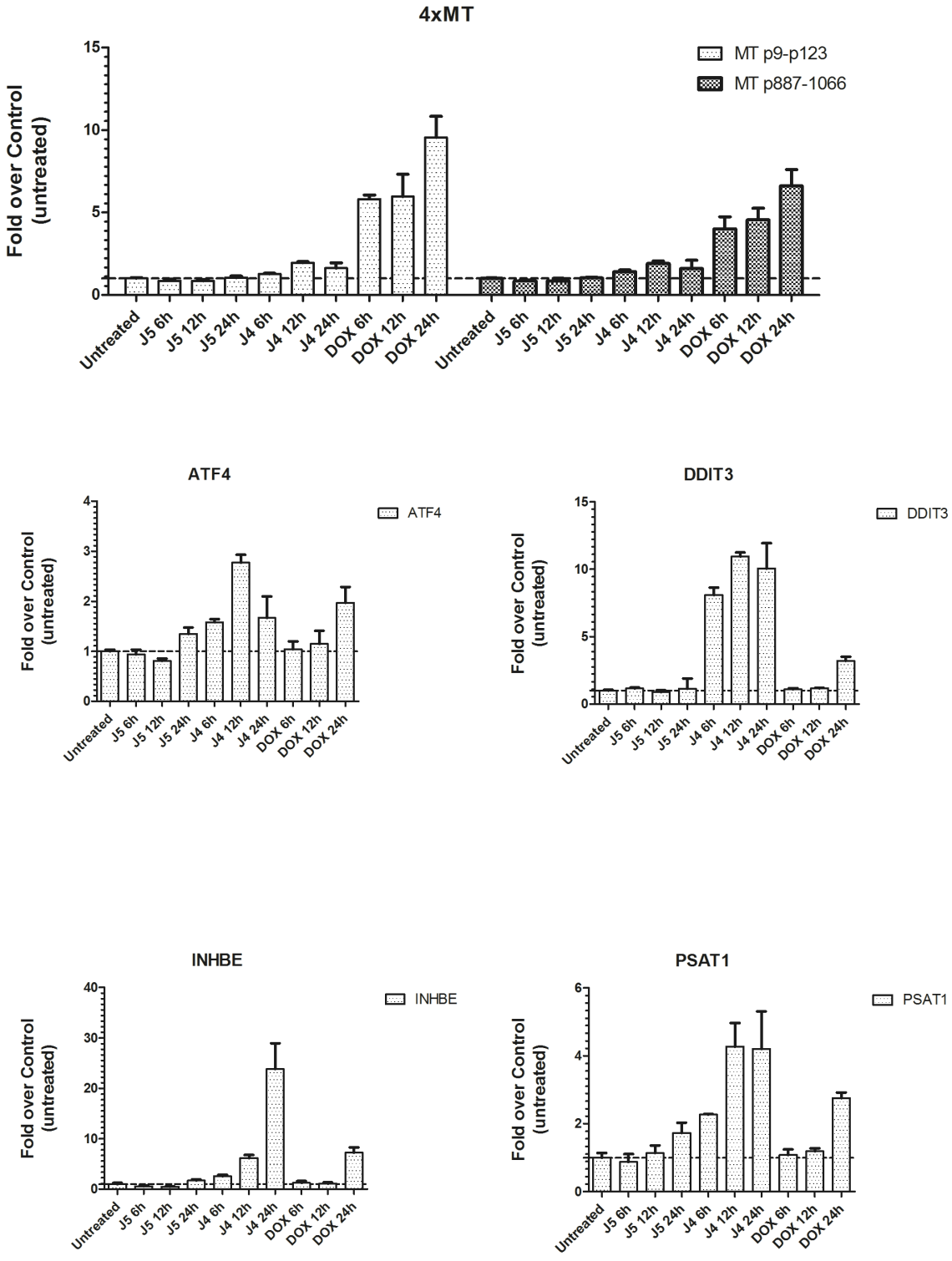

Figure 6.6 qPCR results of ATF4 target genes with overexpression of metallothionein genes in HEK293 cells

Flip-in HEK293 cells were treated with GSK-J4 (10μM), GSK-J5 (10μM) or doxycycline (10μg/ml) for 6, 12 and 24 hours. GSK-J5 is an inactive form of GSK-J4. The expression level of each gene was normalised to untreated samples and ACTB served as housekeeping gene. MT p9-p123 and MT p887-1066 refers to the starting and ending position of the" 4xMT uebergenes". The overexpression of metallothionein genes increases the expression of ATF4, DDIT3 and INHBE. Data plotted represents three biological replicates plus SD.

6.6 Overexpression of MTF1 induces metallothionein expression but does not activate an ATF4 response

Metal regulatory transcription factor 1 (MTF1) is a gene which encodes a transcription factor inducing the expression of metallothioneins and other genes involved in metal homeostasis within the cells (Grzywacz et al. 2015). To further confirm the association between MTs and ATF4 response, a plasmid containing the MTF1 gene was generated by team member Dr Martin Philpott and transfected into a doxycycline-inducible flip-in HEK293 cell line by Dr Federica Lari (Ludwig Institute, University of Oxford, UK). The induction of MTF1 expression induces the expression of MT1X at 6, 12 and 24 hours post-treatment. However, the expression of ATF4 and its downstream target genes did not change significantly after 24 hours post-treatment (**Figure 6.7**). Therefore, the transcription factor MTF1 does not induce ATF4 response.

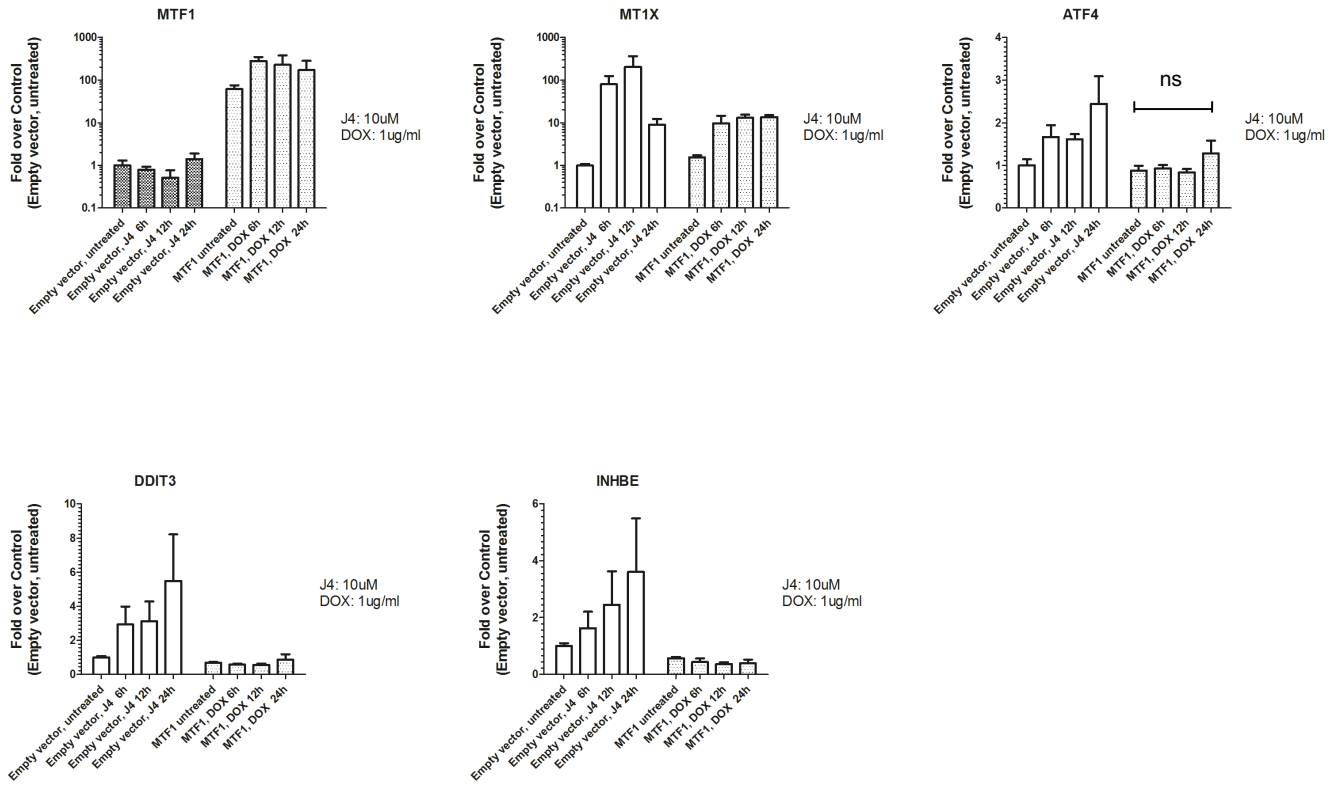

Figure 6.7 qPCR results of cells with overexpression of MTF1

Flip-in HEK293 cells were treated with GSK-J4 (10μM) or doxycycline (10μg/ml) for 6, 12 and 24 hours. The expression level of each gene was normalised to untreated samples and ACTB served as housekeeping gene. The overexpression of MTF1 does not induce ATF4 expression. Data plotted represent three biological replicates plus SD. Pairwised one-way ANOVA as applied to analyse the statistical significance. "ns" refers to no significance.

6.7 Cysteine plays an important role in GSK-J4 effects

Given the unusual high cysteine content of metallothioneins, we hypothesized that the local and transient cysteine depletion at the ribosome due to the metallothionein expression may be responsible for the activation of an ATF stress response. Therefore, three forms of cysteine were employed in this experiment, which are cysteine, N-acetyl-cysteine (NAC) and cystine (**Figure 6.8**).

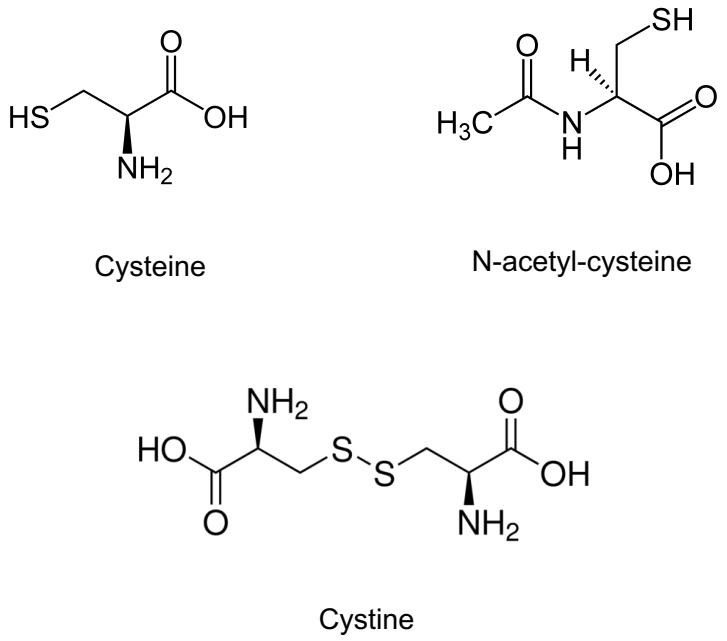

Figure 6.8 The chemical structures of cysteine, N-acetyl-cysteine and cystine

N-acetyl-cysteine (NAC) is the N-acetyl derivative of L-cysteine and cystine is a sulfur-containing derivative obtained from oxidation of cysteine amino acid thiol side chains.

As shown in **Figure 6.9**, the depletion of cysteine in the medium induces the expression of ATF4 and its downstream target genes in the absence of GSK-J4. The fold-change of ATF4 expression in the cysteine depletion sample with DMSO is

slightly higher than in GSK-J4 treated samples. By comparing the samples treated with GSK-J4, the expression level of ATF4 in samples with the depletion of cysteine and the presence of GSK-J4 is higher than it in samples with normal medium plus GSK-J4. Therefore, the depletion of cysteine can induce an ATF4 response and can further enhance the ATF4 stress response in the presence of GSK-J4.

When supplemented with the derivatives of cysteine, NAC attenuated the GSK-J4 effect on MT1X expression whereas the presence of cystine did not make any difference. However, the expression of MT1X in NAC and GSK-J4 treated samples is still a 70-fold over control, which is still very high. Moreover, NAC did not weaken or enhance the 2-fold ATF4 induction by GSK-J4, however it reduced the expression of DDIT3, one of the key downstream targets of the ATF4 response.

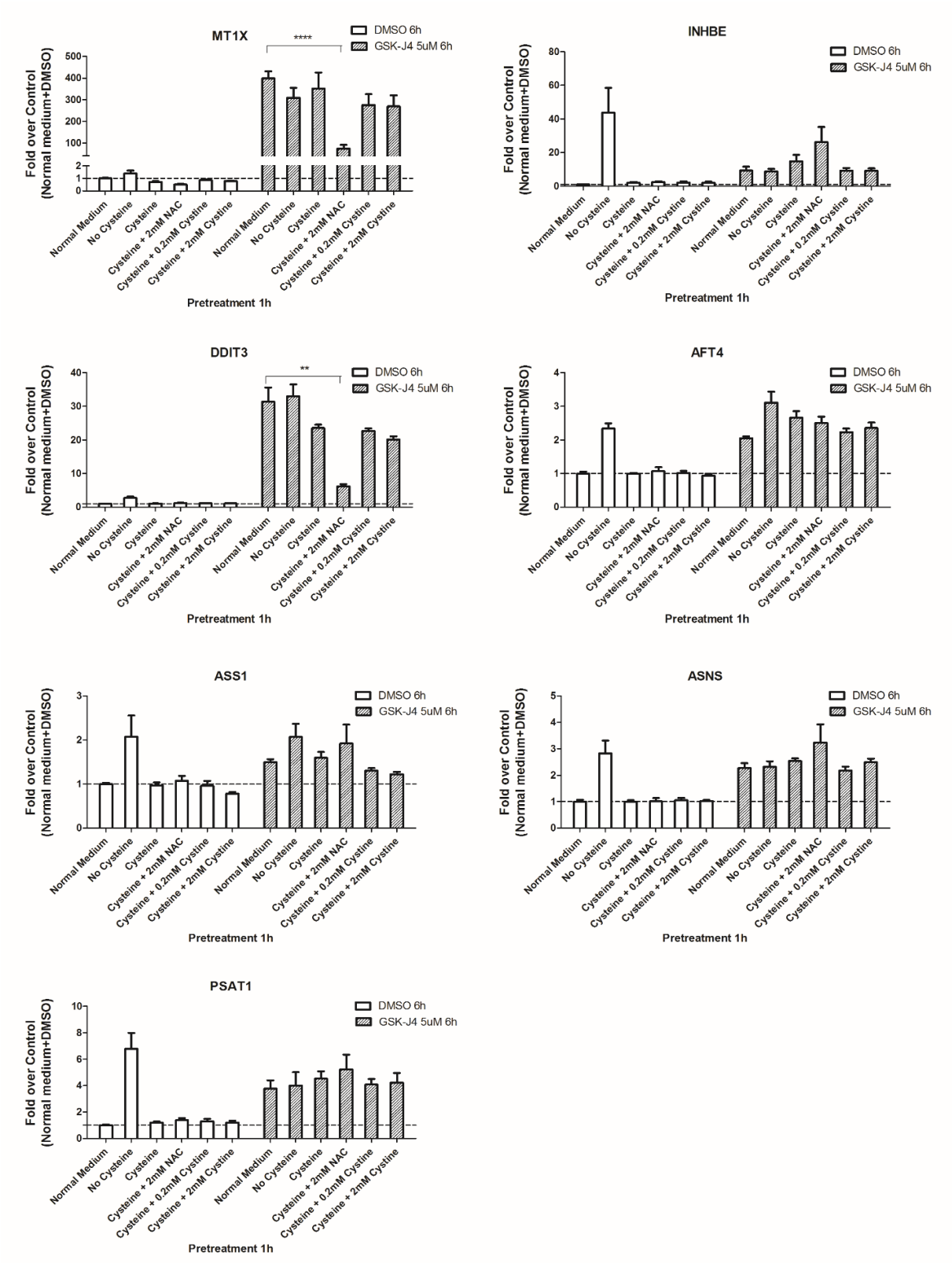

Figure 6.9 qPCR results for cells treated with cysteine and its derivatives

*JJN3 myeloma cells were pre-treated with medium depleted of cysteine or medium supplemented with cysteine and its derivatives for 1 hour and then cells were treated with GSK-J4 (5μM) or DMSO (0.1%) for 6 hours. "Normal medium" refers to complete medium. "No cysteine" refers to cysteine/methionine depletion medium supplemented with only methionine (0.2mM). "Cysteine" refers to cysteine/methionine depletion medium supplemented with methionine (0.2mM) and cysteine (0.2mM). "Cysteine+2mM NAC" refers to cysteine/methionine depletion medium supplemented with methionine (0.2mM), cysteine (0.2mM) and NAC (2mM). "Cysteine+0.2mM Cystine" refers to cysteine/methionine depletion medium supplemented with methionine (0.2mM), cysteine (0.2mM) and cystine (0.2mM). "Cysteine+2mM Cystine" refers to cysteine/methionine depletion medium supplemented with methionine (0.2mM), cysteine (0.2mM) and cystine (2mM). Data plotted represent three biological replicates plus/minus SD. Pairwised one-way ANOVA was applied to analyse the statistical significance. " ** " refers to P values <0.01 and " **** " refers to P values <0.0001 .*

6.8 Discussion

In this chapter, the cellular mechanism of GSK-J4 has been further studied following the previous transcriptomic analysis in myeloma cells in **Chapter 5**. The results in this chapter have validated the previous observation that GSK-J4 increases the expression level of MTs and ATF4 and its downstream targets in JJN3 myeloma cells. In addition, the overexpression of MT1X in HEK293 cells showed that the expression of MT genes in the absence of GSK-J4 can increase the expression level of ATF4 to some extent, which suggests that GSK-J4 may induce MT gene expression first and then the high expression of MT genes is intimately related to the induction of an ATF4 response. Normally, the expression of MTs is involved in a protective effect for the cells against a stressor such as heavy metals (Li, Chen, and Epstein 2004) whereas the ATF4 response is activated by various stressors such as the unfolded protein response or amino acid deficiency (Baird and Wek 2012). However, no previous study has shown a connection between the expression of MTs and the activation of an ATF4-mediated stress response.

Two time-course, 6 hours and 24 hours, were employed in most of the experiments in this chapter. At both time-points, the MT regulation and the ATF4 response activated by GSK-J4 treatment can be observed. However, when using overexpression of MTs to activate ATF4, the increase of ATF4 was slower and was not observed until 24 hours post-treatment. Therefore, both overexpression of MTs and GSK-J4 induced expression of MTs can active ATF4 but with different kinetics.

It has been mentioned previously that the depletion of cysteine induces the expression of genes involved in the amino acid deprivation pathway mediated via the amino acid response (AAR)/ATF4 system in human hepatocellular carcinoma cells

(Lee et al. 2008). The cysteine deprivation experiment described in this chapter and the derived qPCR data confirm that the depletion of cysteine activates an ATF4 response in JJN3 myeloma cells.

Although the supplementation with cysteine or cystine did not show any effect to modulate effects of GSK-J4, the treatment with NAC decreased the expression of MT1X and DDIT3 without affecting the ATF4 expression level (**Figure 6.9**). However, the mechanism of this NAC effect is still unclear. One possible explanation is that NAC may have multiple effects and work independently in respect to the regulation of DDIT3 since it has been shown that ATF4 is not required for the expression of DDIT3 in liver exposed to ER stress (Fusakio et al. 2016).

Chapter 7 Development of a phenotyping platform for myeloma patient bone marrow samples

7.1 Introduction

Building on the results from the epigenetic inhibitor screens in myeloma cell lines, it was of interest to study the effect of selected inhibitors in primary myeloma cells, obtained from bone marrow aspirates of myeloma patients. It is well known that the bone marrow microenvironment plays a major role in development, maintenance, and progression of multiple myeloma and therefore a screen including other marrow cells besides primary malignant plasma cells was of significant interest. The common haematopoietic cell types in the bone marrow are shown in **Figure 7.1**. The cytokines and soluble factors generated by these cells increase tumour proliferation, migration, drug resistance and downregulate apoptotic pathways. These cytokines and soluble factors include IGF-1, IL-6, VEGF, TNF-α, and numerous others (Lawasut et al. 2013, Bianchi and Munshi 2015).

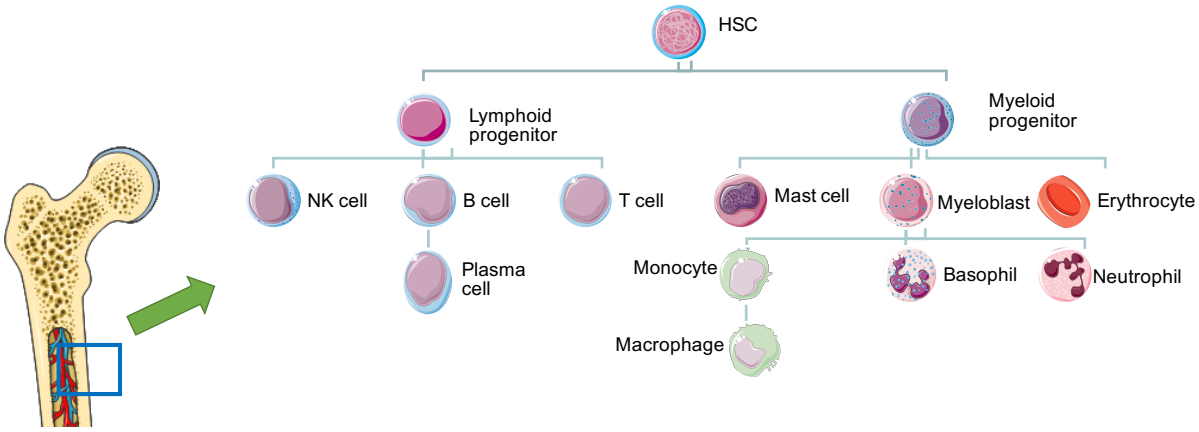

Figure 7.1 Common haematopoietic cell types found in bone marrow

The main cell types derived from HSCs are lymphocytes and myeloid cells. HSC refers to haematopoietic stem cells, and NK cells refer to natural killer cells (Kawano et al. 2017).

Apoptosis of myeloma cells is achieved through two main pathways which lead to the activation of caspases: the death receptor pathway and the mitochondrial pathway. Caspases are members of a cysteine protease family that are synthesised as inactive zymogens. They are responsible for activation of various cellular proteases and endonucleases. The result of activation is cleavage of structural and regulatory cellular proteins and of nuclear DNA, which leads to morphological and biochemical cellular changes that are characteristic of apoptosis (Oancea et al. 2004, Okada and Mak 2004).

Although fluorescence-activated cell sorting (FACS) has been used routinely to measure the effects of a drug at the single-cell level, it has been limited by the number of markers per experiment. In FACS, cells are labelled with fluorescent dye-

conjugated antibodies, and the intensity of each fluorescent parameter is quantitatively measured. However, the actual number of measurable parameters is usually below ten due to the limited number of fluorescent dyes as well as the spectral overlap of fluorescent dyes. Cytometry by Time of Flight (CyTOF), which is a mass cytometry method using transition element isotopes to label antibodies or affinity reagents, has brought significant advancements for deeply phenotyping cells in complex cell populations such as bone marrow or peripheral blood. The quantities of isotopes bound to each cell are analysed by a time-of-flight mass spectrometer, which allows measurement of currently close to 40 parameters in single cells without correction for spectral overlap (Ornatsky et al. 2010, Bendall et al. 2011, Bandura et al. 2009). Using this technique, Bendall, et al. identified differential signalling patterns in different bone marrow populations in response to various cytokines and kinase inhibitors by simultaneous measurement of 34 parameters (Bendall et al. 2011).

In this chapter, the application of mass cytometry is described to identify cellular subsets in myeloma patient bone marrow samples by measuring the expression pattern of cell surface and intracellular markers, and to assess the epigenetic compound effects by identifying the differences between treated and non-treated samples.

7.2 Development of a CyTOF antibody panel for characterisation of myeloma and other marrow cells

Using an established antibody panel (**Table 7.1**) for the characterisation of myeloid, lymphoid and stromal cell types, experiments were carried out to characterise the

phenotypes and composition of bone marrow cells. The antibody panel was designed initially based on an established antibody panel which has been used to detect malignant plasma cells by the combination of CD19, CD28, CD38, CD45, CD56 and CD138 (Robillard et al. 2013). It has been found that normal plasma cells express CD19, CD38, CD45 and CD138 and do not express CD28 and CD56. However, CD28 and CD56 are often seen on abnormal plasma cells and the expression level of CD45 is variable on abnormal plasma cells (Pellat-Deceunynck et al. 1994, Drach, Gattringer, and Huber 1991, Pellat-Deceunynck and Bataille 2004). Besides, CD20, CD33 and CD117, which have been reported to have increased expression in some myeloma cells (Paiva et al. 2010), are also included in our antibody panel. Moreover, common cell type markers, such as the T cell marker CD3 and the NK cell marker CD16, are used in this experiment to reveal the cellular constituents of the bone marrow samples. Additionally, proliferation marker Ki67 and apoptosis marker Caspase3 were included in the panel to assess the compound effect on bone marrow cells.

Table 7.1 Antibody list used in the Cytof study

Marker	Cell/Condition Target
CD38, CD138	plasma cells
CD19, CD20, CD81	B cells
CD3, CD4, CD8 CD28	T cells
CD56	NKs
CD117	mast cells, innate lymphoid cells, NK cells
CD33	myeloid and monocytic cells
CD10	stromal cells
CD45	all haematopoietic cells
CD11c	Dendritic cells, macrophages
Caspase3	apoptosis marker
CD16	NK cells, monocytes/macrophages
Ki67	proliferation marker

Details of each antibody used in the experiment are shown in Appendices Table 3

7.3 Characterizing the bone marrow microenvironment of myeloma patients

Myeloma patient bone marrow samples were obtained from Dr Karthik Ramasamy, Churchill Hospital, Oxford, UK. For each bone marrow sample, mononucleated cells were extracted by Ficoll gradient centrifugation, and the rest of the sample, such as red blood cells, platelets, were discarded. Mononucleated cells were stained with the antibody panel as detailed in **Section 2.12** and were analysed on a CyTOF Helios platform (Fluidigm). Results were analysed using both viSNE analysis (CytoBank) and spanning-tree progression analysis of density-normalised events (SPADE) (CytoBank) software to characterise the cell types and their features in the samples. Based on the expression level of certain markers, the cells were then clustered into different groups.

In the viSNE analysis, only cells with higher frequencies could be clearly clustered. In the sample shown in **Figure 7.2**, hematopoietic cells, B cells, T cells, plasma cells, and myeloid cells are clearly clustered. This patient has a large number of $CD45^-$ $CD38^+$ plasma cells. For $CD38^+$ plasma cells, not all of them were $CD45^-$, which is consistent with the fact that plasma cells in myeloma patients have varying levels of CD45 expression (Pellat-Deceunynck and Bataille 2004).

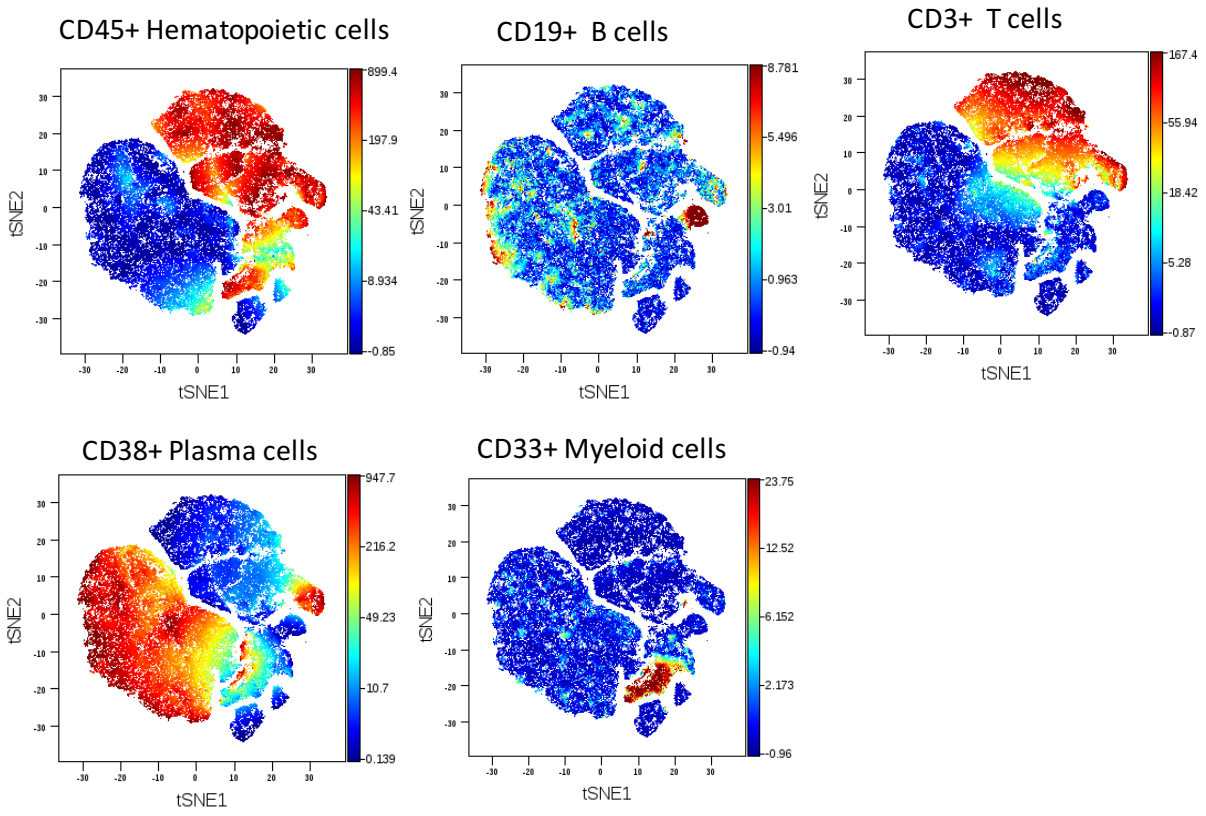

Figure 7.2 viSNE analysis for bone marrow sample (from a newly diagnosed myeloma patient)

The scale bar shows the expression level and the clustered cells with high expression level of certain markers representing different cell types. For example, cells with high expression level of CD3 and CD45 represent T cells.

SPADE analysis allows more detailed clustering and grouping of cells and is superior in representing the cellular subtypes with a low overall proportion in the bone marrow, such as NK cells. **Figure 7.3** shows the SPADE analysis of one relapsed myeloma patient sample after 48 hours treatment with vehicle control (0.1% DMSO). Cells were clustered into different dots based on their characters of marker expressions and then manually grouped into different cell types according to the information in **Table 7.1**. Theoretically, each dot represents a different cell type. However, many subtypes could not be identified due to the limited numbers of markers. Therefore, only common cell types were identified here, which provides a sufficient overview of the bone marrow sample. Plasma cells showed variable expression level of CD45, which is in accordance with the literature (Pellat-Deceunynck and Bataille 2004).

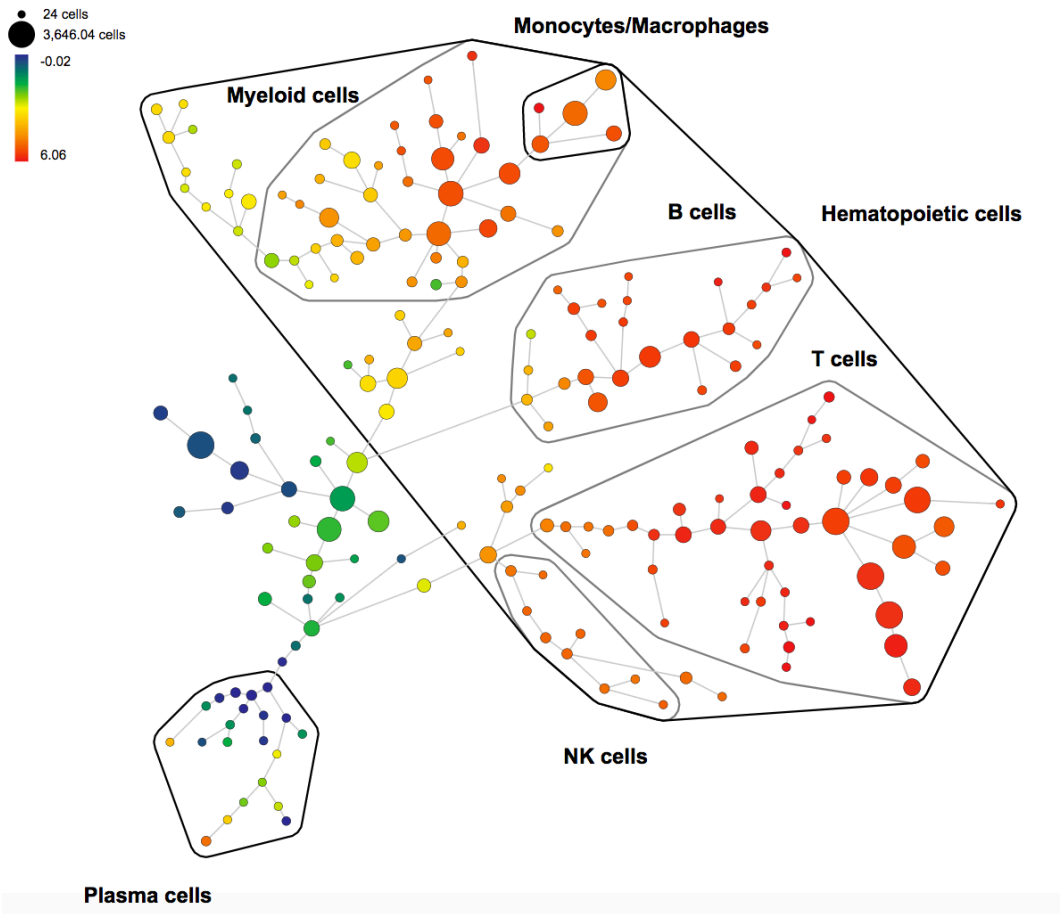

Figure 7.3 SPADE analysis for a relapsed myeloma patient sample (0.1% DMSO treated for 48 hours)

*Cells were clustered based on the characters of marker expressions (**Table 7.1**). The parameter in this figure is the expression level of CD45. Most of the plasma cells were CD45 negative in this sample.*

Figure 7.4 shows the summary of the cell types and their average proportions in the bone marrow samples that were tested in this thesis work. On average, there were 34% of T cells, 11% of B cells, 19% of myeloid cells and 10% of plasma cells. However, the proportions of these cell types are variable across different donors especially for plasma cells, which had a percentage ranging from 2% to 51%. Although the diagnostic criteria for myeloma is over 10% plasma cells in the bone marrow, treated and relapsed myeloma patient typically appear to have less than 10% of plasma cells in the bone marrow. However, on average, 23% of cells were still undefined and they were all $CD45^-$ cells. Therefore, more markers need to be included in the panel to identify this group of cells.

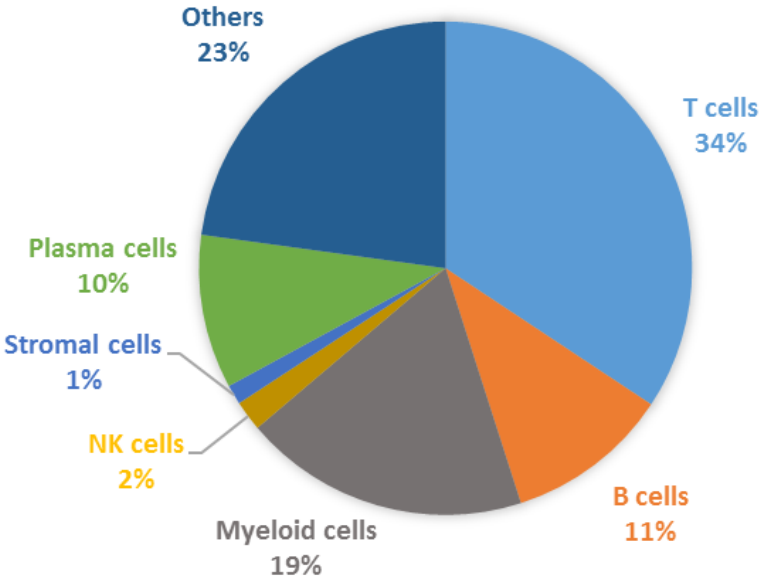

Figure 7.4 Common cell types in bone marrow samples with their average fractions

"Others" refers to undefined cells. Data plotted represents the mean of 10 biological replicates (5 newly diagnosed, 5 relapsed myeloma patient samples). Details of the patient information are shown in Appendices Table 4.

7.4 Investigating the effect of selected epigenetic compounds

GSK-J4 and rocilinostat, which were shown to have strong anti-proliferative effects in myeloma cell lines (**Figure 3.13**), were chosen to be tested in primary myeloma bone marrow samples. The concentration of the compounds used in this experiment was determined by EC_{80} values in the dose-response experiments in human myeloma JJN3 cells. The EC_{80} for GSK-J4 was estimated to be about 5μM and for rocilinostat to be about 3μM in JJN3 cells (**Figure 7.3**).

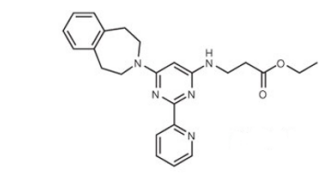

Histone demethylase inhibitor

GSK-J4

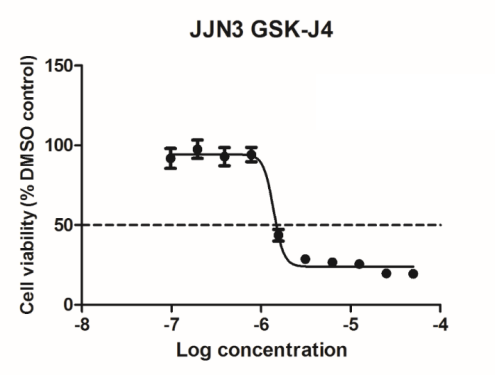

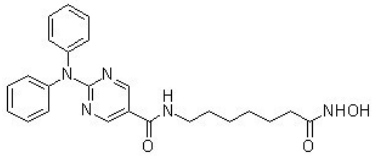

HDAC inhibitor

Rocilinostat

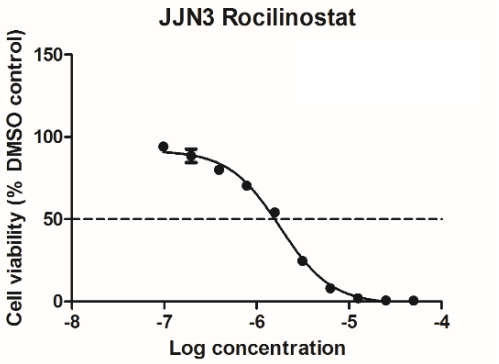

Figure 7.5 The chemical structures of GSK-J4 and rocilinostat and their dose-response curves

(Left) Chemical structures of GSK-J4 and rocilinostat. The chemical structure were obtained from Structural Genomics Consortium (http://www.thesgc.org/chemical-probes).

(Right) The dose-response experiments were performed in JJN3 cells with 72 hours treatment. Log concentration refers to mM range. Data plotted represents the mean plus/minus SD of 3 biological replicates.

These concentrations were used to treat the myeloma bone marrow samples for 48 hours and the samples were then analysed by CyTOF. Over this time course, the proportions of different cell types remained nearly constant between compound treated samples and DMSO treated control samples (**Figure 7.6**). The expected reduction in the cell number of plasma cells after GSK-J4 or rocilinostat treatment, as

predicted from the effect on JJN-3 cells, was not apparent in the primary myeloma experiments. The shorter treatment length and the coculture of plasma cells and all other bone marrow cell types may, therefore, help the survival of plasma cells and reduce the potency of the compounds, as determined previously (**Figure 7.6**).

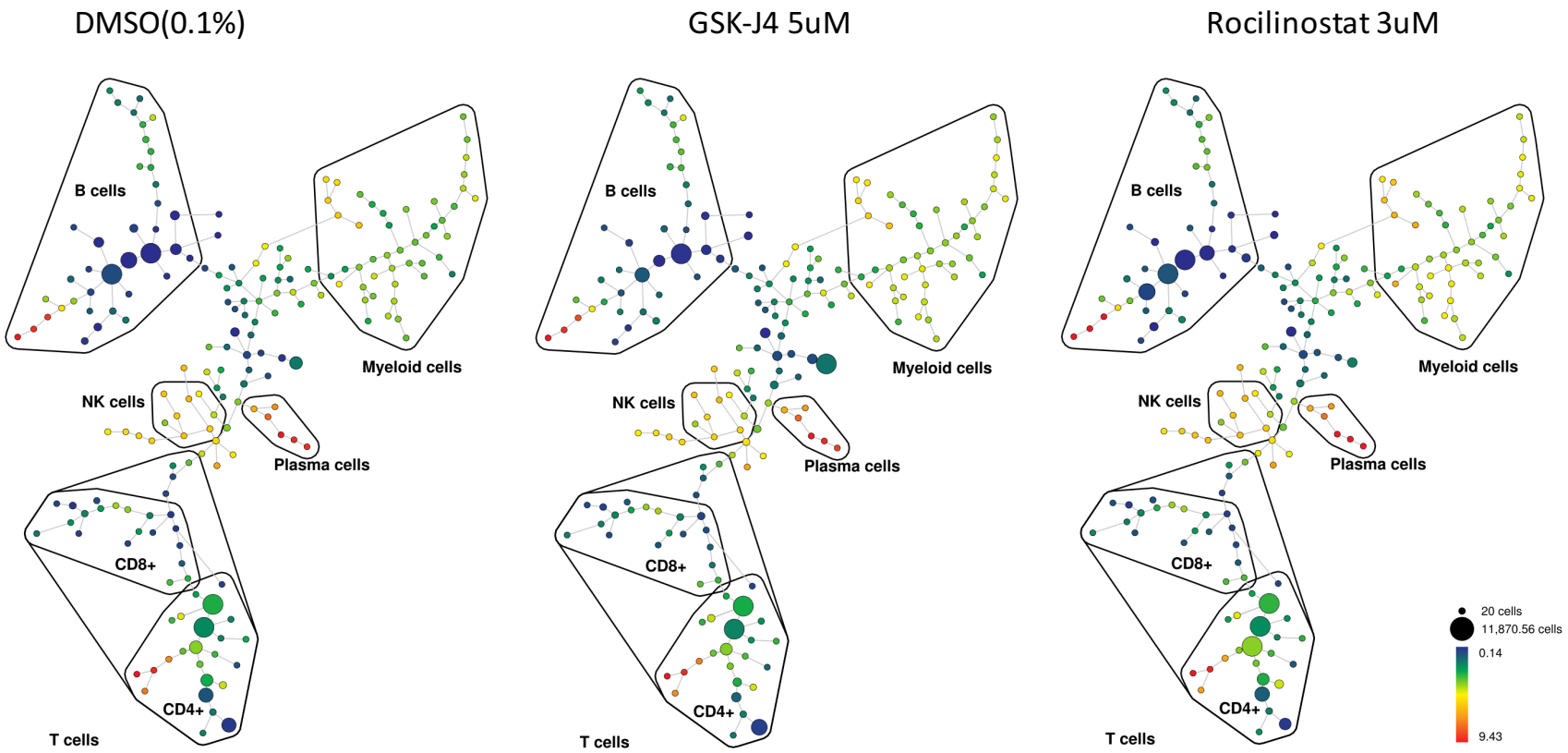

Figure 7.6 SPADE analysis of bone marrow samples after treatment

This sample was obtained from a relapsed myeloma patient. The cells were treated by DMSO (0.1%), GSK-J4 (5uM) and rocilinostat (3uM) for 48 hours. The parameter of the scale bar is the expression level of CD38, which was used to cluster the plasma cells.

However, when investigating markers for apoptosis and proliferation (Caspase activation and Ki67, respectively), the expression level of apoptosis marker Caspase 3 was increased by the treatment of GSK-J4 and rocilinostat, indicating pro-apoptotic effects of these epigenetic inhibitors. Importantly, in primary bone marrow samples, the expression level of proliferation marker Ki67 was low in plasma cells (about 4-5%) and was similar across DMSO, GSK-J4 and rocilinostat treated samples (**Figure 7.7**), indicating further significant differences between cell lines and primary myeloma cells.

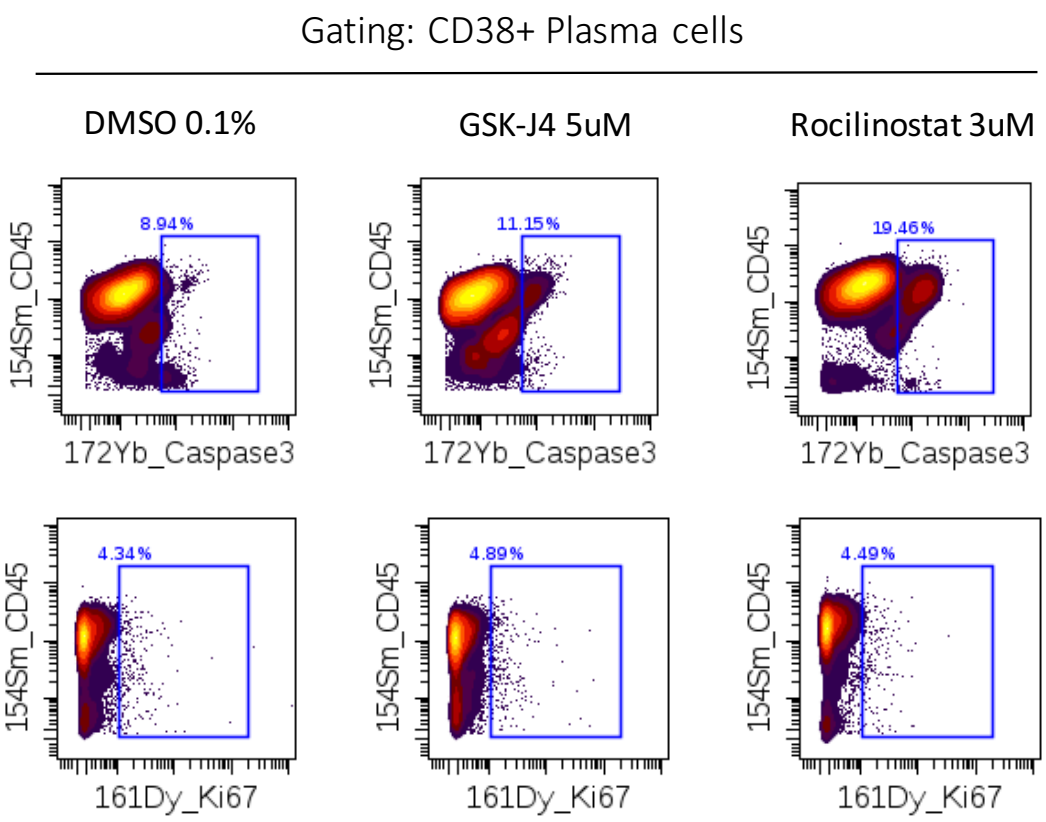

Figure 7.7 GSK-J4 and rocilinostat induces caspase3 in CD38^{+} plasma cells with Ki67 expression levels unchanged

The treatment of GSK-J4 and rocilinostat increased the level of Caspase3 whereas the expression levels of Ki67 remain the same under different conditions. Data plotted was obtained from a relapsed myeloma patient sample.

Of particular importance was the observation that both compounds selectively induced apoptosis in malignant plasma cells but not in non-malignant cell types (such as T cells, B cells or NK cells) in the bone marrow. Resistance to apoptosis is commonly accepted as a hallmark of cancer cells. The results clearly demonstrate that GSK-J4 and rocilinostat target specifically plasma cells in the bone marrow microenvironment and induce apoptosis (**Figure 7.8**), which confirms the anti-proliferative effect from the cell line screening and takes these results a step further by validating these compounds in patient-derived tissue material.

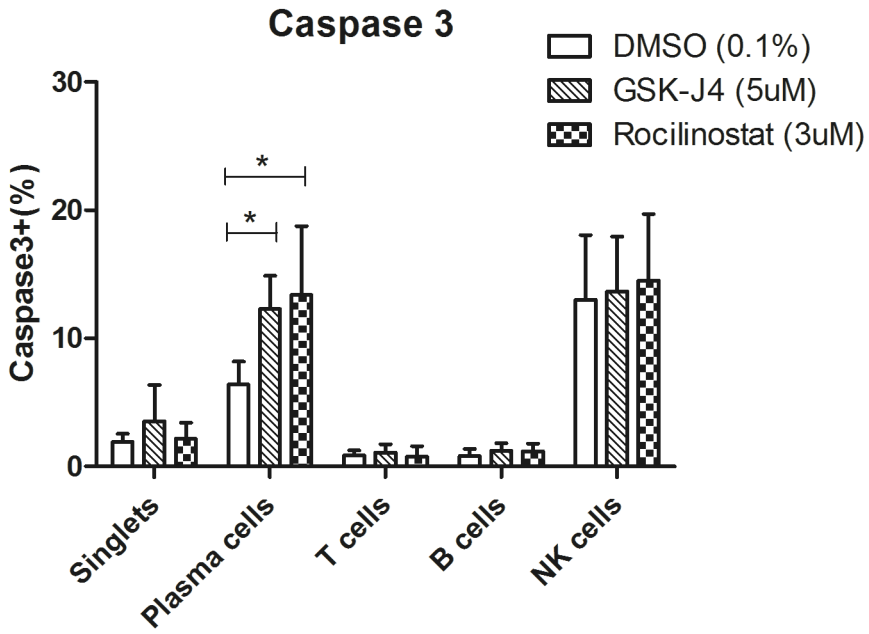

Figure 7.8 The percentage of Caspase3^{+} cells in different cell types shows selective apoptosis of malignant plasma cells but not in non-malignant cells

*Data plotted represents the mean (±) SD in 4 biological replicates (2 newly diagnosed and 2 relapsed myeloma patient samples). Pairwised one-way ANOVA was applied to analyse the statistical significance. " * " refers to p values <0.05.*

7.5 Discussion

In this chapter, CyTOF, which in theory can be used to simultaneously determine the expression of almost 40 markers, was applied to phenotype myeloma patient bone marrow samples. An antibody panel has been successfully set-up to characterise the common cell types in the bone marrow samples and to assess the effects of selected epigenetic inhibitors in primary myeloma cells. This panel contains major haematopoietic cell markers and two intracellular markers. This strategy allowed robust classification of major myeloid and lymphoid cell types besides malignant plasma cells. The intracellular markers included apoptosis marker Caspase3 and the proliferation marker Ki67, which allowed measurements for anti-proliferative compound effects in the bone marrow samples.

Using viSNE and SPADE analyses, the main components of the bone marrow samples could be identified. These experiments provided a clear overview of the bone marrow samples with different treatments, and major subtypes such as B cells, T cells and myeloid cells can be easily identified. Currently, the marker panel has been expanded and tested in the laboratory to identify and characterise these major subtypes further for future, more refined studies.

The experiments also reveal important technical details to be considered. Whereas cell lines are continuously proliferating, primary myeloma cells do not (**Figure 7.7**), at least not at the same rate as cell lines, making it difficult to compare when using proliferation assays or total cell numbers as primary readout over short time periods (such as 2 days in these experiments). Primary myeloma cells are difficult to keep in culture over prolonged periods, therefore the direct measurement of an increased apoptosis marker was successfully used to assess the effects of the compounds.

Another point to consider when comparing compounds in different screening systems, is the apparent change by lowering the potency of these compounds in primary bone marrow samples. Moreover, the constraints in short treatment time makes it difficult to assess the inhibitors with slow effect on-set, such as some of the methyltransferase inhibitors. Therefore, the CyTOF platform was only used for testing inhibitors which were effective in the 3-day time course compound screening.

Not unexpectedly, the relative proportions of cell populations of different donors were variable which may be caused by the diluted bone marrow aspiration by peripheral blood or uneven distribution of cells. For examples, the percentage of plasma cells in bone marrow ranged from 2% to 51% and these plasma cells often had different expression level of CD45 and some other markers. Because of these variabilities, the efficacy of the compounds in patient bone marrow samples showed higher variance compared to myeloma cell lines. Moreover, the limited cell numbers from each patient sample allowed us to investigate only 3-4 conditions at one time. Therefore, many of the potent inhibitors described in **Chapter 5**, have not yet been tested in this CyTOF platform.

Rocilinostat, also known as ACY-1215, is a novel HDAC6-specific histone deacetylase inhibitor. The combination treatment of rocilinostat in conjunction with the novel proteasome inhibitor carfilzomib has shown synergistic effects to myeloma cells resistant to bortezomib in a preclinical setting (Mishima et al. 2015). Proteasome inhibition was shown to enhance the accumulation of misfolded and ubiquitinated proteins within the aggresome, and HDAC6 inhibition by rocilinostat was shown to disrupt proper aggresome formation and function (Mishima et al. 2015) leading to increased apoptosis. Murine models of MM have demonstrated a

significant delay in tumour growth and significant prolongation of survival when treated with a combination of rocilinostat and bortezomib (Santo et al. 2012). In this chapter, rocilinostat was tested in primary human myeloma cells alone indicating a strong pro-apoptotic effect on its own, and confirming its clinical utility in treating MM.

The histone demethylase inhibitor GSK-J4 induces metallothioneins and a strong ATF4 response in myeloma JJN3 cells as described in **Chapter 5 and 6**. Moreover, GSK-J4 has an EC_{50} in the low micromolar range in all tested myeloma cell lines (**Table 3.2**). With the use of this concentration range, it is demonstrated that GSK-J4 induces apoptosis markers specifically in malignant plasma cells in the bone marrow samples without affecting other common cell types.

Taken together, mass cytometry was successfully developed as a phenotyping platform for investigating compound effects of selected epigenetic inhibitors in bone marrow samples from myeloma patients. This platform can be used to characterise the cellular components of bone marrow samples and to assess the efficacy of epigenetic or other inhibitors. GSK-J4 and rocilinostat, which were selected from the epigenetic compound library screening in **Chapter 3**, were confirmed regards their potency in primary myeloma cells and by selectively inducing apoptosis in malignant plasma cells.

Chapter 8 Effects of KDM5B inhibition in multiple myeloma cell lines

8.1 Introduction

Methylation of lysine residues on histone tails is a dynamic epigenetic modification which plays an important role in gene regulation and chromatin structure (Dawson and Kouzarides 2012). The enzymes responsible for the demethylation of methylated histone tails at residue H3K4me3 are the lysine demethylase 5 (KDM5) (also known as JARID1) family of lysine demethylases (Pasini et al. 2008). In mammalian cells, the KDM5 sub-family consists of four enzymes, which are KDM5A (JARID1A), KDM5B (JARID1B), KDM5C (JARID1C) and KDM5D (JARID1D), while KDM5C and KDM5D are encoded on X and Y chromosomes respectively (Tumber et al. 2017). The KDM5 family has important roles both during normal development and in pathological conditions while both KDM5A and KDM5B are involved in the control of cell proliferation, cell differentiation and several cancer types (Rasmussen and Staller 2014, Johansson et al. 2014).

The compound screening described in **Chapter 3** identified several histone demethylase inhibitors that could reduce the cell viability in myeloma cell lines. In particular, GSK-J4, which strongly inhibits KDM6 has proven its strong inhibition in all six myeloma cell lines, and KDOAM25 and GSK467, which inhibit KDM5B, showed inhibition of cell growth in the MM1S myeloma cell line (see **Figure 3.14**). In previous chapters, the mechanisms of GSK-J4 in multiple myeloma was investigated

in detail and I have showed that GSK-J4 could induce a stress response and apoptosis in multiple myeloma cells. In a recent study, enzymatic and cellular based assays demonstrated that GSK-J4 inhibits KDM5 isozymes with appreciable activity, however with 10-30 fold lower potency than its KDM6 inhibition (Heinemann et al. 2014). Moreover, the overexpression of KDM5B in myeloma patients is negatively correlated with the overall survival (Tumber et al. 2017). Therefore, it was of interest to further investigate the functions of the members of the KDM5 family in multiple myeloma using novel tool compounds.

Since KDM5B is likely to play an important role in cell growth and survival and the inhibition of this protein might be beneficial for the treatment of multiple myeloma, several compounds were obtained targeting KDM5B. There are three compounds which were used in this chapter (**Figure 8.1**): KDM5-C70 is a cell-permeable ethyl ester derivative of KDM5-C49, which is a potent inhibitor *in vitro* of KDM5 histone demethylases. KDOAM25 is a KDM5-selective inhibitor, further developed from the KDM5-C49 template. KDM5-C70 was purchased, and KDOAM25 was synthesised by Dr Paul Brennan and Dr Andrea Nuzzi (SGC Oxford). GSK467 was published by GlaxoSmithKline as part of a submicromolar inhibitor series for the KDM4 family and KDM5C with cellular activity (IC_{50} <10μM) in cellular imaging assays (Westaway et al. 2016). However, GSK467 showed a calculated Ki value of 10nM for KDM5B with 180-fold selectivity over KDM4C and no measurable inhibitory effects toward KDM6 in the AlphaScreen format performed by Dr Anthony Tumber (SGC Oxford). According to the results of AlphaScreen, the IC_{50} of KDM5-C70, GSK-467 and KDOAM25 for KDM5B are 4nM, 26nM and19nM respectively (Tumber et al. 2017, Johansson et al. 2016).

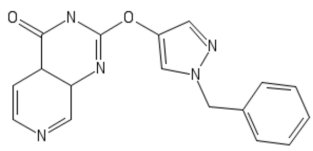

GSK-467

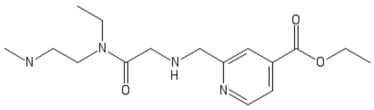

KDM-C70

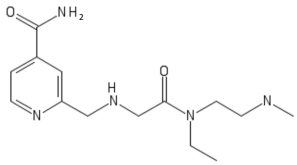

KDOAM25

Figure 8.1 The chemical structures of GSK-467, KDM-C70 and KDOAM25

Chemical structures of GSK-J4 and rocilinostat. The chemical structures were obtained from Structural Genomics Consortium (http://www.thesgc.org/chemical-probes).

8.2 Effects of KDM5B inhibition on cellular proliferation and cell cycle progress

8.2.1 Inhibition of KDM5B leads to reduced viability in MM1S multiple myeloma cells but not in other myeloma cell lines

To assess the cellular activities of these KDM5B inhibitors, dose-response cell viability assays (details of the assay in **Section 2.13**) were conducted in myeloma cells, following the compound screening in **Chapter 3** (**Figure 3.14**). **Figure 8.2** shows the dose-response curves of KDOAM25 with different time courses. After 3-day treatment, KDOAM25 did not show inhibition in MM1S myeloma cells. However, the inhibition of MM1S cells appeared after 5-day and 7-day treatments, and the inhibition was strongest after 7-day treatment.

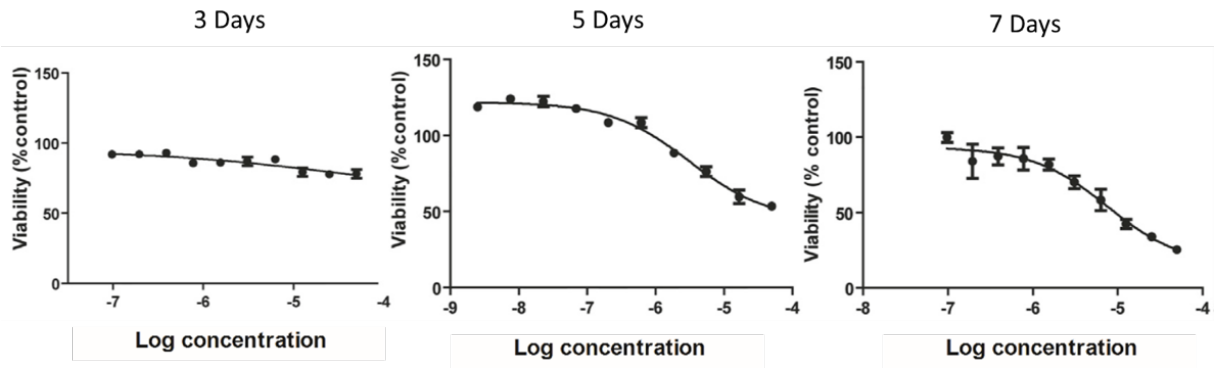

Figure 8.2 The longer the treatment, the stronger the effect of KDOAM25 in MM1S cells

The effect of the compound improved as the treatment time increased. Log concentration refers to mM range. Data plotted represents the mean plus/minus SD of 3 biological replicates.

Since the other two KDM5B inhibitors were supposed to have a similar function compared to KDOAM25, they were tested in cell viability assays with the longer treatment (7 days) as well. **Figure 8.3** shows the dose-response curves of KDM5-C70 and GSK467. Accordingly, all three KDM5B inhibitors, KDOAM25, GSK-467 and KDM5-C70, inhibit cell viability in MM1S myeloma cells. The EC_{50} values of KDOAM25 and GSK-467 are around 50μM and the EC_{50} value of KDM5-C70 is around 20μM for the 7-day treatment.

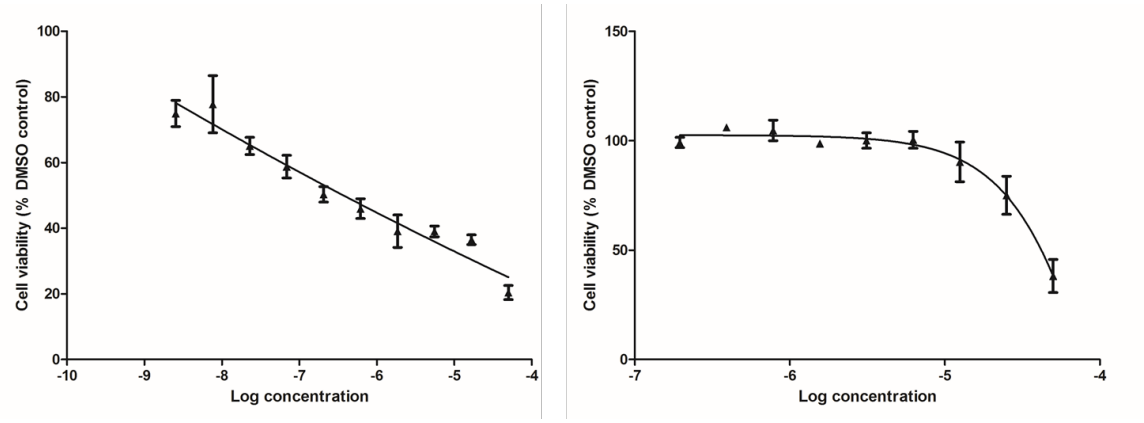

Figure 8.3 Dose response curves of KDM5-C70 (left) and GSK467 (right) in MM1S cells

The cell viability was measured after 7-day treatment of KDM5-C70 and GSK467. The EC_{50} of KDM5-C70 and GSK467 are 20uM and 50uM. Log concentration refers to mM range. Data plotted represents the mean plus/minus SD of 3 biological replicates.

Although GSK-467 and KDOAM25 have shown inhibition for MM1S myeloma cells, they did not show inhibition for all other five myeloma cell lines. **Figure 8.4** shows the dose response curves for GSK-467 and KDOAM25 in JIM3 and KMS11 cells, and similar results were found in other myeloma cell lines (U266, 5TGM1 and JJN3). Therefore, the inhibition of KDM5B only reduces viability of MM1S myeloma cells.

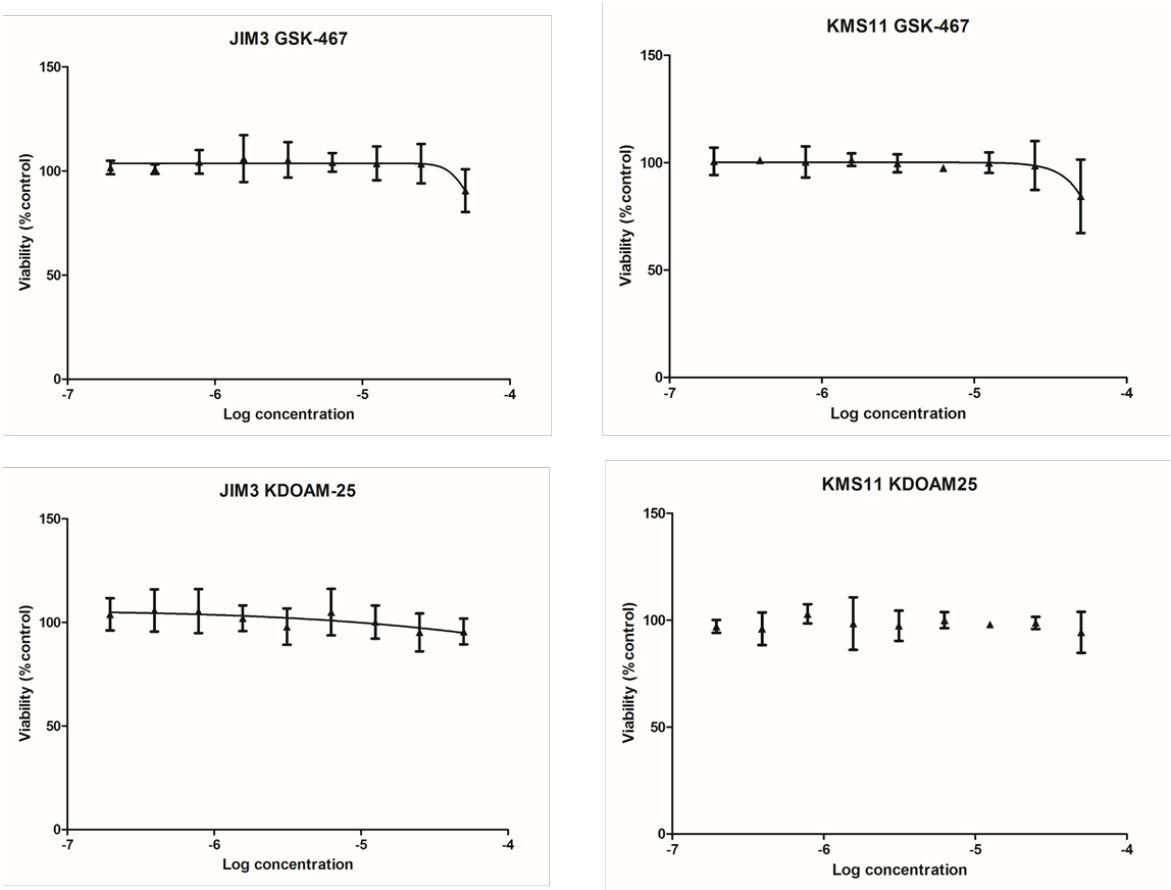

Figure 8.4 Dose response curves of KDOAM-25 and GSK-467 in JIM3 and KMS11 cells

The cell viability was measured after 7days treatment of KDM5-C70 and GSK467. Log concentration refers to mM range. Data plotted represents the mean plus/minus SD of 3 biological replicates.

8.2.2 Inhibition of KDM5B leads to cell cycle arrest and does not induce apoptosis in MM1S multiple myeloma cells

To investigate the mechanisms of the inhibition in MM1S myeloma cells, a study to investigate effects on the cell cycle was conducted. For GSK-467 and KDM5-C70, the cell cycle profile was determined by assessing the phosphorylation status of

retinoblastoma protein (pRb) in treated cells. pRb is responsible for controlling cell growth by inhibiting cell cycle progression from G1 phase to S phase. When pRb is phosphorylated, it becomes inactive and allows the cell cycle to progress. The treatment of KDM5-C70 reduced the phosphorylated pRb while the total pRb remained unchanged (**Figure 8.5**). However, the phosphorylated pRb was not changed by GSK-467. Although GSK-467 only showed slightly less potency in enzymatic assays than KDM5-C70 (Johansson, Velupillai et al. 2016), the cellular activity of GSK-467 was significantly different from KDM5-C70.

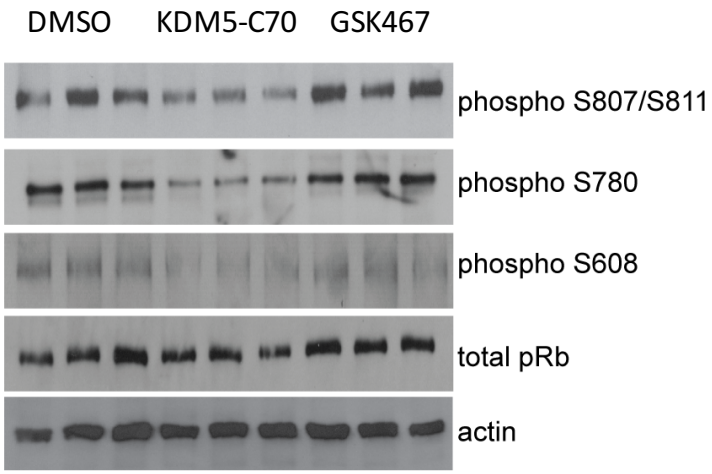

Figure 8.5 KDM5-C70 reduces the level of phosphorylation of retinoblastoma protein in MM1S cells

MM1S cells were treated with KDM5-C70 (50μM), GSK467 (50μM) or vehicle control DMSO (0.1%) for 7 days. There were three biological replicates for each condition, which were represented by three lanes under each condition name. Western blots were performed in collaboration with Dr Shonagh Munro in the laboratory of Prof Nicholas La Thangue, University of Oxford.

For KDOAM25, the cell cycle profile was determined by investigating relative cell proportions in G1 and G2 phases using FACS (details of the assay in **Section 2.9**). The intensity of propidium iodide (PI) staining represents the proportional amount of DNA in the cells while cells in G2 phase have more DNA than cells in G1 phase. The treatment of KDOAM25 (50μM) in MM1S cells for 7 days increased the cells in G1 phase from 52% to 64% and reduced the cells in G2 phase from 26% to 18% (**Figure 8.6**) indicating that the cell cycle was arrested at G1.

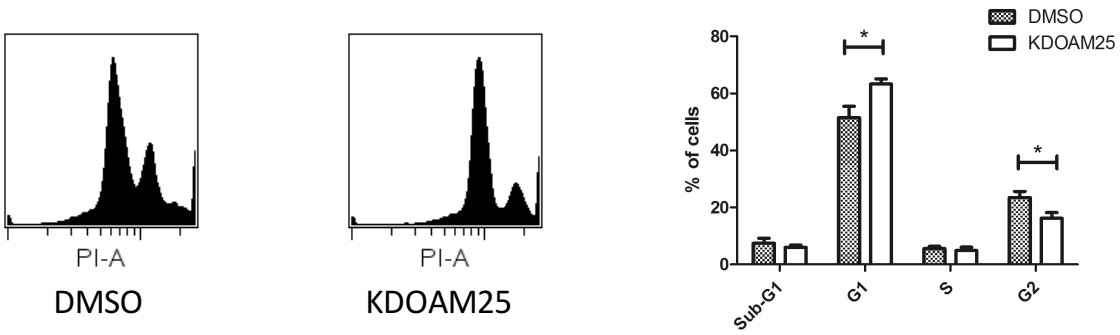

Figure 8.6 Cell cycle profile of KDOAM25 treated MM1S myeloma cells

Cell cycle profile of the samples was measured by propidium iodide staining. MM1S cells were treated with KDOAM25 (50μM) or vehicle control DMSO (0.1%) for 7 days. Significance was calculated using pairwised one-way ANOVA. "" refers to P value <0.05. Data plotted represents the mean plus/minus SD of 3 biological replicates.*

8.2.3 Inhibition of KDM5B does not induce apoptosis in MM1S multiple myeloma cell lines

As shown in **Figure 8.7**, the treatment of MM1S cells with GSK467 (50μM) or KDM5-70C (50μM) for 7 days did not increase the cell apoptosis level compared with the vehicle control. The apoptosis level was determined by the staining of Annexin V and propidium iodide (PI) and analysis by FACS (details of the assay in **Section 2.10**). The portion of non-apoptotic cells in all samples did not show any significant differences. Therefore, GSK-467 does not induce either cell cycle arrest or apoptosis in MM1S myeloma cells while KDM5-70C reduced the cell viability by inhibiting the proliferation of the cells rather than directly killing the cells.

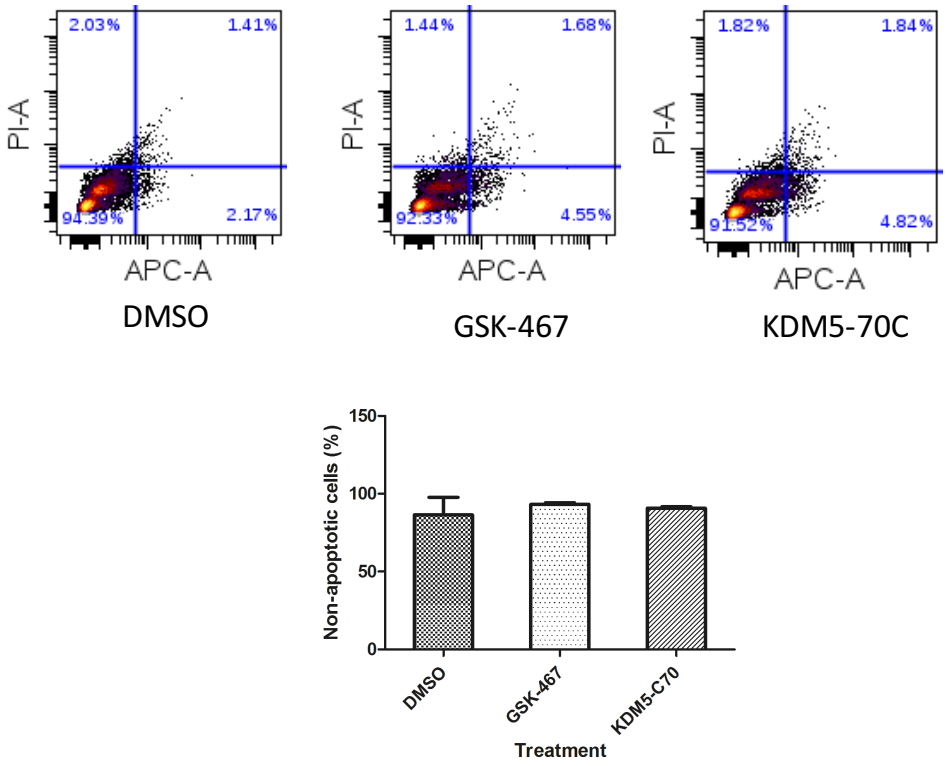

Figure 8.7 GSK-467 and KDM5-70C did not induce apoptosis in MM1S myeloma cells

MM1S cells were treated with KDM5-C70 (50μM), GSK467 (50μM) or vehicle control DMSO (0.1%) for 7 days. Cells were stained with PI and Annexin V (conjugated with APC). The non-apoptotic cells were determined by PI^-APC^- cells. Data plotted represents the mean plus SD of 3 biological replicates.

8.3 Discussion

In this chapter, three inhibitors targeting KDM5B were studied in myeloma cells. KDM5B is a potential oncoprotein and has been shown to be overexpressed in a variety of cancers (Rasmussen and Staller 2014). All of the KDM5B inhibitors have been demonstrated to inhibit proliferation of MM1S myeloma cells. As oppose to GSK-J4, which targets both KDM5 and KDM6 *in vitro* and induces apoptosis in myeloma cells, two of the KDM5B inhibitors (KDM5-70C and KDOAM25) have been shown to cause cell cycle arrest rather than apoptosis in MM1S myeloma cells. Therefore, although *in vitro* study shows that GSK-J4 can inhibit KDM5 to some extent, the experiments in this chapter shows that, in the cells, the GSK-J4 effect is unrelated to a possible KDM5 inhibition.

The KDM5B inhibitors only showed inhibition in MM1S myeloma cells and did not affect other myeloma cell lines. MM1S was established from the peripheral blood cells of a female patient with immunoglobulin A lambda myeloma and the cells have a doubling time of 72 hours, which is slower than other myeloma cells used in this thesis (Greenstein et al. 2003). In the compound screening in myeloma cell lines (**Chapter 3**), there were some inhibitors which showed inhibition only in certain cell lines, such as, methylstat only inhibited growth in JJN3 cells (**Figure 3.13**). However, the reason why these KDM5B compounds inhibited cell growth only in MM1S cells is still unknown.

The results demonstrate that KDM5B inhibitors have an effect on cells growing slowly comparing with other inhibitors. The reason of this slow-onset of effect is unclear. Since the mechanism of KDM5B inhibitors appears to be related to cell

cycle arrest, the slow cell cycle progression in the cells may affect the speed of compound effect.

At present, it is difficult to explain why GSK467 did not cause cell cycle arrest or apoptosis in MM1S myeloma cells. GSK-467 was supposed to have similar functions and mechanisms as KDM5-C70 and KDOAM25 based on the results of enzymatic assays (Johansson, Velupillai et al. 2016). Since GSK467 did show growth inhibition in myeloma cells but not growth arrest or induction of apoptosis, it is possible that the compound might have other functions and off-target effects in cells apart from inhibiting KDM5B. A possible candidate mechanism is the induction of senescence, which, however, has not been further investigated in this thesis.

Chapter 9 Discussion and future perspectives

In this thesis, I have identified and described some underlying mechanisms of epigenetic inhibitors with anti-resorptive and anti-tumour activity for multiple myeloma and its related bone disease. In **Chapter 3**, a library of small molecules with epigenetic targets was tested in both a myeloma viability assay and an osteoclast differentiation assay. In the screening, several compounds with distinct epigenetic targets have been found with inhibitory ability in both assays. These compounds were selected to investigate further the underlying mechanisms in osteoclastogenesis or myeloma cells.

The reduced myeloma cell viability can have several different mechanisms, including apoptotic pathways, cell cycle arrest, senescence, autophagy and mitotic catastrophe (Okada and Mak 2004). In **Chapter 5, 7** and **8**, I have demonstrated that our epigenetic inhibitors reduce cell viability of myeloma cells mainly by activating apoptotic pathways or inducing cell cycle arrest. For example, the KDM6 and KDM5 inhibitor GSK-J4 and HDAC6 inhibitor rocilinostat can induce apoptosis in primary myeloma cells while KDM5B inhibitors KDOAM25 and KDM70C caused cell cycle arrest in MM1S myeloma cells. These mechanisms provide supporting evidence for the selected compounds to become drug candidates for myeloma treatment and help us to understand the functions of the specific epigenetic proteins as well.

In this thesis, GSK-J4 has demonstrated its inhibition in both osteoclast and myeloma assays. The transcriptomic analysis of GSK-J4 treated JJN3 myeloma cells

and the followed qPCR validation reveal and confirm that GSK-J4 induces the ATF4-mediated integrated stress response and the induction of the metallothionein family. Moreover, GSK-J4 increases the expression of apoptosis marker caspase3 in primary myeloma cells without affecting other residential cell populations in the bone marrow. The combined results indicate that in the bone marrow microenvironment GSK-J4 solely induces apoptosis of myeloma cells by upregulation of the metallothionein family and activating the stress response. Additionally, we found that the overexpression of metallothionein genes can induce the ATF-mediated stress response in the absence of GSK-J4, which has not been reported before. The combined results in **Chapter 3**, **5, 6,** and **7** suggests GSK-J4 might be a potent drug candidate for multiple myeloma and its related bone disease.

Rocilinostat (also known as ACY-1215) is a HDAC6-specific inhibitor and has been used in clinical trials in combination with dexamethasone and bortezomib for relapsed or refractory multiple myeloma (Vogl et al. 2017). In this thesis, rocilinostat demonstrated its inhibitory ability in both osteoclast differentiation assay and myeloma cell viability assay. Furthermore, the assessment of rocilinostat in primary bone marrow samples shows that rocilinostat induces apoptosis via upregulating caspase3 in myeloma cells without affecting other cell types in the bone marrow. When I compared this result with the transcriptomic analysis of rocilinostat treated JJN3 myeloma cells, I found rocilinostat upregulates caspase recruitment domain family member 14 (CARD14) and downregulates apoptosis and caspase activation inhibitor (AVEN) in JJN3 myeloma cells. Moreover, a study has demonstrated that rocilinostat in combination with bortezomib increases the expression of caspase3, caspase8 and caspase9 in MM (Santo et al. 2012). These combined results suggest that rocilinostat may cause the death of myeloma cells by inducing apoptosis via

activation of caspase family, in combination with other regimens or as a single drug. Whereas the role of rocilinostat may play in MBD was not deeply studied in this thesis, transcriptomic analysis of rocilinostat in an osteoclast differentiation assay can be conducted in the future, the results of which can be compared with the RNAseq data in **Chapter 5**.

Although the study revealed some interesting and valuable results, there are still some limitations to the work undertaken in this D.Phil project.

Firstly, the eexpression levels of only a limited number of genes were investigated in the osteoclast assay, which leads to insufficient information to fully reveal the inhibition mechanisms of the epigenetic inhibitors. Several inhibitors, such as (+)-JQ1 and belinostat, showed downregulation of RANKL-related genes. However, the detailed mechanisms of these inhibitors cannot be completely explained by the results of RANKL gene card.

Secondly, since MM is a heterogeneous and complex disease, the primary myeloma samples are extremely variable regarding the cell population distribution and the cell viability after short-term in-vitro culturing. Moreover, due to the lack of enough patient number, I did not classify the myeloma bone marrow samples according to the disease stages and previously received treatments. Therefore, in future experiments, it would better to further optimise the *in vitro* culturing conditions for primary bone marrow cells, increase the patient number and compare the samples with similar disease stage and previous treatment.

This D.Phil thesis is not the end of the story but can serve as a starting point for future work.

Firstly, there were many epigenetic compounds which showed potency in both the osteoclast differentiation assay and also the myeloma cell viability assay, however, not all of them have been tested by RANKL gene card, the transcriptomic analysis in myeloma cells or the CyTOF analysis in primary myeloma cells. Therefore, based on the screening results in **Chapter 3**, more compounds will be applied in either transcriptomic analysis of osteoclasts and myeloma cells and the assessment in primary myeloma samples in the future.

Secondly, along with the continuing expansion of our epigenetic compound library, more compounds will be identified with anti-resorptive and anti-cancer activities. In this D.Phil project, an experimental platform has been established to efficiently test the effectiveness of the new compounds in myeloma cells and osteoclasts and then investigate the underlying mechanisms by RNAseq and CyTOF.

Thirdly, apart from the transcriptomic analysis in **Chapter 5**, a more thorough investigation of the exact interactions between epigenetic reader, writer and eraser proteins and the chromain using ChIPseq (chromatin immunoprecipitation sequencing) might reveal fresh insight into the action of the epigenetic inhibitors. Especially, we have demonstrated that some inhibitors that target similar enzymes, such as (+)-JQ1 and DUAL946, have regulated many of the same genes. It would be good to investigate the global inhibition of the epigenetic enzymes and their association with reduced myeloma cell viability.

At last, in this thesis, although several epigenetic inhibitors have been identified with inhibition for both osteoclastogenesis and myeloma cells, all the experiments have been done *in vitro*. It would be of great interest to conduct *in vivo* experiments for compounds like GSK-J4 and rocilinostat to further confirm these valuable results.

Mouse models of myeloma can be applied based on the results from primary human myeloma samples in **Chapter 7**. Also, since some epigenetic inhibitors have potency in both myeloma cells and osteoclast generation, animal models could help us to assess the effectiveness of these compounds in myeloma related bone disease.

List of References

Aggarwal, R., I. M. Ghobrial, and G. D. Roodman. 2006. "Chemokines in multiple myeloma." *Exp Hematol* 34 (10):1289-95. doi: 10.1016/j.exphem.2006.06.017.

Agrawal, N., P. V. Dasaradhi, A. Mohmmed, P. Malhotra, R. K. Bhatnagar, and S. K. Mukherjee. 2003. "RNA interference: biology, mechanism, and applications." *Microbiol Mol Biol Rev* 67 (4):657-85.

Annunziata, C. M., R. E. Davis, Y. Demchenko, W. Bellamy, A. Gabrea, F. Zhan, G. Lenz, I. Hanamura, G. Wright, W. Xiao, S. Dave, E. M. Hurt, B. Tan, H. Zhao, O. Stephens, M. Santra, D. R. Williams, L. Dang, B. Barlogie, J. D. Shaughnessy, Jr., W. M. Kuehl, and L. M. Staudt. 2007. "Frequent engagement of the classical and alternative NF-kappaB pathways by diverse genetic abnormalities in multiple myeloma." *Cancer Cell* 12 (2):115-30. doi: 10.1016/j.ccr.2007.07.004.

Arai, F., and Y. Yamamura. 1990. "Excretion of tetramethyllead, trimethyllead, dimethyllead and inorganic lead after injection of tetramethyllead to rabbits." *Ind Health* 28 (2):63-76.

Aran, D., G. Toperoff, M. Rosenberg, and A. Hellman. 2011. "Replication timing-related and gene body-specific methylation of active human genes." *Hum Mol Genet* 20 (4):670-80. doi: 10.1093/hmg/ddq513.

Asagiri, M., K. Sato, T. Usami, S. Ochi, H. Nishina, H. Yoshida, I. Morita, E. F. Wagner, T. W. Mak, E. Serfling, and H. Takayanagi. 2005. "Autoamplification of NFATc1 expression determines its essential role in bone homeostasis." *J Exp Med* 202 (9):1261-9. doi: 10.1084/jem.20051150.

Attal, M., J. L. Harousseau, A. M. Stoppa, J. J. Sotto, J. G. Fuzibet, J. F. Rossi, P. Casassus, H. Maisonneuve, T. Facon, N. Ifrah, C. Payen, and R. Bataille. 1996. "A prospective, randomized trial of autologous bone marrow transplantation and chemotherapy in multiple myeloma. Intergroupe Français du Myélome." *N Engl J Med* 335 (2):91-7. doi: 10.1056/NEJM199607113350204.

Baird, T. D., and R. C. Wek. 2012. "Eukaryotic initiation factor 2 phosphorylation and translational control in metabolism." *Adv Nutr* 3 (3):307-21. doi: 10.3945/an.112.002113.

Bandura, D. R., V. I. Baranov, O. I. Ornatsky, A. Antonov, R. Kinach, X. Lou, S. Pavlov, S. Vorobiev, J. E. Dick, and S. D. Tanner. 2009. "Mass cytometry: technique for real time single cell multitarget immunoassay based on inductively coupled plasma time-of-flight mass spectrometry." *Anal Chem* 81 (16):6813-22. doi: 10.1021/ac901049w.

Bannister, A. J., and T. Kouzarides. 2011. "Regulation of chromatin by histone modifications." *Cell Res* 21 (3):381-95. doi: 10.1038/cr.2011.22.

Barretina, J., G. Caponigro, N. Stransky, K. Venkatesan, A. A. Margolin, S. Kim, C. J. Wilson, J. Lehár, G. V. Kryukov, D. Sonkin, A. Reddy, M. Liu, L. Murray, M. F. Berger, J. E. Monahan, P. Morais, J. Meltzer, A. Korejwa, J. Jané-Valbuena, F. A. Mapa, J. Thibault, E. Bric-Furlong, P. Raman, A. Shipway, I. H. Engels, J. Cheng, G. K. Yu, J. Yu, P. Aspesi, M. de Silva, K. Jagtap, M. D. Jones, L. Wang, C. Hatton, E. Palescandolo, S. Gupta, S. Mahan, C. Sougnez, R. C. Onofrio, T. Liefeld, L. MacConaill, W. Winckler, M. Reich, N. Li, J. P. Mesirov, S. B. Gabriel, G. Getz, K. Ardlie, V. Chan, V. E. Myer, B. L. Weber, J. Porter, M. Warmuth, P. Finan, J. L. Harris, M. Meyerson, T. R. Golub, M. P. Morrissey, W. R. Sellers, R. Schlegel, and L. A. Garraway. 2012. "The Cancer Cell Line Encyclopedia enables predictive modelling of anticancer drug sensitivity." *Nature* 483 (7391):603-7. doi: 10.1038/nature11003.

Barski, A., S. Cuddapah, K. Cui, T. Y. Roh, D. E. Schones, Z. Wang, G. Wei, I. Chepelev, and K. Zhao. 2007. "High-resolution profiling of histone methylations in the human genome." *Cell* 129 (4):823-37. doi: 10.1016/j.cell.2007.05.009.

Bendall, S. C., E. F. Simonds, P. Qiu, A. D. Amir el, P. O. Krutzik, R. Finck, R. V. Bruggner, R. Melamed, A. Trejo, O. I. Ornatsky, R. S. Balderas, S. K. Plevritis, K. Sachs, D. Pe'er, S. D. Tanner, and G. P. Nolan. 2011. "Single-cell mass cytometry of differential immune and drug responses across a human hematopoietic continuum." *Science* 332 (6030):687-96. doi: 10.1126/science.1198704.

Bereshchenko, O. R., W. Gu, and R. Dalla-Favera. 2002. "Acetylation inactivates the transcriptional repressor BCL6." *Nat Genet* 32 (4):606-13. doi: 10.1038/ng1018.

Bergsagel, D. E., K. M. Griffith, A. Haut, and W. J. Stuckey, Jr. 1967. "The treatment of plasma cell myeloma." *Adv Cancer Res* 10:311-59.

Bergsagel, P. L., and W. M. Kuehl. 2003. "Critical roles for immunoglobulin translocations and cyclin D dysregulation in multiple myeloma." *Immunol Rev* 194:96-104.

Bergsagel, P. L., and W. M. Kuehl. 2005. "Molecular pathogenesis and a consequent classification of multiple myeloma." *J Clin Oncol* 23 (26):6333-8. doi: 10.1200/JCO.2005.05.021.

Bernstein, B. E., A. Meissner, and E. S. Lander. 2007. "The mammalian epigenome." *Cell* 128 (4):669-81. doi: 10.1016/j.cell.2007.01.033.

Bianchi, G., and N. C. Munshi. 2015. "Pathogenesis beyond the cancer clone(s) in multiple myeloma." *Blood* 125 (20):3049-58. doi: 10.1182/blood-2014-11-568881.

Bracken, A. P., and K. Helin. 2009. "Polycomb group proteins: navigators of lineage pathways led astray in cancer." *Nat Rev Cancer* 9 (11):773-84. doi: 10.1038/nrc2736.

Buchman, A. L. 2001. "Side effects of corticosteroid therapy." *J Clin Gastroenterol* 33 (4):289-94.

Cambier, J. C., S. B. Gauld, K. T. Merrell, and B. J. Vilen. 2007. "B-cell anergy: from transgenic models to naturally occurring anergic B cells?" *Nat Rev Immunol* 7 (8):633-43. doi: 10.1038/nri2133.

Cantley, M. D., D. P. Fairlie, P. M. Bartold, K. D. Rainsford, G. T. Le, A. J. Lucke, C. A. Holding, and D. R. Haynes. 2011. "Inhibitors of histone deacetylases in class I and class II suppress human osteoclasts in vitro." *J Cell Physiol* 226 (12):3233-41. doi: 10.1002/jcp.22684.

Chauhan, D., H. Uchiyama, M. Urashima, K. Yamamoto, and K. C. Anderson. 1995. "Regulation of interleukin 6 in multiple myeloma and bone marrow stromal cells." *Stem Cells* 13 Suppl 2:35-9.

Chim, C. S., Y. L. Kwong, and R. Liang. 2008. "Gene hypermethylation in multiple myeloma: lessons from a cancer pathway approach." *Clin Lymphoma Myeloma* 8 (6):331-9. doi: 10.3816/CLM.2008.n.048.

Chohan, T. A., H. Qian, Y. Pan, and J. Z. Chen. 2015. "Cyclin-dependent kinase-2 as a target for cancer therapy: progress in the development of CDK2 inhibitors as anti-cancer agents." *Curr Med Chem* 22 (2):237-63.

Choudhuri, S. 2010. "Small noncoding RNAs: biogenesis, function, and emerging significance in toxicology." *J Biochem Mol Toxicol* 24 (3):195-216. doi: 10.1002/jbt.20325.

Clissold, P. M., and C. P. Ponting. 2001. "JmjC: cupin metalloenzyme-like domains in jumonji, hairless and phospholipase A2beta." *Trends Biochem Sci* 26 (1):7-9.

Collins, A. S., C. E. McCoy, A. T. Lloyd, C. O'Farrelly, and N. J. Stevenson. 2013. "miR-19a: an effective regulator of SOCS3 and enhancer of JAK-STAT signalling." *PLoS One* 8 (7):e69090. doi: 10.1371/journal.pone.0069090.

Collins, S. M., C. E. Bakan, G. D. Swartzel, C. C. Hofmeister, Y. A. Efebera, H. Kwon, G. C. Starling, D. Ciarlariello, S. Bhaskar, E. L. Briercheck, T. Hughes, J. Yu, A. Rice, and D. M. Benson. 2013. "Elotuzumab directly enhances NK cell cytotoxicity against myeloma via CS1 ligation: evidence for augmented NK cell function complementing ADCC." *Cancer Immunol Immunother* 62 (12):1841-9. doi: 10.1007/s00262-013-1493-8.

Crockett, J. C., M. J. Rogers, F. P. Coxon, L. J. Hocking, and M. H. Helfrich. 2011. "Bone remodelling at a glance." *J Cell Sci* 124 (Pt 7):991-8. doi: 10.1242/jcs.063032.

D'Agostino, M., M. Boccadoro, and E. L. Smith. 2017. "Novel Immunotherapies for Multiple Myeloma." *Curr Hematol Malig Rep*. doi: 10.1007/s11899-017-0397-7.

Dabovic, B., R. Levasseur, L. Zambuto, Y. Chen, G. Karsenty, and D. B. Rifkin. 2005. "Osteopetrosis-like phenotype in latent TGF-beta binding protein 3 deficient mice." *Bone* 37 (1):25-31. doi: 10.1016/j.bone.2005.02.021.

Dai, X. M., G. R. Ryan, A. J. Hapel, M. G. Dominguez, R. G. Russell, S. Kapp, V. Sylvestre, and E. R. Stanley. 2002. "Targeted disruption of the mouse colony-stimulating factor 1 receptor gene results in osteopetrosis, mononuclear phagocyte deficiency, increased primitive progenitor cell frequencies, and reproductive defects." *Blood* 99 (1):111-20.

Dalgliesh, G. L., K. Furge, C. Greenman, L. Chen, G. Bignell, A. Butler, H. Davies, S. Edkins, C. Hardy, C. Latimer, J. Teague, J. Andrews, S. Barthorpe, D. Beare,

G. Buck, P. J. Campbell, S. Forbes, M. Jia, D. Jones, H. Knott, C. Y. Kok, K. W. Lau, C. Leroy, M. L. Lin, D. J. McBride, M. Maddison, S. Maguire, K. McLay, A. Menzies, T. Mironenko, L. Mulderrig, L. Mudie, S. O'Meara, E. Pleasance, A. Rajasingham, R. Shepherd, R. Smith, L. Stebbings, P. Stephens, G. Tang, P. S. Tarpey, K. Turrell, K. J. Dykema, S. K. Khoo, D. Petillo, B. Wondergem, J. Anema, R. J. Kahnoski, B. T. Teh, M. R. Stratton, and P. A. Futreal. 2010. "Systematic sequencing of renal carcinoma reveals inactivation of histone modifying genes." *Nature* 463 (7279):360-3. doi: 10.1038/nature08672.

Davila, M. L., I. Riviere, X. Wang, S. Bartido, J. Park, K. Curran, S. S. Chung, J. Stefanski, O. Borquez-Ojeda, M. Olszewska, J. Qu, T. Wasielewska, Q. He, M. Fink, H. Shinglot, M. Youssif, M. Satter, Y. Wang, J. Hosey, H. Quintanilla, E. Halton, Y. Bernal, D. C. Bouhassira, M. E. Arcila, M. Gonen, G. J. Roboz, P. Maslak, D. Douer, M. G. Frattini, S. Giralt, M. Sadelain, and R. Brentjens. 2014. "Efficacy and toxicity management of 19-28z CAR T cell therapy in B cell acute lymphoblastic leukemia." *Sci Transl Med* 6 (224):224ra25. doi: 10.1126/scitranslmed.3008226.

Davis, S. R., and R. J. Cousins. 2000. "Metallothionein expression in animals: a physiological perspective on function." *J Nutr* 130 (5):1085-8.

Dawson, M. A., and T. Kouzarides. 2012. "Cancer epigenetics: from mechanism to therapy." *Cell* 150 (1):12-27. doi: 10.1016/j.cell.2012.06.013.

Day, C. J., M. S. Kim, S. R. Stephens, W. E. Simcock, C. J. Aitken, G. C. Nicholson, and N. A. Morrison. 2004. "Gene array identification of osteoclast genes: differential inhibition of osteoclastogenesis by cyclosporin A and granulocyte macrophage colony stimulating factor." *J Cell Biochem* 91 (2):303-15. doi: 10.1002/jcb.10780.

de Rooij, J. D., I. H. Hollink, S. T. Arentsen-Peters, J. F. van Galen, H. Berna Beverloo, A. Baruchel, J. Trka, D. Reinhardt, E. Sonneveld, M. Zimmermann, T. A. Alonzo, R. Pieters, S. Meshinchi, M. M. van den Heuvel-Eibrink, and C. M. Zwaan. 2013. "NUP98/JARID1A is a novel recurrent abnormality in pediatric acute megakaryoblastic leukemia with a distinct HOX gene expression pattern." *Leukemia* 27 (12):2280-8. doi: 10.1038/leu.2013.87.

Delmore, J. E., G. C. Issa, M. E. Lemieux, P. B. Rahl, J. Shi, H. M. Jacobs, E. Kastritis, T. Gilpatrick, R. M. Paranal, J. Qi, M. Chesi, A. C. Schinzel, M. R.

McKeown, T. P. Heffernan, C. R. Vakoc, P. L. Bergsagel, I. M. Ghobrial, P. G. Richardson, R. A. Young, W. C. Hahn, K. C. Anderson, A. L. Kung, J. E. Bradner, and C. S. Mitsiades. 2011. "BET bromodomain inhibition as a therapeutic strategy to target c-Myc." *Cell* 146 (6):904-17. doi: 10.1016/j.cell.2011.08.017.

Deshpande, A., P. Sicinski, and P. W. Hinds. 2005. "Cyclins and cdks in development and cancer: a perspective." *Oncogene* 24 (17):2909-15. doi: 10.1038/sj.onc.1208618.

Dey, A., J. Ellenberg, A. Farina, A. E. Coleman, T. Maruyama, S. Sciortino, J. Lippincott-Schwartz, and K. Ozato. 2000. "A bromodomain protein, MCAP, associates with mitotic chromosomes and affects G(2)-to-M transition." *Mol Cell Biol* 20 (17):6537-49.

Diamond, P., A. Labrinidis, S. K. Martin, A. N. Farrugia, S. Gronthos, L. B. To, N. Fujii, P. D. O'Loughlin, A. Evdokiou, and A. C. Zannettino. 2009. "Targeted disruption of the CXCL12/CXCR4 axis inhibits osteolysis in a murine model of myeloma-associated bone loss." *J Bone Miner Res* 24 (7):1150-61. doi: 10.1359/jbmr.090210.

Dimopoulos, K., P. Gimsing, and K. Grønbæk. 2013. "Aberrant microRNA expression in multiple myeloma." *Eur J Haematol* 91 (2):95-105. doi: 10.1111/ejh.12124.

Dimopoulos, K., P. Gimsing, and K. Grønbæk. 2014. "The role of epigenetics in the biology of multiple myeloma." *Blood Cancer J* 4:e207. doi: 10.1038/bcj.2014.29.

Djebali, S., C. A. Davis, A. Merkel, A. Dobin, T. Lassmann, A. Mortazavi, A. Tanzer, J. Lagarde, W. Lin, F. Schlesinger, C. Xue, G. K. Marinov, J. Khatun, B. A. Williams, C. Zaleski, J. Rozowsky, M. Röder, F. Kokocinski, R. F. Abdelhamid, T. Alioto, I. Antoshechkin, M. T. Baer, N. S. Bar, P. Batut, K. Bell, I. Bell, S. Chakrabortty, X. Chen, J. Chrast, J. Curado, T. Derrien, J. Drenkow, E. Dumais, J. Dumais, R. Duttagupta, E. Falconnet, M. Fastuca, K. Fejes-Toth, P. Ferreira, S. Foissac, M. J. Fullwood, H. Gao, D. Gonzalez, A. Gordon, H. Gunawardena, C. Howald, S. Jha, R. Johnson, P. Kapranov, B. King, C. Kingswood, O. J. Luo, E. Park, K. Persaud, J. B. Preall, P. Ribeca, B. Risk, D. Robyr, M. Sammeth, L. Schaffer, L. H. See, A. Shahab, J. Skancke, A. M. Suzuki, H. Takahashi, H. Tilgner, D. Trout, N. Walters, H. Wang, J. Wrobel, Y.

Yu, X. Ruan, Y. Hayashizaki, J. Harrow, M. Gerstein, T. Hubbard, A. Reymond, S. E. Antonarakis, G. Hannon, M. C. Giddings, Y. Ruan, B. Wold, P. Carninci, R. Guigó, and T. R. Gingeras. 2012. "Landscape of transcription in human cells." *Nature* 489 (7414):101-8. doi: 10.1038/nature11233.

Dougall, W. C., M. Glaccum, K. Charrier, K. Rohrbach, K. Brasel, T. De Smedt, E. Daro, J. Smith, M. E. Tometsko, C. R. Maliszewski, A. Armstrong, V. Shen, S. Bain, D. Cosman, D. Anderson, P. J. Morrissey, J. J. Peschon, and J. Schuh. 1999. "RANK is essential for osteoclast and lymph node development." *Genes Dev* 13 (18):2412-24.

Drach, J., C. Gattringer, and H. Huber. 1991. "Expression of the neural cell adhesion molecule (CD56) by human myeloma cells." *Clin Exp Immunol* 83 (3):418-22.

Drees, P., A. Eckardt, R. E. Gay, S. Gay, and L. C. Huber. 2007. "Mechanisms of disease: Molecular insights into aseptic loosening of orthopedic implants." *Nat Clin Pract Rheumatol* 3 (3):165-71. doi: 10.1038/ncprheum0428.

Egger, G., G. Liang, A. Aparicio, and P. A. Jones. 2004. "Epigenetics in human disease and prospects for epigenetic therapy." *Nature* 429 (6990):457-63. doi: 10.1038/nature02625.

Eriksen, E. F. 1986. "Normal and pathological remodeling of human trabecular bone: three dimensional reconstruction of the remodeling sequence in normals and in metabolic bone disease." *Endocr Rev* 7 (4):379-408. doi: 10.1210/edrv-7-4-379.

Eriksen, E. F., H. J. Gundersen, F. Melsen, and L. Mosekilde. 1984. "Reconstruction of the formative site in iliac trabecular bone in 20 normal individuals employing a kinetic model for matrix and mineral apposition." *Metab Bone Dis Relat Res* 5 (5):243-52.

Eriksen, E. F., S. F. Hodgson, R. Eastell, S. L. Cedel, W. M. O'Fallon, and B. L. Riggs. 1990. "Cancellous bone remodeling in type I (postmenopausal) osteoporosis: quantitative assessment of rates of formation, resorption, and bone loss at tissue and cellular levels." *J Bone Miner Res* 5 (4):311-9. doi: 10.1002/jbmr.5650050402.

Eriksen, E. F., F. Melsen, and L. Mosekilde. 1984. "Reconstruction of the resorptive site in iliac trabecular bone: a kinetic model for bone resorption in 20 normal individuals." *Metab Bone Dis Relat Res* 5 (5):235-42.

Eslick, R., and D. Talaulikar. 2013. "Multiple myeloma: from diagnosis to treatment." *Aust Fam Physician* 42 (10):684-8.

Falkenberg, K. J., and R. W. Johnstone. 2014. "Histone deacetylases and their inhibitors in cancer, neurological diseases and immune disorders." *Nat Rev Drug Discov* 13 (9):673-91. doi: 10.1038/nrd4360.

Fan, Frank, Wanhong Zhao, Jie Liu, Aili He, Yinxia Chen, Xingmei Cao, Nan Yang, Baiyan Wang, Pengyu Zhang, and Yilin Zhang. 2017. Durable remissions with BCMA-specific chimeric antigen receptor (CAR)-modified T cells in patients with refractory/relapsed multiple myeloma. American Society of Clinical Oncology.

Fang, R., A. J. Barbera, Y. Xu, M. Rutenberg, T. Leonor, Q. Bi, F. Lan, P. Mei, G. C. Yuan, C. Lian, J. Peng, D. Cheng, G. Sui, U. B. Kaiser, Y. Shi, and Y. G. Shi. 2010. "Human LSD2/KDM1b/AOF1 regulates gene transcription by modulating intragenic H3K4me2 methylation." *Mol Cell* 39 (2):222-33. doi: 10.1016/j.molcel.2010.07.008.

Federico, M., and L. Bagella. 2011. "Histone deacetylase inhibitors in the treatment of hematological malignancies and solid tumors." *J Biomed Biotechnol* 2011:475641. doi: 10.1155/2011/475641.

Fernández de Larrea, C., R. A. Kyle, B. G. Durie, H. Ludwig, S. Usmani, D. H. Vesole, R. Hajek, J. F. San Miguel, O. Sezer, P. Sonneveld, S. K. Kumar, A. Mahindra, R. Comenzo, A. Palumbo, A. Mazumber, K. C. Anderson, P. G. Richardson, A. Z. Badros, J. Caers, M. Cavo, X. LeLeu, M. A. Dimopoulos, C. S. Chim, R. Schots, A. Noeul, D. Fantl, U. H. Mellqvist, O. Landgren, A. Chanan-Khan, P. Moreau, R. Fonseca, G. Merlini, J. J. Lahuerta, J. Bladé, R. Z. Orlowski, J. J. Shah, and International Myeloma Working Group. 2013. "Plasma cell leukemia: consensus statement on diagnostic requirements, response criteria and treatment recommendations by the International Myeloma Working Group." *Leukemia* 27 (4):780-91. doi: 10.1038/leu.2012.336.

Fiorelli, G., L. Formigli, S. Zecchi Orlandini, F. Gori, A. Falchetti, A. Morelli, A. Tanini, S. Benvenuti, and M. L. Brandi. 1996. "Characterization and function of the receptor for IGF-I in human preosteoclastic cells." *Bone* 18 (3):269-76.

Franzoso, G., L. Carlson, L. Xing, L. Poljak, E. W. Shores, K. D. Brown, A. Leonardi, T. Tran, B. F. Boyce, and U. Siebenlist. 1997. "Requirement for NF-kappaB in osteoclast and B-cell development." *Genes Dev* 11 (24):3482-96.

Fujikawa, Y., J. M. Quinn, A. Sabokbar, J. O. McGee, and N. A. Athanasou. 1996. "The human osteoclast precursor circulates in the monocyte fraction." *Endocrinology* 137 (9):4058-60. doi: 10.1210/endo.137.9.8756585.

Fuller, K., J. L. Ross, K. A. Szewczyk, R. Moss, and T. J. Chambers. 2010. "Bone is not essential for osteoclast activation." *PLoS One* 5 (9). doi: 10.1371/journal.pone.0012837.

Fusakio, M. E., J. A. Willy, Y. Wang, E. T. Mirek, R. J. Al Baghdadi, C. M. Adams, T. G. Anthony, and R. C. Wek. 2016. "Transcription factor ATF4 directs basal and stress-induced gene expression in the unfolded protein response and cholesterol metabolism in the liver." *Mol Biol Cell* 27 (9):1536-51. doi: 10.1091/mbc.E16-01-0039.

Gadó, K., G. Domján, H. Hegyesi, and A. Falus. 2000. "Role of INTERLEUKIN-6 in the pathogenesis of multiple myeloma." *Cell Biol Int* 24 (4):195-209. doi: 10.1006/cbir.2000.0497.

Gallenkamp, D., K. A. Gelato, B. Haendler, and H. Weinmann. 2014. "Bromodomains and their pharmacological inhibitors." *ChemMedChem* 9 (3):438-64. doi: 10.1002/cmdc.201300434.

Galm, O., H. Yoshikawa, M. Esteller, R. Osieka, and J. G. Herman. 2003. "SOCS-1, a negative regulator of cytokine signaling, is frequently silenced by methylation in multiple myeloma." *Blood* 101 (7):2784-8. doi: 10.1182/blood-2002-06-1735.

Giuliani, N., M. Mangoni, and V. Rizzoli. 2009. "Osteogenic differentiation of mesenchymal stem cells in multiple myeloma: identification of potential therapeutic targets." *Exp Hematol* 37 (8):879-86. doi: 10.1016/j.exphem.2009.04.004.

Giuliani, N., and V. Rizzoli. 2007. "Myeloma cells and bone marrow osteoblast interactions: role in the development of osteolytic lesions in multiple myeloma." *Leuk Lymphoma* 48 (12):2323-9. doi: 10.1080/10428190701648281.

Gohda, J., T. Akiyama, T. Koga, H. Takayanagi, S. Tanaka, and J. Inoue. 2005. "RANK-mediated amplification of TRAF6 signaling leads to NFATc1 induction

during osteoclastogenesis." *EMBO J* 24 (4):790-9. doi: 10.1038/sj.emboj.7600564.

Good-Jacobson, K. L., E. Song, S. Anderson, A. H. Sharpe, and M. J. Shlomchik. 2012. "CD80 expression on B cells regulates murine T follicular helper development, germinal center B cell survival, and plasma cell generation." *J Immunol* 188 (9):4217-25. doi: 10.4049/jimmunol.1102885.

Grayson, A. R., E. M. Walsh, M. J. Cameron, J. Godec, T. Ashworth, J. M. Ambrose, A. B. Aserlind, H. Wang, G. Evan, M. J. Kluk, J. E. Bradner, J. C. Aster, and C. A. French. 2014. "MYC, a downstream target of BRD-NUT, is necessary and sufficient for the blockade of differentiation in NUT midline carcinoma." *Oncogene* 33 (13):1736-1742. doi: 10.1038/onc.2013.126.

Greenstein, S., N. L. Krett, Y. Kurosawa, C. Ma, D. Chauhan, T. Hideshima, K. C. Anderson, and S. T. Rosen. 2003. "Characterization of the MM.1 human multiple myeloma (MM) cell lines: a model system to elucidate the characteristics, behavior, and signaling of steroid-sensitive and -resistant MM cells." *Exp Hematol* 31 (4):271-82.

Grzywacz, A., J. Gdula-Argasińska, B. Muszyńska, M. Tyszka-Czochara, T. Librowski, and W. Opoka. 2015. "Metal responsive transcription factor 1 (MTF-1) regulates zinc dependent cellular processes at the molecular level." *Acta Biochim Pol* 62 (3):491-8. doi: 10.18388/abp.2015_1038.

Görgün, G., M. K. Samur, K. B. Cowens, S. Paula, G. Bianchi, J. E. Anderson, R. E. White, A. Singh, H. Ohguchi, R. Suzuki, S. Kikuchi, T. Harada, T. Hideshima, Y. T. Tai, J. P. Laubach, N. Raje, F. Magrangeas, S. Minvielle, H. Avet-Loiseau, N. C. Munshi, D. M. Dorfman, P. G. Richardson, and K. C. Anderson. 2015. "Lenalidomide Enhances Immune Checkpoint Blockade-Induced Immune Response in Multiple Myeloma." *Clin Cancer Res* 21 (20):4607-18. doi: 10.1158/1078-0432.CCR-15-0200.

Hameed, A., J. J. Brady, P. Dowling, M. Clynes, and P. O'Gorman. 2014. "Bone disease in multiple myeloma: pathophysiology and management." *Cancer Growth Metastasis* 7:33-42. doi: 10.4137/CGM.S16817.

Hanahan, D., and R. A. Weinberg. 2011. "Hallmarks of cancer: the next generation." *Cell* 144 (5):646-74. doi: 10.1016/j.cell.2011.02.013.

Harding, H. P., Y. Zhang, H. Zeng, I. Novoa, P. D. Lu, M. Calfon, N. Sadri, C. Yun, B. Popko, R. Paules, D. F. Stojdl, J. C. Bell, T. Hettmann, J. M. Leiden, and D.

Ron. 2003. "An integrated stress response regulates amino acid metabolism and resistance to oxidative stress." *Mol Cell* 11 (3):619-33.

Hattersley, G., and T. J. Chambers. 1989. "Calcitonin receptors as markers for osteoclastic differentiation: correlation between generation of bone-resorptive cells and cells that express calcitonin receptors in mouse bone marrow cultures." *Endocrinology* 125 (3):1606-12. doi: 10.1210/endo-125-3-1606.

Hayden, M. S., and S. Ghosh. 2004. "Signaling to NF-kappaB." *Genes Dev* 18 (18):2195-224. doi: 10.1101/gad.1228704.

Hayman, A. R. 2008. "Tartrate-resistant acid phosphatase (TRAP) and the osteoclast/immune cell dichotomy." *Autoimmunity* 41 (3):218-23. doi: 10.1080/08916930701694667.

Heinemann, B., J. M. Nielsen, H. R. Hudlebusch, M. J. Lees, D. V. Larsen, T. Boesen, M. Labelle, L. O. Gerlach, P. Birk, and K. Helin. 2014. "Inhibition of demethylases by GSK-J1/J4." *Nature* 514 (7520):E1-2. doi: 10.1038/nature13688.

Helfrich, Miep H., and Stuart Ralston. 2012. *Bone research protocols*. 2nd ed, *Methods in molecular biology,*. New York, NY: Humana Press.

Hideshima, T., D. Chauhan, P. Richardson, C. Mitsiades, N. Mitsiades, T. Hayashi, N. Munshi, L. Dang, A. Castro, V. Palombella, J. Adams, and K. C. Anderson. 2002. "NF-kappa B as a therapeutic target in multiple myeloma." *J Biol Chem* 277 (19):16639-47. doi: 10.1074/jbc.M200360200.

Hodgkinson, C. A., K. J. Moore, A. Nakayama, E. Steingrímsson, N. G. Copeland, N. A. Jenkins, and H. Arnheiter. 1993. "Mutations at the mouse microphthalmia locus are associated with defects in a gene encoding a novel basic-helix-loop-helix-zipper protein." *Cell* 74 (2):395-404.

Hoyer, B. F., K. Moser, A. E. Hauser, A. Peddinghaus, C. Voigt, D. Eilat, A. Radbruch, F. Hiepe, and R. A. Manz. 2004. "Short-lived plasmablasts and long-lived plasma cells contribute to chronic humoral autoimmunity in NZB/W mice." *J Exp Med* 199 (11):1577-84. doi: 10.1084/jem.20040168.

Hull, E. E., M. R. Montgomery, and K. J. Leyva. 2016. "HDAC Inhibitors as Epigenetic Regulators of the Immune System: Impacts on Cancer Therapy and Inflammatory Diseases." *Biomed Res Int* 2016:8797206. doi: 10.1155/2016/8797206.

Hwang, S. Y., and J. W. Putney. 2011. "Calcium signaling in osteoclasts." *Biochim Biophys Acta* 1813 (5):979-83. doi: 10.1016/j.bbamcr.2010.11.002.

Ibragimova, I., M. E. Maradeo, E. Dulaimi, and P. Cairns. 2013. "Aberrant promoter hypermethylation of PBRM1, BAP1, SETD2, KDM6A and other chromatin-modifying genes is absent or rare in clear cell RCC." *Epigenetics* 8 (5):486-93. doi: 10.4161/epi.24552.

Ikeda, F., R. Nishimura, T. Matsubara, S. Tanaka, J. Inoue, S. V. Reddy, K. Hata, K. Yamashita, T. Hiraga, T. Watanabe, T. Kukita, K. Yoshioka, A. Rao, and T. Yoneda. 2004. "Critical roles of c-Jun signaling in regulation of NFAT family and RANKL-regulated osteoclast differentiation." *J Clin Invest* 114 (4):475-84. doi: 10.1172/JCI19657.

Iotsova, V., J. Caamaño, J. Loy, Y. Yang, A. Lewin, and R. Bravo. 1997. "Osteopetrosis in mice lacking NF-kappaB1 and NF-kappaB2." *Nat Med* 3 (11):1285-9.

Ishida, N., K. Hayashi, M. Hoshijima, T. Ogawa, S. Koga, Y. Miyatake, M. Kumegawa, T. Kimura, and T. Takeya. 2002. "Large scale gene expression analysis of osteoclastogenesis in vitro and elucidation of NFAT2 as a key regulator." *J Biol Chem* 277 (43):41147-56. doi: 10.1074/jbc.M205063200.

Jiang, H., C. Acharya, G. An, M. Zhong, X. Feng, L. Wang, N. Dasilva, Z. Song, G. Yang, F. Adrian, L. Qiu, P. Richardson, N. C. Munshi, Y. T. Tai, and K. C. Anderson. 2016. "SAR650984 directly induces multiple myeloma cell death via lysosomal-associated and apoptotic pathways, which is further enhanced by pomalidomide." *Leukemia* 30 (2):399-408. doi: 10.1038/leu.2015.240.

Johansson, C., A. Tumber, K. Che, P. Cain, R. Nowak, C. Gileadi, and U. Oppermann. 2014. "The roles of Jumonji-type oxygenases in human disease." *Epigenomics* 6 (1):89-120. doi: 10.2217/epi.13.79.

Johansson, C., S. Velupillai, A. Tumber, A. Szykowska, E. S. Hookway, R. P. Nowak, C. Strain-Damerell, C. Gileadi, M. Philpott, N. Burgess-Brown, N. Wu, J. Kopec, A. Nuzzi, H. Steuber, U. Egner, V. Badock, S. Munro, N. B. LaThangue, S. Westaway, J. Brown, N. Athanasou, R. Prinjha, P. E. Brennan, and U. Oppermann. 2016. "Structural analysis of human KDM5B guides histone demethylase inhibitor development." *Nat Chem Biol* 12 (7):539-45. doi: 10.1038/nchembio.2087.

Johnson, R. S., B. M. Spiegelman, and V. Papaioannou. 1992. "Pleiotropic effects of a null mutation in the c-fos proto-oncogene." *Cell* 71 (4):577-86.

Jones, P. A. 1986. "DNA methylation and cancer." *Cancer Res* 46 (2):461-6.

Kanwal, R., K. Gupta, and S. Gupta. 2015. "Cancer epigenetics: an introduction." *Methods Mol Biol* 1238:3-25. doi: 10.1007/978-1-4939-1804-1_1.

Kawano, Y., A. M. Roccaro, I. M. Ghobrial, and J. Azzi. 2017. "Multiple Myeloma and the Immune Microenvironment." *Curr Cancer Drug Targets* 17 (9):806-818. doi: 10.2174/1568009617666170214102301.

Keats, J. J., R. Fonseca, M. Chesi, R. Schop, A. Baker, W. J. Chng, S. Van Wier, R. Tiedemann, C. X. Shi, M. Sebag, E. Braggio, T. Henry, Y. X. Zhu, H. Fogle, T. Price-Troska, G. Ahmann, C. Mancini, L. A. Brents, S. Kumar, P. Greipp, A. Dispenzieri, B. Bryant, G. Mulligan, L. Bruhn, M. Barrett, R. Valdez, J. Trent, A. K. Stewart, J. Carpten, and P. L. Bergsagel. 2007. "Promiscuous mutations activate the noncanonical NF-kappaB pathway in multiple myeloma." *Cancer Cell* 12 (2):131-44. doi: 10.1016/j.ccr.2007.07.003.

Khagi, Y., and T. M. Mark. 2014. "Potential role of daratumumab in the treatment of multiple myeloma." *Onco Targets Ther* 7:1095-100. doi: 10.2147/OTT.S49480.

Khoury, G. A., R. C. Baliban, and C. A. Floudas. 2011. "Proteome-wide post-translational modification statistics: frequency analysis and curation of the swiss-prot database." *Sci Rep* 1. doi: 10.1038/srep00090.

Kim, K., S. H. Lee, J. Ha Kim, Y. Choi, and N. Kim. 2008. "NFATc1 induces osteoclast fusion via up-regulation of Atp6v0d2 and the dendritic cell-specific transmembrane protein (DC-STAMP)." *Mol Endocrinol* 22 (1):176-85. doi: 10.1210/me.2007-0237.

Klaus, A., and W. Birchmeier. 2008. "Wnt signalling and its impact on development and cancer." *Nat Rev Cancer* 8 (5):387-98. doi: 10.1038/nrc2389.

Knowles, H. J., and N. A. Athanasou. 2009. "Acute hypoxia and osteoclast activity: a balance between enhanced resorption and increased apoptosis." *J Pathol* 218 (2):256-64. doi: 10.1002/path.2534.

Kobayashi, T., P. T. Walsh, M. C. Walsh, K. M. Speirs, E. Chiffoleau, C. G. King, W. W. Hancock, J. H. Caamano, C. A. Hunter, P. Scott, L. A. Turka, and Y. Choi. 2003. "TRAF6 is a critical factor for dendritic cell maturation and development." *Immunity* 19 (3):353-63.

Koga, T., M. Inui, K. Inoue, S. Kim, A. Suematsu, E. Kobayashi, T. Iwata, H. Ohnishi, T. Matozaki, T. Kodama, T. Taniguchi, H. Takayanagi, and T. Takai. 2004. "Costimulatory signals mediated by the ITAM motif cooperate with RANKL for bone homeostasis." *Nature* 428 (6984):758-63. doi: 10.1038/nature02444.

Kokabu, S., J. W. Lowery, and E. Jimi. 2016. "Cell Fate and Differentiation of Bone Marrow Mesenchymal Stem Cells." *Stem Cells Int* 2016:3753581. doi: 10.1155/2016/3753581.

Kong, Y. Y., H. Yoshida, I. Sarosi, H. L. Tan, E. Timms, C. Capparelli, S. Morony, A. J. Oliveira-dos-Santos, G. Van, A. Itie, W. Khoo, A. Wakeham, C. R. Dunstan, D. L. Lacey, T. W. Mak, W. J. Boyle, and J. M. Penninger. 1999. "OPGL is a key regulator of osteoclastogenesis, lymphocyte development and lymph-node organogenesis." *Nature* 397 (6717):315-23. doi: 10.1038/16852.

Kornak, U., D. Kasper, M. R. Bösl, E. Kaiser, M. Schweizer, A. Schulz, W. Friedrich, G. Delling, and T. J. Jentsch. 2001. "Loss of the ClC-7 chloride channel leads to osteopetrosis in mice and man." *Cell* 104 (2):205-15.

Kovacic, N., P. I. Croucher, and M. M. McDonald. 2014. "Signaling between tumor cells and the host bone marrow microenvironment." *Calcif Tissue Int* 94 (1):125-39. doi: 10.1007/s00223-013-9794-7.

Krizkova, S., M. Ryvolova, J. Hrabeta, V. Adam, M. Stiborova, T. Eckschlager, and R. Kizek. 2012. "Metallothioneins and zinc in cancer diagnosis and therapy." *Drug Metab Rev* 44 (4):287-301. doi: 10.3109/03602532.2012.725414.

Kruidenier, L., C. W. Chung, Z. Cheng, J. Liddle, K. Che, G. Joberty, M. Bantscheff, C. Bountra, A. Bridges, H. Diallo, D. Eberhard, S. Hutchinson, E. Jones, R. Katso, M. Leveridge, P. K. Mander, J. Mosley, C. Ramirez-Molina, P. Rowland, C. J. Schofield, R. J. Sheppard, J. E. Smith, C. Swales, R. Tanner, P. Thomas, A. Tumber, G. Drewes, U. Oppermann, D. J. Patel, K. Lee, and D. M. Wilson. 2012. "A selective jumonji H3K27 demethylase inhibitor modulates the proinflammatory macrophage response." *Nature* 488 (7411):404-8. doi: 10.1038/nature11262.

Krämer, A., B. Schultheis, J. Bergmann, A. Willer, U. Hegenbart, A. D. Ho, H. Goldschmidt, and R. Hehlmann. 2002. "Alterations of the cyclin D1/pRb/p16(INK4A) pathway in multiple myeloma." *Leukemia* 16 (9):1844-51. doi: 10.1038/sj.leu.2402609.

Kubiczkova, L., L. Pour, L. Sedlarikova, R. Hajek, and S. Sevcikova. 2014. "Proteasome inhibitors - molecular basis and current perspectives in multiple myeloma." *J Cell Mol Med* 18 (6):947-61. doi: 10.1111/jcmm.12279.

Kuehl, W. M., and P. L. Bergsagel. 2012. "Molecular pathogenesis of multiple myeloma and its premalignant precursor." *J Clin Invest* 122 (10):3456-63. doi: 10.1172/JCI61188.

Kumar, S. K., V. Rajkumar, R. A. Kyle, M. van Duin, P. Sonneveld, M. V. Mateos, F. Gay, and K. C. Anderson. 2017. "Multiple myeloma." *Nat Rev Dis Primers* 3:17046. doi: 10.1038/nrdp.2017.46.

Kyle, R. A., and S. V. Rajkumar. 2004. "Multiple myeloma." *N Engl J Med* 351 (18):1860-73. doi: 10.1056/NEJMra041875.

Lacey, D. L., E. Timms, H. L. Tan, M. J. Kelley, C. R. Dunstan, T. Burgess, R. Elliott, A. Colombero, G. Elliott, S. Scully, H. Hsu, J. Sullivan, N. Hawkins, E. Davy, C. Capparelli, A. Eli, Y. X. Qian, S. Kaufman, I. Sarosi, V. Shalhoub, G. Senaldi, J. Guo, J. Delaney, and W. J. Boyle. 1998. "Osteoprotegerin ligand is a cytokine that regulates osteoclast differentiation and activation." *Cell* 93 (2):165-76.

Lagasse, E., and I. L. Weissman. 1997. "Enforced expression of Bcl-2 in monocytes rescues macrophages and partially reverses osteopetrosis in op/op mice." *Cell* 89 (7):1021-31.

Lamoureux, F., M. Baud'huin, L. Rodriguez Calleja, C. Jacques, M. Berreur, F. Redini, F. Lecanda, J. E. Bradner, D. Heymann, and B. Ory. 2014. "Selective inhibition of BET bromodomain epigenetic signalling interferes with the bone-associated tumour vicious cycle." *Nat Commun* 5:3511. doi: 10.1038/ncomms4511.

Laubach, J. P., P. Moreau, J. F. San-Miguel, and P. G. Richardson. 2015. "Panobinostat for the Treatment of Multiple Myeloma." *Clin Cancer Res* 21 (21):4767-73. doi: 10.1158/1078-0432.CCR-15-0530.

Lawasut, P., R. W. Groen, E. Dhimolea, P. G. Richardson, K. C. Anderson, and C. S. Mitsiades. 2013. "Decoding the pathophysiology and the genetics of multiple myeloma to identify new therapeutic targets." *Semin Oncol* 40 (5):537-48. doi: 10.1053/j.seminoncol.2013.07.010.

Lee, D. W., J. N. Kochenderfer, M. Stetler-Stevenson, Y. K. Cui, C. Delbrook, S. A. Feldman, T. J. Fry, R. Orentas, M. Sabatino, N. N. Shah, S. M. Steinberg, D.

Stroncek, N. Tschernia, C. Yuan, H. Zhang, L. Zhang, S. A. Rosenberg, A. S. Wayne, and C. L. Mackall. 2015. "T cells expressing CD19 chimeric antigen receptors for acute lymphoblastic leukaemia in children and young adults: a phase 1 dose-escalation trial." *Lancet* 385 (9967):517-528. doi: 10.1016/S0140-6736(14)61403-3.

Lee, J. I., J. E. Dominy, A. K. Sikalidis, L. L. Hirschberger, W. Wang, and M. H. Stipanuk. 2008. "HepG2/C3A cells respond to cysteine deprivation by induction of the amino acid deprivation/integrated stress response pathway." *Physiol Genomics* 33 (2):218-29. doi: 10.1152/physiolgenomics.00263.2007.

Lehenkari, P., T. A. Hentunen, T. Laitala-Leinonen, J. Tuukkanen, and H. K. Vaananen. 1998. "Carbonic anhydrase II plays a major role in osteoclast differentiation and bone resorption by effecting the steady state intracellular pH and Ca2+." *Exp Cell Res* 242 (1):128-37. doi: 10.1006/excr.1998.4071.

Li, C. Y., K. J. Jepsen, R. J. Majeska, J. Zhang, R. Ni, B. D. Gelb, and M. B. Schaffler. 2006. "Mice lacking cathepsin K maintain bone remodeling but develop bone fragility despite high bone mass." *J Bone Miner Res* 21 (6):865-75. doi: 10.1359/jbmr.060313.

Li, J., I. Sarosi, X. Q. Yan, S. Morony, C. Capparelli, H. L. Tan, S. McCabe, R. Elliott, S. Scully, G. Van, S. Kaufman, S. C. Juan, Y. Sun, J. Tarpley, L. Martin, K. Christensen, J. McCabe, P. Kostenuik, H. Hsu, F. Fletcher, C. R. Dunstan, D. L. Lacey, and W. J. Boyle. 2000. "RANK is the intrinsic hematopoietic cell surface receptor that controls osteoclastogenesis and regulation of bone mass and calcium metabolism." *Proc Natl Acad Sci U S A* 97 (4):1566-71.

Li, X., H. Chen, and P. N. Epstein. 2004. "Metallothionein protects islets from hypoxia and extends islet graft survival by scavenging most kinds of reactive oxygen species." *J Biol Chem* 279 (1):765-71. doi: 10.1074/jbc.M307907200.

Li, Y. P., W. Chen, Y. Liang, E. Li, and P. Stashenko. 1999. "Atp6i-deficient mice exhibit severe osteopetrosis due to loss of osteoclast-mediated extracellular acidification." *Nat Genet* 23 (4):447-51. doi: 10.1038/70563.

Li, Z. W., H. Chen, R. A. Campbell, B. Bonavida, and J. R. Berenson. 2008. "NF-kappaB in the pathogenesis and treatment of multiple myeloma." *Curr Opin Hematol* 15 (4):391-9. doi: 10.1097/MOH.0b013e328302c7f4.

Liu, Y. C., S. Szmania, and F. van Rhee. 2014. "Profile of elotuzumab and its potential in the treatment of multiple myeloma." *Blood Lymphat Cancer* 2014 (4):15-27. doi: 10.2147/BLCTT.S49780.

Liu, Y. J., and C. Arpin. 1997. "Germinal center development." *Immunol Rev* 156:111-26.

Lokhorst, H. M., T. Plesner, J. P. Laubach, H. Nahi, P. Gimsing, M. Hansson, M. C. Minnema, U. Lassen, J. Krejcik, A. Palumbo, N. W. van de Donk, T. Ahmadi, I. Khan, C. M. Uhlar, J. Wang, A. K. Sasser, N. Losic, S. Lisby, L. Basse, N. Brun, and P. G. Richardson. 2015. "Targeting CD38 with Daratumumab Monotherapy in Multiple Myeloma." *N Engl J Med* 373 (13):1207-19. doi: 10.1056/NEJMoa1506348.

Lomaga, M. A., W. C. Yeh, I. Sarosi, G. S. Duncan, C. Furlonger, A. Ho, S. Morony, C. Capparelli, G. Van, S. Kaufman, A. van der Heiden, A. Itie, A. Wakeham, W. Khoo, T. Sasaki, Z. Cao, J. M. Penninger, C. J. Paige, D. L. Lacey, C. R. Dunstan, W. J. Boyle, D. V. Goeddel, and T. W. Mak. 1999. "TRAF6 deficiency results in osteopetrosis and defective interleukin-1, CD40, and LPS signaling." *Genes Dev* 13 (8):1015-24.

Lopes-Carvalho, T., and J. F. Kearney. 2004. "Development and selection of marginal zone B cells." *Immunol Rev* 197:192-205.

Lu, G., V. Punj, and P. M. Chaudhary. 2008. "Proteasome inhibitor Bortezomib induces cell cycle arrest and apoptosis in cell lines derived from Ewing's sarcoma family of tumors and synergizes with TRAIL." *Cancer Biol Ther* 7 (4):603-8.

Manasanch, E. E., N. Korde, A. Zingone, N. Tageja, C. Fernandez de Larrea, M. Bhutani, P. Wu, M. Roschewski, and O. Landgren. 2014. "The proteasome: mechanisms of biology and markers of activity and response to treatment in multiple myeloma." *Leuk Lymphoma* 55 (8):1707-14. doi: 10.3109/10428194.2013.828351.

Manz, R. A., M. Lohning, G. Cassese, A. Thiel, and A. Radbruch. 1998. "Survival of long-lived plasma cells is independent of antigen." *Int Immunol* 10 (11):1703-11.

Markovina, S., N. S. Callander, S. L. O'Connor, G. Xu, Y. Shi, C. P. Leith, K. Kim, P. Trivedi, J. Kim, P. Hematti, and S. Miyamoto. 2010. "Bone marrow stromal cells from multiple myeloma patients uniquely induce bortezomib resistant NF-

kappaB activity in myeloma cells." *Mol Cancer* 9:176. doi: 10.1186/1476-4598-9-176.

Martinez, F. O. 2012. "Analysis of gene expression and gene silencing in human macrophages." *Curr Protoc Immunol* Chapter 14:Unit 14 28 1-23. doi: 10.1002/0471142735.im1428s96.

Maruyama, T., A. Farina, A. Dey, J. Cheong, V. P. Bermudez, T. Tamura, S. Sciortino, J. Shuman, J. Hurwitz, and K. Ozato. 2002. "A Mammalian bromodomain protein, brd4, interacts with replication factor C and inhibits progression to S phase." *Mol Cell Biol* 22 (18):6509-20.

Mateos, M. V., R. García-Sanz, R. López-Pérez, M. J. Moro, E. Ocio, J. Hernández, M. Megido, M. D. Caballero, J. Fernández-Calvo, A. Bárez, J. Almeida, A. Orfão, M. González, and J. F. San Miguel. 2002. "Methylation is an inactivating mechanism of the p16 gene in multiple myeloma associated with high plasma cell proliferation and short survival." *Br J Haematol* 118 (4):1034-40.

Mateos, M. V., M. Granell, A. Oriol, J. Martinez-Lopez, J. Blade, M. T. Hernandez, J. Martín, M. Gironella, M. Lynch, E. Bleickardt, P. Paliwal, A. Singhal, and J. San-Miguel. 2016. "Elotuzumab in combination with thalidomide and low-dose dexamethasone: a phase 2 single-arm safety study in patients with relapsed/refractory multiple myeloma." *Br J Haematol* 175 (3):448-456. doi: 10.1111/bjh.14263.

Mateos, M. V., M. T. Hernandez, P. Giraldo, J. de la Rubia, F. de Arriba, L. Lopez Corral, L. Rosinol, B. Paiva, L. Palomera, J. Bargay, A. Oriol, F. Prosper, J. Lopez, E. Olavarria, N. Quintana, J. L. Garcia, J. Blade, J. J. Lahuerta, and J. F. San Miguel. 2013. "Lenalidomide plus dexamethasone for high-risk smoldering multiple myeloma." *N Engl J Med* 369 (5):438-47. doi: 10.1056/NEJMoa1300439.

Mateos, M. V., E. M. Ocio, B. Paiva, L. Rosiñol, J. Martínez-López, J. Bladé, J. J. Lahuerta, R. García-Sanz, and J. F. San Miguel. 2015. "Treatment for patients with newly diagnosed multiple myeloma in 2015." *Blood Rev* 29 (6):387-403. doi: 10.1016/j.blre.2015.06.001.

Matsui, W., Q. Wang, J. P. Barber, S. Brennan, B. D. Smith, I. Borrello, I. McNiece, L. Lin, R. F. Ambinder, C. Peacock, D. N. Watkins, C. A. Huff, and R. J. Jones. 2008. "Clonogenic multiple myeloma progenitors, stem cell properties, and

drug resistance." *Cancer Res* 68 (1):190-7. doi: 10.1158/0008-5472.CAN-07-3096.

McGill, G. G., M. Horstmann, H. R. Widlund, J. Du, G. Motyckova, E. K. Nishimura, Y. L. Lin, S. Ramaswamy, W. Avery, H. F. Ding, S. A. Jordan, I. J. Jackson, S. J. Korsmeyer, T. R. Golub, and D. E. Fisher. 2002. "Bcl2 regulation by the melanocyte master regulator Mitf modulates lineage survival and melanoma cell viability." *Cell* 109 (6):707-18.

McHeyzer-Williams, L. J., D. J. Driver, and M. G. McHeyzer-Williams. 2001. "Germinal center reaction." *Curr Opin Hematol* 8 (1):52-9.

McKercher, S. R., B. E. Torbett, K. L. Anderson, G. W. Henkel, D. J. Vestal, H. Baribault, M. Klemsz, A. J. Feeney, G. E. Wu, C. J. Paige, and R. A. Maki. 1996. "Targeted disruption of the PU.1 gene results in multiple hematopoietic abnormalities." *EMBO J* 15 (20):5647-58.

Medema, R. H., and L. Macůrek. 2012. "Checkpoint control and cancer." *Oncogene* 31 (21):2601-13. doi: 10.1038/onc.2011.451.

Mishima, Y., L. Santo, H. Eda, D. Cirstea, N. Nemani, A. J. Yee, E. O'Donnell, M. K. Selig, S. N. Quayle, S. Arastu-Kapur, C. Kirk, L. H. Boise, S. S. Jones, and N. Raje. 2015. "Ricolinostat (ACY-1215) induced inhibition of aggresome formation accelerates carfilzomib-induced multiple myeloma cell death." *Br J Haematol* 169 (3):423-34. doi: 10.1111/bjh.13315.

Moreau, P., and M. Attal. 2014. "All transplantation-eligible patients with myeloma should receive ASCT in first response." *Hematology Am Soc Hematol Educ Program* 2014 (1):250-4. doi: 10.1182/asheducation-2014.1.250.

Moreaux, J., D. Hose, A. Kassambara, T. Reme, P. Moine, G. Requirand, H. Goldschmidt, and B. Klein. 2011. "Osteoclast-gene expression profiling reveals osteoclast-derived CCR2 chemokines promoting myeloma cell migration." *Blood* 117 (4):1280-90. doi: 10.1182/blood-2010-04-279760.

Morgan, G. J., B. A. Walker, and F. E. Davies. 2012. "The genetic architecture of multiple myeloma." *Nat Rev Cancer* 12 (5):335-48. doi: 10.1038/nrc3257.

Moscatelli, I., C. S. Thudium, C. Flores, A. Schulz, M. Askmyr, N. S. Gudmann, N. M. Andersen, O. Porras, M. A. Karsdal, A. Villa, A. Fasth, K. Henriksen, and J. Richter. 2013. "Lentiviral gene transfer of TCIRG1 into peripheral blood CD34(+) cells restores osteoclast function in infantile malignant osteopetrosis." *Bone* 57 (1):1-9. doi: 10.1016/j.bone.2013.07.026.

Motyckova, G., and D. E. Fisher. 2002. "Pycnodysostosis: role and regulation of cathepsin K in osteoclast function and human disease." *Curr Mol Med* 2 (5):407-21.

Muller, S., P. Filippakopoulos, and S. Knapp. 2011. "Bromodomains as therapeutic targets." *Expert Rev Mol Med* 13:e29. doi: 10.1017/S1462399411001992.

Mócsai, A., M. B. Humphrey, J. A. Van Ziffle, Y. Hu, A. Burghardt, S. C. Spusta, S. Majumdar, L. L. Lanier, C. A. Lowell, and M. C. Nakamura. 2004. "The immunomodulatory adapter proteins DAP12 and Fc receptor gamma-chain (FcRgamma) regulate development of functional osteoclasts through the Syk tyrosine kinase." *Proc Natl Acad Sci U S A* 101 (16):6158-63. doi: 10.1073/pnas.0401602101.

Nair, J. R., L. M. Carlson, C. Koorella, C. H. Rozanski, G. E. Byrne, P. L. Bergsagel, J. P. Shaughnessy, Jr., L. H. Boise, A. Chanan-Khan, and K. P. Lee. 2011. "CD28 expressed on malignant plasma cells induces a prosurvival and immunosuppressive microenvironment." *J Immunol* 187 (3):1243-53. doi: 10.4049/jimmunol.1100016.

Naymagon, L., and M. Abdul-Hay. 2016. "Novel agents in the treatment of multiple myeloma: a review about the future." *J Hematol Oncol* 9 (1):52. doi: 10.1186/s13045-016-0282-1.

Ng, M. H., Y. F. Chung, K. W. Lo, N. W. Wickham, J. C. Lee, and D. P. Huang. 1997. "Frequent hypermethylation of p16 and p15 genes in multiple myeloma." *Blood* 89 (7):2500-6.

Niehrs, C. 2012. "The complex world of WNT receptor signalling." *Nat Rev Mol Cell Biol* 13 (12):767-79. doi: 10.1038/nrm3470.

Nikrad, M., T. Johnson, H. Puthalalath, L. Coultas, J. Adams, and A. S. Kraft. 2005. "The proteasome inhibitor bortezomib sensitizes cells to killing by death receptor ligand TRAIL via BH3-only proteins Bik and Bim." *Mol Cancer Ther* 4 (3):443-9. doi: 10.1158/1535-7163.MCT-04-0260.

Nilsson, K., H. Jernberg, and M. Pettersson. 1990. "IL-6 as a growth factor for human multiple myeloma cells--a short overview." *Curr Top Microbiol Immunol* 166:3-12.

Njau, M. N., J. H. Kim, C. P. Chappell, R. Ravindran, L. Thomas, B. Pulendran, and J. Jacob. 2012. "CD28-B7 interaction modulates short- and long-lived plasma cell function." *J Immunol* 189 (6):2758-67. doi: 10.4049/jimmunol.1102728.

Noll, J. E., S. A. Williams, C. M. Tong, H. Wang, J. M. Quach, L. E. Purton, K. Pilkington, L. B. To, A. Evdokiou, S. Gronthos, and A. C. Zannettino. 2014. "Myeloma plasma cells alter the bone marrow microenvironment by stimulating the proliferation of mesenchymal stromal cells." *Haematologica* 99 (1):163-71. doi: 10.3324/haematol.2013.090977.

Oancea, M., A. Mani, M. A. Hussein, and A. Almasan. 2004. "Apoptosis of multiple myeloma." *Int J Hematol* 80 (3):224-31.

Obeng, E. A., L. M. Carlson, D. M. Gutman, W. J. Harrington, K. P. Lee, and L. H. Boise. 2006. "Proteasome inhibitors induce a terminal unfolded protein response in multiple myeloma cells." *Blood* 107 (12):4907-16. doi: 10.1182/blood-2005-08-3531.

Okada, H., and T. W. Mak. 2004. "Pathways of apoptotic and non-apoptotic death in tumour cells." *Nat Rev Cancer* 4 (8):592-603. doi: 10.1038/nrc1412.

Olsen, E. A., Y. H. Kim, T. M. Kuzel, T. R. Pacheco, F. M. Foss, S. Parker, S. R. Frankel, C. Chen, J. L. Ricker, J. M. Arduino, and M. Duvic. 2007. "Phase IIb multicenter trial of vorinostat in patients with persistent, progressive, or treatment refractory cutaneous T-cell lymphoma." *J Clin Oncol* 25 (21):3109-15. doi: 10.1200/JCO.2006.10.2434.

Ooi, L. L., and C. R. Dunstan. 2009. "CXCL12/CXCR4 axis in tissue targeting and bone destruction in cancer and multiple myeloma." *J Bone Miner Res* 24 (7):1147-9. doi: 10.1359/jbmr.090503.

Ornatsky, O., D. Bandura, V. Baranov, M. Nitz, M. A. Winnik, and S. Tanner. 2010. "Highly multiparametric analysis by mass cytometry." *J Immunol Methods* 361 (1-2):1-20. doi: 10.1016/j.jim.2010.07.002.

Overdijk, M. B., S. Verploegen, M. Bogels, M. van Egmond, J. J. Lammerts van Bueren, T. Mutis, R. W. Groen, E. Breij, A. C. Martens, W. K. Bleeker, and P. W. Parren. 2015. "Antibody-mediated phagocytosis contributes to the anti-tumor activity of the therapeutic antibody daratumumab in lymphoma and multiple myeloma." *MAbs* 7 (2):311-21. doi: 10.1080/19420862.2015.1007813.

Painuly, U., and S. Kumar. 2013. "Efficacy of bortezomib as first-line treatment for patients with multiple myeloma." *Clin Med Insights Oncol* 7:53-73. doi: 10.4137/CMO.S7764.

Paiva, B., J. Almeida, M. Pérez-Andrés, G. Mateo, A. López, A. Rasillo, M. B. Vídriales, M. C. López-Berges, J. F. Miguel, and A. Orfao. 2010. "Utility of flow cytometry immunophenotyping in multiple myeloma and other clonal plasma cell-related disorders." *Cytometry B Clin Cytom* 78 (4):239-52. doi: 10.1002/cyto.b.20512.

Palumbo, A., and K. Anderson. 2011. "Multiple myeloma." *N Engl J Med* 364 (11):1046-60. doi: 10.1056/NEJMra1011442.

Panaroni, C., A. J. Yee, and N. S. Raje. 2017. "Myeloma and Bone Disease." *Curr Osteoporos Rep* 15 (5):483-498. doi: 10.1007/s11914-017-0397-5.

Papamerkouriou, Y. M., E. Kenanidis, Z. Gamie, K. Papavasiliou, T. Kostakos, M. Potoupnis, I. Sarris, E. Tsiridis, and J. Kyrkos. 2015. "Treatment of multiple myeloma bone disease: experimental and clinical data." *Expert Opin Biol Ther* 15 (2):213-30. doi: 10.1517/14712598.2015.978853.

Pasini, D., K. H. Hansen, J. Christensen, K. Agger, P. A. Cloos, and K. Helin. 2008. "Coordinated regulation of transcriptional repression by the RBP2 H3K4 demethylase and Polycomb-Repressive Complex 2." *Genes Dev* 22 (10):1345-55. doi: 10.1101/gad.470008.

Patel, N., J. Black, X. Chen, A. M. Marcondes, W. M. Grady, E. R. Lawlor, and S. C. Borinstein. 2012. "DNA methylation and gene expression profiling of ewing sarcoma primary tumors reveal genes that are potential targets of epigenetic inactivation." *Sarcoma* 2012:498472. doi: 10.1155/2012/498472.

Pellat-Deceunynck, C., and R. Bataille. 2004. "Normal and malignant human plasma cells: proliferation, differentiation, and expansions in relation to CD45 expression." *Blood Cells Mol Dis* 32 (2):293-301. doi: 10.1016/j.bcmd.2003.12.001.

Pellat-Deceunynck, C., R. Bataille, N. Robillard, J. L. Harousseau, M. J. Rapp, N. Juge-Morineau, J. Wijdenes, and M. Amiot. 1994. "Expression of CD28 and CD40 in human myeloma cells: a comparative study with normal plasma cells." *Blood* 84 (8):2597-603.

Pichiorri, F., S. S. Suh, M. Ladetto, M. Kuehl, T. Palumbo, D. Drandi, C. Taccioli, N. Zanesi, H. Alder, J. P. Hagan, R. Munker, S. Volinia, M. Boccadoro, R. Garzon, A. Palumbo, R. I. Aqeilan, and C. M. Croce. 2008. "MicroRNAs regulate critical genes associated with multiple myeloma pathogenesis." *Proc Natl Acad Sci U S A* 105 (35):12885-90. doi: 10.1073/pnas.0806202105.

Puthier, D., S. Derenne, S. Barille, P. Moreau, J. L. Harousseau, R. Bataille, and M. Amiot. 1999. "Mcl-1 and Bcl-xL are co-regulated by IL-6 in human myeloma cells." *Br J Haematol* 107 (2):392-5.

Radbruch, A., G. Muehlinghaus, E. O. Luger, A. Inamine, K. G. Smith, T. Dorner, and F. Hiepe. 2006. "Competence and competition: the challenge of becoming a long-lived plasma cell." *Nat Rev Immunol* 6 (10):741-50. doi: 10.1038/nri1886.

Rajkumar, S. V. 2016. "Multiple myeloma: 2016 update on diagnosis, risk-stratification, and management." *Am J Hematol* 91 (7):719-34. doi: 10.1002/ajh.24402.

Rajkumar, S. V., M. A. Dimopoulos, A. Palumbo, J. Blade, G. Merlini, M. V. Mateos, S. Kumar, J. Hillengass, E. Kastritis, P. Richardson, O. Landgren, B. Paiva, A. Dispenzieri, B. Weiss, X. LeLeu, S. Zweegman, S. Lonial, L. Rosinol, E. Zamagni, S. Jagannath, O. Sezer, S. Y. Kristinsson, J. Caers, S. Z. Usmani, J. J. Lahuerta, H. E. Johnsen, M. Beksac, M. Cavo, H. Goldschmidt, E. Terpos, R. A. Kyle, K. C. Anderson, B. G. Durie, and J. F. Miguel. 2014. "International Myeloma Working Group updated criteria for the diagnosis of multiple myeloma." *Lancet Oncol* 15 (12):e538-48. doi: 10.1016/S1470-2045(14)70442-5.

Rajkumar, S. V., S. Jacobus, N. S. Callander, R. Fonseca, D. H. Vesole, M. E. Williams, R. Abonour, D. S. Siegel, M. Katz, P. R. Greipp, and Eastern Cooperative Oncology Group. 2010. "Lenalidomide plus high-dose dexamethasone versus lenalidomide plus low-dose dexamethasone as initial therapy for newly diagnosed multiple myeloma: an open-label randomised controlled trial." *Lancet Oncol* 11 (1):29-37. doi: 10.1016/S1470-2045(09)70284-0.

Rajkumar, S. V., and R. A. Kyle. 2005. "Multiple myeloma: diagnosis and treatment." *Mayo Clin Proc* 80 (10):1371-82. doi: 10.4065/80.10.1371.

Rana, T. M. 2007. "Illuminating the silence: understanding the structure and function of small RNAs." *Nat Rev Mol Cell Biol* 8 (1):23-36. doi: 10.1038/nrm2085.

Rasmussen, P. B., and P. Staller. 2014. "The KDM5 family of histone demethylases as targets in oncology drug discovery." *Epigenomics* 6 (3):277-86. doi: 10.2217/epi.14.14.

Reik, W. 2007. "Stability and flexibility of epigenetic gene regulation in mammalian development." *Nature* 447 (7143):425-32. doi: 10.1038/nature05918.

Ribourtout, B., and M. Zandecki. 2015. "Plasma cell morphology in multiple myeloma and related disorders." *Morphologie* 99 (325):38-62. doi: 10.1016/j.morpho.2015.02.001.

Rimondi, E., M. Zweyer, E. Ricci, R. Fadda, and P. Secchiero. 2007. "Receptor activator of nuclear factor kappa B ligand (RANKL) modulates the expression of genes involved in apoptosis and cell cycle in human osteoclasts." *Anat Rec (Hoboken)* 290 (7):838-45. doi: 10.1002/ar.20550.

Rizzi, M., R. Knoth, C. S. Hampe, P. Lorenz, M. L. Gougeon, B. Lemercier, N. Venhoff, F. Ferrera, U. Salzer, H. J. Thiesen, H. H. Peter, U. A. Walker, and H. Eibel. 2010. "Long-lived plasma cells and memory B cells produce pathogenic anti-GAD65 autoantibodies in Stiff Person Syndrome." *PLoS One* 5 (5):e10838. doi: 10.1371/journal.pone.0010838.

Robillard, N., M. C. Béné, P. Moreau, and S. Wuillème. 2013. "A single-tube multiparameter seven-colour flow cytometry strategy for the detection of malignant plasma cells in multiple myeloma." *Blood Cancer J* 3:e134. doi: 10.1038/bcj.2013.33.

Rosean, T. R., V. S. Tompkins, G. Tricot, C. J. Holman, A. K. Olivier, F. Zhan, and S. Janz. 2014. "Preclinical validation of interleukin 6 as a therapeutic target in multiple myeloma." *Immunol Res* 59 (1-3):188-202. doi: 10.1007/s12026-014-8528-x.

Ross, F. P., and S. L. Teitelbaum. 2005. "alphavbeta3 and macrophage colony-stimulating factor: partners in osteoclast biology." *Immunol Rev* 208:88-105. doi: 10.1111/j.0105-2896.2005.00331.x.

Röllig, C., S. Knop, and M. Bornhäuser. 2015. "Multiple myeloma." *Lancet* 385 (9983):2197-208. doi: 10.1016/S0140-6736(14)60493-1.

Saftig, P., E. Hunziker, O. Wehmeyer, S. Jones, A. Boyde, W. Rommerskirch, J. D. Moritz, P. Schu, and K. von Figura. 1998. "Impaired osteoclastic bone resorption leads to osteopetrosis in cathepsin-K-deficient mice." *Proc Natl Acad Sci U S A* 95 (23):13453-8.

Salo, J., P. Lehenkari, M. Mulari, K. Metsikkö, and H. K. Väänänen. 1997. "Removal of osteoclast bone resorption products by transcytosis." *Science* 276 (5310):270-3.

Santo, L., T. Hideshima, A. L. Kung, J. C. Tseng, D. Tamang, M. Yang, M. Jarpe, J. H. van Duzer, R. Mazitschek, W. C. Ogier, D. Cirstea, S. Rodig, H. Eda, T. Scullen, M. Canavese, J. Bradner, K. C. Anderson, S. S. Jones, and N. Raje. 2012. "Preclinical activity, pharmacodynamic, and pharmacokinetic properties of a selective HDAC6 inhibitor, ACY-1215, in combination with bortezomib in multiple myeloma." *Blood* 119 (11):2579-89. doi: 10.1182/blood-2011-10-387365.

Schenk, T., W. C. Chen, S. Göllner, L. Howell, L. Jin, K. Hebestreit, H. U. Klein, A. C. Popescu, A. Burnett, K. Mills, R. A. Casero, L. Marton, P. Woster, M. D. Minden, M. Dugas, J. C. Wang, J. E. Dick, C. Müller-Tidow, K. Petrie, and A. Zelent. 2012. "Inhibition of the LSD1 (KDM1A) demethylase reactivates the all-trans-retinoic acid differentiation pathway in acute myeloid leukemia." *Nat Med* 18 (4):605-11. doi: 10.1038/nm.2661.

Seales, E. C., K. J. Micoli, and J. M. McDonald. 2006. "Calmodulin is a critical regulator of osteoclastic differentiation, function, and survival." *J Cell Biochem* 97 (1):45-55. doi: 10.1002/jcb.20659.

Seifert, M., R. Scholtysik, and R. Kuppers. 2013. "Origin and pathogenesis of B cell lymphomas." *Methods Mol Biol* 971:1-25. doi: 10.1007/978-1-62703-269-8_1.

Sekiguchi, N., K. Ootsubo, M. Wagatsuma, K. Midorikawa, A. Nagata, S. Noto, K. Yamada, and N. Takezako. 2014. "Impact of C-Myc gene-related aberrations in newly diagnosed myeloma with bortezomib/dexamethasone therapy." *Int J Hematol* 99 (3):288-95. doi: 10.1007/s12185-014-1514-1.

Shapiro-Shelef, M., and K. Calame. 2005. "Regulation of plasma-cell development." *Nat Rev Immunol* 5 (3):230-42. doi: 10.1038/nri1572.

Sharma, A., C. J. Heuck, M. J. Fazzari, J. Mehta, S. Singhal, J. M. Greally, and A. Verma. 2010. "DNA methylation alterations in multiple myeloma as a model for epigenetic changes in cancer." *Wiley Interdiscip Rev Syst Biol Med* 2 (6):654-69. doi: 10.1002/wsbm.89.

Sharma, S., T. K. Kelly, and P. A. Jones. 2010. "Epigenetics in cancer." *Carcinogenesis* 31 (1):27-36. doi: 10.1093/carcin/bgp220.

Shi, Y., F. Lan, C. Matson, P. Mulligan, J. R. Whetstine, P. A. Cole, and R. A. Casero. 2004. "Histone demethylation mediated by the nuclear amine oxidase homolog LSD1." *Cell* 119 (7):941-53. doi: 10.1016/j.cell.2004.12.012.

Siegel, D. S., T. Martin, M. Wang, R. Vij, A. J. Jakubowiak, S. Lonial, S. Trudel, V. Kukreti, N. Bahlis, M. Alsina, A. Chanan-Khan, F. Buadi, F. J. Reu, G. Somlo, J. Zonder, K. Song, A. K. Stewart, E. Stadtmauer, L. Kunkel, S. Wear, A. F. Wong, R. Z. Orlowski, and S. Jagannath. 2012. "A phase 2 study of single-agent carfilzomib (PX-171-003-A1) in patients with relapsed and refractory multiple myeloma." *Blood* 120 (14):2817-25. doi: 10.1182/blood-2012-05-425934.

Siegel, D. S., P. Richardson, M. Dimopoulos, P. Moreau, C. Mitsiades, D. Weber, J. Houp, C. Gause, S. Vuocolo, J. Eid, T. Graef, and K. C. Anderson. 2014. "Vorinostat in combination with lenalidomide and dexamethasone in patients with relapsed or refractory multiple myeloma." *Blood Cancer J* 4:e182. doi: 10.1038/bcj.2014.1.

Silbermann, R., and G. D. Roodman. 2013. "Myeloma bone disease: Pathophysiology and management." *J Bone Oncol* 2 (2):59-69. doi: 10.1016/j.jbo.2013.04.001.

Singhal, S., J. Mehta, R. Desikan, D. Ayers, P. Roberson, P. Eddlemon, N. Munshi, E. Anaissie, C. Wilson, M. Dhodapkar, J. Zeddis, and B. Barlogie. 1999. "Antitumor activity of thalidomide in refractory multiple myeloma." *N Engl J Med* 341 (21):1565-71. doi: 10.1056/NEJM199911183412102.

Smith, D., and K. Yong. 2013. "Multiple myeloma." *BMJ* 346:f3863. doi: 10.1136/bmj.f3863.

Soriano, P., C. Montgomery, R. Geske, and A. Bradley. 1991. "Targeted disruption of the c-src proto-oncogene leads to osteopetrosis in mice." *Cell* 64 (4):693-702.

Stenbeck, G. 2002. "Formation and function of the ruffled border in osteoclasts." *Semin Cell Dev Biol* 13 (4):285-92.

Stewart, A. K., S. V. Rajkumar, M. A. Dimopoulos, T. Masszi, I. Spicka, A. Oriol, R. Hajek, L. Rosinol, D. S. Siegel, G. G. Mihaylov, V. Goranova-Marinova, P. Rajnics, A. Suvorov, R. Niesvizky, A. J. Jakubowiak, J. F. San-Miguel, H. Ludwig, M. Wang, V. Maisnar, J. Minarik, W. I. Bensinger, M. V. Mateos, D. Ben-Yehuda, V. Kukreti, N. Zojwalla, M. E. Tonda, X. Yang, B. Xing, P. Moreau, A. Palumbo, and Aspire Investigators. 2015. "Carfilzomib, lenalidomide, and dexamethasone for relapsed multiple myeloma." *N Engl J Med* 372 (2):142-52. doi: 10.1056/NEJMoa1411321.

Subramaniam, D., R. Thombre, A. Dhar, and S. Anant. 2014. "DNA methyltransferases: a novel target for prevention and therapy." *Front Oncol* 4:80. doi: 10.3389/fonc.2014.00080.

Sundaram, K., R. Nishimura, J. Senn, R. F. Youssef, S. D. London, and S. V. Reddy. 2007. "RANK ligand signaling modulates the matrix metalloproteinase-9 gene expression during osteoclast differentiation." *Exp Cell Res* 313 (1):168-78. doi: 10.1016/j.yexcr.2006.10.001.

Syed, Y. Y. 2017. "Lenalidomide: A Review in Newly Diagnosed Multiple Myeloma as Maintenance Therapy After ASCT." *Drugs* 77 (13):1473-1480. doi: 10.1007/s40265-017-0795-0.

Szabo, A. G., A. O. Gang, M. Pedersen, T. S. Poulsen, T. W. Klausen, and P. Nørgaard. 2016. "Overexpression of c-myc is associated with adverse clinical features and worse overall survival in multiple myeloma." *Leuk Lymphoma* 57 (11):2526-34. doi: 10.1080/10428194.2016.1187275.

Tai, Y. T., P. A. Mayes, C. Acharya, M. Y. Zhong, M. Cea, A. Cagnetta, J. Craigen, J. Yates, L. Gliddon, W. Fieles, B. Hoang, J. Tunstead, A. L. Christie, A. L. Kung, P. Richardson, N. C. Munshi, and K. C. Anderson. 2014. "Novel anti-B-cell maturation antigen antibody-drug conjugate (GSK2857916) selectively induces killing of multiple myeloma." *Blood* 123 (20):3128-38. doi: 10.1182/blood-2013-10-535088.

Takayanagi, H. 2007. "The role of NFAT in osteoclast formation." *Ann N Y Acad Sci* 1116:227-37. doi: 10.1196/annals.1402.071.

Takayanagi, H., S. Kim, T. Koga, H. Nishina, M. Isshiki, H. Yoshida, A. Saiura, M. Isobe, T. Yokochi, J. Inoue, E. F. Wagner, T. W. Mak, T. Kodama, and T. Taniguchi. 2002. "Induction and activation of the transcription factor NFATc1 (NFAT2) integrate RANKL signaling in terminal differentiation of osteoclasts." *Dev Cell* 3 (6):889-901.

Terpos, E., J. Berenson, N. Raje, and G. D. Roodman. 2014. "Management of bone disease in multiple myeloma." *Expert Rev Hematol* 7 (1):113-25. doi: 10.1586/17474086.2013.874943.

Terpos, E., D. Christoulas, M. Gavriatopoulou, and M. A. Dimopoulos. 2017. "Mechanisms of bone destruction in multiple myeloma." *Eur J Cancer Care (Engl)* 26 (6). doi: 10.1111/ecc.12761.

Tokoyoda, K., T. Egawa, T. Sugiyama, B. I. Choi, and T. Nagasawa. 2004. "Cellular niches controlling B lymphocyte behavior within bone marrow during development." *Immunity* 20 (6):707-18. doi: 10.1016/j.immuni.2004.05.001.

Tondravi, M. M., S. R. McKercher, K. Anderson, J. M. Erdmann, M. Quiroz, R. Maki, and S. L. Teitelbaum. 1997. "Osteopetrosis in mice lacking haematopoietic transcription factor PU.1." *Nature* 386 (6620):81-4. doi: 10.1038/386081a0.

Touzeau, C., and P. Moreau. 2016. "Pomalidomide in the management of relapsed multiple myeloma." *Future Oncol* 12 (17):1975-83. doi: 10.2217/fon-2016-0184.

Travers, A., and G. Muskhelishvili. 2015. "DNA structure and function." *FEBS J* 282 (12):2279-95. doi: 10.1111/febs.13307.

Tsukada, Y., J. Fang, H. Erdjument-Bromage, M. E. Warren, C. H. Borchers, P. Tempst, and Y. Zhang. 2006. "Histone demethylation by a family of JmjC domain-containing proteins." *Nature* 439 (7078):811-6. doi: 10.1038/nature04433.

Tumber, A., A. Nuzzi, E. S. Hookway, S. B. Hatch, S. Velupillai, C. Johansson, A. Kawamura, P. Savitsky, C. Yapp, A. Szykowska, N. Wu, C. Bountra, C. Strain-Damerell, N. A. Burgess-Brown, G. F. Ruda, O. Fedorov, S. Munro, K. S. England, R. P. Nowak, C. J. Schofield, N. B. La Thangue, C. Pawlyn, F. Davies, G. Morgan, N. Athanasou, S. Müller, U. Oppermann, and P. E. Brennan. 2017. "Potent and Selective KDM5 Inhibitor Stops Cellular Demethylation of H3K4me3 at Transcription Start Sites and Proliferation of MM1S Myeloma Cells." *Cell Chem Biol* 24 (3):371-380. doi: 10.1016/j.chembiol.2017.02.006.

Uchiyama, H., B. A. Barut, A. F. Mohrbacher, D. Chauhan, and K. C. Anderson. 1993. "Adhesion of human myeloma-derived cell lines to bone marrow stromal cells stimulates interleukin-6 secretion." *Blood* 82 (12):3712-20.

Vallet, S., and K. C. Anderson. 2011. "CCR1 as a target for multiple myeloma." *Expert Opin Ther Targets* 15 (9):1037-47. doi: 10.1517/14728222.2011.586634.

Vallet, S., and N. Raje. 2011. "Bone anabolic agents for the treatment of multiple myeloma." *Cancer Microenviron* 4 (3):339-49. doi: 10.1007/s12307-011-0090-7.

van Haaften, G., G. L. Dalgliesh, H. Davies, L. Chen, G. Bignell, C. Greenman, S. Edkins, C. Hardy, S. O'Meara, J. Teague, A. Butler, J. Hinton, C. Latimer, J. Andrews, S. Barthorpe, D. Beare, G. Buck, P. J. Campbell, J. Cole, S. Forbes, M. Jia, D. Jones, C. Y. Kok, C. Leroy, M. L. Lin, D. J. McBride, M. Maddison, S. Maquire, K. McLay, A. Menzies, T. Mironenko, L. Mulderrig, L. Mudie, E. Pleasance, R. Shepherd, R. Smith, L. Stebbings, P. Stephens, G. Tang, P. S. Tarpey, R. Turner, K. Turrell, J. Varian, S. West, S. Widaa, P. Wray, V. P. Collins, K. Ichimura, S. Law, J. Wong, S. T. Yuen, S. Y. Leung, G. Tonon, R. A. DePinho, Y. T. Tai, K. C. Anderson, R. J. Kahnoski, A. Massie, S. K. Khoo, B. T. Teh, M. R. Stratton, and P. A. Futreal. 2009. "Somatic mutations of the histone H3K27 demethylase gene UTX in human cancer." *Nat Genet* 41 (5):521-3. doi: 10.1038/ng.349.

Varettoni, M., A. Corso, G. Pica, S. Mangiacavalli, C. Pascutto, and M. Lazzarino. 2010. "Incidence, presenting features and outcome of extramedullary disease in multiple myeloma: a longitudinal study on 1003 consecutive patients." *Ann Oncol* 21 (2):325-30. doi: 10.1093/annonc/mdp329.

Vogelstein, B., D. Lane, and A. J. Levine. 2000. "Surfing the p53 network." *Nature* 408 (6810):307-10. doi: 10.1038/35042675.

Vogl, Dan T, Noopur S Raje, Sundar Jagannath, Paul G. Richardson, Parameswaran Hari, Robert Z. Orlowski, Jeffrey G Supko, David Tamang, Min Yang, Simon S. Jones, Catherine Wheeler, Robert J. Markelewicz, and Sagar Lonial. 2017. "Ricolinostat, the first selective histone deacetylase 6 inhibitor, in combination with bortezomib and dexamethasone for relapsed or refractory multiple myeloma." *Clinical Cancer Research*. doi: 10.1158/1078-0432.ccr-16-2526.

Väänänen, H. K., H. Zhao, M. Mulari, and J. M. Halleen. 2000. "The cell biology of osteoclast function." *J Cell Sci* 113 (Pt 3):377-81.

Wada, T., T. Nakashima, A. J. Oliveira-dos-Santos, J. Gasser, H. Hara, G. Schett, and J. M. Penninger. 2005. "The molecular scaffold Gab2 is a crucial component of RANK signaling and osteoclastogenesis." *Nat Med* 11 (4):394-9. doi: 10.1038/nm1203.

Waldmann, T., and R. Schneider. 2013. "Targeting histone modifications--epigenetics in cancer." *Curr Opin Cell Biol* 25 (2):184-9. doi: 10.1016/j.ceb.2013.01.001.

Wang, Z. Q., C. Ovitt, A. E. Grigoriadis, U. Möhle-Steinlein, U. Rüther, and E. F. Wagner. 1992. "Bone and haematopoietic defects in mice lacking c-fos." *Nature* 360 (6406):741-5. doi: 10.1038/360741a0.

Warde, N. 2010. "Rituximab targets short-lived autoreactive plasmablasts." *Nat Rev Rheumatol* 6 (5):246. doi: 10.1038/nrrheum.2010.53.

Wehrli, N., D. F. Legler, D. Finke, K. M. Toellner, P. Loetscher, M. Baggiolini, I. C. MacLennan, and H. Acha-Orbea. 2001. "Changing responsiveness to chemokines allows medullary plasmablasts to leave lymph nodes." *Eur J Immunol* 31 (2):609-16. doi: 10.1002/1521-4141(200102)31:2<609::AID-IMMU609>3.0.CO;2-9.

Wei, B., S. Yang, B. Zhang, and Y. Feng. 2016. "Clinicopathological significance of p15 promoter hypermethylation in multiple myeloma: a meta-analysis." *Onco Targets Ther* 9:4015-22. doi: 10.2147/OTT.S102733.

Weilbaecher, K. N., G. Motyckova, W. E. Huber, C. M. Takemoto, T. J. Hemesath, Y. Xu, C. L. Hershey, N. R. Dowland, A. G. Wells, and D. E. Fisher. 2001. "Linkage of M-CSF signaling to Mitf, TFE3, and the osteoclast defect in Mitf(mi/mi) mice." *Mol Cell* 8 (4):749-58.

West, A. C., and R. W. Johnstone. 2014. "New and emerging HDAC inhibitors for cancer treatment." *J Clin Invest* 124 (1):30-9. doi: 10.1172/JCI69738.

Westaway, S. M., A. G. Preston, M. D. Barker, F. Brown, J. A. Brown, M. Campbell, C. W. Chung, G. Drewes, R. Eagle, N. Garton, L. Gordon, C. Haslam, T. G. Hayhow, P. G. Humphreys, G. Joberty, R. Katso, L. Kruidenier, M. Leveridge, M. Pemberton, I. Rioja, G. A. Seal, T. Shipley, O. Singh, C. J. Suckling, J. Taylor, P. Thomas, D. M. Wilson, K. Lee, and R. K. Prinjha. 2016. "Cell Penetrant Inhibitors of the KDM4 and KDM5 Families of Histone Lysine Demethylases. 2. Pyrido[3,4-d]pyrimidin-4(3H)-one Derivatives." *J Med Chem* 59 (4):1370-87. doi: 10.1021/acs.jmedchem.5b01538.

Williams, G. H., and K. Stoeber. 2012. "The cell cycle and cancer." *J Pathol* 226 (2):352-64. doi: 10.1002/path.3022.

Wright, L. M., W. Maloney, X. Yu, L. Kindle, P. Collin-Osdoby, and P. Osdoby. 2005. "Stromal cell-derived factor-1 binding to its chemokine receptor CXCR4 on precursor cells promotes the chemotactic recruitment, development and survival of human osteoclasts." *Bone* 36 (5):840-53. doi: 10.1016/j.bone.2005.01.021.

Wu, J., T. Yamauchi, and J. C. Izpisua Belmonte. 2016. "An overview of mammalian pluripotency." *Development* 143 (10):1644-8. doi: 10.1242/dev.132928.

Wu, S. Y., A. Y. Lee, S. Y. Hou, J. K. Kemper, H. Erdjument-Bromage, P. Tempst, and C. M. Chiang. 2006. "Brd4 links chromatin targeting to HPV transcriptional silencing." *Genes Dev* 20 (17):2383-96. doi: 10.1101/gad.1448206.

Xing, L., T. P. Bushnell, L. Carlson, Z. Tai, M. Tondravi, U. Siebenlist, F. Young, and B. F. Boyce. 2002. "NF-kappaB p50 and p52 expression is not required for RANK-expressing osteoclast progenitor formation but is essential for RANK- and cytokine-mediated osteoclastogenesis." *J Bone Miner Res* 17 (7):1200-10. doi: 10.1359/jbmr.2002.17.7.1200.

Xu, F. H., S. Sharma, A. Gardner, Y. Tu, A. Raitano, C. Sawyers, and A. Lichtenstein. 1998. "Interleukin-6-induced inhibition of multiple myeloma cell apoptosis: support for the hypothesis that protection is mediated via inhibition of the JNK/SAPK pathway." *Blood* 92 (1):241-51.

Yagi, M., T. Miyamoto, Y. Sawatani, K. Iwamoto, N. Hosogane, N. Fujita, K. Morita, K. Ninomiya, T. Suzuki, K. Miyamoto, Y. Oike, M. Takeya, Y. Toyama, and T. Suda. 2005. "DC-STAMP is essential for cell-cell fusion in osteoclasts and foreign body giant cells." *J Exp Med* 202 (3):345-51. doi: 10.1084/jem.20050645.

Yasuda, H., N. Shima, N. Nakagawa, K. Yamaguchi, M. Kinosaki, S. Mochizuki, A. Tomoyasu, K. Yano, M. Goto, A. Murakami, E. Tsuda, T. Morinaga, K. Higashio, N. Udagawa, N. Takahashi, and T. Suda. 1998. "Osteoclast differentiation factor is a ligand for osteoprotegerin/osteoclastogenesis-inhibitory factor and is identical to TRANCE/RANKL." *Proc Natl Acad Sci U S A* 95 (7):3597-602.

Zannettino, A. C., A. N. Farrugia, A. Kortesidis, J. Manavis, L. B. To, S. K. Martin, P. Diamond, H. Tamamura, T. Lapidot, N. Fujii, and S. Gronthos. 2005. "Elevated serum levels of stromal-derived factor-1alpha are associated with increased osteoclast activity and osteolytic bone disease in multiple myeloma patients." *Cancer Res* 65 (5):1700-9. doi: 10.1158/0008-5472.CAN-04-1687.

Zhang, D. E., K. Fujioka, C. J. Hetherington, L. H. Shapiro, H. M. Chen, A. T. Look, and D. G. Tenen. 1994. "Identification of a region which directs the monocytic activity of the colony-stimulating factor 1 (macrophage colony-stimulating

factor) receptor promoter and binds PEBP2/CBF (AML1)." *Mol Cell Biol* 14 (12):8085-95.

Zhao, Q., J. Shao, W. Chen, and Y. P. Li. 2007. "Osteoclast differentiation and gene regulation." *Front Biosci* 12:2519-29.

Appendices

Table 1 Primer list for Chapter 4 (RANKL gene card)

Gene	Forward	Reverse
BCL2	GTGAACTGGGGGAGGATTGT	GGAGAAATCAAACAGAGGCC
CCND1	CGCCCCACCCCTCCAG	CCGCCCAGACCCTCAGACT
DCSTAMP	GGTTCACTTGAAACTGCACG	TAACACTGAGAGGAACCCAG
MYC	TCAAGAGGCGAACACACAAC	GGCCTTTTCATTGTTTTCCA
CTSK	TGAGGCTTCTCTTGGTGTCCATAC	AAAGGGTGTCATTACTGCGGG
TCIRG1	AGCTCGATGGAGGAGGGAGT	CAAACAGGAAGGGGAAGGTG
NFATC1	CGAGCCGTCATTGACTGTGC	GAGCGCTGGGAGCATTCGAT
CA2	ACTGGGGTTCACTTGATGGA	CTGCACAGCTTTCCCAAAAT
ACP6	GACCACCTTGGCAATGTCTCTG	TGGCTGAGGAAGTCATCTGAGTTG
TNF	CTCTCTCCCCTGGAAAGGAC	GCCAGAGGGCTGATTAGAGA
FBP1	CATGGCGATGGACCGGGA	AGGTTTGTCAGCACCAGTGT
GABPA	AAAGAGCGCCGAGGATTTCAG	CCAAGAAATGCAGTCTCGAG
CALM1	GGCATTCCGAGTCTTTGACAA	CCGTCTCCATCAATATCTGCT
CD44	TGGCACCCGCTATGTCCAG	GTAGCAGGGATTCTGTCTG
ILF3	AGGCCTACGCTGCTCTTGCT	GCCGAAGCCAGGGTTATGTG
GABPB1	CCCAGAGAGTCCTGACACT	TCTGAAGAATTGGACAATGG
CSF2RA	GGCACGAGGCGAGAGAAGA	ACGCAAACATCGCCGCTTCT
CDK7	ATGGCTCTGGACGTGAAGTC	CTTAATGGCGACAATTTGGTTG
CALCR	TGGTGCCAACCACTATCCATGC	CACAAGTGCCGCCATGACAG
MMP9	CAGTCCACCCTTGTGCTCTT	CCAGAGATTTCGACTCTCCAC
c-Fos	AAAAGGAGAATCCGAAGGGAAA	GTCTGTCTCCGCTTGGAGTGTAT
IGFBP4	CCCACTCCCAAAGCTCAGACT	CCAAGCAGATGGTGCAACAA
FAM89A	TGTCCTTGCTCTGCCAACTG	GCCGTTCTCCAGAGCGTAAG
COL6A2	GTCCTGCCCACCTCTCCTC	GAAGTTCTGCTCACCCAGCC
COL6A1	ACCTACACCGACTGCGCTAT	CGTCGGTCACCACAATCAGG
COL11A2	CGTTTCGGCTTCTCAGCCAT	GCACCAGAGGTAGGAGGAGG
TMEM132A	TTCTGCTCCTACAGCCCTGG	GTAGGGCTCTGCTGGAGTCA
CSPG	CAGCTCTACTCTGGACGCCT	GATGGAGTCACTCAGCAGCG
CDC42EP5	GGCTAGAGCTGGAGTCGTGA	CGATCAGGCCGCTTCTTGG
PRPSAP1	CCAGGGAAATGGAGGTATTG	AGAGGCCAACTGGATAGTAA
LIF	TGTCTTACAACACAGGCTCCAG	TCCAGTGCAGAACCAACAGC
NEURL3	CCAAAGCCACACCAGGAGAG	CACTTGGCCGTATCGCTGAA
MEGF6	CTGCCAGACAAGGTGCTCTT	GCCCAGTATCACAGGCTCTC
CKB	CACCATGCACCCCTGATGT	CTCTACCAAGGGTGACGGAAGT
ACTB	CAAGTCCACACAGGGGAGGT	AGACCAAAAGCCTTCATACATCTC
B2M	TGTCTGGGTTTCATCCATCCG	AGTCACATGGTTCACACGGC

Table 2 Primer list for Chapter 6

Gene	Forward	Reverse
MT1X	TCTCCTTGCCTCGAAATGG	CACAGCTGTCCTGGCATCA
ATF4	ATGACCGAAATGAGCTTCCTG	GCTGGAGAACCCATGAGGT
ASNS	GGAAGACAGCCCCGATTTACT	AGCACGAACTGTTGTAATGTCA
ASS1	TCCGTGGTTCTGGCCTACA	GGCTTCCTCGAAGTCTTCCTT
INHBE	ATCTTCCGATGGGGACCAAG	AGAGTTAAGGTATGCCAGCCC
PSAT1	TGCCGCACTCAGTGTTGTTAG	GCAATTCCCGCACAAGATTCT
DDIT3	AGGCACTGAGCGTATCATGT	TGAAGATACACTTCCTTCTTGAACA
MTF1	GTCTGTCAGAAGTGAATA	TGTAGTCGACGTTAGAAT

Table 3 Antibody list for Chapter 7

Marker	Target	Metal	Clone	Company	Concentration (µl/100µl)
CD19	B cells	142Nd	HIB19	Fluidigm	1
CD117	Mast cells, ILCs, NKs	143Nd	104D2	Fluidigm	0.75
CD38	Plasma cells	144Nd	HIT2	Fluidigm	1
CD81	B cells	145Nd	5A6	Fluidigm	0.3
CD4	T helper cells	145Nd	RPA-T4	Fluidigm	0.5
CD20	B cells	147Sm	2H7	Fluidigm	0.3
CD16	NK cells	148Nd	3G8	Fluidigm	0.5
CD45	All hemaetopoitic cells	154Sm	HI30	Fluidigm	0.1
CD10	Stromal cells	156Gd	HI10a	Fluidigm	0.5
CD33	Myeloid cells	158Gd	WM53	Fluidigm	1
CD11c	Macrophages/Monocytes	159Tb	Bu15	Fluidigm	0.3
CD28	T cells	160Gd	CD28.2	Fluidigm	1
CD8a	Cytotoxic T cells	162Dy	RPA-T8	Fluidigm	0.5
CD138	Plasma cells	168Er	DL101	Fluidigm	1
CD3	T cells	170Er	UCHT1	Fluidigm	0.5
CD56	NK cells	176Yb	N901	Fluidigm	0.5
Caspase 3	Apoptosis	172Yb	5A1E	Fluidigm	1
Ki67	Proliferating	161Dy	B56	Fluidigm	1

Table 4 Patient information for Chapter 7

No.	Disease	Previous treatment lines	Plasma cell proportion (%)
1	IgG kappa Myeloma(replased)	CTD induction and HDM/ASCT 2012, CCD (MUK5 trial) 2014 until Jan 2015.	4.1
2	Myeloma(new)	No prior treatments	6.1
3	MGUS(new)	No prior treatments	5.5
4	Myeloma(replased)	History not available	2.5
5	Myeloma(replased)	CTD and HDM/ASCT 2013	6.1
6	Myeloma	CTD 2011, 1st auto Nov 2011, VCD, second auto 30/12/2015	6.1
7	IgG lambda Myeloma(replased)	CTD induction and HDM/ASCT 2009, VCD 6 cycles March to July 2016	8.3
8	IgA lambda Myeloma(replased)	VCD induction and HDM/ASCT July 2015, Ixazomib/plb maintenance on the C16019 study	8.3
9	IgG kappa MGUS(new)	No prior treatments	2.1
10	IgG lambda Smouldering Myeloma(new)	No prior treatments	51.9

Table 5 EC_{50} (μM) and its 95% confidential interval (CI) or SD for selected compounds in Chapter 3

Target	Compound	Cell line					
		JJN3		5TGM1		JIM3	
		EC50	95% CI	EC50	95% CI	EC50	95% CI
Bromodomain	(+)-JQ1	0.10	0.08-0.2	0.08	0.05-0.11	0.16	0.1-0.25
Bromodomain	CBP/BRD4(0383)	7.58	4.9-11.8	7.45	5.8-10.4	3.30	1.8-5.4
Bromodomain/HDAC	DUAL946	2.29	1.9-2.8	4.44	3.2-6.1	17.24	7.5-25.2
HDAC	CXD101	0.15	0.09-0.22	0.13	0.11-0.15	0.15	0.13-0.17
HDAC	Rocillinostat	1.79	1.6-2	2.16	1.9-2.4	4.71	4.3-5.2
DNMT	5-Aza-deoxy-cytidine	1.29	0.5-3.2	0.08	/	1.78	0.9-3.9
		EC50	95% CI	EC50	SD	EC50	SD
Histone demethylase	GSK-J4	1.50	1.1-1.7	/	/	1.0	0.1
Target	Compound	Cell line					
		KMS11		MM1S		U266	
		EC50	95% CI	EC50	95% CI	EC50	95% CI
Bromodomain	(+)-JQ1	0.09	0.07-0.11	0.03	0.02-0.04	0.07	0.05-0.08
Bromodomain	CBP/BRD4(0383)	9.44	6.8-12.9	3.64	2.4-3.9	7.80	5.6-12.2
Bromodomain/HDAC	DUAL946	5.00	4.2-6	1.02	0.8-1.2	5.30	4.5-5.2
HDAC	CXD101	0.25	0.20-0.31	0.26	0.21-0.32	0.19	0.15-0.23
HDAC	Rocillinostat	4.92	4.3-5.5	2.85	2.4-3.3	5.54	4.8-6.3
DNMT	5-Aza-deoxy-cytidine	1.47	0.6-3.3	>50	/	3.62	1.4-5.5
		EC50	SD	EC50	SD	EC50	SD
Histone demethylase	GSK-J4	2.3	1.1	1.9	0.3	1.6	0.2

The EC_{50} of GSK-J4 in JIM3, KMS11, MM1S and U266 was obtained from Dr Edward Hookway in our research group.

Table 5 Full list of viability mean (%) and SD (%) in compound screening in myeloma cell lines (Chapter 3)

Target	Compound	JIM3		KMS11	
		Mean	SD	Mean	SD
Lysine demethylases	Tranylcypromine	91.6	13.9	96.8	6.6
Histone methyltransferase	SGC0946 (DOT1L probe)	75.9	16.4	90.3	6.1
Methyl Lysine Binder	UNC1215 (L3MBTL3 Probe)	89.4	3.2	100.1	5.9
Histone methyltransferase	(R)-PFI-2 (SETD7 Probe)	73.6	7.2	89.9	15.6
Histone demethylase	JIB-04	89.8	8.6	100.2	5.4
HDAC	CI-994	88.0	6.9	93.2	11.1
Lysine demethylases	GSK-J4 (KDM Probe)	0.3	0.4	3.2	6.2
Lysine demethylases	GSK-J5 (control)	88.9	8.4	109.9	5.2
HDAC	CXD101	36.2	17.5	28.3	26.3
Histone methyltransferase	UNC0642 (G9a/GLP Probe)	87.1	19.6	92.1	2.0
Bromodomains	(+)-JQ1 (active enantiomer)	78.2	26.7	12.0	14.5
Bromodomains	(-)-JQ1 (inactive stereoisomer)	89.5	6.2	99.3	1.4
Bromodomains	PFI-1 (BET Probe)	38.3	6.5	16.7	14.7
Bromodomains	CBP/BRD4 (0383)	69.2	24.4	71.0	8.9
Histone methyltransferase	UNC0638 (G9a Probe)	72.0	7.3	95.3	9.4
Lysine demethylases	IOX1 (5COOH-8HQ)	83.6	11.5	102.6	4.5
Prolyl-Hydroxylases	IOX2 (PHD2 Probe)	80.8	4.3	98.4	9.4
DNMT	5-Aza-deoxy-cytidine	20.0	17.0	20.1	13.1
HDAC	Valproic acid	81.0	21.7	74.2	38.2
Kinase inhibitor	K00135	86.0	22.3	100.6	7.3
Bromodomains	SMARCA	65.1	12.3	86.6	11.6
Bromodomains	I-BET (BET Probe)	56.6	9.5	25.0	23.4
PARP	Rucaparib	71.5	3.3	95.6	18.5
Bromodomains	GSK2801 (BAZ2B/A Probe)	92.3	17.3	99.4	3.2
Histone methyltransferase	Chaetocin	90.0	15.3	104.1	9.0
Kinase inhibitor	5-Iodotubercidin "HASPIN"	1.7	2.1	0.0	0.0
Histone methyltransferase	A-366 (G9a/GLP Probe)	79.4	12.1	91.0	6.0
PARP	Olaparib	84.5	12.3	106.0	11.1
HDAC	Entinostat (MS-275)	83.2	7.5	93.1	8.6
HDAC	Trichostatin A	7.3	14.5	20.8	25.8
HDAC	SAHA	62.1	7.5	82.0	9.5
Histone demethylase	Methylstat	81.4	10.4	96.2	9.1
Bromodomains	Bromosporin	85.5	7.2	95.2	10.6
Bromodomains	I-CBP112 (CREBBP/EP300 Probe)	76.7	10.7	94.4	16.0
Bromodomains	RVX-208	80.8	15.5	86.2	13.4
HDAC	Belinostat	17.1	29.1	0.9	1.6
HDAC	SRT1720	90.4	8.3	100.9	11.2
HDAC	EX 527	63.1	12.5	89.7	13.4
Histone methyltransferase	GSK343 (EZH2 Probe)	92.9	11.7	91.5	11.3
DNMT	5-Azacitidine	29.3	34.0	45.0	26.6
HAT	C646	96.2	9.6	98.2	12.8
Lysine demethylases	GSK-LSD1	94.8	7.0	89.3	14.3

Target	Compound	JIM3		KMS11	
		Mean	SD	Mean	SD
Histone demethylase	KDOBA67	8.2	5.4	26.1	30.7
Histone methyltransferase	UNC1999 (EZH2/1 Probe)	89.0	23.7	73.5	26.7
Bromodomains	SGC-CBP30 (CREBBP/EP300 Probe)	102.3	25.1	83.6	11.8
Halofuginone	MAZ1392	101.2	11.8	96.1	6.0
Halofuginol	MAZ1805	83.1	5.4	101.4	5.9
HDAC/Bromo	DUAL946 (High)	70.3	19.0	81.7	15.8
PADI4	GSK484 (High)	96.9	21.3	90.8	12.4
Histone methyltransferase	CPI.360	91.1	23.7	92.4	12.6
Histone methyltransferase	CPI.413 (Low)	106.7	7.9	98.0	7.3
Bromodomain	PFI4	84.4	12.1	94.5	7.2
Bromodomain	PFI3	91.6	11.9	97.3	3.1
Arginine methyltransferase	OICR	92.2	4.0	99.5	2.2
	SGC707	94.8	12.6	91.9	14.1
Histone methyltransferase	LLY507	91.1	5.8	99.3	1.0
Histone demethylase	ML324	79.6	5.3	91.6	4.0
HDAC	PCI-34051	73.1	6.8	88.0	15.2
HDAC	Tubastatin A HCI	68.8	9.0	81.3	13.0
Bromodomain	BAZ-ICR	93.6	8.7	101.0	2.7
Bromodomain	NI57	93.7	7.3	108.1	6.5
HDAC	RGFP 966	74.0	16.1	91.5	24.8
HDAC	Rocilinostat	14.3	2.3	31.3	33.9
Bromodomain	OF-1	68.6	38.1	58.3	50.5
Bromodomain	LP99	105.5	1.2	105.5	10.4
Histone demethylase	KDOAM25	93.11	0.75	89.62	0.37
Histone demethylase	GSK467	96.44	1.03	87.14	9.90
PRMT5	J556-42R	88.6	1.9	59.0	8.8
PRMT5	J556-63R	66.5	3.7	41.7	9.5
PRMT5	J556-70P	52.6	3.9	58.2	7.9
PRMT5	J556-143	74.5	3.3	41.9	5.4

Target	Compound	U266		MM1S	
		Mean	SD	Mean	SD
Lysine demethylases	Tranylcypromine	94.2	12.0	91.8	4.6
Histone methyltransferase	SGC0946 (DOT1L probe)	96.4	14.2	28.6	19.7
Methyl Lysine Binder	UNC1215 (L3MBTL3 Probe)	109.3	14.9	99.0	9.5
Histone methyltransferase	(R)-PFI-2 (SETD7 Probe)	84.9	5.3	89.8	6.8
Histone demethylase	JIB-04	113.5	18.2	88.4	4.9
HDAC	CI-994	99.5	10.7	86.0	4.7
Lysine demethylases	GSK-J4 (KDM Probe)	0.4	0.0	0.9	1.9
Lysine demethylases	GSK-J5 (control)	102.4	8.0	99.1	3.8
HDAC	CXD101	58.8	11.7	25.4	29.3
Histone methyltransferase	UNC0642 (G9a/GLP Probe)	85.7	15.6	73.2	24.9
Bromodomains	(+)-JQ1 (active enantiomer)	30.8	16.3	7.5	14.3
Bromodomains	(-)-JQ1 (inactive stereoisomer)	96.2	3.7	83.1	3.2
Bromodomains	PFI-1 (BET Probe)	48.8	23.5	61.8	21.3
Bromodomains	CBP/BRD4 (0383)	76.3	12.6	26.0	7.5
Histone methyltransferase	UNC0638 (G9a Probe)	103.1	2.1	53.1	16.9
Lysine demethylases	IOX1 (5COOH-8HQ)	99.0	8.5	90.0	4.9
Prolyl-Hydroxylases	IOX2 (PHD2 Probe)	99.0	13.7	89.8	5.1
DNMT	5-Aza-deoxy-cytidine	47.0	15.8	0.1	0.1
HDAC	Valproic acid	88.4	5.6	88.0	3.5
Kinase inhibitor	K00135	101.3	5.9	94.2	9.0
Bromodomains	SMARCA	79.1	6.6	86.2	9.7
Bromodomains	I-BET (BET Probe)	27.4	4.2	34.5	8.4
PARP	Rucaparib	105.4	13.6	70.9	8.6
Bromodomains	GSK2801 (BAZ2B/A Probe)	99.0	10.8	95.7	13.9
Histone methyltransferase	Chaetocin	87.8	25.4	1.8	3.6
Kinase inhibitor	5-Iodotubercidin "HASPIN"	23.1	30.2	3.3	4.1
Histone methyltransferase	A-366 (G9a/GLP Probe)	88.0	10.2	69.1	24.4
PARP	Olaparib	100.5	11.1	88.2	7.8
HDAC	Entinostat (MS-275)	87.5	3.5	87.2	9.6
HDAC	Trichostatin A	26.3	10.5	0.0	0.0
HDAC	SAHA	75.6	7.9	66.3	2.3
Histone demethylase	Methylstat	101.1	3.5	84.9	9.5
Bromodomains	Bromosporin	100.7	3.4	77.7	3.1
Bromodomains	I-CBP112 (CREBBP/EP300 Probe)	92.3	13.1	79.3	17.8
Bromodomains	RVX-208	67.2	17.9	77.5	32.6
HDAC	Belinostat	18.4	25.5	0.0	0.0
HDAC	SRT1720	96.2	9.6	94.5	4.1
HDAC	EX 527	80.8	7.4	93.1	5.2
Histone methyltransferase	GSK343 (EZH2 Probe)	97.7	12.6	91.0	5.3
DNMT	5-Azacitidine	70.6	12.9	86.9	1.8
HAT	C646	98.9	8.0	96.8	8.6
Lysine demethylases	GSK-LSD1	91.6	14.6	106.1	7.8
Histone demethylase	KDOBA67	20.9	11.0	12.7	6.3
Histone methyltransferase	UNC1999 (EZH2/1 Probe)	81.8	16.3	43.6	22.6
Bromodomains	SGC-CBP30	96.1	15.4	46.8	14.5

	(CREBBP/EP300 Probe)				
Target	**Compound**	**U266**		**MM1S**	
		Mean	**SD**	**Mean**	**SD**
Halofuginone	MAZ1392	95.6	6.1	95.2	3.2
Halofuginol	MAZ1805	104.1	4.5	91.9	4.1
HDAC/Bromo	DUAL946 (High)	78.4	3.6	66.5	36.4
PADI4	GSK484 (High)	95.8	11.4	93.8	12.7
Histone methyltransferase	CPI.360	103.7	10.4	93.4	13.2
Histone methyltransferase	CPI.413 (Low)	104.4	9.5	100.7	12.9
Bromodomain	PFI4	103.7	12.8	84.4	15.4
Bromodomain	PFI3	94.8	8.5	92.9	5.1
Arginine methyltransferase	OICR	95.4	3.1	92.0	3.0
	SGC707	99.7	18.1	91.3	5.2
Histone methyltransferase	LLY507	104.9	7.1	88.3	3.0
Histone demethylase	ML324	88.6	3.8	80.4	4.0
HDAC	PCI-34051	84.3	5.1	74.4	4.7
HDAC	Tubastatin A HCl	87.0	4.2	61.2	10.9
Bromodomain	BAZ-ICR	103.4	11.1	91.9	5.8
Bromodomain	NI57	96.5	4.6	88.1	9.4
HDAC	RGFP 966	73.7	14.4	78.4	9.7
HDAC	Rocilinostat	21.5	32.7	8.5	5.6
Bromodomain	OF-1	80.1	45.1	65.5	4.8
Bromodomain	LP99	98.9	2.1	83.0	5.8
Histone demethylase	KDOAM25	102.11	1.20	48.87	2.52
Histone demethylase	GSK467	104.58	1.66	51.04	0.91
PRMT5	J556-42R	40.1	2.6	41.0	4.6
PRMT5	J556-63R	34.2	1.5	24.7	1.1
PRMT5	J556-70P	29.4	0.6	21.6	1.4
PRMT5	J556-143	29.6	0.7	3.6	0.3

Target	Compound	5TGM3	
		Mean	SD
Lysine demethylases	Tranylcypromine	92.3	13.5
Histone methyltransferase	SGC0946 (DOT1L probe)	71.4	16.7
Methyl Lysine Binder	UNC1215 (L3MBTL3 Probe)	88.7	11.4
Histone methyltransferase	(R)-PFI-2 (SETD7 Probe)	76.1	12.4
Histone demethylase	JIB-04	91.1	10.0
HDAC	CI-994	75.5	10.9
Lysine demethylases	GSK-J4 (KDM Probe)	23.8	18.5
Lysine demethylases	GSK-J5 (control)	98.4	5.1
HDAC	CXD101	38.0	22.3
Histone methyltransferase	UNC0642 (G9a/GLP Probe)	85.3	12.2
Bromodomains	(+)-JQ1 (active enantiomer)	57.0	22.1
Bromodomains	(-)-JQ1 (inactive stereoisomer)	89.9	17.8
Bromodomains	PFI-1 (BET Probe)	28.5	23.2
Bromodomains	CBP/BRD4 (0383)	49.1	20.9
Histone methyltransferase	UNC0638 (G9a Probe)	77.1	17.1
Lysine demethylases	IOX1 (5COOH-8HQ)	90.6	17.6
Prolyl-Hydroxylases	IOX2 (PHD2 Probe)	78.6	24.6
DNMT	5-Aza-deoxy-cytidine	34.4	24.6
HDAC	Valproic acid	88.1	16.9
Kinase inhibitor	K00135	103.9	13.4
Bromodomains	SMARCA	77.9	17.2
Bromodomains	I-BET (BET Probe)	36.8	28.1
PARP	Rucaparib	58.5	25.0
Bromodomains	GSK2801 (BAZ2B/A Probe)	95.1	11.0
Histone methyltransferase	Chaetocin	92.9	16.4
Kinase inhibitor	5-Iodotubercidin "HASPIN"	41.3	24.8
Histone methyltransferase	A-366 (G9a/GLP Probe)	87.7	27.5
PARP	Olaparib	82.8	32.2
HDAC	Entinostat (MS-275)	89.8	14.5
HDAC	Trichostatin A	12.4	18.5
HDAC	SAHA	40.3	31.2
Histone demethylase	Methylstat	73.7	27.4
Bromodomains	Bromosporin	78.4	31.4
Bromodomains	I-CBP112 (CREBBP/EP300 Probe)	86.3	13.5
Bromodomains	RVX-208	65.4	21.0
HDAC	Belinostat	22.0	21.8
HDAC	SRT1720	103.3	4.0
HDAC	EX 527	80.3	9.8
Histone methyltransferase	GSK343 (EZH2 Probe)	95.4	15.2
DNMT	5-Azacitidine	43.5	19.6
HAT	C646	97.2	6.3
Lysine demethylases	GSK-LSD1	98.2	12.2
Histone demethylase	KDOBA67	20.2	26.8
Histone methyltransferase	UNC1999 (EZH2/1 Probe)	84.4	11.1
Bromodomains	SGC-CBP30	86.2	25.3

	(CREBBP/EP300 Probe)		
Target	**Compound**	**5TGM3**	
		Mean	**SD**
Halofuginone	MAZ1392	83.6	13.4
Halofuginol	MAZ1805	79.7	24.4
HDAC/Bromo	DUAL946 (High)	76.2	35.3
PADI4	GSK484 (High)	81.2	27.9
Histone methyltransferase	CPI.360	96.4	10.5
Histone methyltransferase	CPI.413 (Low)	88.5	23.1
Bromodomain	PFI4	88.1	8.7
Bromodomain	PFI3	84.2	5.3
Arginine methyltransferase	OICR	81.2	18.7
	SGC707	65.1	47.0
Histone methyltransferase	LLY507	34.4	51.3
Histone demethylase	ML324	38.3	34.5
HDAC	PCI-34051	68.7	33.5
HDAC	Tubastatin A HCl	53.5	38.7
Bromodomain	BAZ-ICR	80.9	30.8
Bromodomain	NI57	91.4	13.6
HDAC	RGFP 966	66.7	27.7
HDAC	Rocilinostat	68.9	58.0
Bromodomain	OF-1	50.9	27.3
Bromodomain	LP99	101.0	8.2
Histone demethylase	KDOAM25	93.58	7.85
Histone demethylase	GSK467	83.99	5.39
PRMT5	J556-42R	66.2	2.5
PRMT5	J556-63R	70.3	4.1
PRMT5	J556-70P	57.4	3.4
PRMT5	J556-143	61.0	14.7

The SD of compound screening results in JJN3 cells has already been represented in **Figure 3.15**.